



# **Cell and tissue specific functional genomics of psoriasis and psoriatic arthritis**

Alicia Lledó Lara  
Hertford College  
University of Oxford

*A thesis submitted in partial  
fulfilment of the requirements for the degree of  
Doctor of Philosophy  
Hilary Term, 2019*

# **Abstract**

**Functional genomics of psoriasis**

Alicia Lledó Lara, Hertford College, Hilary Term 2019

A thesis submitted in partial fulfilment of the requirements for the degree of  
Doctor of Philosophy of the University of Oxford

This is my abstract...

# Acknowledgements

Thank you, thank you, thank you.

## eclarations

I declare that unless otherwise stated, all work presented in this thesis is my own. Some aspects of the thesis were a collaboration, with some of the work conducted with or by others.

All the healthy volunteers and psoriasis patients samples were collected by myself and processing was part of a collaborative effort with past and current lab members Dr Anna Sanniti, Dr Andrew Brown and Giuseppe Scozzafava. The psoriatic arthritis samples processed for ATAC, qPCR array and mass cytometry were part of the Immune Function in Inflammatory Arthritis (IFIA) study established in 2006 and sample collection was a collaborative effort with Dr Hussein Al-Mossawi and Dr Nicole Yager.

The fixation protocol for sorted primary cells using DSP was optimised by Moustafa Attar. RNA extraction, ATAC and ChIPm processing for the healthy controls and psoriasis cohorts was carried out together with the ankylosing spondylitis samples in collaboration with Dr Anna Sanniti and Dr Andrew Brown. Advice for ATAC and ChIPm library indexing and sequencing was provided by Amy Trebes. RNA-seq and 10X Genomics technology Chromium single cell 3' expression library preparations and sequencing together with ATAC and ChIPm sequencing were performed by Oxford Genomics Centre at the Wellcome Centre for Human Genetics. Processing of the qPCR array and mass cytometry samples was conducted by UCB and measurement of synovial fluid cytokine and chemokine abundance was carried out by collaborators in Basle.

Regarding analysis, mass cytometry data was analysed by Dr Nicole Yager. ATAC and ChIPm NGS data processing was conducted using in house  pipelines developed by Dr Gabriele Migliorini towards which I actively contributed by performing literature review analysis of the most appropriate methods, facilitating code for some of the parts and performing additional analysis to test and validate some of the tools and approaches. ~~The~~ peak filtering strategy for ATAC using IDR was proposed and implemented by Dr Gabriele Migliorini and I conducted additional analysis to validate it. The strategy to perform filtering of chromatin accessible regions based on an empirical cut-off to remove excessive noise was developed and implemented together with Dr Hai Fang. RNA-seq NGS data processing was performed using the in-house pipeline developed by Dr Katie Burnham. All the resources for fine-mapping analysis using genotyping or summary statistics data were provided by Dr Adrián Cortés. General advice ~~for analysis of different datasets~~ were provided by Dr Silvia Salatino, Dr Hai Fang, Dr Katie Burnham, Dr Félicie Constantino, Dr Gabriele Migliorini, Dr Adrián Cortés and Enrique Vázquez de Luis. The script to calculate enrichment across TSS was provided by Dr Silvia Salatino ~~(part of the Oxford Genomics Centre resources)~~. ~~The function for colour coding KEGG pathways based on gene expression data was developed by Dr Hai Fang and I contributed together with Dr Anna Sanniti to manual curation of the pathways.~~

# **Submitted Abstracts**

<b>Title</b>	<b>Year</b>
Authors	

# Other Publications

## Title

Journal

Authors

# Contents

<b>Abstract</b>	i
<b>Acknowledgements</b>	ii
<b>Declarations</b>	iii
<b>Submitted Abstracts</b>	iv
<b>Contents</b>	vi
<b>List of Figures</b>	xi
<b>List of Tables</b>	xiii
<b>Abbreviations</b>	xiv
<b>1 Introduction</b>	1
1.1 Psoriasis and psoriatic arthritis . . . . .	1
1.1.1 Epidemiology and global impact . . . . .	2
1.1.2 Psoriasis and inflammatory dermatoses . . . . .	3
1.1.3 PsA and spondyloarthropathies . . . . .	4
1.2 Pathophysiology of psoriasis and psoriatic arthritis . . . . .	5
1.2.1 Clinical presentation and diagnosis . . . . .	5
1.2.2 Aetiology of psoriasis and PsA . . . . .	7
1.2.3 Cell types involved in psoriasis and PsA pathogenesis . . . . .	11
1.2.4 Therapeutic intervention . . . . .	16
1.3 Genetics of psoriasis and psoriatic arthritis . . . . .	17
1.3.1 Heritability . . . . .	17
1.3.2 Non-GWAS and linkage studies . . . . .	18
1.3.3 Genome-wide association studies . . . . .	19
1.3.4 Relevance of non-coding variants in disease susceptibility .	23
1.3.5 The role of GWAS in highlighting immune-relevant cell types and pathways . . . . .	24
1.3.6 Limitations and future of GWAS . . . . .	29
1.4 Functional interpretation of GWAS in complex diseases . . . . .	30
1.4.1 Overcoming the limitations of GWAS: post-GWAS studies .	30
1.4.2 Understanding the epigenetic landscape in complex diseases	31
1.4.3 The chromatin landscape . . . . .	32
1.4.4 Transcriptional profiles in disease . . . . .	38
1.4.5 Transcriptional regulation in complex diseases . . . . .	41
1.4.6 The use of fine-mapping to prioritise functional causal variants . . . . .	42
1.4.7 Integration and interpretation of genomic data . . . . .	43

## CONTENTS

---

1.4.8	Aims and objectives . . . . .	45
<b>2</b>	<b>Material and Methods</b>	<b>47</b>
2.1	Ethical approval and recruitment of study participants . . . . .	47
2.1.1	Psoriasis patient recruitment . . . . .	47
2.1.2	PsA patient recruitment . . . . .	48
2.1.3	Healthy volunteer recruitment . . . . .	48
2.2	Sample processing . . . . .	49
2.2.1	PBMCs and synovial fluid cells isolation . . . . .	49
2.2.2	Skin biopsies processing and adherence assays . . . . .	50
2.2.3	Fixation, cryopreservation and cell culture . . . . .	50
2.2.4	Primary cell isolation using magnetic-activated cell sorting	51
2.2.5	Primary cell isolation using fluorescence-activated cell sorting . . . . .	52
2.3	Experimental protocols . . . . .	53
2.3.1	ATAC - Chromatin Accessibility . . . . .	53
2.3.2	Chromatin immunoprecipitation with sequencing library preparation by Tn5 transposase . . . . .	56
2.3.3	RNA extraction and gene expression quantification . . . . .	57
2.3.4	DNA extraction and rs4672405 genotyping . . . . .	60
2.3.5	Mass cytometry using cytometry by time of flight (CyTOF)	60
2.4	Computational and statistical analysis . . . . .	61
2.4.1	ATAC data analysis . . . . .	61
2.4.2	ChIPm data analysis . . . . .	65
2.4.3	Gene expression analysis . . . . .	66
2.4.4	Genomic region annotation, enrichment analysis, gene-network analysis and pathway visualisation . . . . .	69
2.4.5	Statistical fine-mapping . . . . .	71
2.4.6	Mass cytometry data analysis . . . . .	73
<b>3</b>	<b>Defining the genome-wide chromatin accessibility landscape and gene expression profile in psoriasis</b>	<b>74</b>
3.1	Introduction . . . . .	74
3.1.1	The systemic and skin-specific manifestations of psoriasis .	74
3.1.2	The personalised epigenome in disease . . . . .	75
3.1.3	Transcriptional profiles in psoriasis . . . . .	76
3.1.4	Chromatin accessibility, gene expression and genetic variability . . . . .	80
3.1.5	Fine-mapping using summary stats . . . . .	81
3.2	Aims . . . . .	82
3.3	Results . . . . .	83
3.3.1	Psoriasis and healthy controls: cohort description and datasets . . . . .	83
3.3.2	Investigation of psoriasis-specific changes in the enhancer mark H3K27ac in different peripheral blood immune cell populations . . . . .	88

## CONTENTS

---

3.3.3	Identifying global changes in chromatin accessibility between psoriasis patients and healthy controls for different peripheral blood immune cell populations . . . . .	94
3.3.4	Differential gene expression analysis in circulating immune cells in psoriasis . . . . .	101
3.3.5	RNA-seq in epidermis from psoriasis patients . . . . .	111
3.3.6	Comparison of systemic and tissue-specific gene expression signatures in psoriasis . . . . .	122
3.3.7	Integration of chromatin accessibility and expression data for peripheral blood immune cells in psoriasis . . . . .	123
3.3.8	Fine-mapping of psoriasis GWAS loci and functional interpretation . . . . .	126
3.3.9	Allele-specific differences in chromatin accessibility at the GWAS locus 2p15 . . . . .	131
3.4	Discussion . . . . .	137
3.4.1	Chromatin accessibility and H3K27ac landscape in psoriasis immune cells . . . . .	137
3.4.2	Dysregulation of gene expression in psoriasis circulating immune cells . . . . .	139
3.4.3	Correlation between changes in chromatin accessibility and gene expression . . . . .	142
3.4.4	Tranciptomic profiles in lesional and uninvolved psoriatic epidermis . . . . .	143
3.4.5	LncRNAs in psoriasis . . . . .	145
3.4.6	Differences in transcriptional dysregulation in peripheral blood and skin . . . . .	147
3.4.7	Fine-mapping using summary statistics and integration with epigenetic data . . . . .	148
3.4.8	Limitations in the approach . . . . .	151
3.4.9	Conclusions . . . . .	152
	<b>Appendices</b>	<b>153</b>
<b>A</b>	<b>Tables</b>	<b>155</b>
A.1	Chapter 3 Tables . . . . .	155
A.2	Chapter 4 Tables . . . . .	155
A.3	Chapter 5 Tables . . . . .	162
<b>B</b>	<b>Additional figures</b>	<b>165</b>
B.1	Chapter 3 Figures . . . . .	165
B.2	Chapter 4 Figures . . . . .	168
B.3	Chapter 5 Figures . . . . .	171
	<b>Bibliography</b>	<b>206</b>

# List of Figures

1.1	Environmental triggers and genetic predisposition leading to psoriasis and PsA (adapted from Nestle <i>et al.</i> , 2009). . . . .	14
3.1	Quality control evaluation of the H3K27ac ChIPm libraries in immune cells isolated from psoriasis and control samples. . . . .	89
3.2	PCA and chromatin annotation states of the consensus list of H3K27ac called peaks in four immune primary cell types from psoriasis and healthy control samples. . . . .	91
3.3	Differential H3K27ac modification at a putative intergenic enhancer region in circulating CD14 <sup>+</sup> monocytes between psoriasis patients and healthy controls. . . . .	93
3.4	Quality control assessment of the ATAC libraries generated from circulating immune cells in psoriasis and control samples. . . . .	94
3.5	Clustered heatmap and conserved TFBS enrichment analysis in the consensus list of called ATAC peaks in CD14 <sup>+</sup> monocytes, CD4 <sup>+</sup> , CD8 <sup>+</sup> and CD19 <sup>+</sup> cells from the patients and controls cohort. . . . .	96
3.6	Epigenetic landscape at two ATAC differential accessible regions between patients and controls in CD8 <sup>+</sup> cells. . . . .	99
3.7	Epigenetic landscape at <i>DTD1</i> locus showing differential H3K27ac and chromatin accessibility between psoriasis patients and controls in CD8 <sup>+</sup> cells. . . . .	100
3.8	PCA and sample distance heatmap with hierarchical clustering illustrating the sample variability based on the gene expression profiles for all 72 samples. . . . .	103
3.9	Magnitude and significance of the gene expression changes between psoriasis patients and healthy controls in four immune cell types. . . . .	104
3.10	RNA-seq expression levels of the lncRNA <i>HOTAIRM1</i> and its experimentally validated target <i>UPF1</i> in psoriasis and healthy controls CD14 <sup>+</sup> monocytes. . . . .	107
3.11	Differential expression between psoriasis and healthy controls of MAPK and DUSP genes contributing to MAPK signalling enrichment in CD14 <sup>+</sup> monocytes and CD8 <sup>+</sup> T cells. . . . .	110
3.12	Mapping of the DEGs identified in CD8 <sup>+</sup> cells between psoriasis patients and healthy controls onto the TNF- $\alpha$ and the chemokine signalling pathways. . . . .	112
3.13	PCA for the RNA-seq data in the uninvolved and lesional epidermis from psoriasis patients. . . . .	113
3.14	Magnitude and significance of the gene expression changes between matched lesional and uninvolved epidermal biopsies from three psoriasis patients. . . . .	114

## LIST OF FIGURES

---

3.15 Overlap of the significantly differentially expressed genes between lesional and uninvolved epidermal sheets, split epidermis and whole skin biopsies. . . . .	116
3.16 Mapping of the DEGs between lesional and uninvolved epidermis from psoriasis patients onto the HIF-I signalling pathway. . . . .	119
3.17 Mapping of the DEGs between lesional and uninvolved epidermis from psoriasis patients onto the NOD-like signalling pathway. . . . .	121
3.18 Differential gene expression and chromatin accessibility landscape for <i>TIAM1</i> and <i>TRAT1</i> genes in CD8 <sup>+</sup> cells. . . . .	125
3.19 Epigenetic landscape at the location of the SNPs in the 4 SNPs in the 90% credible set for the <i>SLC45A1/TNFRSF9</i> psoriasis GWAS locus. . . . .	132
3.20 Epigenetic landscape at the location of the 95% credible set of AS fine-mapped SNPs for the chr2p15. . . . .	134
3.21 rs4672505 genotype and chromatin accessibility at chr2:62,559,749-62,561,442 in CD8 <sup>+</sup> cells. . . . .	135
3.22 Potential role of rs4672505 in regulating <i>B3GNT2</i> gene expression. . . . .	136
 B.1 Distribution of the background read counts from all the master list peaks absent in each sample. . . . .	165
B.2 Pre-sequencing profiles of relative abundance of DNA library fragment sizes for a psoriatic lesional keratinocytes ATAC 1 library generated using 40 min of transposition. . . . .	165
B.3 Assessment of TSS enrichment from ATAC 1 and Fast-ATAC in healthy and psoriasis KCs isolated from skin biopsy samples. . . . .	166
B.4 Fast-ATAC and Omni-ATAC NHEK pre-sequencing profiles of relative abundance of DNA library fragment sizes. . . . .	167
B.5 Percentage of MT reads and called peaks after IDR p-value filtering in the ATAClibraries generated in CD14 <sup>+</sup> monocytes, CD4 <sup>+</sup> , CD8 <sup>+</sup> and CD19 <sup>+</sup> isolated from psoriasis patients and healthy controls. . . . .	168
B.6 PCA analysis illustrating batch effect in ATAC and RNA-seq samples. . . . .	169
B.7 Mapping rate and total reads after filtering (million) mapping to Ensembl genes in all the RNA-seq samples from psoriasis patients and controls in four cell types. . . . .	169
B.8 Mapping quality control for the RNA-seq data in the uninvolved and lesional epidermis from psoriasis patients. . . . .	170
B.9 Correlation in gene expression between the miRs <i>MIR31HG</i> and the target gene <i>HIF-1A</i> in lesional and uninvolved skin. . . . .	170
B.10 Assessment of the percentage of mitochondrial and duplicated reads and the number of called peaks after filtering in the ATAC data from peripheral blood and synovial fluid of PsA patients samples. . . . .	171
B.11 Enrichment of eQTL SNPs for the consensus list of ATAC peaks used to perform differential chromatin accessibility analysis in each cell type. . . . .	171
B.12 Permutation analysis SF vs PB in CD14 <sup>+</sup> monocytes,CD4m <sup>+</sup> ,CD8m <sup>+</sup> and NK. . . . .	172

## **LIST OF FIGURES**

---

B.13 Enrichment of DARs in the 15 chromatin states of the cell type specific Roadmap Epigenomic Project segmentation maps. . . . .	173
B.14 Heatmap for the top 20 marker genes of the CC-mixed and CC-IL7R CD14 <sup>+</sup> monocytes subpopulations. . . . .	174
B.15 Identification of the CD14 <sup>+</sup> monocytes populations from bulk SFMCs and PBMCs using scRNA-seq transcriptomes. . . . .	175
B.16 Quantification of cytokine levels in plasma and synovial fluid from 10 PsA patients. . . . .	176

# List of Tables

1.1	Variables and scoring used in the Psoriasis Area and Severity Index (PASI) . . . . .	7
1.2	Variables and scoring used in the Psoriatic Arthritis Response Criteria (PsARC) . . . . .	8
1.3	Main GWAS studies in psoriasis and PsA . . . . .	21
2.1	Summary table of samples/cohorts recruited in this thesis for generation of various datasets. . . . .	49
2.2	Antibody panel used for FACS separation of primary cell populations in Chapter 3 controls and Chapter 5 PsA samples. . .	53
2.3	Molecules targeted by the mass cytometry antibody panel for peripheral blood and synovial fluid samples. . . . .	62
3.1	Summary table of the most comprehensive transcriptional studies in psoriasis skin and blood. . . . .	77
3.2	Description and metadata of the psoriasis patients cohort. . . . .	84
3.3	Description of the healthy control cohort. . . . .	87
3.4	Summary results from the differential H3K27ac analysis between psoriasis patients and healthy controls in CD14 <sup>+</sup> monocytes, CD4 <sup>+</sup> , CD8 <sup>+</sup> and CD19 <sup>+</sup> cells. . . . .	92
3.5	Summary results from the differential chromatin accessibility analysis between psoriasis patients and healthy controls in CD14 <sup>+</sup> monocytes, CD4 <sup>+</sup> , CD8 <sup>+</sup> and CD19 <sup>+</sup> cells. . . . .	98
3.6	Summary results from the DGE analysis between psoriasis patients and healthy controls in CD14 <sup>+</sup> monocytes, CD4 <sup>+</sup> , CD8 <sup>+</sup> and CD19 <sup>+</sup> cells. . . . .	102
3.7	Overlap between putative psoriasis GWAS genes and the reported significantly DEGs in CD14 <sup>+</sup> monocytes, CD4 <sup>+</sup> , CD8 <sup>+</sup> and CD19 <sup>+</sup> cells. . . . .	105
3.8	Pathways enriched for DEGs between psoriasis patients and healthy controls in CD14 <sup>+</sup> monocytes and CD8 <sup>+</sup> cells. . . . .	108
3.9	Summary results of the DGE analysis between uninvolved and lesional psoriatic epidermal biopsies. . . . .	114
3.10	Most relevant pathways enriched for DEGs between lesional and uninvolved epidermis isolated from psoriasis patients skin biopsies.	118
3.11	Overlap between the DEGs in the four circulating immune cell types (psoriasis patients versus controls) and the DEGs in psoriasis patients skin biopsies (lesional versus uninvolved). . . . .	123
3.12	Summary table of the psoriasis Immunochip GWAS loci presenting $\log_{10}ABF > 3$ for the fine-mapping lead SNP. . . . .	127

## LIST OF TABLES

---

3.13 SNPs from the 90% credible set of the successfully fine-mapped psoriasis loci overlapping ATAC accessible chromatin in four cell types. . . . .	130
A.1 Enrichment of ATAC-seq reads across the TSS for the CD14 <sup>+</sup> monocytes and CD4 <sup>+</sup> samples fresh, frozen and fixed. . . . .	155
A.2 Evaluation of ChiPm library complexity for the psoriasis and control chort 1B ChiPm assay. . . . .	156
A.3 Size of the master lists generated by DiffBind for the H3K27ac differential analysis between psoriasis patients and healthy controls in CD14 <sup>+</sup> monocytes, CD4 <sup>+</sup> , CD8 <sup>+</sup> and CD19 <sup>+</sup> cells. . . . .	157
A.4 Functional interactions and overlap with another study for the differentially expressed lncRNAs in each cell type. . . . .	157
A.5 Additional enriched pathways for DEGs between psoriasis and healthy controls in CD14 <sup>+</sup> monocytes and CD8 <sup>+</sup> cells. . . . .	158
A.6 Additional enriched pathways for DEGs between lesional and uninvolved epidermis isolated from psoriasis patients skin biopsies.	159
A.7 Loci from the psoriasis GWAS Immunochip presenting log <sub>10</sub> ABF< 3 for the fine-mapping lead SNP in the association analysis. . . . .	161
A.8 Additional enriched pathways for the DEGs between SF and PB CD14 <sup>+</sup> monocytes from the CC-mixed and CC-IL7R subpopulations.	162
A.9 PsA GWAS Immunochip loci presenting log <sub>10</sub> ABF< 3 for the fine-mapping lead SNP in the association analysis. . . . .	163

# Abbreviations

Abbreviation	Definition
<b>Ab</b>	Antibody
<b>ATAC-seq</b>	
<b>Atopic dermatitis</b>	AD
<b>ChIPm</b>	
<b>CLE</b>	cutaneous lupus erythematosus
<b>DMARDs</b>	disease-modifying antirheumatic drugs
<b>Fast-ATAC</b>	
<b>IDR</b>	
<b>GWAS</b>	Genome-wide association studies
<b>KC</b>	Keratinocytes
<b>NSAID</b>	nonsteroidal antiinflammatory drug
<b>Omni-ATAC</b>	
<b>PCA</b>	
<b>PI</b>	Protein inhibitor
<b>PsA</b>	
<b>QC</b>	
<b>qPCR</b>	quantitative polymerase chain reaction
<b>RA</b>	Rheumatoid arthritis
<b>ROS</b>	Reactive oxygen species
<b>SDS</b>	Sodium dodecyl sulfate
<b>SF</b>	Synovial fluid

# Chapter 1

## Introduction

Our growing knowledge of genetic associations with susceptibility to psoriasis and psoriatic arthritis (PsA) has not been matched by understanding of the functional basis of these associations and translation to patient benefit. To address this challenge, it is important to understand the regulatory genomic landscape within which disease associated genetic variants may act. This thesis describes functional genomic approaches to establish genome-wide epigenetic and expression profiles for disease relevant tissues and blood-isolated immune cells in psoriasis and PsA, and explore their potential significance for disease pathogenesis and genetic variation. In this chapter, I begin by reviewing current knowledge of the pathophysiology of psoriasis and psoriatic arthritis, the role of genetic variation, and the challenge of functionally characterising genome-wide association studies (GWAS) in complex traits, including the different functional genomics approaches that can be applied.

### 1.1 Psoriasis and psoriatic arthritis

Psoriasis and PsA have been described as two distinct common complex disease entities that nonetheless share certain clinical features and genetic architecture. Psoriasis is a chronic inflammatory skin disease characterised by episodes of relapse and remittance, most commonly manifesting as well-demarcated erythematous plaques with silver scale and associated with increased risk of joint, eye and systemic disorders (Nestle et al. 2009). On the other hand,

## **Introduction**

---

PsA is a seronegative chronic inflammatory disease within the spondyloarthritis (SpA) family that usually develops after psoriasis skin manifestations (Moll et al. 1973; Coates et al. 2016a; Villanova et al. 2013). Understanding similarities and differences between these conditions at the pathological level is helpful before we consider sharing and specificity at the genetic level as well as implications for the identification of new therapeutic targets.

### **1.1.1 Epidemiology and global impact**

Psoriasis represents a serious global health problem that currently affects about 100 million people worldwide, including both children and adults with no sex bias (Organization 2016). Although the mean age of onset is 33 years, a bimodal distribution with psoriasis patients being classified as early-onset/ type I (with peaks between 16 and 22 years) or late-onset / type II (between 50-60 years) has also been described (Henseler and Christophers 1985; Perera et al. 2012). This classification based on the age of onset also ~~has~~ correlates with distinctive clinical features including severity, relapse frequency and family history.

The risk of developing psoriasis shows ethnic differences with a lower prevalence among adult African, African American and Asian populations (between 0.4 and 0.7%) compared to American and Canadian (4.6 and 4.7 %, respectively) (Jacobson et al. 2011). In the UK the prevalence of psoriasis ranges between 2 and 3%, affecting approximately 1.8 million people (Perera et al. 2012). On the other hand, cases of PsA in the general population varies between 0.04 and 1.2% (Perera et al. 2012) occurring in 10 to 30% of psoriasis patients, evidencing the strong association between the two diseases (Gelfand et al. 2005; Reich et al. 2015; Perera et al. 2012). Overall, data suggest ~~an~~ steady increase in both psoriasis and PsA prevalence over the last thirty years (Springate et al. 2017; Organization 2016).

## **Introduction**

---

Several severe comorbidities have are associated with psoriasis and PsA, with comparatively greater prevalence in PsA. For example, intraocular inflammation (uveitis) affects 8% of PsA patients compared to only 2% of psoriasis patients (Husted et al. 2011; Oliveira et al. 2015). Other comorbidities include inflammatory bowel disease (IBD), cardiovascular disease (CVD), type 2 diabetes (T2D) and metabolic syndrome (Gelfand et al. 2006; Shapiro et al. 2007; Cohen et al. 2008). Psoriasis and PsA have also been associated with an increased prevalence of depression and suicidal ideation (Sampogna et al. 2012). Overall, psoriasis and PsA represent a significant burden for the economy due to treatment costs and associated morbidity. Treatment and management-associated costs per psoriasis patient per year in 2015 in the UK accounted for £4,000 to £14,000, before and after requirements of biological therapy, respectively, and were further increased in PsA (Burgos-Pol and Dermo 2016; Poole et al. 2010).

### **1.1.2 Psoriasis and inflammatory dermatoses**

The skin is the biggest organ in the human body constituting an effective barrier between the environment and the internal organs. The most external layer, the epidermis, plays an important role in innate and adaptive immunity and its alterations, ~~due to exogenous or endogenous factors~~, can lead to development of inflammatory skin conditions, such as psoriasis or atopic dermatitis (Johnson-Huang 2009; Proksch et al. 2008).

Lesions in psoriasis are very heterogeneous in type (pustular and non-pustular), location and severity, which complicates its clinical classification (Perera et al. 2012). As a result, several phenotypes including chronic plaque psoriasis (psoriasis vulgaris), guttate psoriasis, pustular psoriasis, erythrodermic psoriasis and nail psoriasis have been defined (Marrakchi et al. 2011).

## **Introduction**

---

### **1.1.3 PsA and spondyloarthropathies**

PsA belongs to the SpA family, which includes diseases such as ankylosing spondylitis (AS), reactive arthritis (ReA), idiopathic inflammatory bowel disease (IBD) and undifferentiated SpA (Goldman and Schafer 2011). All these SpA subtypes are characterised by structural damage (bone formation and erosion) as well as inflammation of joints and extra-articular sites such as eyes, gut and skin. Broadly, SpA has been classified into axial and peripheral based on the affected joints (spine/sacroiliac or peripheral) and the presence of extra-articular features (Rudwaleit et al. 2009).

Major histocompatibility (MHC) class I molecules present intracellular peptides (self or from infectious agents) to T cells, encoded by the human leukocyte antigen (HLA) A, B and C genes. HLA-B27 is the strongest genetic association for the SpA family. Studies in human families and rat models with HLA-B27 positive status have shown manifestation of different SpA, such as psoriasis and inflammatory bowel disease (IBD)–, within a single family or individual (Said-Nahal2001; Hammer et al. 1990). Based on ~~the~~ common pathophysiological foundations, some studies have supported the concept of SpA as a single disease that presents heterogeneous phenotypic manifestations based on current knowledge (Baeten et al. 2013). Interestingly, the axial and peripheral classification of SpA may be supported by true immunopathological differences between the two (Porcher et al. 2005; Appel et al. 2011; Vandooren et al. 2004). Nevertheless, the knowledge of cellular and molecular processes contributing to pathophysiology is still limited and further research will impact on the classification and understanding of SpA family.

As a phenotype, PsA can be further subdivided in five clinical groups as per the Moll and Wright criteria: distal, destructive, symmetric, asymmetric and spinal (Moll et al. 1973). These subclasses mainly differ in the location, number and distribution of the affected joints and have been later modified to

## **Introduction**

---

also include dactylitis (diffuse swelling of a digit), a distinctive feature of PsA (Reich 2012). Importantly, the phenotypic heterogeneity of SpA and also within PsA difficults the design and achievement of meaningful outcomes from clinical studies due to the incomplete understanding of disease classification. This may obscure findings and conclusion in pathophysiological and clinical studies and needs to be considered when interpreting the results.

## **1.2 Pathophysiology of psoriasis and psoriatic arthritis**

### **1.2.1 Clinical presentation and diagnosis**

Approximately 90% of all psoriasis cases are psoriasis vulgaris, which manifests with well demarcated plaques, erythema and scaling. Plaque formation is the result of thickening (acanthosis) and vascularisation of the epidermis and can vary in size and distribution, with the most common locations being the elbows, knees and scalp (Perera et al. 2012; Griffiths and Barker 2007). The second most common clinical presentation is guttate psoriasis (10% of all cases) characterised by acute onset of small droplike papules usually in the trunk and proximal extremities (Vence et al. 2015). ~~Despite psoriasis vulgaris and guttate representing an important burden for patient wellbeing but are generally not life threatening forms of disease.~~

Early and late onset psoriasis (type I and type II) differ in clinical presentation. Type I psoriasis patients commonly present with guttate lesions followed very often by bacterial infection, particularly *Streptococcus* throat infection, and have a stronger family history with a high prevalence of HLA-C\*06:02 (85.4% of the cases) (Telfer et al. 1992). In contrast, in type II psoriasis only in 14.6% of the cases are positive for HLA-C\*06:02 and most commonly manifests as spontaneous chronic plaques (psoriasis vulgaris) (Perera et al. 2012).

## **Introduction**

---

For PsA, symmetric/polyarticular PsA constitutes the most common manifestation (more than 50% of the cases) followed by asymmetric/oligoarticular PsA (around 30%), which exclusively affects single or few distal interphalangeal or phalangeal joints (Reich et al. 2009; McGonagle et al. 2011). Skin psoriatic lesions precede joint inflammation in approximately 60 to 70% of the cases (Gladman et al. 2005; McGonagle et al. 2011). In particular, nail pitting and scalp and intergluteal skin lesions constitute a predictive biomarker for development of joint inflammation (Moll et al. 1973; Griffiths and Barker 2007; McGonagle et al. 2011).

The diagnosis of psoriasis and PsA is primarily based on clinical assessment of the patient's symptoms due to the lack of molecular biomarkers at early stages of the disease (Villanova et al. 2013). The evaluation of skin lesion severity poses an additional challenge, and different measures have been implemented for criteria unification. The Psoriasis Area and Severity Index (PASI) is the most widely quantitative rating score of skin lesion severity in research and clinical trials (Fredriksson and Pettersson 1978; Finlay 2005). PASI quantifies the lesional burden by body part based on area of affected surface and the severity of erythema, induration and scale at each location (Table 1.1). Disease is considered mild for PASI scores below 7 and is classified as moderate-to-severe for PASI scores between 7 to 12, depending on the study (Finlay 2005; Schmitt and Wozel 2005; Langewouters et al. 2008).

 To diagnose PsA, modified Moll and Wright criteria known as Classification Criteria for Psoriatic Arthritis (CASPAR) are most widely used (Taylor et al. 2006). A positive diagnosis based on CASPAR requires the presence of inflammatory arthritis, enthesitis, and/or spondylitis and three points from a list of associated elements. In terms of disease activity and treatment efficacy, the PsA Response Criteria (PsARC) is the preferred measure (Mease 2011; Clegg et al. 1996). PsARC considers the number of tender joints (TJC) and swollen

## Introduction

---

PASI	Description
Body location	Head and neck, upper limbs, trunk and lower limbs
Clinical signs	Redness, thickness and scaling
Severity scale	Absent, mild, moderate, severe or very severe
Affected area (%)	0, 1-9, 10-29, 30-49, 50-69, 70-89 or 90-100

**Table 1.1: Variables and scoring used in the Psoriasis Area and Severity Index (PASI).** For each of the locations the test quantifies the percentage of affected area and the severity of those three clinical signs (redness, thickness and scaling). The percentage of affected area is scored in a scale 1 to 6 (1=1-9%; 2=10-29%; 3=30-49%; 4=50-69%; 5=70-89%; 6=90-100%) and the severity of the three clinical signs in a scale from 0 to 4 (from none to maximum). A combined score for each of the body regions is calculated as the sum of the clinical signs severity scores for that region multiplied by score of that percentage affected area and the proportion of body surface represented by that body region (0.1 for head and neck, 0.2 for upper limbs, 0.3 for trunk and 0.4 for lower limbs). The final PASI score is the addition of each of those scores for each body region. PASI ranges from 0 (no disease) to 72 (maximal disease severity).

joints (SJC) over 68 and 66, respectively, as well as patient and physician global assessment of the individual's general health based on a short questionnaire (Table 1.2).

### 1.2.2 Aetiology of psoriasis and PsA

Psoriasis and PsA are chronic inflammatory diseases characterised by a dysregulated immune response ~~initiated~~ as the result of genetic predisposition and exposure to ~~particular~~ environmental cues (Figure 1.1). The origin of both pathologies, as well as the connection between skin and joint inflammation, still remain controversial.

#### Environmental factors and disease

A variety of exposures are proposed as risk factors for the development and worsening of psoriasis and PsA. A wide range of drugs including anti-depressants, anti-hypertensives and anti-cytokine therapies have been associated

## Introduction

---

PsARC	Description
TJC68	Number of tender joints over 68
SJC66	Number of swollen joints over 66
Patients global health assessment	Evaluation of the patient's health by the patient (scale 0 to 5)
Physician global health assessment	Evaluation of the patient's health by the physician (scale 0 to 5)

**Table 1.2: Variables and scoring used in the Psoriatic Arthritis Response Criteria (PsARC).** The patient's global health assessment by the patient and the physician is scored using a 5-point Likert scale, where 0 corresponds to very good, no symptoms and 5 corresponds to very poor and severe symptoms. When used to evaluate overall improvement after 12 weeks of treatment, improvement in at least two of the four variables evaluated (one of which must be TJC or SJC score) with no worsening of any criteria is required.

with initiation, exacerbation and worsening of psoriasis (Kim et al. 2010).

Bacterial and viral infections are associated with triggering and exacerbation of psoriasis, notably guttate psoriasis after group C *Streptococcus* throat infection as well as human immunodeficiency virus (HIV) infection (Gudjonsson and Karason 2003; Valdimarsson and Thorleifsdottir 2009; Diluvio et al. 2006).

~~In PsA, statistical association with antibody production against *Streptococcus pyogenes*, *Yersinia enterocolitica*, *Chlamydophila psittaci* and HIV have also been reported (Thrastardottir and international 2018). Recent studies have also observed perturbation in the composition of the gut and skin microbiota of psoriasis and PsA patients (Eppinga and rheumatology 2014; Yan et al. 2017),~~

Physical trauma and mechanical stress can also trigger the appearance of skin lesions and digit joint inflammation (Weiss et al. 2002; Nestle et al. 2009). Increased risk of PsA onset amongst psoriasis patients was indeed associated with lifting cumulative heavy loads as well as with several types of injuries and infections that require treatment with antibiotics (Eder et al. 2011). Smoking has been the most confidently associated ~~with an odds ratio (OR) of 1.78 (95%~~

## **Introduction**

---

~~CI 1.52–2.06) for psoriasis, in particular palmoplantar pustulosis (Armstrong et al. 2014). Psoriasis has also shown association with obesity, alcohol dependency, vitamin D deficiency and stress, but evidence remains controversial (Meglio et al. 2014).~~

## **Histopathological alterations in skin and joints**

The epidermis is the most external compartment of the skin, comprising approximately 90% keratinocytes and organised in a layer-like structure that self-renews in an spatial and time-dependent manner (Wikramanayake et al. 2014). Keratinocyte differentiation is associated with changes in morphology, replication ability and keratin composition of the intracellular matrix. In the context of psoriasis, impaired epidermis cell renewal leads to histological alterations and lesion development. Importantly, keratinocytes undergo upregulation in proliferation rate (hyperplasia) that causes aberrant cell differentiation (parakeratosis), thickening of the epidermis and subsequent scale formation (Ruchusatsawat et al. 2011). Concomitantly, inflammation causes immune cell infiltration and hypervascularisation of the lesion driven by upregulation in the expression of angiogenic factors and activation of the endothelium (Perera et al. 2012).

In PsA, the affected joint shows a wide range of histological changes (Haddad and Chandran 2013). One of the most common structural changes is arthritis caused by the swelling and inflammation of the joints (Schett et al. 2011). As a result of this inflammation, alterations in bone remodeling lead to osteolysis with subsequent bone resorption and erosion at the affected joints (Mensah et al. 2008). Bone erosion is also the main histopathological process driving dactylitis, where bone lysis resolves in shortening of the digits (Gladman et al. 2005). Moreover, 35% of PsA patients also undergo inflammation of the connective tissue at the insertion of tendons or ligaments, a phenomenon known

## **Introduction**

---

as enthesitis (McGonagle et al. 2011; Polachek et al. 2017). The inflammatory environment at the entheses favours bony spurs formation along the insertion sites, similar to RA, causing structural debilitation of the joints (Benjamin and McGonagle 2009; Finzel et al. 2014).

### **Dysregulation of the innate and adaptive immune response**

The dysregulated immune response in psoriasis and PsA is the result of the interaction between innate and adaptive immune cells through feedback loops and a complex cytokine milieu (Figure 1.1). Interferon (IFN)- $\alpha$  and  $\gamma$  are innate immune cytokines involved in disease initiation and mainly produced by circulating plasmacytoid dendritic cells (pDCs) and myeloid DC (mDCs), respectively, as well as by T cells in lesional skin (Leanne et al. 2009; Perera et al. 2012; Hijnen et al. 2013). Increased mRNA levels for both IFNs have been detected in skin plaques and shown to contribute to lymphocyte recruitment and maintenance of DC activation (Schmid et al. 1994). Tumour necrosis factor (TNF)- $\alpha$  is another key cytokine involved in the dysregulated innate immune response observed in psoriasis and PsA. TNF- $\alpha$  is produced by activated keratinocytes, mast cells, natural killer (NK) cells and also adaptive immune cell types, including T helper (Th)/CD4 $^{+}$  cells activated Th-1 and Th-17 subsets infiltrate skin lesions and inflamed joints (Perera et al. 2012; Lizzul et al. 2005). TNF- $\alpha$  causes activation of the nuclear factor kappa-light-chain-enhancer of activated B cells (NF- $\kappa$ B), a master transcriptional regulator which induces expression of pro-inflammatory cytokines, antiapoptotic genes and genes involved in maintenance of chronic inflammation (Lizzul et al. 2005; Johansen et al. 2004). Moreover, TNF- $\alpha$  has a prominent role in bone turnover and bone remodeling, key histopathological features of PsA (Mensah et al. 2008).

Interleukin-23 (IL-23) and interleukine-17 (IL-17) constitute a link between the innate and adaptive immunity as well as a key loop for the perpetuation of

## **Introduction**

---

the psoriasis and PsA inflammatory response. IL-23 is an innate immune cytokine mainly produced by the mDCs and macrophages in inflamed skin and to a lesser degree by psoriatic keratinocytes (Lee et al. 2004; Li et al. 2018). IL-23 ~~exerts its function through binding~~ to the IL-23 receptor (IL23R), highly expressed by the lesion-resident DCs and T cells and also by circulating CD4<sup>+</sup> (Tonel et al. 2010). In psoriasis, IL-23 mediates the pathogenic loop between activated keratinocytes and T cells, where activation of the IL-23 pathway ~~importantly~~ leads to Th-17 cell differentiation and increased IL-17 cytokine levels as a result of NF-κB activation (McGeachy et al. 2009). IL-17 signalling maintains the Th-17 immune ~~mediated~~ response through recruitment and activation of neutrophils, induction of pro-inflammatory cytokines, including interleukine-1 $\beta$  (IL-1 $\beta$ ) and interleukine-6 (IL-6), and sustained KCs activation (Doyle and Arthritis 2012).

More recently, interleukin 22 (IL-22) has gained relevance as mediator of dysregulated crosstalk between the innate and adaptive immune response. IL-22 levels are increased in the skin lesions and plasma of psoriatic patients and is mainly produced by a subset of CD4<sup>+</sup> cells known as Th-22 (Wolk et al. 2006). ~~IL-22 contributes to some of the histological changes in skin as well as to antimicrobial peptides (AMPs) production by keratinocytes (Eyerich et al. 2009).~~

### **1.2.3 Cell types involved in psoriasis and PsA pathogenesis**

Psoriasis and PsA are complex dynamic pathophysiological processes, and the understanding of the relative importance of different cell types at different disease stages still remains challenging.

**T cells.** T lymphocytes have been considered the most relevant cell types in the initiation and maintenance of psoriasis and PsA. Skin-resident memory T cells have been demonstrated to have a key role in psoriatic lesion development in mice models (Boyman et al. 2004). In human case reports,  bone marrow transplantation has shown to cause initiation or termination of psoriasis

## **Introduction**

---

(Gardembas 1990; Eedy et al. 1990). *In vivo* studies demonstrated that transition to psoriatic lesions following engrafted human pre-lesional skin in immune-deficient mice was only dependent on T cells requiring injection of autologous activated CD4<sup>+</sup> not CD8<sup>+</sup> cells (Wrone-Smith and Nickoloff 1996). Nevertheless, preferential migration into the epidermis and clonal populations T cells have only been isolated for CD8<sup>+</sup> cells (Wrone-Smith and Nickoloff 1996; Chang et al. 1994). In psoriasis and PsA, IL-23 together with other cytokines, including IL-1 $\beta$  and IL6, induce activation and differentiation of naïve CD4<sup>+</sup> and CD8<sup>+</sup> into pathogenic Th-17 and Tc17 cells producing IL-17 (Weaver et al. 2007). IL-17<sup>+</sup> CD8<sup>+</sup> cells have been found in psoriatic skin and are enriched in PsA synovial fluid when compared to peripheral blood, showing correlation with markers of inflammation and structural changes in the joint (Menon et al. 2014; Ortega et al. 2009). Likewise, Th-17 infiltrated cells have been found in the epidermis of psoriatic lesions (Lowes et al. 2008; Pène et al. 2008). Additionally, IL-12 and IFN- $\gamma$  lead to expansion of Th-1 and Tc-1 cells, which contribute to perpetuation of the immune response through IFN $\gamma$  and IL-18 production in psoriasis and PsA (Austin et al. 1999; Perera et al. 2012).

**Keratinocytes.** In psoriasis keratinocytes have ~~demonstrated~~ a role as a bridge between the innate and adaptive immune response. Karatinocytes have ~~shown~~ ability to act as immune sentinels through MHC-class II antigen presentation to CD4<sup>+</sup> and T cytotoxic(Tc)/CD8<sup>+</sup> cells (Black and ArdernJones 2007). Upon damage by environmental triggers keratinocytes release cationic AMP LL-37 and self-DNA/RNA that form a complex which acts as an antigen for skin-resident DCs activation and initiation of ~~the~~ inflammatory response (Lande et al. 2007). Moreover, pro-inflammatory cytokines such as IL-17A or IL-22 also ~~activate keratinocytes inducing proliferation~~ and in turn production of cytokines, including IL-1, IL-6 and TNF- $\alpha$ , and chemokines (e.g CXCL1, CXCL2, CXCL5, CXCL8 and CCL20) leading to recruitment of neutrophils and T cell to the site of

## **Introduction**

---

inflammation (Feldmeyer et al. 2007; Arend et al. 2008; Nestle et al. 2009; Nestle et al. 2005). Keratinocytes also release vein endothelial growth factor (VEGF), a pro-angiogenic factor that activates endothelial cells and leads to pathogenic angiogenesis (Xia et al. 2003). The relevance of keratinocytes in the dysregulated immune response in psoriasis is further reinforced by the genetic association with ~~genetic~~ variants located at <sup>at</sup> keratinocyte-specific genes from the late cornified envelope (LCE) family (Tsoi et al. 2012).

**Dendritic cells.** mDCs and pDCs are important innate immune cells in initiation of the psoriasis dysregulated immune response through antigen presentation and T cell activation (Mahil et al. 2016). pDCs are circulating professional antigen presentation cells (APCs) that on activation through Toll-like receptor (TLR)7/9 by the keratinocytes self-DNA and LL-37 complex ~~and~~ infiltrate into the lesional and uninvolved dermis of psoriasis patients (Nestle et al. 2005; Lande et al. 2007). In contrast, quiescent mDCs are epidermal resident cells that undergo maturation in presence of the IFN- $\alpha$  secreted by pDCs, expanding up to 30-fold in lesional skin (Zaba2007). Activated mDCs mediate the Th-1 and Th-17 response as well as perpetuation of KC activation through IL-23 production (Lee et al. 2004).

**Monocytes and macrophages.** Resident macrophages in the healthy dermis undergo a 3-fold increase in psoriatic skin lesions and contribute to disease development through TNF $\alpha$  production (Perera et al. 2012; Mahil et al. 2016). Similarly, mouse models for chronic psoriasiform skin inflammation have demonstrated macrophage migration into affected skin and how production of TNF- $\alpha$  contributes to maintenance of skin lesions (Stratis et al. 2006; Wang et al. 2006). Initial studies showed greater phagocytic and bactericidal activity in monocytes from psoriasis patients compared to those from healthy individuals (M et al. 1979). Additionally, increased circulating intermediate monocytes ( $CD14^{high}$   $CD16^{high}$ ) and monocyte aggregation was also observed

## Introduction

---

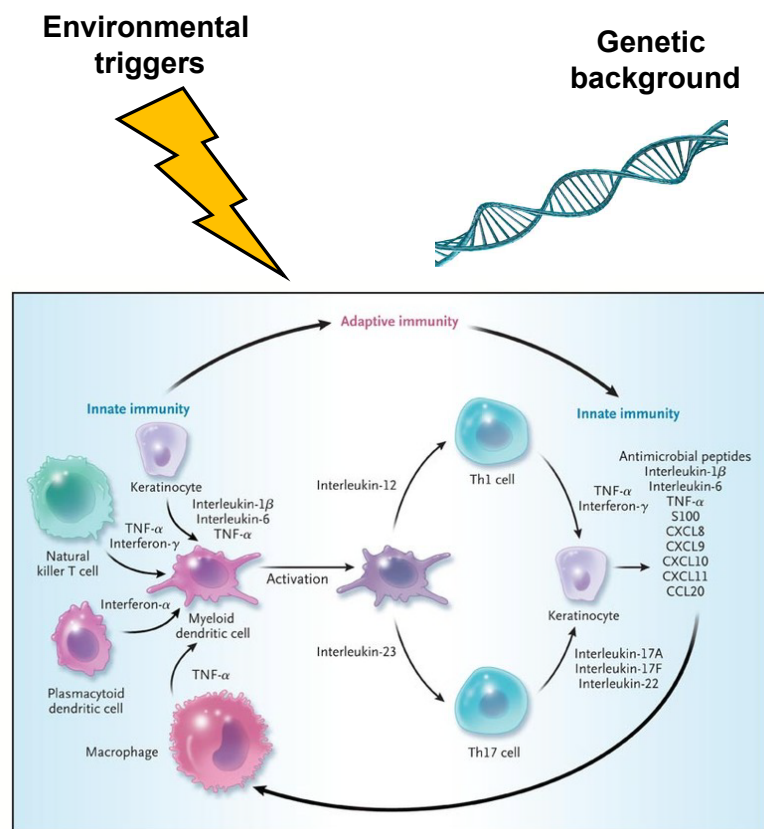


**Figure 1.1: Environmental triggers and genetic predisposition leading to psoriasis and PsA (adapted from Nestle *et al.*, 2009).** The main cell types, cytokines and chemokines involved in the dysregulated innate and adaptive immune response found in these conditions are shown.

## **Introduction**

---

in psoriasis patients, resulting in enhanced platelet activation and angiogenesis (**Golden2015**). In PsA synovial membranes, the levels of monocytes/macrophage metalloproteinases responsible for bone erosion through differentiation into osteoclasts have been found to be similar to those found in RA joints (Hitchon et al. 2002).

**Natural killer.** NK cells are lymphoid-derived innate immune cells identified as CD3<sup>-</sup> CD56<sup>+</sup>. The majority of circulating NK cells (90%) are CD56<sup>dim</sup> and show strong cytotoxicity driven by high content of perforin and granzymes (**Mandal2014**). In contrast, CD56<sup>bright</sup> commonly infiltrate into second lymph organs and other tissues, where they are activated by DCs and produce immunoregulatory cytokines such as IFN- $\gamma$ , promoting Th-1 expansion and the adaptive immune response (Martin-Fontech et al. 2004; Ferlazzo et al. 2004). In psoriasis, significant increase of cells expressing NK markers have been found in lesional compared to uninvolved skin (**Cameron2002**; Ottaviani et al. 2006). Expansion of NK CD3<sup>-</sup> CD56<sup>bright</sup> cells in inflamed joints was observed in a cohort including RA, PsA and AS patients (Dalbeth and Callan 2002). Moreover, NK cells in RA have shown to trigger osteoclastogenesis and bone destruction in vitro and in mice models (**Soderstrom2010**) . Amongst the target cells receptors regulating NK cells function, the killer immunoglobulin-like receptor (KIR) family includes activating and inhibitory members. The inhibitory receptor KIR2DL1 and the activatory receptor KIR2DS1 recognise HLA- Cw\*06:02, strongly associated with psoriasis and PsA (Tobin et al. 2011). Interestingly, gene based studies have shown genetic variability in *KIR2DS1* gene, associated with psoriasis and PsA susceptibility ~~and also reported for~~ AS and RA (**Luszczek 2004**; Williams et al. 2005; Carter et al. 2007; Yen et al. 2001).

**Neutrophils.** Neutrophils are implicated in disease initiation through their ability to form neutrophil extracellular traps (NET) that contain host DNA and LL-37 (Hu et al. 2016). Evidence of increased NET formation in peripheral blood

## **Introduction**

---

and lesional skin of psoriasis patients has been found and seem to contribute to pDC and CD4<sup>+</sup> T cell activation (Hu et al. 2016). Neutrophils have also been identified in recent studies as one of the main sources of IL-17 production in the skin lesions and release a wide range of proteases, some of which induce keratinocyte proliferation (Mahil2006; Lin et al. 2011).

**B cells.** The role of B cells in the pathophysiology of psoriasis and PsA has remained unclear. B cells are mainly known as key players of the humoral adaptive immune response through antibody production. However, they also act as APCs, regulate CD4<sup>+</sup> activation and differentiation into Th effector cells by providing co-estimulatory signals and actively secrete cytokines (Bouaziz et al. 2007; Constant et al. 1995; Harris et al. 2000; Linton et al. 2003). Recent studies in the imiquimod-induced psoriasis mice model have demonstrated more severe inflammation in CD19<sup>-/-</sup> mice a regulatory B cell subset producing IL 10 (Yanaba et al. 2013; Alrefai et al. 2016). Furthermore, different B cell subsets have been found in PBMCs from psoriasis patients and in lesional skin and correlation with disease severity has been identified for some clinical subtypes (Lu et al. 2016).

### **1.2.4 Therapeutic intervention**

Psoriasis and PsA are currently incurable diseases, with treatments available focused on alleviating symptoms. For instance, topical therapies are advocated in cases of mild-to-moderate psoriasis, including emollients and short-term corticosteroids (Menter et al. 2009). Other treatments may be used in combination with corticosteroids, such as ultraviolet (UV) light therapy and vitamin D analogues, directed to inhibit T-cell and KC proliferation and stimulate KC differentiation (Rizova and Coroller 2001). In the case of PsA, for patients presenting with swelling of two or fewer joints, nonsteroidal anti-inflammatory drugs (NSAID) to control the inflammatory symptoms and intra-

## **Introduction**

---

articular injection of glucocorticosteroids together with joint aspiration are used to reduce pain and inflammation (Coates et al. 2016a).

Treatment of most forms of PsA and moderate-to-severe psoriasis require the use of systemic therapies. More severe forms of PsA require disease-modifying antirheumatic drugs (DMARDs) including ~~the~~ antagonist of folic acid methotrexate (MTX) and ~~the~~ phosphodiesterase 4 inhibitor Apremilast, which act as immunosuppressors of activated T cells and cytokine production, respectively (Keating 2017; Schmitt and of 2014; Gossec et al. 2016; Polachek et al. 2017). ~~Remarkably,~~ biologic systemic agents represent the most specific treatment option for severe psoriasis and PsA notably TNF-alpha inhibitors (TNFi). Three TNFi have been approved for the treatment of psoriasis: etanercept, infliximab and adalimumab (Ahil2016). In addition, certolizumab pegol and golimumab are often used in the management of PsA (Coates et al. 2016b). However, side effects such as increased risk of infection or reactivation of latent infections have been identified  (Nickoloff and Nestle 2004). Moreover, ~~between 20 to 50%~~ of patients fail to respond to the first TNFi administrated, requiring switching to an alternative TNFi (Abramson and Khattri 2016). New biologic therapies have been developed to target other key cytokines, such as IL-12, IL-23 (ustekinumab) or IL-17 (secukinumab and ixekizumab), which represent a substantial advance in treating patients failing to respond to TNFi Mahil2016, Coates2016a.

## **1.3 Genetics of psoriasis and psoriatic arthritis**

### **1.3.1 Heritability**

The risk of developing psoriasis and PsA is not only influenced by environmental conditions but also by the genetic background of each individual. The concordance of psoriasis is greater in monozygotic (33-55%) compared to dizygotic twins (13-21%), giving a heritability estimate of 80%, while no

## **Introduction**

---

difference in concordance is reported for PsA, probably due to lack of statistical power and appropriate diagnosis (Farber et al. 1974; Duffy et al. 1993; Pedersen et al. 2008). In the general population, approximately 40% of patients with psoriasis or PsA have a family history in first degree relatives (Gladman et al. 1986). Interestingly, the recurrence rate in first-degree relatives has been shown to be greater in PsA (40%) compared to psoriasis (8%) in a study in the Icelandic population (Chandran et al. 2009). ~~Altogether, this may suggest differences in the heritability between the two phenotypes and a stronger genetic contribution in PsA.~~

### **~~1.3.2 Non GWAS and linkage studies~~**

Linkage analysis of psoriasis and PsA in family pedigrees presenting an autosomal dominant condition yielded nine psoriasis susceptibility loci (PSORS1-9) with PSORS1 showing the strongest genetic association (**Consortium2003**; Capon 2017). PSORS1 locus lies within the MHC class I region, initially associated with psoriasis susceptibility in serological studies (Russell et al. 1972; Tiilikainen et al. 1980). Rare highly penetrant mutations have also been identified for two genes within PSORS2 (17q25): zinc finger protein 750 (ZNF750) and caspase domain family member 14 (CARD14), with common variants in CARD14 also reported in psoriasis and PsA patients, implicating genetic variation in this gene in Mendelian and multi-factorial forms of disease (Tomfohrde et al. 1994; Jordan et al. 2012b; Jordan et al. 2012a; Tsoi et al. 2012). Nevertheless, the inability of independent studies to reproduce these results for regions other than PSOR1, 2 and 4, highlights the limitations of linkage studies to understand the genetics of complex diseases (Capon 2017).

## **Introduction**

---

### **1.3.3 Genome-wide association studies**

Genome-wide association studies (GWAS) have benefited from the understanding of common single base-pair changes known as single nucleotide polymorphisms (SNPs) in different populations and are focused on identifying disease-associated common SNPs (with minor allele frequency (MAF)  $\geq 1$  to 5% ) showing differences in allele frequency between patients and controls (Ku et al. 2010). GWAS are thus based on the hypothesis that complex diseases are caused by the interaction of multiple common variants, which association with disease have only modest effect size with OR between 1.2 and 2 (Schork et al. 2009; Cui et al. 2010). The genotyped SNPs in GWAS are solely used a proxy for the disease causative variant, for instance non-genotyped SNPs or other type of genetic variability such as copy number variants (CNVs) (Hirschhorn 2005; Ku et al. 2010).

The first psoriasis and PsA GWAS were published in 2007 and a total of 63 genetic associations have been identified at genome-wide significance ( $p\text{val} \leq 5 \times 10^{-8}$ ) up to date (Table ??), explaining 28% of the psoriasis and PsA heritability (Tsoi et al. 2017). The majority of studies have been performed in Caucasian European or North American cohorts but increasing numbers of GWAS in large Chinese cohorts are also being published (Zhang et al. 2009; Sun et al. 2010; Yin et al. 2015). Early GWAS with moderate power confirmed association with loci overlapping the PSOR1 and PSOR2 genomic regions identified by linkage studies (Cargill et al. 2007; Strange et al. 2010). HLA-C has been consistently identified as the most significant locus with the greatest effect size. Additional MHC-I and MHC-II associations with disease risk have been identified for HLA-A, HLA-B and HLA-DQA1 through step-wise conditional analysis(Okada et al. 2014).

The informativeness of GWAS was significantly enhanced with the use of the Immunochip genotyping chip, which covers 186 immune relevant loci

## **Introduction**

---

identified in previous GWAS studies across different inflammatory diseases at a greater genotyping density (Tsoi et al. 2012). The psoriasis Immunochip study uncovered 15 new associations, including the PSOR4 *CARD14* and also included meta-analysis with the largest available psoriasis cohorts at the time (Tsoi et al. 2012). This meta-analysis has since been further expanded yielding 16 additional associations and ~~reinforcing the importance of NFκB and cytotoxicity pathways in disease pathophysiology~~ (Tsoi et al. 2015; Tsoi et al. 2017). Meta-analysis of GWAS across Caucasian and Chinese populations revealed 4 new associations as well as population-specific effect or allelic heterogeneity in 11 loci, including MHC-I genes, demonstrating the value of this trans-ethnic approach to further understand the heterogeneous genetic susceptibility to psoriasis ~~in different populations~~ (Yin et al. 2015).

Conducting independent GWAS for psoriasis and PsA has shown differences in HLA-C and HLA-B alleles frequencies. Interestingly, comparative higher association with HLA-B has been found in PsA individuals compared to psoriasis patients not developing joint inflammation (Winchester et al. 2012; Okada et al. 2014). GWAS association for previously identified psoriasis loci such as *IFNLR1*, *IFIH1* and *NFKBIA* were also found genome-wide significant when using only PsA cases, and PsA-specific independent signals for *IL23R* and *TNFAIP3* showing stronger association when compared to psoriasis patients not developing joint inflammation were also found (Ellinghaus et al. 2010; Stuart et al. 2015). Furthermore, PsA GWAS using Immunochip has also revealed a specific association in chromosome 5q31 not reported previously (Bowes et al. 2015).

## Introduction

---

**Table 1.3: Main GWAS studies in psoriasis and PsA.** Summary table describing the most relevant psoriasis and PsA GWAS studies. Information regarding sample size, patients phenotypes and the main reported associations in each study is included. The Ellinghaus *et al.*, 2010 and the Stuart *et al.*, 2015 studies included stratified association analysis of psoriasis and PsA independently. WA=white American; Eur=European; \* Meta-analysis performed.

Study	Etnicity	Sample size (Cases/Controls)	Phenotype	Main associations (putative genes)
(Cargill et al. 2007)	WA	1,446/1,432	Psoriasis, PsA	HLA-C (PSOR1) and <i>IL-12B</i>
(Nair et al. 2009)	Eur	1,409/1,436	Psoriasis, PsA	<i>IL-23A</i> , <i>IL23R</i> , <i>IL-12B</i> , <i>TNIP1</i> , <i>TNFIP3</i> , <i>IL-4</i> and <i>IL-13</i>
(Stuart et al. 2010)	WA, Eur	1,831/2,546	Psoriasis, PsA	<i>NOS2</i> , <i>FBXL19</i> , <i>PSMA6</i> - <i>NFKBIA</i>
(Ellinghaus et al. 2010)	German	472/1,146	Psoriasis	<i>TRAF3IP2</i>
(Strange et al. 2010)	Eur	2,622/5,667	Psoriasis, PsA	<i>LCE3D</i> (PSOR2), <i>IL28RA</i> , <i>REL</i> , <i>IFIH1</i> , <i>ERAP1</i> , <i>TYK2</i> and <i>HLA-C/ERAP1</i>
(Zhang et al. 2008)	Chinese	1,139/1,132	Psoriasis	(type <i>LCE</i> gene family and <i>IL-12B</i> ) I)

## Introduction

---

(Sun et al. 2010)	Chinese	8,312/12,919	Psoriasis, PsA	<i>ERAP1</i> , <i>PTTG1</i> , <i>CSMD1</i> , <i>GJB2</i> , <i>SERPINB8</i> , <i>ZNF816A</i>
(Tsoi et al. 2012)†	WA, Eur	10,588/22,806	Psoriasis, PsA	<i>CARDI4</i> ( <i>PSOR4</i> ), <i>RUNX3</i> , <i>B3GNT2</i> , <i>ELMO1</i> , <i>STAT3</i>
(Tsoi et al. 2015)†	WA, Eur	15,000/27,000	Psoriasis, PsA	1q31.1, 5p13.1, <i>PLCL2</i> , <i>NFKBIZ</i> , <i>CAMK2G</i>
(Bowes et al. 2015)	British, Australians	Irish, 1,962/8,923	PsA	5q31 PsA-specific
(Stuart et al. 2015)	WA and Eur	1,430/1,417	Psoriasis, PsA	PsA-specific secondary signals (main text), new psoriasis-specific ( <i>CDKAL1</i> and <i>CAMK2G</i> ), stronger psoriasis <i>LCE</i> association
(Yin et al. 2015)	WA, Eur, Asian	15,369/19,517	Psoriasis, PsA	<i>LOC144817</i> , <i>COG6</i> , <i>RUNX1</i> and <i>TP63</i> ; signals with ethnic heterogeneity
(Tsoi et al. 2017)†	WA, Eur	19,032/39,498	Psoriasis, PsA	<i>CHUK</i> , <i>IKBKE</i> , <i>FASLG</i> , <i>KLRK1</i> , <i>PTEN</i>

## **Introduction**

---

Overall, GWAS studies have demonstrated shared and distinct genetic architectures for psoriasis and PsA. It is important to take into account that these results are affected by imprecise phenotyping of cases, which is one of the many challenges in the systematic comparison between the two diseases.

### **1.3.4 Relevance of non-coding variants in disease susceptibility**

Approximately 88% of all GWAS associations map within non-coding regions (Welter et al. 2013). Psoriasis exome association studies in Chinese and Caucasian populations have increased the number of coding variants with putative effects on the protein structure (Tang et al. 2014; Zuo et al. 2015; Dand et al. 2017). These studies have confirmed some previously identified missense associations in *CARD14* and *ERAP1*, revealed new common coding variants at these previously associated loci and identified rare protective missense changes, for example in the *TYK2* gene (Tang et al. 2014; Dand et al. 2017). Nevertheless, results from extensive exome studies suggest that non-synonymous SNPs have a limited contribution to the overall genetic risk of psoriasis compared to non-coding variants (Tang et al. 2014).

The association of non coding variants with disease can be explained by their ability to regulate gene expression in a cell and context specific manner (Fairfax et al. 2012). These variants can be located in different regulatory elements, including enhancers, silencers, promoters and the 5' and 3' untranslated region (UTR) of genes (Ward and Kellis 2012). Non-coding GWAS variants can alter the expression of target genes through different mechanisms including changes in chromatin accessibility, histone modifications, protein binding such as transcription factors (TFs), DNA methylation and binding of non-coding RNA molecules (Knight 2014) (1.4.2).

Identification of the target gene regulated by non-coding variants represents a challenge in the field of functional genetics. This limitation can

## **Introduction**

---

be partially addressed by conducting expression quantitative trait loci (eQTL) analysis, which identifies genome-wide statistical associations between gene transcript levels and SNPs in *cis* (<1Mb) or *trans* to the gene. For instance, in T2D ~~an~~ such approach revealed a *cis*-eQTL involving the TF *KLF4* and a haplotype of non-coding GWAS SNPs located 14kb up-stream (Small et al. 2011). Moreover, this haplotype also showed association with genes in *trans*, highlighting downstream targets regulated by KLF4. Nonetheless, eQTL mapping alone only provides statistical suggestion of transcriptomic regulation, and additional functional assays, such as chromatin conformation and genome editing, are required to demonstrate causality (Edwards et al. 2013).

### **1.3.5 The role of GWAS in highlighting immune-relevant cell types and pathways**

GWAS represent a biologically unbiased approach to shed ~~some~~ light on pathophysiological ~~relevant~~ cell types and molecular pathways associated with disease. ~~GWAS have underlined some of the most important cell types for which genetic variation may be functionally relevant~~ by overlapping them with epigenetic features mapped in cell lines or primary cells isolated from healthy control (Farh et al. 2015). In psoriasis and PsA, ~~enrichment of associated variants has been found for regulatory elements~~ in several cell types (e.g Th-1 and Th-17 cells) and the majority of GWAS risk loci have been linked to genes that belong to a limited number of pathways, as detailed below (Tsoi et al. 2017; Capon 2017). ~~A number of these candidate genes are selected by proximity to the associated variant and genes unknown to be regulated at a distance fail to be included~~ a limitation when interpreting GWAS results. Additional criteria ~~has~~ also been used to link non-coding GWAS variants to a target gene, including LD with a deleterious variant, direct functional characterisation of the regulatory element and/or genetic variant or association of gene expression with the genotype of the

## **Introduction**

---

GWAS lead SNP (Capon et al. 2008; Tsoi et al. 2012; Tsoi et al. 2017; Meglio et al. 2011).

Systematic comparison of ~~the~~ genetic architecture across different conditions has revealed associated psoriasis and PsA risk loci shared, in the same or opposite directions, with AS, Crohns disease (CD), multiple sclerosis (MS), RA or type 1 diabetes (T1D) (<https://www.immunobase.org>). This has also supported the use of therapeutic interventions such as anti- IL-23 and anti- IL-17 antibodies across a number of immune-related phenotypes including psoriasis, PsA, AS and IBD, amongst others (Visscher et al. 2017).

## **Antigen presentation**

In psoriasis *HLA-Cw*\*0602 represents the strongest GWAS association, also shared with other diseases such as hepatitis C, primary sclerosing cholangitis and Graves disease (Blais et al. 2011). No differences at the transcript level have been identified for HLA-Cw\*0602 when comparing psoriasis patients versus controls, suggesting alterations in antigen presentation as the mechanism ~~explaining disease association~~ (Hundhausen et al. 2012). The relevance of antigen presentation in psoriasis and PsA has been reinforced by the GWAS association of the endoplasmic reticulum aminopeptidase 1 *ERAP1* gene, involved in the trimming of peptide antigens. Moreover, ~~GWAS studies identified that~~ *ERAP1* was associated with psoriasis and PsA only in individuals carrying one copy of the rs10484554 *HLA-C* risk allele (Strange et al. 2010). ~~These epistatic phenomena,~~ whereby association of one gene is dependent on the presence of another, ~~have~~ also been reported between *HLA-B*\*27 and *ERAP1* in AS (Cortes2015b; Evans et al. 2011). Interestingly, the *ERAP1* haplotype associated with increased risk of SpA increases *ERAP1* expression and also alters splicing, resulting in an *ERAP1* protein isoform with increased activity in monocyte-derived DCs and lymphoblastoid B cell lines (Constatino2015; Hanson et al. 2018).

## **Introduction**

---

### **Skin barrier**

GWAS have highlighted keratinocyte-specific genes such ~~the previously mentioned~~ *LCE* gene cluster and genes with a key role in skin biology such as *CARD-14*. ~~Further studies in the *PSORS2* region have revealed that~~ association with disease is driven by a deletion ~~in two of the genes within this family,~~ *LCE3B* and *LCE3C* (*LCE3C\_LCE3B\_del*) (Cid et al. 2009). Lack of *LCE3B* and *LCE3C* expression in psoriasis patients has been hypothesised to impair the repair following skin disruption, potentially facilitating microorganism infection and triggering a dysregulated immune response (Bergboer et al. 2011). Similarly to the *LCE* gene cluster, common and rare pathogenic mutations of the PSOR4 *CARD-14* gene lead to increased activation of NF- $\kappa$ B as well as overexpression of psoriasis pathophysiological relevant genes (including *IL-6* and *TNFA*) in keratinocyte cell lines (Jordan et al. 2012b).

### **NF- $\kappa$ B and TNF pathways**

The NF- $\kappa$ B pathway is involved in the regulation of the innate and adaptive immune response and NF- $\kappa$ B contributes to the development of many chronic inflammatory diseases (Liu et al. 2017). In fact, elevated levels of NF- $\kappa$ B are present in psoriatic lesional compared to uninvolved and normal skin (Lizzul et al. 2005).

Several psoriasis and PsA GWAS loci have been mapped to gene members of the NF- $\kappa$ B and TNF signalling pathways including *TNIP1*, *TNFAIP3*, *NFKBIA*, *REL*, *TRAF3IP2*, *CHUK*, *IKBKE* and *FASLG* (Huffmeier 2010; Nair et al. 2008; Ellinghaus et al. 2010; Wang et al. 2008; Idel et al. 2003; Bowes et al. 2012; Tsoi et al. 2017). For example, a haplotype including missense mutations and intronic variants in *TRAF3IP2* has been reported to drive psoriasis and PsA association by reducing its affinity for TRAF interacting proteins and concomitantly altering NF- $\kappa$ B activation and the IL-17/IL-23 axis (Huffmeier 2010; Ellinghaus et al.

## **Introduction**

---

2010). In addition, exome-sequencing studies have identified variants with predicted influence on protein structure and function at *TNFSF15*, a TNF ligand family protein which regulates NF- $\kappa$ B and MAP kinases activation in endothelial cells (Dand et al. 2017; Wang et al. 2014).

### **Type I IFN and innate host defense**

Members of the type-I IFN signalling pathway have ~~also~~ been associated with psoriasis and PsA, highlighting ~~the role of~~ genes ~~contributing to the~~ host response to viruses and bacteria ~~in the disease pathophysiology~~. Exome-sequencing and GWAS have identified two independent protective missense mutations predicted to impair the catalytic activity of the Janus kinases (JAK) protein member TYK2, and thus the initiation of the IFN-I downstream inflammatory cascade in psoriasis and PsA (Strange et al. 2010; Tsoi et al. 2012; Dand et al. 2017). A JAK inhibitor approved for RA is currently undergoing clinical trials in psoriasis and PsA, alongside with development of more specific JAK inhibitors and drugs targeting ~~upstream type I IFN pathway members~~, such as *TLR7* and *TLR9* (Yogo et al. 2016; Baker and diseases 2017).

### **IL-17/IL-23 axis**

Together with the TNF pathway, the IL-17/IL-23 axis is the most common target of biological therapeutics. In fact, some studies have reported greater efficacy of individual IL-17A or IL-23 blockade compared to TNF inhibition in the treatment of psoriasis and PsA (Griffiths et al. 2015; Blauvelt et al. 2017). The cytokine IL-23 is formed of two subunits: IL-23A/p19 and IL-12B/p40. Transcriptional studies have shown increased levels of p40 and p19 in psoriasis lesional skin and a role ~~for~~ both subunits in abnormal KC differentiation (Zhu 2011; Lee et al. 2004). Psoriasis and PsA GWAS associations with *IL23R* ~~have been reported~~, including a protective two SNP haplotype shared with ~~CD~~ (Nair

## **Introduction**

---

et al. 2008; Strange et al. 2010; Tsoi et al. 2012). GWAS associations have also been established implicating *IL 23A* and *IL 12* (Cargill et al. 2007; Strange et al. 2010; Tsoi et al. 2012). Interestingly, an *IL-23* signal secondary to that reported by Tsoi *et al.*, 2012 has been specifically associated with PsA (Tsoi et al. 2012; Bowes et al. 2015). Regarding the genetics of the Th-17 pathway, its relevance is partly explained through the cross-talk with the IL-23 response, which mediates Th-17 cell differentiation and activation. Additionally, GWAS associations implicating TFs regulating Th-17 polarisation, such as *IRF4* and *STAT3*, have also been identified for psoriasis and PsA (Tsoi et al. 2012; Huber et al. 2008; Harris et al. 2007).

### **Genome-wide pathway enrichment analysis and intergenic regions**

New approaches using genetic association data have disclosed relevant biological processes by conducting genome-wide pathway analysis. In psoriasis, this has revealed association of novel processes, such as retinol metabolism, transport of inorganic ions and aminoacids and post-translational protein modifications (PTMs) (Aterido2015).

As previously mentioned, the majority of the non-coding GWAS associations are located in intergenic regions and often lack functional characterisation. Therefore these variants tend to be associated to the nearest gene but may occur in intergenic regions at a distance from any gene, including chr1p36.23, chr2p15 and chr9q31.2 in psoriasis and PsA. One of the most interesting regions the chr1p36.23, shared with UC and proximal to a number of gene candidates including *RERE*, *SLC45A1*, *ERRFI1* and *TNFRSF9* (Tsoi et al. 2012). Unpublished capture-HiC data using the immortalised keratinocyte cell line HaCaT has revealed interaction of SNPs in this locus with the promoter of the *ERRFI1* gene, an inhibitor of the epidermal growth factor receptor signalling required for normal keratinocyte proliferation (Ray-Jones et al. 2017).

## Introduction

---

### 1.3.6 Limitations and future of GWAS

GWAS have made a great contribution to our understanding of the genetic basis of complex diseases. However, this approach has a number of limitations ~~that need to be considered~~.

One ~~of the major limitations~~ is the challenge of fine-mapping due to linkage disequilibrium (LD). An association between a genetic locus and a trait does not reveal the causal variant, which could potentially be any of the highly correlated SNPs in the same LD block at the lead SNP. This can be addressed in part by dense genotyping, statistical fine-mapping methods and incorporation of epigenetic data while ultimately application of genome-wide editing may be needed to define the GWAS causal SNP.

Another concern is the missing heritability when that explained by the GWAS is compared to the estimated heritability from twin and family studies (Ku et al. 2010; Yang et al. 2010). Since complex traits are influenced by polygenic effects, where the genetic contribution is driven by multiple variants with small effect size, larger experimental cohorts have led to the discovery of new genome-wide significant associations (Visscher et al. 2017). For example, in human height, most of the missing heritability could be explained by GWAS associated variants with nominal significance that failed to pass the stringent threshold due to their small effect size (Yang et al. 2010).

Another source of unexplained heritability may be rare putative causal variants poorly tagged by common SNPs (Wray 2005). Such limitations have partly been overcome by improved genotyping arrays like Immunochip, which incorporates SNPs with MAF<1% (Cortes and Brown 2011). Moreover, exome studies have also demonstrated the contribution of coding and intronic rare variants (MAF<5%) in the genetic architecture of complex traits such as height or psoriasis (Marouli et al. 2017; Dand et al. 2017). In addition to rare variants, other sources of structural variation such as copy number variants

## **Introduction**

---

(CNVs), small (<1Kb) insertions/deletions (indels) and inversions could all contribute to missing heritability. Incorporation of new genotyping platforms has allowed ~~the~~ genome-wide identification of CNV while ~~the~~ accurate detection of translocations and inversions relies on the implementation of long read whole genome sequencing (WGS) technologies (Glessner et al. 2009; Marshall et al. 2017; Visscher et al. 2017). Lastly, the missing heritability may also be the consequence of the overestimated heritability in complex traits as the result of assuming additive genetic effect instead of epistatic interaction between the different associated loci (Zuk et al. 2012).

## **1.4 Functional interpretation of GWAS in complex diseases**

### **1.4.1 Overcoming the limitations of GWAS: post-GWAS studies**

GWAS report associations with disease for ~~a~~ particular locus but typically fail to identify the true causal variant(s) within the haplotype block, yielding a large number of SNPs in high LD with the lead variant (Edwards et al. 2013). Thus, refinement of the number of putative causal variants for each GWAS association is required previous to functional validation of their putative pathogenic effect ~~through molecular and cellular assays and *in vivo* models~~. Statistical fine-mapping partially overcomes some of the GWAS limitations by further refining the number of most likely causal variants ~~driving disease association~~ within each GWAS LD block. The integration of statistical fine-mapping with cell type and context specific epigenetic data, including chromatin accessibility, histone modifications and DNA methylation, can help to determine the chromatin state where the fine-mapped variants are located and its potential ~~in~~ regulating gene expression (Petronis 2010). Additionally, the incorporation of

## **Introduction**

---

gene expression, eQTL analysis and chromatin interaction data can establish a relationship between non-coding variants and putative gene targets.

### **1.4.2 Understanding the epigenetic landscape in complex diseases**

Epigenetic ~~modifications consist of heritable~~ changes in the phenotype and/or gene expression that do not involve changes in the DNA sequence (Feil and Fraga 2012). ~~These changes include a wide range of modification in the proteins which serve as scaffold for the DNA, known as histones, as well as DNA methylation and non coding RNAs.~~ Environmental and intrinsic factors can trigger changes in the epigenome that result in dysregulation of gene expression and, ~~consequently, in alteration of gene~~ function.

Genetic background can increase the predisposition to epigenetic changes ~~caused by extrinsic factors.~~ Studies have demonstrated differences in response to environmental factors by different mice breeds as well as greater differences in the epigenetic landscape between human dizygotic twins when compared to monozygotic (Pogribny et al. 2009; Kaminsky et al. 2009). Importantly, disease-associated GWAS variants have consistently shown enrichment for DNA regulatory elements, characterised by the combination of epigenetic marks, including accessible chromatin, histone modifications and DNA methylation (Trynka and Raychaudhuri 2013a; Trynka and Raychaudhuri 2013b; Gusev et al. 2014).

The plasticity of the epigenetic landscape is required for cell differentiation and identity and particularly important in the immune system to ensure adaptation and response to ~~different pathogen~~ infections (Yosef and Regev 2016). The role of cell type specificity in the epigenetic landscape has been demonstrated in eQTL studies, where 50 to 90% the genetic variants regulating gene expression are cell type and stimulus dependent (Dimas et al. 2009; Nica

## Introduction

---

et al. 2011; Fairfax et al. 2012; Fairfax et al. 2014; Raj et al. 2014; Naranbhai et al. 2015; Kasela et al. 2017). Recent methodological advances have made the personalised study and understanding of the epigenome possible by the implementation of low-cell-input high-throughput techniques coupled to next generation sequencing (NGS) (Schmidl 2016; Buenrostro et al. 2013; Oudelaar et al. 2017). Understanding of cell-to-cell epigenomic heterogeneity is also being addressed with single-cell methods and may help to elucidate the impact of genetic variability in regulation of gene expression and disease mechanisms (Buenrostro et al. 2015; Cusanovich et al. 2015; Rotem et al. 2015; Nagano et al. 2013; Smallwood et al. 2014).

### 1.4.3 The chromatin landscape

 In the cell nucleus, DNA is compacted into a highly organised structure known as chromatin. The nucleosome is the basic repeating unit of chromatin and is formed by a 147bp segment of DNA wrapped around an octameric core of histone proteins regularly spaced by 10bp of linker DNA (Luger et al. 1997). In general, highly compacted DNA will remain more inaccessible for the assembly of the transcriptional machinery, consequently preventing gene expression. Chromatin accessibility can be altered by PTM of the histone proteins that affects their affinity with the DNA within the nucleosome as well as the interaction between nucleosomes in the vicinity (Polach et al. 2000; Pepenella et al. 2014). Additionally, chromatin structure can also be influenced by adenosine triphosphate (ATP)-remodelling complexes that facilitate sliding of individual nucleosomes to neighboring DNA segments, increasing temporary chromatin accessibility at particular sites (Cosma et al. 1999). From the biochemical point of view, the signature of chromatin accessibility, histone modifications, transcription factor occupancy and DNA methylation has been used to identifying cis-regulatory elements such as promoters, enhancers,

## **Introduction**

---

silencers, insulators and locus control regions, and define the cellular chromatin landscape (Boyle et al. 2012; Kundaje et al. 2015).

### **Methods to ascertain chromatin accessibility**

Accessible chromatin constitutes about  of the human genome and represents a very robust marker for histone modifications, early replication regions, transcription start sites (TSS) and TF binding sites (TFBSs) (ENCODE 2007). The informativeness of chromatin accessibility ~~for understanding~~ gene regulation has driven the development of several high-throughput techniques for accurately tagging these regions. Amongst those techniques, the “gold standard” is DNase I hypersensitive sites sequencing (DNase-seq), which uses the non-specific double strand endonuclease DNase I to preferentially cut ~~on~~ nucleosome-free regions known as DNase hypersensitive sites (DHSs). In this approach, ~~isolation of the chromatin free DNA is followed by further enzymatic digestion and DNA library preparation prior to NGS~~ (John et al. 2013). DNase-seq also provides high quality information regarding , generating footprints that identify TF binding ~~in relation to chromatin structure~~ (Hesselberth et al. 2009; Boyle et al. 2010).

Another method to interrogate the accessible genome is formaldehyde-assisted isolation of regulatory elements (FAIRE-seq), which uses formaldehyde cross-linking, sonication and phenol-chloroform extraction to remove the DNA-protein complexes and retain only the nucleosome-depleted regions ~~that undergo NGS~~ (Giresi et al. 2006). Both methods have enabled ENCODE to map regulatory elements in several cell lines, primary cells and tissues, revealing that 76.6% of all non-coding GWAS SNPs together with those in complete LD are located within broadly accessible chromatin ~~tagged by DHSs~~ (ENCODE 2007; Buck et al. 2014; Gaulton et al. 2010; Maurano et al. 2012). Indirect measurement of ~~the~~ chromatin accessibility has ~~also~~ been performed using micrococcal

## **Introduction**

---

nuclease-sequencing (MNase-seq), which retains nucleosome-bound material for downstream sequencing, providing a qualitative and quantitative comprehensive map for nucleosome positioning and also TF occupancy (Axel 1975; Ponts et al. 2010). The high number of cells (5 to 10 millions or more) required by these assays for good quality data limits their application to particular biological and clinical samples.

Recently, a new technique assay for transposase-accessible chromatin using sequencing (ATAC-seq) has represented a groundbreaking step in characterisation of the genomic regulatory landscape (Buenrostro et al. 2013). ATAC-seq is based on an engineered hyperactive transposase enzyme, known as Tn5, that preferentially accesses and tags nucleosome-free and inter-nucleosomal DNA using lower number of cells and shorter processing times compared to DNase-seq (Gradman et al. 2008; Adey et al. 2010). This makes ATAC-seq a very versatile technique to interrogate the chromatin landscape in a clinical set-up, where sample availability and time-efficiency are key factors (Scharer et al. 2016; Qu et al. 2015; Qu et al. 2017).

## **The role of histone modifications and TF occupancy in the chromatin landscape**

Identifying the combination of histone modifications and binding of TF is essential to characterise regulatory regions of the genome. Histone modifications take place in the NH<sub>2</sub> terminal tail that protrudes from the nucleosome, the most common modifications being acetylation, phosphorylation and methylation. The co-localisation of different histone marks modulates the affinity for DNA-binding proteins and the interaction with neighboring nucleosomes in varied manners, contributing to the overall chromatin accessibility landscape of the cells (Jenuwein and Allis 2001; Bannister and Kouzarides 2011). The combination of histone modifications can be used to broadly divide chromatin into

## Introduction

---

condensed non-transcribed heterochromatin and accessible transcriptionally active euchromatin. Further studies have identified facultative and constitutive heterochromatin, which distinguishes spatially and temporally regulated genes from those permanent<sup>1</sup> silenced, respectively. Facultative heterochromatin is enriched for H3K27me3 and the polycomb repressor complexes (PRCs), whilst constitutive heterochromatin is marked by H3K9me3 (Hansen et al. 2008; Bannister et al. 2001).

Several types of chromatin corresponding to different regulatory elements have also been defined. Enhancers and promoters, regardless of their activation state, are tagged by high levels of H3K4me1 or H3K4me3, respectively, and both features co-localise with H3K4me2 modifications (Heintzman et al. 2007; Hon et al. 2009). H3K9ac is specifically enriched at active promoters whereas H3K27ac generally designates activation at both promoters and enhancers (Hon et al. 2009; Creyghton and the 2010). Conversely, H3K27me3 together with the heterochromatin mark H3K9me3 indicates gene repression ~~at promoter elements~~ (Hansen et al. 2008; Bannister et al. 2001; Pan et al. 2007). Interestingly, GWAS variants for different complex diseases have<sup>2</sup> demonstrated to be relatively enriched for some of those modifications, importantly H3K4me3, H3K9ac, H3K79me2, H3K4me1 and H3K36r<sup>3</sup> (Ernst et al. 2011; Trynka and Raychaudhuri 2013a). Overall, functional understanding and interpretation of histone mark co-localisation remains challenging and incorporation of additional epigenetic information is usually required. Together with histone modifications, TF<sup>4</sup> also play a role in nucleosome positioning as well as in acting as boundary elements to separate chromatin states (Vierstra et al. 2014; Zhang et al. 2009; Bell and Nature 2000). ~~TF occupancy is indirectly tagged by chromatin accessibility assays, such as DHS, through reduced cutting sensitivity of DNase I due to protein binding and steric hindrance.~~ 

## Introduction

---

Chromatin immunoprecipitation sequencing (ChIP-seq) has been widely used to precisely locate histone modifications and TF binding in the genome. This technique assays protein-DNA binding *in vivo* using Abs that specifically recognise histone modifications or TF after DNA-protein cross-linking and sonication. Following immunoprecipitation of the desired DNA-protein complexes with the appropriate Ab, the cross-linking is reversed and the proteins digested prior to DNA library preparation and sequencing (Solomon et al. 1988; Barski et al. 2007; Johnson et al. 2007). ChIP-seq has been used to analyse a wide range of histone modifications and TF binding in different cell lines, primary cells and tissues (ENCODE2012; Bernstein and Nature 2010; Adams et al. 2012). Similarly to the first generation of chromatin accessibility techniques, chromatin immunoprecipitation sequencing (ChIP-seq) requires at least between 5 to 10 million cells per experiment, restricting its application to the availability of biological material. In order to overcome this limitation, a wide range of protocols have been developed, of which ChIPmentation (ChIPm) appears as the simplest and most cost-effective method, only requiring 10,000 and 100,000 cells to assay histone modifications or TF binding, respectively (Schmidl2016). ChIPm involves the use of the Tn5 transposase, accelerating library preparation and increasing the sensitivity of the results.

## DNA methylation

DNA methylation involves the transferal of a methyl group to the 5' carbon of a cytosine that precedes a guanine nucleotide (CpG sites) by a group of enzymes known as DNA methyl-transferase (DNMTs). CpG islands are found along the entire genome and their methylation generally associates with repression of gene expression (Herman and Baylin 2003). Together with histone modifications, DNA methylation has a pivotal role in the differentiation of haematopoietic stem cells and the maturation and activation of immune cells

## Introduction

---

(Sellars et al. 2015; Lai et al. 2013). The pathogenicity of changes in the methylome has been studied in a range of diseases including RA, systemic lupus erythematosus (SLE), psoriasis and PsA (Lei et al. 2009; Liu et al. 2013; Zhang et al. 2010). For example, regulation of TNF- $\alpha$  production upon inflammatory stimuli involves a complex network of DNMTs that alter the methylation signature at the locus (Sullivan et al. 2007).

### Chromatin interactions and gene expression

The functional understanding of non-coding variants has benefited from eQTL studies. Nevertheless, eQTLs only provide indirect evidence of the effect of a SNP on regulating expression of a particular gene. Since enhancers may not control expression of the closest gene, functional interpretation of GWAS variants requires genome-wide mapping of those chromatin interactions (Smemo et al. 2014). Chromatin is organised into topologically associating domains (TADs) of several hundred kb insulated from other TADs by the binding of CTCF protein, amongst others (Nora et al. 2017). Chromatin loops between promoters and the corresponding regulatory elements mostly take place within the same TAD and are highly cell- and context-specific (Smith et al. 2016). Hence, interrogation of chromatin interactions provides additional evidence for physical contact between enhancers and gene promoters coordinating assembly of the transcriptional machinery and consequently regulating expression. As an example, obesity risk non-coding variants located within the *FTO* gene appeared to regulate expression through chromatin looping of the *IRX3* gene, located 1Mb downstream (Smemo et al. 2014).

A wide range of genome wide and high throughput methods to investigate the 3D chromatin conformation have been developed, being of particular interest  Capture C, as simultaneously scales up the number of interactions investigated at high resolution and minimises the number of cells required (Davies et al. 2017;

## **Introduction**

---

Oudelaar et al. 2017). Other techniques such as promoter capture HiC have yielded comprehensive immune specific maps of promoter enhancer interactions in seventeen human primary hematopoietic cell types (Javierre 2016).

### **1.4.4 Transcriptional profiles in disease**

The role of environmental and genetic factors in altering gene expression regulation in complex diseases has been investigated through extensive comparison of case-control transcriptional profiles. The informativeness of this approach is conditional on studying the relevant disease tissue, which sometimes remains challenging due to a lack of pathophysiological understanding of disease mechanisms or difficulties in accessing it. In immune mediated diseases, peripheral blood mononuclear cells (PBMCs) differential gene expression (DGE) analysis between patients and controls has enabled identification of relevant pathways and biochemical functions in a number of chronic immune diseases, including psoriasis and PsA (further detailed in Chapter 3 and ??, respectively) (Miao et al. 2013; Junta and 2009; Baechler et al. 2003; Assassi et al. 2010; Batliwalla et al. 2005). The growing evidence supporting cell type and context specificity has also prioritised the use of disease-specific affected tissue over PBMCs, when available, including skin biopsies in psoriasis, synovial-isolated macrophages in RA and B cells and monocytes in SLE (Katschke et al. 2001; Dozmorov et al. 2015; Jabbari et al. 2012).

Likewise, the extensive overlap of GWAS variants with non-coding regions potentially dysregulating gene expression has highlighted the importance of performing context-specific eQTL studies. In this respect, consortia such as the Genotype Tissue Expression (GTEx) have generated publicly accessible comprehensive tissue-specific eQTL studies that have greatly contributed to the functional understanding of GWAS risk alleles in many complex diseases (Lonsdale et al. 2013; Fagny et al. 2017).

## Introduction

---

### Long non-coding RNAs and enhancer RNAs

In addition to protein coding mRNAs, non-coding RNAs have been demonstrated to have a role in regulation of gene expression. One category of non-coding RNAs are the long non-coding RNAs (lncRNAs), transcripts between 200 and 100Kb ~~long~~ that undergo splicing, 5' capping and 3' polyadenylation (Derrien et al. 2012). LncRNAs can positively and negatively regulate transcription through different mechanisms including guidance of chromatin modifiers such as DMTs and PRCs to specific loci, alteration of mRNA stability, translational control, and acting as a decoy for other non-coding RNAs and regulatory proteins (Pandey et al. 2008; Faghihi et al. 2008; Gong and Maquat 2011; Carrieri et al. 2012; Kino et al. 2010).

Amongst the characterised lncRNAs, many have been demonstrated to play a role in the regulation of the innate and adaptive immune response, for example in T cell activation and host-pathogen interactions (Pang et al. 2009; Rossetto and Pari 2012). Moreover, differential case-control gene expression analyses have underscored the contribution of lncRNAs in several chronic inflammatory conditions, including RA, SLE and psoriasis (Ahn 2016; Müller et al. 2014; Shi et al. 2014; Li et al. 2014).

A particularly relevant type of lncRNAs are the enhancer RNAs (eRNAs), shorter molecules compared to the canonical lncRNAs (approximately 346  nucleotides) that do not undergo splicing or polyadenylation (Forrest et al. 2014). Although traditionally chromatin segmentation maps have defined enhancers as DNA regions with particular epigenetic characteristics, later studies have shown their ability to be bi-directionally transcribed into eRNAs molecules (De Santa 2010; Kim et al. 2010). Importantly, the transcriptional activity of enhancers has been demonstrated to be an excellent proxy to identify functionally active regulatory regions, which have also been successfully validated by reporter assays (Anderssen 2014; Forrest et al. 2014).

## **Introduction**

---

Another class of non-coding RNAs are micro-RNAs (miRNAs), between 21 to 24 nucleotides long (Lee et al. 2002). Under particular conditions, expression of genes containing complementary sequences to miRNAs ~~are commonly~~ negatively regulated through assembly of the miRNA-induced silencing complex followed by mRNA degradation, mRNA destabilisation or translational repression ~~with~~ <sup>in</sup> 30 ~~and~~ 80% of human genes predicted to be under transcriptional control of miRNAs (Ameres et al. 2010; Braun et al. 2011; Petersen et al. 2006; Lewis et al. 2005; Friedman et al. 2008).

## **Methods to assay gene expression**

RNA sequencing (RNA-seq) involves reverse-transcription of the extracted RNA into cDNA and PCR amplification preserving relative abundance of each transcript, followed by library preparation and NGS (Mortazavi et al. 2008). Systematic comparison has shown superior dynamic range of detection for RNA-seq compared to micro-arrays, particularly for low abundance transcripts (Zhao et al. 2014). Furthermore, RNA-seq allows the capture of additional information ~~to the expression profile~~, including the identification of new exons, alternative splicing events and allele-specific expression (ASE). Quantification of ASE through RNA-seq has provided direct evidence for local/*cis*-eQTLs driven by allele-specific mechanism in up to 88% of the genes with an associated *cis*-eQTL(Yan et al. 2002; Pickrell et al. 2010).

Additionally, 5end RNA-sequencing methods such as cap analysis of gene expression (CAGE) has been used to quantify eRNAs by the ~~functional annotation of the mammalian genome~~ 5' (FANTOM5) Consortium, contributing to a better definition of enhancers and their spatial and temporal specificity in hundreds of human primary cells and tissues (Forrest et al. 2014; Andersson et al. 2014). Lastly, development of single-cell RNA-seq (scRNA-seq) has enabled the

## **Introduction**

---

identification of cell sub-populations within a tissue in an unbiased way (Tang et al. 2009; Tang et al. 2010).

### **1.4.5 Transcriptional regulation in complex diseases**

Non-coding GWAS variants can exert pathogenic effects by affecting one or many of the previously described mechanisms responsible for the fine regulation of gene expression in homeostatic conditions. For example, intronic SNPs can influence mRNA splicing through exon skipping, resulting in truncated but functional proteins. For instance, exon skipping caused by an intronic risk allele at the TNF Receptor Superfamily Member 1A (*TNFRSF1A*) associated with MS results in a soluble isoform of the *TNFRSF1A* protein with TNF antagonistic function (Gregory et al. 2012). On the other hands, non-coding variants at enhancers, silencers and promoters can dysregulate gene expression by altering affinity at TFBS, histone modifications and chromatin accessibility. For instance, in thyroid autoimmunity, the risk allele of an intronic SNP in the thyroid stimulating hormone receptor (*TSHR*) gene reduces *TSHR* protein expression in IFN- $\alpha$  stimulated thyroid cells (Stefan et al. 2014). ~~The risk SNP increases the affinity of the repressor promyelocytic leukemia zinc finger protein (*PLZF*) that recruits histone acetylases (HDACs) to the locus, resulting in impaired tolerance to thyroid auto antigens.~~ Alterations in TF binding can also affect looping and long-range chromatin interactions between enhancers and promoters. For instance, in prostate cancer this phenomenon causes upregulated expression of the oncogene *SOX9* due to increased enhancer activity and enhancer-promoter interaction (Zhang et al. 2012).

Alternatively, non-coding SNPs can regulate gene expression by creating a new promoter-like element, as in the  $\alpha$ -thalassemia disease, where this phenomenon leads to dysregulated downstream activation of all  $\alpha$ -like globin genes in erythroid cells (Gobbi et al. 2006). ~~Genetic variants at eRNAs can also~~

## **Introduction**

---

affect regulation of gene expression as it has been demonstrated in the nuclear receptor for anti diabetic drugs PPAR $\gamma$  in mice (Soccio et al. 2015). Lastly, non coding variants placed in UTRs and intergenic regions can affect binding of miRNAs and lncRNA to the target genes. This is the case of a CD associated variant at the 3'UTR of the gene immunity related GTPase M *IRGM* which reduces binding of the miR 196, increasing its mRNA stability and translation, ultimately resulting in disrupted autophagy (Brest et al. 2011). In psoriasis and PsA, some specific SNPs located at 3' UTR of genes such as *IL-23*, *TRAF3IP2* or *SOCS1* have been hypothesised to disrupt or create *de novo* miRNA binding sites, but no experimental evidence has been provided yet (Pivarcsi et al. 2014).

### **1.4.6 The use of fine-mapping to prioritise functional causal variants**

The aim of fine-mapping is to reduce the size of GWAS genomic intervals and yield a minimal set of SNPs containing the causal variant that will explain most of the association for that particular locus (Spain and Barrett 2015). Fine-mapping studies require extensive genotyping to meet the assumption that the putative causal variant will be likely interrogated in the analysis. This can be achieved by WGS, dense genotyping arrays and *in silico* imputation using publicly available data. The use of the Immunochip array across most of the immune-mediated inflammatory diseases has increased the genotyping density at previously associated immune-relevant loci ~~in a cost effective manner~~ (Trynka et al. 2011). Similarly, imputation methods using WGS reference panels, such as HapMap and 1000 Genomes Project, have offered genome-wide coverage for SNPs and CNVs with MAF >1% across different ancestry groups (Abecasis et al. 2012). More recently, the UK10K project has improved the quality of imputation specifically for rare variants with MAF between 0.01 and 0.5% (Chou et al. 2016).

## Introduction

---

Bayesian statistical analysis has been chosen over the frequentist approach (based on p-value calculations) to increase the resolution of the GWAS associations and facilitate the identification of relevant genes and disease mechanism. Bayesian fine-mapping quantifies the evidence of association for each of the genotyped or imputed SNPs as Bayes Factor (BF). BFs are later used to calculate posterior probabilities (PP) which represent the probability of each SNP to drive a particular association (Wakefield 2007). Since including only the most significant fine-mapped SNP would miss the causal variant in approximately 97.5% of loci, the Bayesian strategies report a credible set of SNPs which includes those variants capturing 95 or 99% of the cumulative PP in each loci (Bunt et al. 2015). This strategy has proven further refinement and reduction of false-positives compared to inclusion of all the SNPs in high LD (e.g  $r^2 \geq 0.8$ ) with the lead variant (Bunt et al. 2015). Furthermore, inclusion of functional data from publicly available sources as priors of the approximate Bayesian model has demonstrated a reduction of the number of SNPs in the credible set and also increased the proportion of successfully fine-mapped loci (Bunt et al. 2015; Kichaev and Pasaniuc 2015). The integration of fine-mapping data generated with the Bayesian probabilistic identification of causal SNPs (PICS) method and a map of genomic regulatory elements, revealed that approximately 60% of the top fine-mapped SNPs overlapped enhancer elements (importantly stimulus-specific) and were very close but not within TF binding sites (TFBS) (Farh et al. 2015).

### 1.4.7 Integration and interpretation of genomic data

The evolution of different omics methods towards generation of paired datasets at a high-throughput scale presents a challenge in terms of interpretation and integration. This is particularly important in the field of complex diseases resulting from the interaction of many risk variants, with small

## **Introduction**

---

or moderate effect, that involve several genes and signalling pathways through alteration of epigenetic features and dysregulation of gene expression.

Tools such as RegulomeDB allow the querying of a large number of publicly available epigenetic and functional datasets, including DHSs, TFBS, histone modification and DNA-protein interactions, at the SNP level (Boyle et al. 2012). Other powerful tools include the University of California Santa Cruz (UCSC) genome browser, a resource to display in-house and publicly accessible annotation data (Kent et al. 2002). In addition to this, international consortia generating large-scale epigenetic and expression data such as ENCODE, Blueprint, the Roadmap Epigenomics Project, GTEx or FANTOM have created comprehensive website resources for browsing and downloading data (Adams2012 ; ENCODE 2007; Lonsdale et al. 2013; Forrest et al. 2014). These collaborations have also led to the integration of epigenetic datasets and assembling of cell type specific chromatin states maps. This consists of the segmentation and labelling of the genome with a chromatin state based on concurrence of several epigenetic marks using Hidden Markov Model algorithms such as ChromHMM, amongst others (Kundaje2015 ; Ernst and Kellis 2010; Ernst et al. 2011; Hoffman et al. 2013).

In addition to data integration, the other main bottleneck encountered by functional genomics is determining the clinical relevance of GWAS SNPs, eQTLs, differentially expressed genes or differentially epigenetic modified regions. This can be addressed by performing enrichment analysis, which tests for statistically significant over-representation of particular annotation terms (e.g ontologies, signalling pathways or functional elements) within the entities of interest. For instance, pathway enrichment analysis uses functional units containing related genes defined by prior knowledge. Amongst the most comprehensive and informative pathways sources are The Kyoto Encyclopedia of Genes and Genomes (KEGG) and the REACTOME, which also considers biochemical reactions such as

## **Introduction**

---

binding, activation or protein translocation (Kanehisa and Goto 2000; Fabregat et al. 2018). Such annotation sources may be used to interpret, for example, a set of differentially expressed genes or a list of genes obtained through annotation of non coding regions using proximity, chromatin interaction data or eQTL studies. Similarly, this type of analysis can be used to find enrichment of genomic regions of interest for a varied collection of epigenomic features tagging regulatory elements in relevant cell types.

From the number of tools designed to perform this type of analysis, eXploring Genomic Relations (XGR) is particularly powerful (Fang et al. 2016). XGR is an open source R package and web-app that allows handling of different types of input data (SNPs, genes and regions). XGR integrates a wide range of ontologies and up to date publicly available functional data to perform different types of annotation and enrichment analysis, facilitating background customisation for reliable and meaningful output results. Moreover, XGR also performs gene network analysis from the same inputs as the pathway analysis. This leverages experimentally validated interaction information to identify gene networks modulated by putative pathogenic variants, improving interpretation through consideration of network connectivity.

### **1.4.8 Aims and objectives**

The aim of this thesis is to investigate the epigenetic regulatory landscape in psoriasis and PsA to identify disease and cell type specific changes in putative regulatory regions and differences in gene expression, with the longer-term goal of advancing understanding of the pathophysiology of these diseases and informing interpretation of genetic associations arising from GWAS.

Specific objectives are:

1. To establish ATAC protocol(s) appropriate for cells and tissues of interest and samples taken in the clinic, with optimisation of

## Introduction

---

required methodologies and analytical tools including quality control measurements, peak filtering, differential analysis,  position time, approaches to reduce mitochondrial DNA contamination, application to skin biopsies, and utility of cryopreservation and fixation (Chapter ??).

2. To determine chromatin accessibility, histone modification and gene expression differences between psoriasis patients and controls ~~in peripheral blood~~ for four major circulating immune cell types in peripheral blood ( $CD14^+$  monocytes,  $CD4^+$  and  $CD8^+$  T cells, and  $CD19^+$  B cells) as well as gene expression differences in psoriasis lesional and uninvolved epidermis, and further integrate them with psoriasis GWAS fine-mapped variants (Chapter 3).
3. To identify cell subsets contributing to pathophysiological relevant pathways in PsA by assaying chromatin accessibility and gene expression in  $CD14^+$  monocytes, memory  $CD4^+$  and  $CD8^+$  T cells, and NK cells for peripheral blood and synovial fluid, determining transcriptional differences at the single-cell level in cell types of interest and relating findings to PsA GWAS (Chapter ??).

# Chapter 2

## Material and Methods

### 2.1 Ethical approval and recruitment of study participants

A summary of the samples and cohorts recruited for this thesis is included in Table 2.1.

#### 2.1.1 Psoriasis patient recruitment

Patient blood samples and skin biopsies were collected in collaboration with Professor Graham Ogg at the Weatherall Institute of Molecular Medicine, University of Oxford, and the Dermatology Department research nurses at the Churchill Hospital, Oxford University Hospitals NHS Trust. This was under approval from the Oxfordshire Research Ethics Committee (REC 14/SC/0106 and REC 14/NW/1153). After written informed consent, up to 60mL of blood from eligible psoriasis patients were collected into 10mL anticoagulant ethylenediaminetetraacetic acid (EDTA)-containing blood tubes (Vacutainer System, Becton Dickson) (Table 2.1). Detailed clinical information describing the recruited psoriasis cohorts is included in Chapter 3 Table 3.2.

*Eligibility criteria.* Psoriasis patients were eligible for recruitment when aged 18 years or older, previously or newly diagnosed as having psoriasis (fulfilling the Psoriasis Area and Severity Index (PASI) classification, Table 1.1) and in a flare (active disease state). Recruited patients were required

## **Material and Methods**

---

to have moderate to severe disease (PASI>5), not to have taken antibiotics in the two weeks before sampling and to be naïve for biological therapy.

### **2.1.2 PsA patient recruitment**

Sample recruitment was performed as part of the Immune Function in Inflammatory Arthritis (IFIA) study established in 2006 (REC/06/Q1606/139) in collaboration with Dr Hussein Al-Mossawi at the Botnar Research Centre and research nurses at the Nuffield Orthopaedic Centre, Oxford University Hospitals NHS Trust. Following informed written consent, approximately 30mL of both blood and synovial fluid aspirate (variable upon disease severity) were collected into 10mL anticoagulant sodium heparin coated tubes (Vacutainer System, Becton Dickson) (Table 2.1). Further details about the cohort and collected clinical information can be found in Chapter ?? Table ??.

***Eligibility criteria..*** Eligible patients were aged 18 years or older, previously or newly diagnosed with PsA according to the PsA Response Criteria (PsARC) (Table 1.2) and a physician global assessment questionnaire, with concomitant psoriasis and in a flare. Patients had to present an oligoarticular phenotype, not having taken antibiotics in the two weeks before sampling and be naïve for biological therapy and preferably for any other treatment.

### **2.1.3 Healthy volunteer recruitment**

Recruitment of healthy volunteers was conducted as part of the Genetic Diversity and Gene Expression in White Blood Cells study with approval from the Oxford Research Ethics Committee (REC 06/Q1605/55). Up to 80mL of blood were collected into 10mL anticoagulant EDTA-containing blood tubes. Healthy individuals recruited in the study were required to be 18 years old or older, preferably British or European, without family history of psoriasis, PsA, RA or SpA and not having suffered from an infection in the two weeks prior to

## **Material and Methods**

---

sample recruitment (Table 2.1). Detailed information describing the recruited matched healthy control volunteers for psoriasis patients is included in Chapter 3 Table 3.3.

<b>Chapter</b>	<b>Samples/cohorts</b>	<b>Description</b>
Chapter ??	Healthy controls	CD14 <sup>+</sup> monocytes and CD4 <sup>+</sup> cells from peripheral blood (fresh, frozen and fixed)
	Skin biopsies	Healthy and psoriatic skin
Chapter 3	Cohort 1A and 1B	Psoriasis and healthy control cells isolated from peripheral blood
Chapter ??	PsA samples	Cells isolated from synovial fluid and peripheral blood

**Table 2.1: Summary table of samples/cohorts recruited in this thesis for generation of various datasets.** For each of the chapters, the samples or name of the cohorts (when applicable) recruited and used to generate different types of data together with a short description are included. Detailed explanation is included in each of the chapters where the results for the processed samples are presented.

## **2.2 Sample processing**

Blood, synovial fluid and skin biopsies were processed straight after recruitment, following the appropriate protocols.

### **2.2.1 PBMCs and synovial fluid cells isolation**

PBMCs were isolated from blood samples through density gradient separation using Ficoll-Paque (GE Healthcare) with centrifugation at 500g for 30 minutes at room temperature with minimum acceleration and no braking. Total synovial fluid mononuclear cells (SFMCs) were isolated by centrifugation at 500g for 5 min at room temperature in absence of density gradient. Samples were placed on ice, washed twice in ice cold Hanks balanced salt solution (HBSS) without calcium or magnesium (Thermo Fisher Scientific) and resuspended in phosphate saline buffer (PBS, Gibco) supplemented with 0.5% fetal calf serum

## **Material and Methods**

---

(FCS, Invitrogen) and 2mM EDTA (Sigma), prior to separation of the different cell types. Cell numbers and viability were determined by manual counting using a haemocytometer with trypan blue (Sigma) for viability assessment.

### **2.2.2 Skin biopsies processing and adherence assays**

Keratinocytes enrichment from skin biopsies was performed as described in Gutowska-Owsiaak and colleagues (GutowskaOwsiaak and Schaupp 2012). Skin biopsies (approximately 4mm) were washed with PBS, cut in 1mm width strips and incubated in 2U/mL of dispase II (Sigma) overnight at 4°C. Following incubation, the epidermis was separated from the dermis. For RNA extraction, the epidermis was snap-frozen in liquid nitrogen. For chromatin accessibility assay, the epidermis was further digested in trypsin (Invitrogen) at 37°C for 5 min to obtain a cell suspension that was filtered through a 70µm nylon strainer (BD) and washed with PBS. In some instances cells were manually counted and aliquoted in PBS prior to chromatin accessibility assay. In others, cells from each of the biopsies were resuspended in KGM-2 BulletKit (Lonza) supplemented with 0.06mM Ca<sup>2+</sup> and cultured in a collagen IV coated 96-well plate at 37°C 5% CO<sub>2</sub> for 3 hours. After culture, cells in 96-well plates were washed twice with 200µL of PBS and kept at 37°C for downstream chromatin accessibility processing.

### **2.2.3 Fixation, cryopreservation and cell culture**

Cells (50,000) were fixed using dithio-bis(succinimidyl propionate) (DSP) as described in Attar and colleagues and stored at 4°C for 24h (Attar et al. 2018).

Liquid nitrogen storage of 40-50x10<sup>6</sup> PBMCs was carried out using a modified version of the protocol described by Kent and colleagues(Kent 2009), where cells were pre-conditioned in RPMI 1640 complete medium (Lonza) supplemented with 2 mM L-glutamine (Sigma), 100U penicillin and streptomycin 100µg/mL (Sigma) and 50% FCS for 30 minutes and,

## **Material and Methods**

---

afterwards, diluted 1 in 2 in complete RPMI 1640 (supplemented as previously described) with 20% dimethyl sulfoxide (DMSO, Sigma). PBMCs followed slow cryopreservation at -80°C at -1°C per minute and then transferred and stored for a minimum of two weeks in liquid nitrogen.

PBMCs were thawed quickly in a 37°C water bath, resuspended in supplemented complete RPMI 1640 with 10% FCS at a density of  $10^6$  cells/mL and rested for 30 min at 37°C, 5% CO<sub>2</sub> in 25mL non-adherent polypropylene cell culture flasks (Greiner) followed by filtering through a 40µm cell strainer to obtain a homogenous cell suspension for FACS separation. Cryopreserved normal human epidermal keratinocytes (NHEK, Lonza) in passage three were recovered and cultured at a cell density of  $5 \times 10^6$  cells/mL in a 75 mL adherent cell culture flask (Greiner) in EpiLife basal medium (Gibco), following manufacturer's instructions. After recovery, NHEKs were trypsinised at room temperature for 8 minutes and trypsin was inactivated with EpiLife 10% FCS. Cells were centrifuged at 180g for 10 min at room temperature and then manually counted with trypan blue for viability staining. NHEKs (16,000 cells) were seeded in a 96-well plate in 100uL of medium and cultured for 2 days at 37C, 5% CO<sub>2</sub> to reach 90-100% confluence (approximately 50,000 cells) before performing any ATAC protocol on the plate (further detailed in Chapter ??). When used for Omni-ATAC, NHEKs after trypsinisation were processed through Ficoll density gradient (as previously explained for PBMCs isolation) to remove dead cells as recommended by Corces and colleagues (Corces et al. 2017).

### **2.2.4 Primary cell isolation using magnetic-activated cell sorting**

Primary cell subpopulations were separated using magnetic-activated cell sorting (MACS, Miltenyi) following the manufacturer's instructions. Consecutive positive selection was performed using Miltenyi beads for CD19<sup>+</sup>, CD8<sup>+</sup>, CD14<sup>+</sup>

## **Material and Methods**

---

monocytes and CD4<sup>+</sup> cells (catalogue numbers 130-050-201, 130-045-101, 130-045-201 and 130-050-301, respectively) and AutoMACS Pro (Miltenyi) followed by a manual cell count with trypan blue. MACS separation was chosen over fluorescence-associated cell sorting (FACS) due to time and logistic constraints during sample processing.

### **2.2.5 Primary cell isolation using fluorescence-activated cell sorting**

Isolation of cell subpopulations from PBMCs and SFMCs (Chapter ?? and ?? in Table 2.1) was performed by FACS. PBMCs and SFMCs were resuspended in 1mM EDTA PBS (FACS buffer) at 10x10<sup>6</sup> cells/mL, stained with the appropriate antibody cocktail (Table 2.2) for 30 min at 4°C, washed with FACS buffer and centrifuged at 500g for 5 min at 4°C. For the cell separation in the Chapter 3 samples (Table 2.1), a modified FACS buffer supplemented with 3mM EDTA , 2% FCS and 25mM 4-(2-hydroxyethyl)-1-piperazineethanesulfonic acid (HEPES, Invitrogen) was used to avoid cell clumping after cryopreservation and short recovery in culture (as detailed previously). After removing the supernatant, cells were resuspended in FACS buffer prior to separation.

From the healthy control samples of Chapter ?? (Table 2.1), CD14<sup>+</sup> monocytes and CD3<sup>+</sup> CD14<sup>-</sup> CD4<sup>+</sup> T cells were isolated using the SONY SH800 cell sorter. For the PsA samples (Chapter ?? in Table 2.1 and Table ??), separation of CD19<sup>+</sup> B cells, memory T cells (CD3<sup>+</sup> CD14<sup>-</sup> CD4<sup>+</sup> CD45RA<sup>-</sup> and CD3<sup>+</sup> CD14<sup>-</sup> CD8<sup>+</sup> CD45RA<sup>-</sup>), CD14<sup>+</sup> monocytes and CD56<sup>+</sup> NK from PBMCs and SFMCs was performed using FACS Aria (BD) cell sorter. Sorted cells were collected in 1.5mL tubes containing PBS 1% FCS when used for ATAC-seq or only PBS when processed for scRNA-seq to avoid potential RNase contamination. OneComp eBeads (eBioscience) were used for compensation of fluorescence spill over.

## Material and Methods

---

Surface marker	Fluorochrome PsA/Control	Manufacturer PsA/Control	Clone PsA/Control	Dilution PsA/Control
Viability	eFluor780	-	eBioscience	1:500/1:250
CD3	FITC/AF700	SK7/UCHT1	BioLegend	1:50/1:50
CD4	APC	RPA-T4/RPA-T4	BioLegend	1:50/1:50
CD8a	PE	RPA-T8	BioLegend	1:100/-
CD45RA	BV421	HI100	BioLegend	1:25/-
CD19	PerCP-Cy5.5	SJ25C1	BioLegend	1:50/-
CD14	Pe-Cy7/FITC	M5E2/TUK4	BioLegend/Miltenyi	1:50/1:100
CD56	BV510	HCD56	Biolegend	1:25/-

**Table 2.2: Antibody panel used for FACS separation of primary cell populations in Chapter 3 controls and Chapter 5 PsA samples.** Details regarding target molecule, fluorochrome, clone, supplier and dilution used for PBMCs and SFMCs staining are provided for each surface marker in the panel. For cell separation from Chapter 3, control PBMCs staining was only performed for CD3, CD4, CD14 and viability markers.

## 2.3 Experimental protocols

### 2.3.1 ATAC - Chromatin Accessibility

Three different versions of the ATAC-seq protocol were progressively used in this thesis for assessment of chromatin accessibility in different primary cells, including CD14<sup>+</sup> monocytes, CD4<sup>+</sup> and CD8<sup>+</sup> T cells, CD19<sup>+</sup> B cells and CD56<sup>+</sup> NK cells, as well as in epidermal keratinocytes isolated from skin biopsies. ATAC (used in this thesis to refer to any of the three protocols in subsequent chapters) interrogates accessible chromatin using the transposase enzyme Tn5 to simultaneously access nucleosome-free and inter-nucleosomal DNA and tag both ends of the fragments with Illumina adapters. Fast-ATAC and Omni-ATAC were two subsequent protocols following the ATAC-seq protocol from Buenrostro and colleagues (Buenrostro et al. 2013), aiming to reduce the amount of mitochondrial DNA in the sequencing libraries and improve the signal-to-noise ratio of the original protocol. When using MACS separation, primary cells were manually counted, as specified above, and resuspended in PBS 1% FCS.

## **Material and Methods**

---

### **ATAC-seq**

ATAC-seq was used to generate data from NHEKs, skin biopsies and healthy volunteers (Chapter ?? in Table 2.1) as well as cohort 1A primary immune cells isolated from blood of psoriasis and control samples (Chapter 3 in Table 2.1 and Tables 3.2 and 3.3). ATAC-seq was performed using an estimated number of 50,000 cells as described in Buenrostro and colleagues with minor modifications (Buenrostro *et al.* 2013). Cells lysis was carried out for 10 min, the isolated nuclei were transposed for 40 min at 37°C using the Nextera Tn5 transposase (Illumina) and DNA was purified with the PCR MinElute kit (Qiagen), following the manufacturer's instructions. When using DSP fixed cells, two washes with 50µL of PBS were performed to remove any remaining fixative prior to the ATAC-seq protocol. After the transposition reaction, the Tn5 enzyme was inactivated with 500 mM EDTA for 30 min at 70°C followed by de-crosslinking using 50 mM dithiothreitol (DTT) for 30 min at 37°C and DNA column purification, as previously detailed. All transposed samples were simultaneously amplified and singled indexed for 11 PCR cycles using modified Nextera primers from Buenrostro *et al.*, 2013, after appropriate assessment of the approximate required number of qPCR cycles. The resulting DNA libraries were purified using the MinElute PCR purification kit (Qiagen) and a 1.8X (v/v) of Agencourt AMPure XP Magnetic Beads (Beckman Coulter) to remove adapters excess and primer dimers.

Additional modifications of the protocol were implemented when processing keratinocytes isolated from skin biopsies and NHEKs in 96-well plates (Bao *et al.* 2015) (as later detailed in Chapter ??).

### **Fast-ATAC**

An improved ATAC-seq protocol was published in Nature Methods by Corces and colleagues called Fast-ATAC (Corces *et al.* 2016). Optimised for

## **Material and Methods**

---

hematopoietic cells, the protocol combined cell lysis and transposition into a single step. In this thesis, Fast-ATAC was performed in skin biopsies (Chapter ?? in Table 2.1), cohort 1B primary immune cells isolated from blood of psoriasis and control samples (Chapter 3 in Table 2.1 and Tables 3.2 and 3.3) and primary immune cells isolated from blood and synovial fluid of PsA patients (Chapter ?? in Table 2.1 and Table ??). Fast-ATAC was conducted as described by Corces and colleagues with minor modifications. Following the advice from the authors, approximately 20,000 cells (MACS or FACS sorted) were washed with 200µL of PBS, centrifuged at 500g for 5 min at 4°C and incubated in the lysis/transposition buffer containing digitonin (Roche) for 30 min at 37°C and agitation at 400rpm. Following transposition DNA was prepared and purified as per the protocol except 13 cycles of PCR amplification were used after appropriate cell cycle determination in a pilot set of samples.

### **Omni-ATAC**

Omni-ATAC was performed in 50,000 viable NHEKs in suspension (Chapter ??), as described in the latest publication from Corces and colleagues (Corces et al. 2017). Transposed DNA was simultaneously amplified and indexed, as detailed in the ATAC-seq standard protocol, for 8 PCR cycles and purified using MinElute PCR purification columns (Qiagen) only.

### **Quality control and sequencing**

Indexed and amplified ATAC samples were assessed for fragmentation profile on an Agilent 2200 or 4200 Tapestation with the D1000 high sensitivity DNA tape (Agilent) as part of the quality control. Quantification of the library concentration was performed by qPCR using the Kapa assay from Roche, following the manufacturer's instructions. Pools of 12 to 16 libraries were sequenced on up to 3 lanes of the HiSeq4000 Illumina platform aiming for 30

## **Material and Methods**

---

million paired-end reads. NGS was performed at the Oxford Genomics Centre, at the Wellcome Centre for Human Genetics (WHG) for this and all other work involving NGS in this thesis.

### **2.3.2 Chromatin immunoprecipitation with sequencing library preparation by Tn5 transposase**

For chromatin immunoprecipitation (ChIP) a low cell input protocol known as ChIPmentation (ChIPm) was used (Schmidl et al. 2015). This protocol combines DNA cross-linking and chromatin sonication and immunoprecipitation, as per standard ChIP-seq, with sequencing library preparation by tagmentation using Tn5 transposase. ChIPm introduces sequencing-compatible adapters by performing the transposition reaction directly on bead-bound chromatin, prior to de-crosslinking, preventing overtagmentation of the DNA and thus reducing required input material. Overall ChIPm represents a more time- and cost-effective protocol compared to ChIP-seq or other low-input ChIP-seq protocols.

The H3K27ac histone mark (active enhancer and promoter marker) was assayed in four cells types ( $CD14^+$  monocytes, total  $CD4^+$ , total  $CD8^+$  and  $CD19^+$ ) from samples of cohort 1B (Chapter ?? in Table 2.1 and Tables 3.2 and 3.3). For each sample and cell type, 600,000 MACS sorted cells, as described in 2.2, were fixed with 1% formaldehyde (Sigma) and snap frozen in dry ice and ethanol prior to storage at -80°C. Fixed cells were thawed, resuspended in SDS lysis buffer and sonicated for 8 min using Covaris M220 (Covaris) with a duty factor of 5%. After sonication, chromatin was split into 6 aliquots (100,000 cells per aliquot), snap frozen and stored at -80°C. Aliquots as needed were thawed on ice and then processed downstream for ChIPm as described by Schmidl and colleagues for immunoprecipitation, tagmentation of bed-bound chromatin, de-crosslinking and DNA amplification (Schmidl et al. 2015). Immunoprecipitation was carried out with 1 $\mu$ g of the Diagenode antibody (C15410196). For each

## **Material and Methods**

---

sample, an aliquot of chromatin was processed in parallel without incubation with the anti-H3K27ac antibody (control input). Tagmentation of the control input was performed using 1ng of DNA. Amplification by qPCR was carried out in each of the samples and control inputs to determine the appropriate number of full cycles required to reach one-third of the final fluorescence to minimise the presence of PCR replicates upon NGS. Libraries were then amplified for the number of determined cycles minus one and simultaneously dual indexed using the primers optimised by Buenrostro and colleagues (Buenrostro et al. 2015). A pool of 64 libraries (including control input samples) were sequenced over a number of lanes in the HiSeq4000 Illumina platform aiming for 25 million paired-end reads

### **2.3.3 RNA extraction and gene expression quantification**

#### **RNA extraction**

Following MACS isolation of the different cell types 2 to  $3 \times 10^6$  cells were resuspended in 350 $\mu$ L of RNAProtect (Qiagen) or RLT buffer (Qiagen) supplemented with 0.1% of beta-mercaptoethanol (BM, Sigma) and snap frozen in dry ice before storage at -80°C. Cells isolated from Cohort 1A psoriasis and control samples (Chapter 3 in Table 2.1 and Tables 3.2 and 3.3) were preserved in RNAProtect, which stops any biochemical reaction and transcriptional activity whilst maintaining cell integrity. At early stages of the project, the time frame to process the acquired samples was uncertain and RNAProtect was chosen as the most appropriate strategy to preserve cells for future RNA extraction to guarantee high quality in case storage exceeded 6 months. In the psoriasis and control samples from Cohort 1B (Chapter 3 in Table 2.1 and Tables 3.2 and 3.3) and in the PsA samples (Chapter ?? in Table 2.1 and Table ??), cells were resuspended in 0.1% BM supplemented RLT buffer, which lysis cells and prevents RNA degradation. When starting from RNAProtect preserved material,

## **Material and Methods**

---

cells were centrifuged at 300g for 10 min at room temperature, the supernatant were removed and the pellets were resuspended in 350µL of RLT 0.1% BM buffer. All cell lysates were homogenised using the QIAshredder (Qiagen) prior to RNA extraction.

Total RNA was extracted using the AllPrep DNA/mRNA/microRNA Universal kit (Qiagen) following the manufacturer's instructions. RNA extractions were performed in batches of 12 samples, including all cell types from each individual processed and balanced numbers of psoriasis and control samples, to minimise batch effect correlating with phenotype. Basic quantification was performed with NanoDrop (Thermo Scientific) before storage at -80°C.

### **RNA-seq**

RNA-seq quality control (QC), quantification and library preparation were carried out by Oxford Genomics Centre followed by NGS in two independent batches of samples, each including Cohort 1A or Cohort 1B, respectively (Chapter 3 in Table 2.1 and Tables 3.2 and 3.3). Processing of samples in two batches was due to logistics of patient recruitment in the project. RNA quality control and quantification were assessed with the Bioanalyzer (Agilent). Samples were depleted from ribosomal RNA using Ribo-Zero rRNA Removal kit (Illumina) prior to cDNA synthesis and library preparation using TruSeq Stranded Total RNA (Illumina). This method preserves non-polyadenylated transcripts including nascent pre-mRNA (unspliced) and functionally relevant lncRNAs. For each of the cohorts, all libraries were pooled together and sequenced over several lanes of HiSeq4000 aiming a depth of approximately 50 million total reads per sample to maintain an appropriate level of sensitivity for subsequent expression analysis.

## **Material and Methods**

---

### **Gene expression quantification by qPCR array**

Expression of immune-relevant genes for a number of the PsA cohort samples (Chapter ?? in Table 2.1 and Table ??) was profiled using the RT2 Profiler PCR Array (PAHS-3803Z, Qiagen) by UCB collaborators UCB. RT2 Profiler PCR Array consisted of a 384-well plate which includes SYBR Green-optimised primers assays to test expression for 370 key genes involved in immune response during autoimmunity and inflammation, as well as appropriate house-keeping genes for normalisation of expression. This PCR array allows simultaneous amplification of different gene-specific products under the same PCR conditions. In brief, RNA was extracted, as detailed previously, from CD14<sup>+</sup> monocytes, memory CD4<sup>+</sup> and CD8<sup>+</sup> cells, followed by reverse-transcription for cDNA synthesis using RT Primer Mix (Qiagen). Synthesised cDNA was mixed with the ready-to-use PCR mastermix and equal volumes were aliquoted to each well of the plate as specified in the manufacturers instructions. Real-time PCR cycling program was run and abundance of the amplified product quantified by measuring SYBR Green fluorescence.

### **Single-cell RNA-seq**

scRNA-seq data was generated using 10X Genomics technology Chromium single cell 3' expression library preparation kit (PN-120267) by the Oxford Genomics Centre at the WHG for a number of the PsA cohort samples (Chapter ?? in Table 2.1 and Table ??). Briefly, PBMCs and SFMCs were made into a cell suspension. Approximately 3,000 cells from the PBMCs or SFMCs suspensions were partitioned into single-cell gel beads in emulsion (GEMs) using the 10X Chromium controller system. Reverse-transcription for cDNA synthesis was performed within the GEMs, which included a 16bp 10x barcode, a 10bp unique molecular identifier (UMI) and poly-dT primers. The cDNA was released from the GEMs, followed by PCR amplification, enzymatic fragmentation

## **Material and Methods**

---

and size selection. Afterward, appropriate sequencing Illumina indexes were incorporated into the samples through library preparation. Sequencing was performed using PE HiSeq4000 with 26bp for read 1 and 98bp for read 2 at a depth of approximately 50,000 reads per cell, following standard 10X library sequencing requirements.

### **2.3.4 DNA extraction and rs4672405 genotyping**

DNA isolation was performed using the AllPrep DNA/mRNA/microRNA Universal kit (Qiagen) following the manufacturer's instructions. Quantification was performed using NanoDrop (Thermo Scientific) and samples were kept at -80°C for long term storage. The extracted DNA was amplified by PCR using forward (5'-CACTGTGGAGGGAGGAACAA-3') and reverse (5'-CGTGTG GCCAGGATAGTCT-3') primers annealing up and down stream the SNP rs4672505, respectively. An aliquot of the sample was run on a 1% agarose gel to check for amplification of a 390bp PCR fragment. The remaining was purified using MinElute PCR purification kit, quantified by dsDNA Qubit kit (Invitrogen) according to the manufacturer's instructions and prepared for Sanger sequencing using the Mix2Seq kit and service (Eurofins). The forward and reverse sequences were analysed with BioEdit software (<http://www.mbio.ncsu.edu/BioEdit/bioedit.html>).

### **2.3.5 Mass cytometry using cytometry by time of flight (CyTOF)**

CyTOF represents an improved version of flow cytometry that allows a single-cell high-dimensional phenotypic and functional analysis. CyTOF interrogates up to 42 intracellular and surface markers by using antibodies coupled to metal isotopes instead of fluorescence molecules. Replacement of fluorescence molecules by metal isotopes allows increasing the number of

## **Material and Methods**

---

functional markers simultaneously assayed and minimises the spillover of signal, two of the main limitations in flow cytometry.

Mass cytometry using CyTOF was performed by Dr Nicole Yager in collaboration with UCB for all the PsA samples (Chapter ?? in Table 2.1 and Table ??). Briefly, an aliquot of peripheral blood and synovial fluid were fixed for 5 min with 1.6% paraformaldehyde (PFA) within 30 min of venipuncture/aspiration, respectively. These samples were defined as time 0h. In addition, another aliquot of peripheral blood and synovial fluid were incubated at 37°C for 6h in the presence of the protein transport inhibitors 1X BD GolgiStop (BD) and 1X BD GolgiPlug (BD), containing monesin and brefeldin A, respectively. Treatment with monensin and brefeldin A prevents the extracellular transport of cytokines from the cells and allowed measuring the intrinsic cytokine production rate in basal conditions. After 5h 45 mins the samples were treated with cisplatin to facilitate discrimination of dead cells, and then fixed 5 min with 1.6% PFA. These samples were defined as time 6h. After fixation of time 0h or 6h samples, red blood cells were lysed and cell suspensions were washed with PBS and stained with antibodies against the cell surface markers (Table 2.3). The samples were then permeabilised and labelled with antibodies for intracellular functional markers (Table 2.3) and data was acquired on a CyTOF Helios instrument.

## **2.4 Computational and statistical analysis**

### **2.4.1 ATAC data analysis**

ATAC-seq, Fast-ATAC and Omni-ATAC data were analysed using an in house pipeline. The pipeline performs single sample data processing and also builds a combined master list for each of the conditions of interest for chromatin accessibility characterisation and differential analysis.

## Material and Methods

---

### Markers from the CyTOF antibody panel

---

CD248, CD19, GP38, FAP, CD8a, IL8, CD16, CD25, CD123,  
IL-17F, IL-17A, IL-10, CD11c, CD14, IL6, IFN- $\gamma$ , CD-11b  
CD45RO, CD56, HLA-DR, IL-13, CD117, CD4, IL4, IL-2, TNF $\alpha$ ,  
IL-21, FceR, CD3, CD161, MCP-1, GM-CSF, CD45,  
MCP-1<sup>(\*)</sup>, osteopontin

**Table 2.3: Molecules targeted by the mass cytometry antibody panel for peripheral blood and synovial fluid samples.** The molecules targeted by the isotope-conjugated antibodies used in the CyTOF staining panel are listed. Note the panel includes antibodies targeting intra-cellular molecules and also surface markers, to identify the cell populations of interest for further analysis of the intracellular cytokine and chemokine production.

### Next generation sequencing data processing

NGS data for each sample was trimmed for low quality base pairs and Nextera adapter sequences using cutadapt (M. 2011) before general QC assessment using fastqc (S. 2010). Trimmed reads were aligned to the reference genome (build hg19) using bowtie2 (Langmead and Salzberg 2012) and the following parameters were used, -k 4 -X 2000 -I 38 --mm -1, consistent with other publications (Buenrostro et al. 2013; Corces et al. 2016). Samtools (Li et al. 2009) was used to remove PCR duplicate reads marked with Picard Tools (<http://broadinstitute.github.io/picard/>) as well as low MAPQ (<30), non-uniquely mapping and non-properly paired reads. The resulting bam file was additionally filtered to remove mitochondrial DNA and reads were adjusted by +4bp on the plus strand and by -5bp on the minus strand to represent the center of the transposition binding event. Pileup tracks (bigWig files) representing the number of reads per bp position were generated using bedtools genomeCoverageBed (Quinlan and Hall 2010) and the UCSC genome browser bedGraphToBigWig tool (Kent et al. 2010). For visualisation purposes, normalised bigWig files were generated from normalised bedgraph files with

## **Material and Methods**

---

bedtools genomecov and the library size factor estimated by the differential analysis algorithm.

### **Peak calling, filtering and sample quality assessment**

Peak calling was performed using MACS2 callpeak (Zhang et al. 2008) and the parameters --nomodel --shift -100 --extsize 200 --p 0.1 --keep-dup all --call-summits. Peaks overlapping blacklisted features from the ENCODE project (<https://www.encodeproject.org/annotations>) were removed. The --shift and --extsize parameters were set according to the recommendations of MACS2 for DHS and following other ATAC-seq publications (Buenrostro et al. 2015; Corces et al. 2016). The pval cut off for filtering called peaks was determined for each cell type using Irreproducibility Discovery Rate (IDR) analysis (as further detailed in Chapter ??ch:Results1). For this, the filtered bam file of each sample was partitioned into two equal size files (pseudoreplicates). Peak calling was performed in each pseudoreplicate, followed by filtering for a range of pvals (from 0 to  $10^{-45}$ ) and IDR analysis done for the resulting pairs of filtered peak sets. For each of the filtering pvals, the percentage of peaks sharing IDR rank between the two pseudoreplicates was determined, and the optimal pval filter identified. When more than one summit was identified in a peak, the median of the summits was used. For all peaks, summits were extended  $\pm 250\text{bp}$  to create a non-overlapping homogenous 500bp peak list for each sample (Buenrostro et al. 2015; Corces et al. 2016).

Sample quality was determined by the fold enrichment of ATAC-seq signal across all the hg19 TSSs annotated by Ensembl (175,114 features), computed as in (Buenrostro et al. 2015) using a script provided by Dr Silvia Salatino. In brief, transposition events were calculated in 1bp bins  $\pm 1,000\text{bp}$  surrounding all TSSs and normalised to the mean value of background reads (signal from -1,000 to -800). For overall library quality assessment all ATAC fragments

## **Material and Methods**

---

were considered. When assessing chromatin structure within or across the TSS, fragments of <150bp or 260340bp were used, respectively (Scharer et al. 2016). Fraction of reads in peaks (FRiP) was calculated for samples in Chapter ?? as the overlap between the peak list filtered for FDR<0.01 and all ATAC fragments using bedtools intersect with the parameter --f 0.1.

### **Combined peak master list and differential analysis**

To perform differential open chromatin analysis a non-overlapping 500bp peak master list including all samples for a particular contrast was built. Each master list was built by union of all the peaks present in at least 30% of the samples included, regardless of the subgroup to which they belonged (e.g patients or controls, synovial fluid or peripheral blood). Reads overlapping each of the peaks in the master list were retrieved for each sample using the HTSeq-count algorithm (Anders et al. 2015). Principal component analysis (PCA) was performed on all counts normalised with the vsd function from the DESeq2 v1.20 R package (Love et al. 2014).

For differential chromatin accessibility analysis, an empirical 80% confidence cut-off was calculated and used to pre-filter peaks with high noise that could be confounding the analysis (detailed in Chapter ??). Differential analysis was performed using DESeq2 with a paired design (in Chapter ?? and Chapter ??) or including batch as a covariate in the model (in Chapter 3). Peaks were annotated with proximal genes ( $\leq 5\text{Kb}$ ) using xGR2nGenes function from the XGR R package (Fang et al. 2016). These gene lists were intersected with differentially expressed genes (DEGs) from RNA-seq/scRNA-seq analysis or genes reported by psoriasis and PsA GWAS.

### 2.4.2 ChIPm data analysis

#### Next generation sequencing data processing

ChIPm NGS data from samples and inputs were processed similarly to ATAC-seq (see Section ATAC-seq, Fast-ATAC and Omni-ATAC data analysis) for trimming, mapping and filtering with minor modifications. Specifically, the MAPQ30 score for filtering reads was lowered to 10. For visualisation, bedgraph files with noise subtracted using the control input were generated using MACS2 bdgcmp -m subtract followed by conversion to bigWig with bedGraphToBigWig tools.

#### Peak calling, filtering and sample quality

Peak calling for each ChIPm sample was performed accounting for background signal using the control input samples with MACS2 callpeak --bw 200 --p 0.1 --keep-dup all --call-summits. In this case the average library fragment size (--bw) was used by MACS2 to first empirically find the model that best represents the precise protein-DNA interactions and calculate the appropriate --shift parameter. For ChIPm PCA, filtering and downstream analysis peak homogenisation was performed similarly to Section 2.4.1 to build a combined master list for all samples and cell types from cohort 1B (Chapter 3 Table 3.2 and 3.3).

Sample quality was determined by a combination of measurements. For library complexity the non-redundant fraction and PCR bottleneck coefficients (PBC1 and PBC2) were calculated following ENCODE guidelines (<https://www.encodeproject.org/chip-seq/histone/>) from unfiltered bam files. Enrichment of the ChIPm signal was evaluated based on the normalised strand cross-correlation coefficient (NSC) and relative strand cross-correlation

## **Material and Methods**

---

coefficient (RSC), calculated with SPP using bam files filtered for low MAPQ30, duplicated and non-properly paired reads.

### **Combined peak master list and differential analysis**

DiffBind (default parameters unless specified) was used to build a peak master list and perform differential H3K27ac analysis between psoriasis patients and healthy controls for each cell type. DiffBind used the unfiltered sample peak files generated by MACS2 and the filtered bam files (from samples and control inputs) to generate a master list including high quality reproducible peaks present in at least 50% of the samples (modification from default parameters) and retrieve counts of the reads mapping at the location of each peak.

### **2.4.3 Gene expression analysis**

#### **qPCR analysis**

Pre-processing of the qPCR data up to calculation of fold changes (FCs) for each gene was conducted by UCB collaborators. When comparing synovial fluid and peripheral blood isolated cells from patients, FC was calculated for each patient as the ratio between the  $2^{-dCt}$  in each of the tissues. Therefore, in a particular cell type three FCs (one per individual) were provided for each gene. When comparing expression in cells isolated from peripheral blood of PsA patients versus healthy controls, the FC for each gene and each individual was calculated as the ratio between the average  $2^{-dCt}$  in the three controls and the  $2^{-dCt}$  of a particular patient. In order to determine the significance of the FCs, one sample t-test was performed with the null hypothesis being  $H_0 : \mu = 1$  (no change) and the alternative hypothesis  $H_1 : \mu \neq 1$ .

## **Material and Methods**

---

### **Bulk RNA-seq analysis**

NGS RNA-seq data processing was performed using an in-house pipeline developed by Dr Katie Burnham. Ribo-depleted RNA-seq data was mapped against the reference genome (build hg19) using the aligner STAR (Dobin et al. 2013). Mapping allowed multiple alignments and only retained those with the best score and a mis-match percentage lower than 0.04%. Duplicates were marked and removed using Picard Tools. Gene counts were retrieved using HTSeq-count and the gencode hg19 annotation file comprising 2,840,278 gene entities, including lnc-RNAs. Differential gene expression analysis was performed with DESeq2 on genes with five or more reads in at least eight samples (smallest group size corresponding to the psoriasis patients' samples). Independent filtering of genes with low expression levels, outlier removal using Cook's distance and moderation of  $\log_2 FC$  were enabled when using DESeq2. Differentially expressed transcripts were identified based on False discovery rate (FDR)<0.05. Batch effect was included as a covariate in the contrast between psoriasis patients and healthy controls. This effect related to the RNA extraction, library preparation and sequencing of cohort 1A and cohort 1B samples from the psoriasis study (including healthy controls). Lnc-RNAs were annotated using the list provided by gencode.v19 <https://www.gencodegenes.org/releases/19.html>. The paired design of the psoriasis skin DGE analysis was taken into account by the DESeq2 model.

### **Single-cell RNA-seq analysis**

Raw Illumina sequencing data from the 10X Genomics technology Chromium single cell 3' expression libraries generated in bulk PBMCs and SFMCs from three PsA patients (see ??) were first processed using Cell Ranger v2.2 software provided by 10X Genomics technology <https://support.10xgenomics.com/single-cell-gene-expression/software/pipelines/>.

## Material and Methods

---

Illumina sequencing base call files (BCLs) were demultiplexed and converted into fastq files using cellranger mkfastq. For each of the samples, mapping of the fastq files to the compatible human transcriptome reference (GRCh38-1.2.0) and retrieval of counts for each transcript included in the reference genome were performed with cellranger count using default parameters.

The count matrix files were fully processed downstream using the R package Seurat 2.3.4 (Butler et al. 2018). Each of the PBMCs and SFMCs individual count matrices were downsampled to 3,500 cells after removing all the genes expressed in fewer than 30 cells (drop-out events). Additional filtering was conducted to remove cells presenting more than 7.5% of mitochondrial reads, a number of genes larger than  $500 \pm 1SD$  (approximately 1,800 genes in all the samples) and a maximum of 10,000 UMI. After filtering, individual PBMCs and SFMCs count matrices were processed for data scaling and normalisation (regressing number of UMI and percentage of mitochondrial counts) and PCA analysis. The first eight PCs (capturing most of the variation in the data according to jackstraw analysis) were then used to identify clusters (groups of cells with similar expression profiles) built by a shared nearest neighbor (SNN) modularity optimisation algorithm (default resolution 0.6) followed by visualisation using t-Distributed Stochastic Neighbor Embedding (t-SNE) dimensional reduction. CD14<sup>+</sup> monocyte clusters were selected based on co-expression of appropriate cell specific markers (*CD14* and *LYZ*). For each of the CD14<sup>+</sup> monocyte populations, the top variable genes were quantified by dispersion of expression (variance/mean) ratio, using a cut-off for maximum mean expression of 4 and minimum dispersion of 0.25. The union of the 1,000 most variable genes across the six CD14<sup>+</sup> monocyte samples (three from PBMCs and three from SFMCs) were used to perform canonical correlation analysis (CCA). The first nine canonical correlation vectors (CCs) were used to align all the CD14<sup>+</sup> monocyte populations. This alignment using CCA was applied in order

## **Material and Methods**

---

to merge all the CD14<sup>+</sup> monocyte datasets, removing batch effects and allowing further downstream analysis. Cluster identification and visualisation using t-SNE in the combined CD14<sup>+</sup> monocytes from the six samples was performed (further detailed in Chapter ??) followed by DGE analysis between the SFMCs and PBMCs CD14<sup>+</sup> monocyte populations.

### **2.4.4 Genomic region annotation, enrichment analysis, gene-network analysis and pathway visualisation**

Genomic region annotation with chromatin states was performed by overlapping peaks with the appropriate cell type chromatin segmentation map from Epigenome Roadmap ([https://egg2.wustl.edu/roadmap/web\\_portal/chr\\_state\\_learning.html](https://egg2.wustl.edu/roadmap/web_portal/chr_state_learning.html)).

Genomic feature enrichment analysis was performed using XGR built-in data (including eQTLs, FANTOM enhancers, histone marks and TFBS, amongst others) and the function xGRviaGenomicAnno (Fang et al. 2016). When annotating regions (ATAC or ChIPm peaks) the summit of the peaks were used to increase the specificity of the analysis. Pathway enrichment analysis was conducted for the built-in KEGG, Reactome MsigdbC2BIOCARTA and MsigdbC2CPall pathways with the xEnricherGenesAdv XGR functionality. Input data used were genes annotating differentially accessible ATAC peaks or differentially expressed genes, and background was defined as all the annotated ATAC peaks from the differential analysis master list or all the gencode hg19 detected genes, depending on the analysis.

Gene network analysis was carried out with xSubneterGenes XGR functionality using as the input list all the qPCR array genes and as significance-level the best pval across the three cell types where the expression was assayed. This list of genes was superposed onto the STRING interaction network (including known and predicted proteinprotein interactions) to obtain

## Material and Methods

---

a maximum-scoring gene subnetwork (30 genes) containing as many highly significant (highly scored) genes as possible and a lesser number of non-significant genes as linkers.

LD-based enrichment analysis of psoriasis and PsA GWAS LD blocks for differentially accessible regions (DARs) was conducted with the XGR function xLDenricher. This function allows to compute enrichment of the psoriasis and PsA GWA LD blocks for an annotation feature, in this case differentially accessible ATAC peaks, by comparing this overlap (observed) to the overlap between differential ATAC regions and a null distribution of LD blocks generated via sampling from all common SNPs (background). The sampling strategy to generate this null distribution of LD blocks respects the minor allele frequency (MAF) and the distance of the lead SNP to the nearest gene in each of the GWAS LD blocks. A number of 20,000 permutations were conducted. Similarly, enrichment analysis for PsA GWAS fine-mapped SNPs and differentially accessible regions or consensus ATAC peaks was conducted using 1,000 backgrounds of SNPs generated by SNPsnap ([https://data.broadinstitute.org/mpg/snpsnap/match\\_snps.html](https://data.broadinstitute.org/mpg/snpsnap/match_snps.html)). These backgrounds included SNPs that preserved the same LD structure, allele frequencies and proximity to genes as the fine-mapped SNPs. The fine-mapped SNPs and the matched backgrounds were co-localised using an in-house R script with (1) differentially accessible regions (DARs) or consensus ATAC peaks and (2) a window of 10Kb around the DARs or the consensus ATAC peaks for each of the cell types. Empirical p-value was computed to determine the significance of the overlap between fine-mapped SNPs and each of the features using binomial test.

Visualisation of the signalling-pathway enrichment from the RNA-seq results was performed using an R function part of the Atlas and Analysis of systems-biology-led pathways website resource, developed by Dr. Hai Fang

## **Material and Methods**

---

(manuscript in preparation). The manually curated KEGG pathways expanded with genes for each gene family were coloured based on the FC from the corresponding RNA-seq differential analysis and highlighted in bold when passing the FDR threshold for significance.

### **2.4.5 Statistical fine-mapping**

Fine mapping of the psoriasis and PsA GWAS signals was performed using a Bayesian approach, aiming to overcome the incomplete coverage of genotyping arrays and the hundreds of associations per locus due to the LD structure of the genome. Fine-mapping was conducted using two different strategies due to availability of summary statistics or genotyping data from the psoriasis and PsA Immunochip GWAS studies, respectively. Both strategies include the same main steps of imputation, association testing and calculation of PP and were implemented in collaboration with Dr Adrián Cortés.

#### **Psoriasis fine-mapping using Immunochip summary statistics**

Fine mapping was performed for X of the risk loci reported by the psoriasis Immunochip GWAS study from Tsoi and colleagues, for which only the summary statistics of the GPC Immunochip cohort (2,997 cases and 9,183 controls) were available (Tsoi et al. 2012). The summary statistics file included the pval, OR, z-score and standard error (SE) calculated for each of the genotyped SNPs using a logarithmic regression model and correcting for ten principal components. The statistic z-scores from the genotyped SNPs were used in the direct imputation of summary statistics (DIST) method to impute the z-scores for allele 1 of the missing SNPs based on the correlation in linkage disequilibrium ( $r^2$ ) from the 1000 Genome Project Version 3 (Lee et al. 2013). Imputation was performed genome-wide for all autosomes and the results were filtered based on the quality of the imputation ( $>0.8$ ). Association analysis and calculation of the ABF were

## **Material and Methods**

---

performed using Wakefield approximation for a 2Mb window around the GWAS lead SNP of each locus of interest. This approximation was applied under the priors of (1) normally distributed OR with mean and variance ( $\sigma^2$ ); (2) the greater the variance the bigger the size effects obtained will be; (3) mean is 0 and variance is fixed to 0.2 (accepted variance for GWAS studies). In this approach ABF was calculated using effect size ( $\beta$ ) and standard error (SE). SE is calculated as  $\sqrt{\sigma^2}$  and  $\beta$  is determined using the z-scores of each of the interrogated SNPs as:  $\beta = \text{z-score} * \text{SE}$ . It is important to note that step-wise conditional analysis is not performed when using summary statistics imputation. Similarly to the genotyping fine-mapping approach, PP for the SNPs in a particular window (signal) were calculated and ranked to set the threshold of the 50 and 90 % credible set of SNPs.

### **PsA fine-mapping using Immunochip genotyping data**

Fine-mapping was performed for a number of non-MHC PsA Immunochip GWAS susceptibility loci using the UK cohort (1,103 patients and 8,900 controls) from Bowes and colleagues PsA Immunochip (Bowes et al. 2015). Access to the data post-quality control was kindly provided by Dr Anne Barton (The University of Manchester) PCA analysis was performed using only pruned SNPs with flashpca (Abraham and Inouye 2014) and the calculated PCs were used as covariates in the association analysis to correct for population stratification.

For each of the fine-mapped loci a 2Mb window around the lead SNP was defined and SNPs extracted from the data using PLINK 1.9 (Chang et al. 2015). Phasing of the genotype data was performed with SHAPEIT (Delaneau et al. 2012) and used to impute missing genotypes with IMPUTE2 (Howie et al. 2009) and the 1000 Genomes Project Version 3 as the reference panel (October 2015 release). SNPs for which imputation was not successful in at least 70% of the samples (info-score<0.7) were filtered out using QCtool. The

## **Material and Methods**

---

association and conditional analysis was conducted using a Bayesian additive model implemented with SNPTEST and including the previously calculated PCs as covariates (Burton 2007). Approximated Bayes Factors (ABF) were calculated for the lead signal and step-wise conditional analysis was performed if  $\log_{10}ABF > 3$ . Credible sets of SNPs containing the variants likely to explain 50% and 90% of that association were identified for each of the signals in the locus, along with their corresponding posterior probabilities (PP) as further detailed in Bunt and colleagues (Bunt et al. 2015).

### **2.4.6 Mass cytometry data analysis**

Mass cytometry analysis was performed by Dr Nicole Yager. Cell populations in synovial fluid and peripheral blood at 0h and 6h were identified using manual annotation. For the CD14<sup>+</sup> monocyte population identified within each tissue at 0h and 6h, the percentage of TNF- $\alpha$ , MCP-1 and osteopontin positive staining cells were calculated. Significance of the differences in the percentage of positive staining cells for each cytokine between synovial fluid and peripheral blood isolated CD14<sup>+</sup> monocytes was determined using Wilcoxon signed-rank test.

# Chapter 3

## Defining the genome-wide chromatin accessibility landscape and gene expression profile in psoriasis

### 3.1 Introduction

#### 3.1.1 The systemic and skin-specific manifestations of psoriasis

In psoriasis, skin lesions represent the main manifestation of the dysregulated innate immune response triggered by the interaction between genetic and environmental factors (reviewed in Chapter 1). In addition to keratinocytes, other circulating immune cells, such as T cells or DCs, are actively recruited to the site of inflammation contributing to disease initiation and progression (Leanne et al. 2009). A number of studies have identified systemic components of psoriasis, including an increase of circulating Th-17, Th-1 and Th-22 cells in patients' blood and the impaired inhibitory function of circulating Tregs (Sugiyama 2005; Kagami et al. 2010). Activated T cells isolated from psoriasis patients' blood have demonstrated their ability to induce skin lesions in xenotransplantation models of psoriasis (Wrone-Smith and Nickoloff 1996; Nickoloff and Wrone-Smith 1999). Psoriasis patients also present increased risk for PsA following skin lesions as well as other co-morbidities, such as CVD (Ibrahim et al. 2009; Shapiro et al. 2007). Overall, these findings reinforce

## **Defining the genome-wide chromatin accessibility landscape and gene expression profile in psoriasis**

---

there being a systemic component in psoriasis and highlight the importance of investigating relevant circulating immune cells to better understand disease pathophysiology.

### **3.1.2 The personalised epigenome in disease**

The technical revolution in the epigenetics field has opened an avenue to profile the epigenome of individual cell type populations in clinical samples, contributing to the interpretation and understanding of GWAS non-coding variants. ATAC-seq and ChIPm have enabled the interrogation of chromatin accessibility, histone modifications and TF binding using a few thousand cells (Buenrostro et al. 2013; Schmidl et al. 2015). This has facilitated mapping the regulatory landscape in a wide range of cell types and tissues from clinical samples, providing details about the molecular programming of cells and the location and status of *cis*-regulatory elements in a disease-specific manner.

ATAC-seq has been used to identify inter- and intra-individual differences and pathological changes in chromatin accessibility (Qu et al. 2015). For example, differential analysis in B cells isolated from SLE patients and healthy controls has revealed changes in chromatin accessibility near genes involved in B cell activation and enriched for TFBS potentially regulating pathogenic processes (Scharer et al. 2016). Similarly, a study in age-related macular degeneration (AMD) has identified the retina epithelium as the main tissue driving disease onset through global loss of chromatin accessibility in comparison to healthy tissue (Wang et al. 2018).

In addition to the study of chromatin accessibility, the characterisation of histone modifications provides further functional information to understand the cell type specificity of the regulatory landscape. For example, in chronic lymphocytic leukaemia ChIPm has been used to identify subtype-specific epigenome signatures based on the interrogation of several histone marks

## **Defining the genome-wide chromatin accessibility landscape and gene expression profile in psoriasis**

---

(Rendeiro et al. 2016). As GWAS SNPs are mostly located in intergenic regions that may act as gene expression regulatory elements, assessing the active enhancer mark H3K27ac is of particular interest here. However, disease-specific data to use in this type of analysis is currently unavailable for most of the complex diseases. A relevant example of enhancer profiling through H3K27ac assay has been conducted in the autoimmune disease juvenile idiopathic arthritis, where a disease-specific H3K27ac super-enhancer (those spanning up to 50Kb) signature has been identified in SF mCD4<sup>+</sup> cells (Peeters et al. 2015). In addition to this, inhibitors of histone de-acetylases (HDACs) are being investigated as potential therapeutic agents for RA and SLE, amongst others (Hsieh et al. 2014; Shu et al. 2017).

### **3.1.3 Transcriptional profiles in psoriasis**

#### **Trancriptomics in psoriatic skin**

Characterisation of transcriptional profiles in complex diseases has been performed to better understand disease pathophysiology and assess the role of genetic variability in regulating gene expression. In psoriasis, the majority of transcriptional studies have been performed for inflamed skin (lesional) using pre-lesional (uninvolved) skin, adjacent to the lesion, as the best internal control accounting for biological variability (Table 3.1).

**Defining the genome-wide chromatin accessibility landscape and gene expression profile in psoriasis**

**Table 3.1: Summary table of the most comprehensive transcriptional studies in psoriasis skin and blood.** SB= whole skin biopsy; EpB=epidermal biopsy; CK=cultured keratinocytes; C=control; L= psoriatic lesional skin; U=psoriatic uninvolved skin.

Author and year	Sample type and size	Technology	Description
(Jabbari et al. 2012)	SB (L=3, U=3)	RNA-seq microarray	and Technology discrepancies
(Li et al. 2014)	SB (L=92, C=82)	RNA-seq microarray	and Technology discrepancies and lncRNAs targets
(Keermann et al. 2015)	SB (L=12, U=12, C=12)	RNA-seq	co-regulation Dormant psoriasis signature and <i>IL36</i> expression in psoriasis skin
(Tsoi et al. 2015)	SB (L=97, U=29, C=90)	RNA-seq	Psoriatic skin-specific new lncRNAs
(Swindell and Remmer 2015)	SB (L=14, U=14)	RNA-seq and mass-spectrometry	209 co-regulated mRNA-proteins
(Swindell et al. 2017)	CK (L=4, U=4, C=4)	RNA-seq	Decreased differentiation gene signature in lesional skin
(Tervaniemi et al. 2016)	EpB (L=6, U=6, C=9)	RNA-seq	NOD-like and inflammasome pathways

## Defining the genome-wide chromatin accessibility landscape and gene expression profile in psoriasis

---

(Coda et al. 2012)	PBMCs (PS=6, C=5) and SB (L=5, U=5)	Microarray	Partial overlap between PBMCs and skin DEGs
(Lee et al. 2009)	PBMCs (PS=5, C=8)	Microarray	202 DEGs, circulating gene expression signature
(Mesko et al. 2010)	PBMCs(PS=15, IBD=12,RA=12, C=18)	TaqMan customised array (96 genes)	6 psoriasis-specific DEGs
(Palau et al. 2013)	Activated CD4+ <sup>+</sup> and CD8 <sup>+</sup> (PS=17, C=7)	Microarray	42 DEGs in T cell activation ( <i>SPATS2L</i> and <i>KLF6</i> )
(Jung et al. 2004)	IL-10 stimulated PBMCs and CD14 <sup>+</sup> (C=5), IL-10 therapy PBMCs (PS=4)	Microarray	High correspondence between <i>in vitro</i> and <i>in vivo</i> IL-10 driven DEGs

## **Defining the genome-wide chromatin accessibility landscape and gene expression profile in psoriasis**

---

Other studies have also incorporated healthy control skin biopsies to ascertain the extent of dysregulation of the transcriptomic profile prior to lesion development in uninvolved skin (Table 3.1). Interestingly, discrepancies regarding the transcriptional similarities between normal and uninvolved skin have been identified, likely due to different filtering criteria for magnitude of effect (Keermann et al. 2015; Tsoi et al. 2015).

The latest transcriptomic studies in psoriasis using RNA-seq have demonstrated greater sensitivity as well as the ability to identify non-coding RNA species, such as lncRNAs, in an unbiased way (Jaabari 2011; Li et al. 2014). LncRNAs expression has also been proven to have a role in psoriasis pathophysiology, showing approximately 1,000 species differentially expressed between lesional and uninvolved skin (Tsoi et al. 2015). Interestingly, comparison of protein abundance and DGE in psoriatic skin has revealed that only 5% of the dysregulated transcripts present a similar trend at the protein level (Swindell and Remmer 2015).

The majority of the transcriptional studies have been performed in whole skin biopsies containing a mix of tissues from the epidermis, dermis, basal layer, muscle and adipose tissue (Table 3.1). Lately, studies in psoriatic cultured keratinocytes (from lesional and uninvolved biopsies) and epidermis from split-thickness skin grafts have identified differences in gene expression and functional pathway enrichment compared to the studies based on whole skin biopsies (Swindell et al. 2017; Tervaniemi et al. 2016). These results reinforce the importance of using homogenous tissue and cell type samples to better dissect the altered biological processes contributing to the development of psoriasis at the site of inflammation.

### **Transcriptomics in circulating immune cells**

A limited number of comprehensive transcriptional studies comparing circulating immune cells between psoriasis patients and healthy controls have been conducted. The majority of these studies have investigated changes in gene expression between psoriasis and healthy controls in mixed PBMC populations using microarray technologies (Table 3.1).

A study conducted by Coda and colleagues explored the overlap between the differentially expressed genes (DEGs) in PBMCs (psoriasis versus controls) and comparing lesional and uninvolved skin biopsies (Coda et al. 2012). The results revealed a limited overlap with more than 50% of the common genes presenting opposite directions of modulation in the two tissues. At the cell type specific level, some studies have performed *in vitro* culture and stimulation of T cells and monocytes (Palau et al. 2013; Jung et al. 2004). For instance, Palau and colleagues found forty-two DEGs enriched for cytokine and IFN ( $\alpha$ ,  $\beta$  and  $\gamma$ ) signalling pathways when comparing activated CD4 $^{+}$  and CD8 $^{+}$  T cell from psoriasis patients and healthy controls. Further understanding of psoriasis-specific systemic gene dysregulation has also been approached through comparison with other chronic inflammatory diseases (Mesko et al. 2010).

#### **3.1.4 Chromatin accessibility, gene expression and genetic variability**

As described in Chapter 1, accessible chromatin is more likely to be bound by TFs and other co-regulatory proteins, and so can be used as a proxy to tag genomic loci involved in regulation of gene expression and to infer the putative functional relevance of GWAS SNPs. The orchestration of cell type specific changes in the chromatin landscape and gene expression is pivotal for an appropriate immune response (Goodnow et al. 2005). For example,

## **Defining the genome-wide chromatin accessibility landscape and gene expression profile in psoriasis**

---

integration of ATAC-seq data and gene expression in pancreatic islets has revealed chromatin accessibility to be a better predictor for gene activation in  $\alpha$ - compared to  $\beta$  cells, which could be explained by the heterogeneity within each cell population or cell type intrinsic differences in gene regulation. In AMD clinical samples, integration of ATAC and gene expression found moderate correlation between the two in retina and pigmented epithelium retina (Wang et al. 2018). In the context of genetic variability, the relationship between chromatin accessibility and gene expression in homeostasis and stimulated conditions has been addressed by integrating eQTL and chromatin accessibility QTLs (ca-QTLs). For example, enhancer priming events have been described in human iPS derived macrophages, where the same genetic variants leads to changes in chromatin accessibility in the naïve state prior to changes in gene expression upon stimulation (Alasoo et al. 2018).

### **3.1.5 Fine-mapping using summary stats**

The generation of cell type specific epigenetic maps can be used to inform statistical fine-mapping in the effort to identify putative causal SNPs to undergo functional validation (detailed in Chapter 1). Integration of Bayesian fine-mapping for twenty-one complex immune diseases performed by Farh and colleagues demonstrated greatest enrichment of fine-mapped causal variants in immune cell enhancer elements, particularly from activated conditions (**Farh2014**). In this study, psoriasis PICS showed the most significant enrichment for Th-1, Th-2 and Th-17 subsets. Furthermore, exhaustive fine-mapping using a customised genotyping array has been conducted for eight psoriasis GWAS loci using a frequentist approach which measure the association of each SNP through p-values (Das et al. 2014).

Traditional Bayesian fine-mapping requires genotyping data from the GWAS cohorts to perform genotype phasing and imputation prior to association

## **Defining the genome-wide chromatin accessibility landscape and gene expression profile in psoriasis**

---

analysis and calculation of posterior probabilities (PP) and credible sets of SNPs. Restricted access to GWAS genotyping data, commonly due to ethical reasons, can be a limitation when performing this type of analysis. Since summary statistics from GWAS studies are widely available, methods like DIST have been developed to impute summary statistics instead of genotypes for the unmeasured SNPs in the study (Lee et al. 2013). In addition to this, summary statistics Bayesian fine-mapping methods using functional annotation as a prior in the model have also been developed (Li et al. 2016).

### **3.2 Aims**

The aim of this chapter is to determine chromatin accessibility, histone modification and gene expression differences between psoriasis patients and controls in four circulating immune cell types ( $CD14^+$  monocytes,  $CD4^+$  and  $CD8^+$  T cells and  $CD19^+$  B cells) and to complement this with analysis of differential gene expression in lesional and uninvolved epidermis isolated from psoriatic skin biopsies. The long term goal is to identify disease and cell type specific changes in putative regulatory regions and integrate them with observed differences in gene expression to improve the understanding of systemic and skin inflammatory features of psoriasis and prioritise putative causal GWAS variants.

The specific aims for this chapter are:

1. To identify differences in chromatin accessibility and the H3K27ac active enhancer mark between psoriasis patients and healthy controls in immune cells isolated from peripheral blood.
2. To determine changes in genes expression between psoriasis patients and healthy controls in immune cells isolated from peripheral blood.
3. To identify differentially expressed genes between lesional and uninvolved epidermis isolated from psoriatic skin biopsies.

4. To compare the differences in the transcriptomic profile from circulating immune cells between patients and controls with the transcriptional differences from contrasting lesional and uninvolved epidermis.
5. To conduct fine-mapping analysis for a number of psoriasis GWAS loci using summary statistics.
6. To integrate fine-mapped credible set of SNPs with disease and cell type specific epigenetic maps, gene expression profiles and publicly available data to narrow down the putative causal variants from GWAS risk loci.

### **3.3 Results**

#### **3.3.1 Psoriasis and healthy controls: cohort description and datasets**

Peripheral blood samples were collected from a cohort of psoriasis patients and healthy individuals in order isolate four relevant immune cells types ( $CD14^+$  monocytes,  $CD4^+$ ,  $CD8^+$  and  $CD19^+$ ) and perform ATAC-seq, RNA-seq and ChIPm analysis. Additionally, the epidermis from paired uninvolved and lesional skin biopsies collected from three psoriasis patients were processed downstream for RNA-seq analysis.

A total of 8 psoriasis patients, 6 males and 2 females (Table 3.2) were recruited following eligibility criteria detailed in Chapter 2 .

**Defining the genome-wide chromatin accessibility landscape and gene expression profile in psoriasis**

---

**Table 3.2: Description and metadata of the psoriasis patients cohort.** For each of the individuals information relating to sex, age , disease duration (in months), PASI score, nail involvement and family history has been recorded. Patients are divided into cohort 1A and cohort 1B based on the timing (batch) of ATAC and RNA-seq processing and type of ATAC-seq protocol applied. PASI score is detailed in Table 1.1. Available datasets from peripheral blood isolated cells (ATAC, ChIPm, RNA-seq) and skin biopsies (skin RNA-seq) are indicated for each sample. The skin RNA-seq samples include lesional and uninvolved paired-skin biopsies from each of the three individuals.

Sample ID	Sex	Age (years)	Disease duration	PASI	Nails affected	Family history	ATAC	ChIPm	RNA-seq	Skin RNA-seq
Cohort 1A										
PS1011	Male	55	420	11	Yes	No	Yes	No	Yes	Yes
PS2014	Female	65	588	17	No	No	Yes	No	Yes	No
PS2015	Male	56	384	5	Yes	No	Yes	No	Yes	Yes
PS2016	Male	40	180	10	No	No	Yes	No	Yes	Yes
Cohort 1B										
PS2000	Male	61	156	10	No	Yes	Yes	Yes	Yes	No
PS2001	Male	56	432	10	Yes	No	Yes	Yes	Yes	No
PS2314	Male	42	120	6.5	Yes	No	Yes	Yes	Yes	No
PS2319	Female	64	372	10.2	No	Yes	Yes	Yes	Yes	No

**Defining the genome-wide chromatin accessibility landscape and gene expression profile in psoriasis**

---

Mean ( $\pm$ SD)	55 ( $\pm$ 9.4)	331.5 ( $\pm$ 163.3)	10 ( $\pm$ 3.5)

## **Defining the genome-wide chromatin accessibility landscape and gene expression profile in psoriasis**

---

The mean age of the cohort was 55 years old and the mean disease duration 331.5 months. All the patients presented active skin disease and none of them had reported joint involvement at the time of sample collection. Disease severity was quantified using the PASI score, previously reviewed in Chapter 1, with the mean cohort score being 10. Currently, there is no consensus on PASI thresholds to define mild and moderate-to-severe disease. A review study regarding the use of PASI as an instrument to determine disease severity of chronic-plaque psoriasis have suggested considering psoriasis as moderate when PASI ranges between 7 to 12 and severe for PASI>12 (Schmitt and Wozel 2005). On the other hand, NICE and other studies had defined psoriasis as severe based on PASI $\geq$ 10 (Woolacott et al. 2006; Finlay 2005). In this cohort, six out of ten patients had PASI $\geq$ 10, and so were categorised as having severe psoriasis. Only two of them showed PASI<7 showing a mild psoriasis phenotype. All patients were naïve for biologics therapies. PS2319 was currently on methotrexate therapy and the remaining patients had only been treated occasionally with topical steroids or UVB therapy. Interestingly, PS2014 showed the most severe PASI score (17) and was a non-responder to methotrexate. Patients PS1011, PS2015, PS2001 and PS2314 presented nail pitting, which has been defined as one of the markers for increased risk of developing joint affection and PsA (Moll et al. 1973; Griffiths and Barker 2007; McGonagle et al. 2011). A family history of psoriasis was reported by PS2000 and PS2319. In addition to the psoriasis samples, peripheral blood was collected from 10 sex and age-matched healthy individuals (Table 3.3).

For both cohorts, ATAC-seq and RNA-seq data were generated from CD14 $^{+}$  monocytes, CD4 $^{+}$ , CD8 $^{+}$  and CD19 $^{+}$  cells (Tables 3.2 and 3.3). For cohort 1A, ATAC data was generated using the ATAC-seq protocol from Buenrostro *et al.*, 2013, which was replaced by the Fast-ATAC method from Corces and colleagues (Corces et al. 2016) in cohort 1B, due to the improvements of this protocol as explained in Chapter ???. Additionally, samples from cohort 1B were also

## Defining the genome-wide chromatin accessibility landscape and gene expression profile in psoriasis

---

Sample ID	Sex	Age (years)	ATAC	ChIPm	RNA-seq
<b>Cohort 1A</b>					
CTL1	Male	36	Yes	No	Yes
CTL2	Male	53	Yes	No	Yes
CTL3	Male	34	Yes	No	Yes
CTL4	Female	46	Yes	No	Yes
CTL5	Male	42	Yes	No	Yes
<b>Cohort 1B</b>					
CTL6	Male	31	Yes	Yes	Yes
CTL7	Male	57	Yes	Yes	Yes
CTL8	Female	50	Yes	Yes	Yes
CTL9	Male	50	Yes	Yes	Yes
CTL10	Male	67	Yes	Yes	Yes
Mean ( $\pm$ SD)	–	46.6 11.2			

**Table 3.3: Description of the healthy control cohort.** Controls are divided in cohort 1A and cohort 1B based on the timing (batch) of ATAC and RNA-seq processing and type of ATAC protocol, similarly to the psoriasis patients samples. For each of the samples, availability of ATAC, ChIPm and RNA-seq generated from peripheral blood isolated cells are indicated.

processed to assess differences in H3K27ac modification between patients and controls using ChIPm. For 3 of the psoriasis patients (PS2014, PS2015 and PS2016) paired biopsies from lesional and uninvolved skin were collected and the epidermal sheets were isolated to perform RNA-seq differential analysis (Table 3.2). This should be considered as a pilot study aiming to refine the previous RNA-seq studies performed in whole skin biopsies, with a more heterogeneous cell type composition compared to epidermis, which could not be expanded due to time and cost constraints.

### **3.3.2 Investigation of psoriasis-specific changes in the enhancer mark H3K27ac in different peripheral blood immune cell populations**

#### **Data processing and quality control**

A total of 32 ChIPm libraries from four patients and four controls in four peripheral blood immune cell types were sequenced, and reads filtered as detailed in Chapter 2. After filtering, the total number of reads ranged between 46.9 and 60.5 million, compliant with the 40 million total reads recommended by ENCODE (Figure 3.1A). As part of the quality control, library complexity for each of the samples was measured based on non-redundant fraction and the PCR bottlenecking coefficients PBC1 and PBC2. According to the ENCODE standards, most of the libraries had appropriate complexity and moderate to mild bottlenecking (Table A.2). The CD8<sup>+</sup> CTL7 and the CD19<sup>+</sup> PS2000 and PS2314 libraries failed the recommended complexity non-redundant fraction values and also had more severe PCR bottlenecking (based on PBC1 coefficient threshold). These observations were consistent with the greater number of duplicated reads identified in these libraries compared to the rest (>50% of the total sequenced reads) and consequently lower number of reads after filtering (Figure 3.1A).

Cross-correlation analysis was performed to determine the NSC and RSC coefficients, which provide a measure for the signal-to-noise ratios in the samples. All the ChIPm libraries showed appropriate signal-to-noise following ENCODE standards (Landt et al. 2012), with NSC and RSC values equal or greater than 1.05 and 0.8, respectively (Figure 3.1B and C). Interestingly, the CD14<sup>+</sup> monocytes and CD4<sup>+</sup> ChIPm libraries had lower signal enrichment compared to the CD8<sup>+</sup> and CD19<sup>+</sup> libraries, which correlates with the cell type grouping during sample processing. Following QC, the CD8<sup>+</sup> CTL7 and the CD19<sup>+</sup> PS2000 and PS2314 libraries were removed for downstream analysis.

## Defining the genome-wide chromatin accessibility landscape and gene expression profile in psoriasis

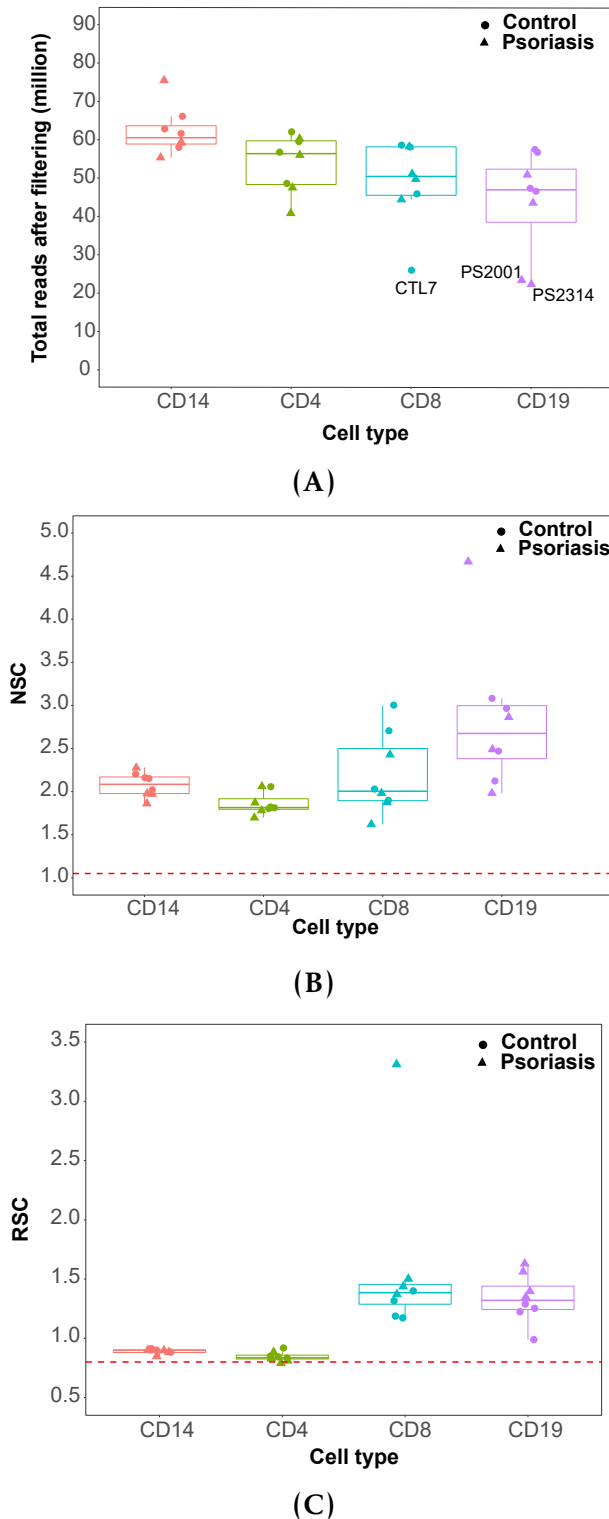


**Figure 3.1: Quality control evaluation of the H3K27ac ChIPm libraries in immune cells isolated from psoriasis and control samples.** For each of the cell types boxplots representing (A) million of reads after filtering, (B) normalised strand cross-correlation coefficient (NSC) and (C) relative strand cross-correlation coefficient (RSC). NSC and RSC are measures of signal enrichment independent of peak calling, where 1 and 0 indicate no enrichment, respectively. In (C) and d) the dashed red line indicates the ENCODE threshold for low enrichment (NSC<1.05 and RSC<0.8). For each point, colour codes for cell type and shape for phenotype (psoriasis or control).

## **Defining the genome-wide chromatin accessibility landscape and gene expression profile in psoriasis**

---

PCA using a combined list of consensus H3K27ac called peaks in the 32 samples, which included patients and controls in all 4 cell types (excluding the aforementioned low quality samples), confirmed the ability of this data to identify cell type specific differences in the enhancer landscape and reinforced the appropriate quality of the data (Figure 3.2A). When PCA was then conducted per cell type, PS2314 CD8<sup>+</sup> library appeared as an outlier compared to the rest of CD8<sup>+</sup> H3K27ac ChIPm samples and was also removed for downstream analysis (data not shown).

### **H3K27ac differential analysis**

Following data quality control, an exploratory analysis was conducted to find differences in H3K27ac modifications between patients and controls using DiffBind in each cell typ. For each of the 4 cell types analysed, DiffBind assembled a consensus list of H3K27ac peaks used to perform differential analysis (as explained in Chapter 2 and Table Table A.3). Annotation with chromatin states of each consensus list of H3K27ac peaks showed a high percentage of sites annotated as heterochromatin or repetitive (Figure 3.2B), ranging from 20.8% in CD14<sup>+</sup> monocytes to 51.39% in CD8<sup>+</sup> cells. Such sites are less likely to be relevant since H3K27ac is a histone modification mainly enriched at enhancer regulatory elements. Therefore, the differential analysis for H3K27ac modifications between psoriasis and healthy control samples in each cell type was restricted to those H3K27ac peaks annotated as enhancers (weak and strong) (Table A.3). CD14<sup>+</sup> monocytes had the greatest number of differentially modified enhancers (8 significant sites), followed by CD4<sup>+</sup> (4) and CD8<sup>+</sup> (1) (Table 3.4).

Some of the H3K27ac differentially modified regions when comparing patients versus controls appeared to be proximal to potentially relevant genes in chronic inflammation. FOr example, a differential H3K27ac regions in CD14<sup>+</sup> monocytes was located between the *SLC15A2* and *ILDR2* genes (Figure 3.3).

## Defining the genome-wide chromatin accessibility landscape and gene expression profile in psoriasis

---

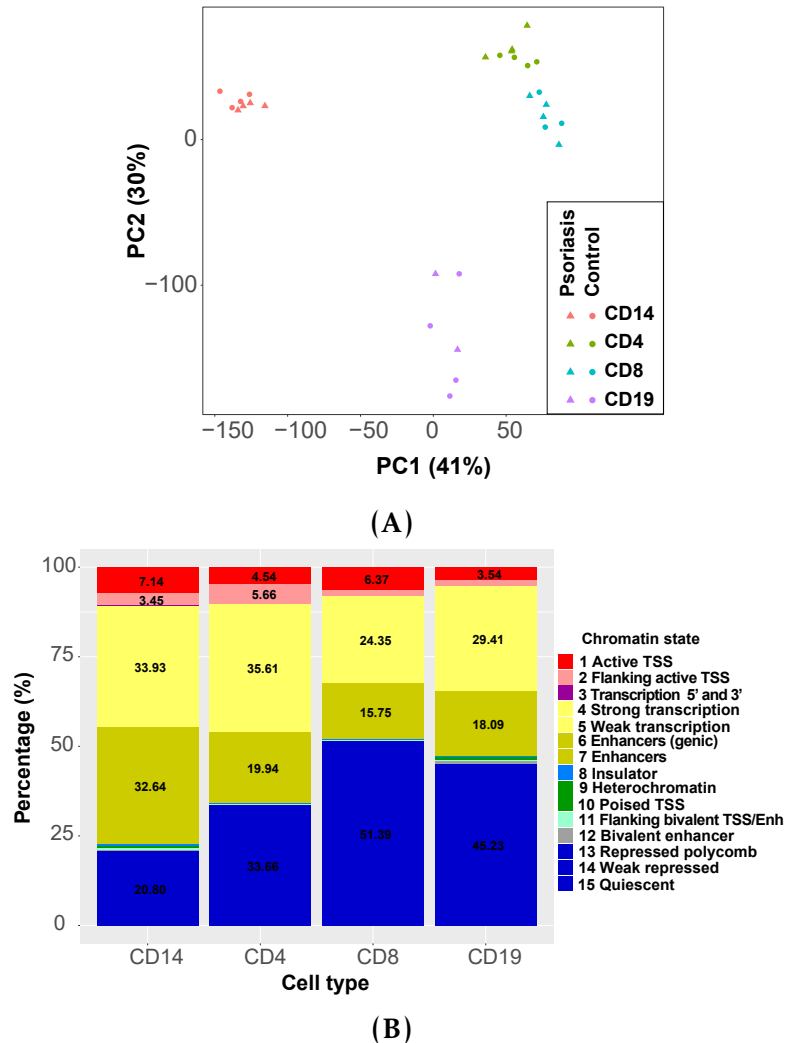


**Figure 3.2: PCA and chromatin annotation states of the consensus list of H3K27ac called peaks in four immune primary cell types from psoriasis and healthy control samples.** (A) PCA analysis was performed using the normalised counts across a consensus master list of the combined H3K27ac enriched regions in psoriasis patients and healthy control samples across CD14<sup>+</sup> monocytes, CD4<sup>+</sup>, CD8<sup>+</sup> and CD19<sup>+</sup> cells. (B) Annotation of the H3K27ac list of consensus enriched sites built by DiffBind for each cell was performed using the appropriate cell type specific Roadmap Epigenomic Project chromatin segmentation maps. Results are expressed as the percentage of regions annotated with a particular chromatin state over the total number of H3K27ac enriched sites in each individual cell type master list.

## Defining the genome-wide chromatin accessibility landscape and gene expression profile in psoriasis

---

Cell type	Differential regions genome-wide	Differential regions enhancers
CD14 <sup>+</sup>	15	8
CD4 <sup>+</sup>	0	4
CD8 <sup>+</sup>	8	1
CD19 <sup>+</sup>	12	0

**Table 3.4: Summary results from the differential H3K27ac analysis between psoriasis patients and healthy controls in CD14<sup>+</sup> monocytes, CD4<sup>+</sup>, CD8<sup>+</sup> and CD19<sup>+</sup> cells.** Differential analysis was performed genome-wide in all the DiffBind H3K27ac consensus sites or only at the consensus sites annotated as enhancers (according to the chromatin segmentation map from Roadmap Epigenomics Project). Genome-wide differential significant sites in CD14<sup>+</sup> monocytes and CD8<sup>+</sup> also contain the sites identified in the enhancer restricted analysis. Significant differentially H3K27ac modified regions were determined using FDR<0.05 and no fold change threshold.

*ILDR2* has recently been identified as relevant for negative regulation of T cells response in RA (Hecht et al. 2018). This region showed lower H3K27ac levels in psoriasis patients compared to controls and was annotated as enhancer by the Roadmap Epigenomics Project chromatin segmentation map. Additionally this site was overlapping a DHS and H3Kme1 (enhancer mark) modification and a CTCF-binding site identified by ChIP-seq in K562 cells.

Genome-wide differential analysis revealed additional H3K27ac differential regions between psoriasis and control samples in CD14<sup>+</sup> monocytes and CD8<sup>+</sup> cells, which also included those already identified in the restricted enhancer analysis (Table 3.4).

Overall, restricting the analysis to enhancer annotated regions based on chromatin segmentation maps did not significantly increase the number of observed differentially modified H3K27ac sites when compared to the genome-wide analysis in any of the 4 cell types. The results in this pilot cohort did not show relevant global epigenetic changes in H3K27ac sites between psoriasis patients and controls for these cell types and sample size.

## Defining the genome-wide chromatin accessibility landscape and gene expression profile in psoriasis

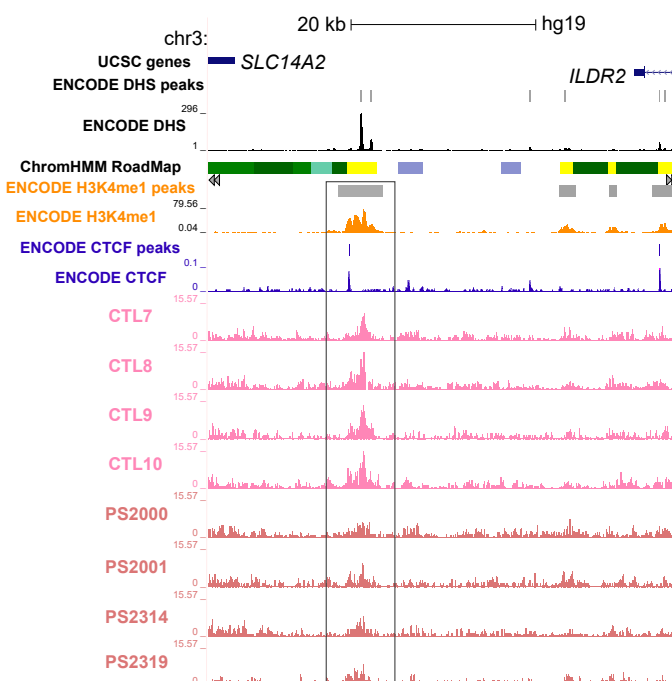


**Figure 3.3: Differential H3K27ac modification at a putative intergenic enhancer region in circulating CD14<sup>+</sup> monocytes between psoriasis patients and healthy controls.** UCSC Genome Browser view illustrating the normalised H3K27ac fold-enrichment (y-axis) at an intergenic differentially modified region located between *SLC14A2* and *ILDR2* genes (x-axis) in CD14<sup>+</sup> monocytes (lower H3K27ac enrichment in psoriasis patients compared to healthy controls). CD14<sup>+</sup> monocytes publicly available epigenetic data from ENCODE (including DHS, H3K4me1 and CTCF ChIP-seq) and the Epigenome Roadmap chromatin segmentation track are also shown. Differential H3K27ac modified regions were considered significant based on FDR<0.05 and no fold change cut-off. H3K27ac tracks are colour-coded by condition: control(CTL)=pink and psoriasis (PS)=sienna.

## Defining the genome-wide chromatin accessibility landscape and gene expression profile in psoriasis

### 3.3.3 Identifying global changes in chromatin accessibility between psoriasis patients and healthy controls for different peripheral blood immune cell populations

In order to interrogate genome-wide changes in chromatin accessibility between patients and controls, ATAC-seq was performed in the same four cell types in eight patients and ten controls (Table ??) giving a total of 72 libraries.

#### Data processing and quality control

The median total reads of the ATAC libraries after filtering ranged between 39.2 and 49.8 million in CD4<sup>+</sup> and CD19<sup>+</sup> cells, respectively (over 15 million reads determined as appropriate minimum in Chapter ??) for all samples (Figure 3.4A).

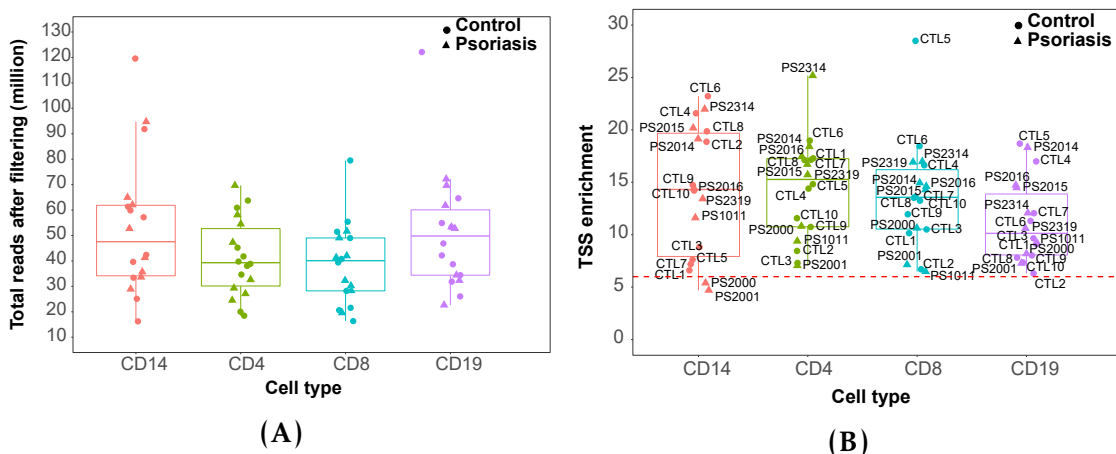


**Figure 3.4: Quality control assessment of the ATAC libraries generated from circulating immune cells in psoriasis and control samples.** For each of the cell types and samples, boxplots showing (A) million of reads after filtering and (B) values for fold-enrichment of ATAC fragments across the Ensembl annotated TSS. In (B) the dashed red line indicates the recommended ENCODE threshold for TSS enrichment values. For each point, colour codes for cell type and shape for phenotype (psoriasis or control). In (B) sample IDs are included.

Differences in the percentage of mitochondrial reads were noticeable between samples from cohort 1A generated with ATAC-seq protocol from Buenrostro *et al.*, 2013 and the Fast-ATAC libraries from cohort 1B using the later

## **Defining the genome-wide chromatin accessibility landscape and gene expression profile in psoriasis**

---

modified (Corces et al. 2016) protocol (Figure B.5A). All the samples showed the required characteristic ATAC-seq fragment size distribution recapitulating nucleosome periodicity (previously detailed in Chapter ??). Analysis of ATAC signal enrichment across gene TSSs revealed that most of the samples had enrichment over 6 (Figure 3.4B) and only PS2000 and PS2001 CD14+ monocytes were removed from downstream analysis due to low signal-to-noise ratios (<6). When comparing the number of peaks passing IDR filtering in each samples versus the number of reads after filtering, most of the samples showed between 10,000 and 35,000 peaks (Figure B.5B) and the majority of the differences in number of called peaks were intrinsic to the cell type and the signal-to-noise differences in the samples (previously studied in Chapter ??). Importantly, CD19<sup>+</sup> CTL2 appeared to be an outlier, with a noticeably lower number of peaks for its high sequencing depth (Figure 3.4 c). This observation together with its border line TSS enrichment supported removal of the CD19<sup>+</sup> CTL2 sample from downstream analysis.

A heatmap illustrating sample distance using the combined consensus list of called ATAC peaks across all the samples (named here as CP\_all) showed successful separation of the samples according to the cell type into three main clusters corresponding to CD14<sup>+</sup> monocytes, CD19<sup>+</sup> and CD4+/CD8<sup>+</sup> T cells (Figure 3.5A). Within each of the cell type clusters, samples did not separate based on disease condition, suggesting the absence of major global differences in the chromatin accessibility landscape between psoriasis patients and control samples. Conversely, within the cell types some grouping of ATAC samples by batch was observed (Figure 3.5A).

## Defining the genome-wide chromatin accessibility landscape and gene expression profile in psoriasis

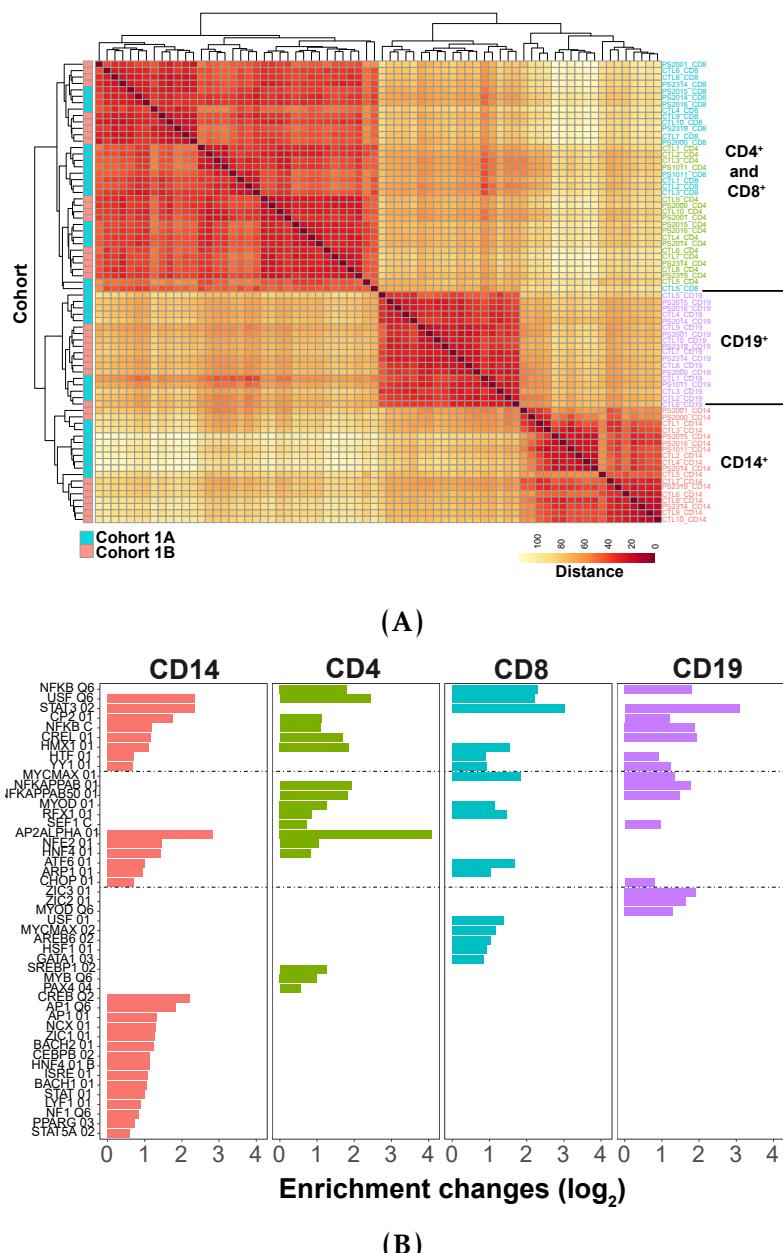


**Figure 3.5: Clustered heatmap and conserved TFBS enrichment analysis in the consensus list of called ATAC peaks in CD14<sup>+</sup> monocytes, CD4<sup>+</sup>, CD8<sup>+</sup> and CD19<sup>+</sup> cells from the patients and controls cohort.** (A) Distance matrix and hierarchical clustering for the 72 samples was performed based on the normalised read counts retrieved for each sample at the regions included in a combined consensus list of called ATAC peaks across all 4 cell types (CP\_all). Clusters have been additionally annotated using cohort identity. (B) Enrichment analysis for the conserved TFBS was performed for each of the consensus list of ATAC peaks per cell type used for downstream differential analysis between psoriasis and control individuals (named here as CP\_CD14, CP\_CD4, CP\_CD8, and CP\_CD19). Enrichment was tested for 258 human conserved TFBS identified by Transfac using position-weight matrices based on experimental results in the scientific literature. Significant enrichment using FDR<0.01.

## Defining the genome-wide chromatin accessibility landscape and gene expression profile in psoriasis

---

### Differential chromatin accessibility analysis

To perform differential chromatin accessibility analysis between patients and controls, a consensus list of called ATAC peaks (accessible chromatin regions) was built for each of the 4 cell types (named here as CP\_CD14, CP\_CD4, CP\_CD8, and CP\_CD19) (detailed in Chapter 2). Each cell type consensus list of called peaks was significantly enriched ( $FDR < 0.01$ ) for conserved TFBS (Figure 3.5B). For example, enrichment of conserved NF $\kappa$ B binding motifs was identified across each cell type list consensus ATAC peaks. Conserved binding motifs for TF involved in T cell biology, such as AREB6 (ZEB1), ATF6 and the heat-shock transcription factor HSF1 (Guan et al. 2018; Yamazaki et al. 2009; Gandhapudi et al. 2013), were enriched in the CP\_CD8. Enrichment for relevant cell type specific *cis*-eQTLs was also observed. For example, eQTLs from unstimulated and stimulated (LPS or IFN- $\gamma$ ) monocytes were the most significantly enriched ( $FDR < 0.01$ ) in the CP\_CD14 (unstimulated fold-enrichment 5.1, LPS 2h fold-enrichment 4.7 and IFN- $\gamma$  fold-enrichment 5.0 from Fairfax et al., 2014 data) when compared to the other eQTL datasets. The observed enrichment of eQTL SNPs and conserved TFBS demonstrated functional relevance of the consensus list of ATAC called peaks used in the downstream differential analysis between psoriasis and control samples for each cell type and further confirmed the quality of the ATAC data.

The differential analysis between patients and controls was performed on the ATAC normalised read counts for CP\_CD14, CP\_CD4, CP\_CD8, and CP\_CD19 using DESeq2. PCA performed in the count data of each cell type consensus list of called ATAC peaks prior to the differential analysis revealed a batch effect correlating with the different ATAC protocols used in cohort 1A and cohort 1B (ATAC-seq and Fast-ATAC, respectively) (Figure B.6A). Therefore, the ATAC-seq protocol was included as a covariate in the differential analysis model. Moreover,

## **Defining the genome-wide chromatin accessibility landscape and gene expression profile in psoriasis**

---

CTL5 appeared as a cohort 1A outlier for all the cell types (representative example Figure B.6A) and was also removed from the differential analysis.

Genome-wide differential chromatin accessibility analysis revealed 55 significant ( $\text{FDR} < 0.05$ ) differentially accessible regions (DARs) between psoriasis patients and healthy controls in  $\text{CD8}^+$  cells (Table 3.5), of which 17 showed  $\text{FDR} < 0.01$ . Conversely,  $\text{CD14}^+$  monocytes,  $\text{CD4}^+$  and  $\text{CD19}^+$  cells only showed one or no DARs.

Cell type	Number of DARs $\text{FDR} < 0.05$
$\text{CD14}^+$	1
$\text{CD4}^+$	0
$\text{CD8}^+$	55
$\text{CD19}^+$	1

**Table 3.5: Summary results from the differential chromatin accessibility analysis between psoriasis patients and healthy controls in  $\text{CD14}^+$  monocytes,  $\text{CD4}^+$ ,  $\text{CD8}^+$  and  $\text{CD19}^+$  cells.** The number of DARs refers to those statistically significant when using a cut-off for background reads of 80% (see Chapter ??) and a  $\text{FDR} < 0.05$ . No threshold for the fold change was applied.

Annotation of the 55  $\text{CD8}^+$  DARs using cell type specific Roadmap Epigenomics chromatin segmentation maps revealed the potential for some of the regions to be involved in regulation of gene expression, including 24 (44.4%) weak enhancers, 7 (12.9%) active promoters, 6 (11.1%) weak promoter and 2 (3.7%) strong enhancers. The functional relevance of the DARs in terms of regulation of gene expression was further investigated by integration of the  $\text{CD8}^+$  T cell eRNA data from the FANTOM5 project. Of the  $\text{CD8}^+$  DARs, 8 overlapped significantly expressed eRNAs in the same cell type. These included a region at the TSS of the *TNSF11* gene and another upstream the *IL7R* promoter, which were more accessible in the psoriasis patients compared to the healthy controls (Figure 3.6A and B). The two DARs also overlap chromatin harbouring H3K4me3, a histone mark indicating an active promoter, and

## Defining the genome-wide chromatin accessibility landscape and gene expression profile in psoriasis

H3K27ac consistent with the transcription of those regions as eRNAs in CD8<sup>+</sup> cells according to FANTOM5.

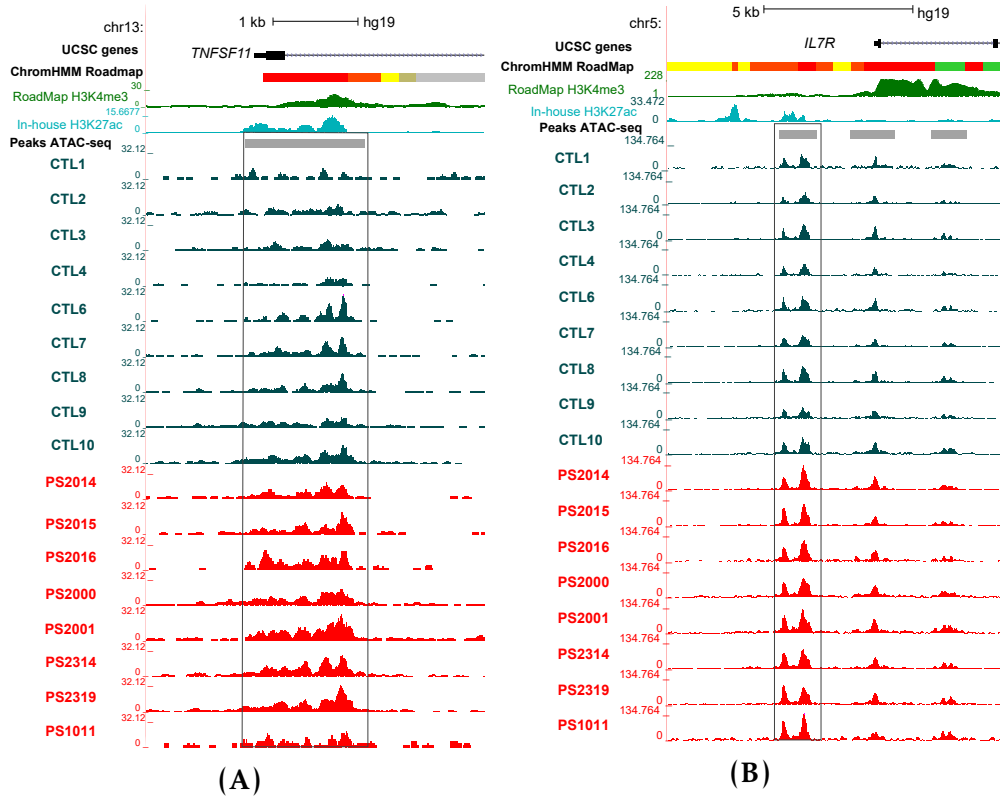


**Figure 3.6: Epigenetic landscape at two ATAC differential accessible regions between patients and controls in CD8<sup>+</sup> cells.** UCSC Genome Browser view illustrating the normalised ATAC read density (y-axis) in DARs located at (A) the promoter of *TNFSF11* gene and (B) up-stream the *IL7R* gene (x-axis). Both DARs were more open in CD8<sup>+</sup> cells from psoriasis compared to controls. Tracks are colour-coded by condition: control(CTL)=dark turquoise and psoriasis (PS)=red. The Epigenome Roadmap chromatin segmentation map and H3K4me3 for CD8<sup>+</sup> cells are also shown, together with a representative track from the in-house ChIPm H3K27ac in this cell type. All DARs were significant based on FDR<0.05 and no fold change cut-off.

Other potentially interesting CD8<sup>+</sup> DARs were found nearby genes such as the MAPK *MAP3K7CL* and *NFKB1*; however they were not at regions annotated as enhancers or overlapping with experimentally validated eRNA changes in DNA methylations.

### Integration of H3K27ac ChIPm and ATAC-seq chromatin accessibility profiles

Integration of the observed H3K27ac ChIPm and ATAC differential analysis between patients and controls of only showed co-localisation for one region in

## Defining the genome-wide chromatin accessibility landscape and gene expression profile in psoriasis

CD8<sup>+</sup> cells within an intron of the D-tyrosyl-tRNA deacylase 1 (*DTD1*) gene (Figure 3.7). Lower levels of H3K27ac and chromatin accessibility were found in the psoriasis patients when compared to healthy controls. This differential region was annotated as an active enhancer according to the CD8<sup>+</sup> Roadmap Epigenomics Project segmentation map and did not interact with the promoter of any gene according to Hi-C and promoter Hi-C data in CD8<sup>+</sup> cells (Javierre2016). Conversely, SNPs within this region are reported to be eQTL for *DTD1* in whole blood (<https://gtexportal.org/home/eqtls>).

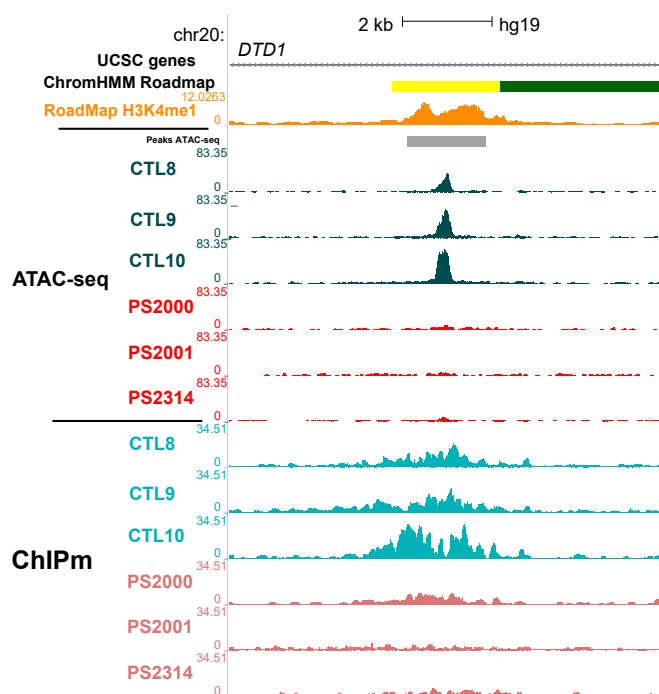


**Figure 3.7: Epigenetic landscape at *DTD1* locus showing differential H3K27ac and chromatin accessibility between psoriasis patients and controls in CD8<sup>+</sup> cells.** UCSC Genome Browser view illustrating the normalised ATAC read density and H3K27ac normalised fold-enrichment (y-axis). Tracks are colour-coded by condition and assay: control (CTL)=dark and light turquoise and psoriasis (PS)=light and dark red, for ATAC and ChIPm respectively. The Roadmap Epigenomics Project chromatin segmentation map and H3K4me1 for CD8<sup>+</sup> cells are also shown.

### **3.3.4 Differential gene expression analysis in circulating immune cells in psoriasis**

#### **Data processing and quality control**

In addition to characterising the chromatin accessibility landscape, gene expression profiles in psoriasis and healthy individuals were analysed for the same four primary circulating immune cell types using RNA-seq. The percentage of RNA-seq reads mapping to a unique location in the genome using STAR (see Chapter 2) was appropriate (minimum recommended 70 to 80%), ranging between 79.64 and 86.19% across the 72 samples (Figure B.7A). After appropriate filtering, all the samples had at least 20 million reads (as required by ENCODE standards) mapping to a comprehensive list of Ensembl features, including protein coding genes and lncRNAs (Figure B.7B). In all 4 cell types, greater mapping rates and total reads mapping to Ensembl features were observed for cohort 1B samples when compared to cohort 1A. These differences were attributed to the library preparation and sequencing of each cohort in two different batches.

PCA using the normalised number of reads mapping to each of the 20,493 Ensembl genes passing quality control (see Chapter 2) showed that most variability was driven by cell type differences (Figure 3.8A). A heatmap illustrating sample distance based on the expression profile of each sample followed by hierarchical clustering revealed three main clusters corresponding to CD14<sup>+</sup> monocytes, CD4<sup>+</sup> and CD8<sup>+</sup> T cells, and CD19<sup>+</sup> cells (Figure 3.8A). Within each cell type cluster, samples were further grouped by cohort (1A and 1B) but not by condition (psoriasis and control), consistent with the differences in mapping rate and total reads mapping to Ensembl genes observed across the two cohorts (Figure B.7A and B). Clear correlation of sample batch with PC4 from the PCA analysis led to a very clear separation of the samples into cohort 1A and

## Defining the genome-wide chromatin accessibility landscape and gene expression profile in psoriasis

---

1B, explaining 3% of the total variance (Figure B.6B). Consequently, batch was included in the DGE model as a covariate.

### mRNA and lncRNA differential expression

DGE analysis between 8 psoriasis patients and 10 healthy controls in CD14<sup>+</sup> monocytes, CD4<sup>+</sup> and CD8<sup>+</sup> T cells and CD19<sup>+</sup> B cells was performed using DESeq2, including cohort identity as a covariate. For each of the cell types a number of mRNAs were identified as differentially expressed at an FDR <0.05 or 0.01 (Table 3.6).

Cell type	mRNA FDR<0.05/0.01	lncRNA FDR<0.05/0.01	Up-regulated FDR<0.05/0.01	Down-regulated FDR<0.05/0.01
CD14 <sup>+</sup>	671/229	28/8	331/112	368/125
CD4 <sup>+</sup>	108/40	12/4	56/20	64/24
CD8 <sup>+</sup>	651/175	31/5	269/67	418/113
CD19 <sup>+</sup>	167/71	6/2	29/13	144/60

**Table 3.6: Summary results from the DGE analysis between psoriasis patients and healthy controls in CD14<sup>+</sup> monocytes, CD4<sup>+</sup>, CD8<sup>+</sup> and CD19<sup>+</sup> cells.** The number of statistically differentially expressed mRNAs and lncRNAs are listed for two FDR threshold (FDR<0.05 and FDR<0.01). No threshold for the fold change was applied in this analysis. For each of the FDR thresholds the number of up- and down- regulated genes is included.

CD14<sup>+</sup> monocytes and CD8<sup>+</sup> showed the largest number of differentially expressed mRNAs between psoriasis patients and controls with the highest magnitude of fold change (Figure 3.9). **CD14<sup>+</sup> monocytes and CD4<sup>+</sup> T cells showed similar numbers of genes up-regulated and down-regulated in psoriasis patients when compared to the healthy controls. In contrast, in CD8<sup>+</sup> and CD19<sup>+</sup> cells a larger number of modulated genes were down-regulated in patients compared to controls. In CD14<sup>+</sup> monocytes, the most significant differentially up-regulated genes with largest fold changes (fold change $\geq$ 1.5) included genes such as SDC2, CD83 and MIR22G (Figure 3.9A). In CD8<sup>+</sup> most significant differentially expressed genes showing fold**

## Defining the genome-wide chromatin accessibility landscape and gene expression profile in psoriasis

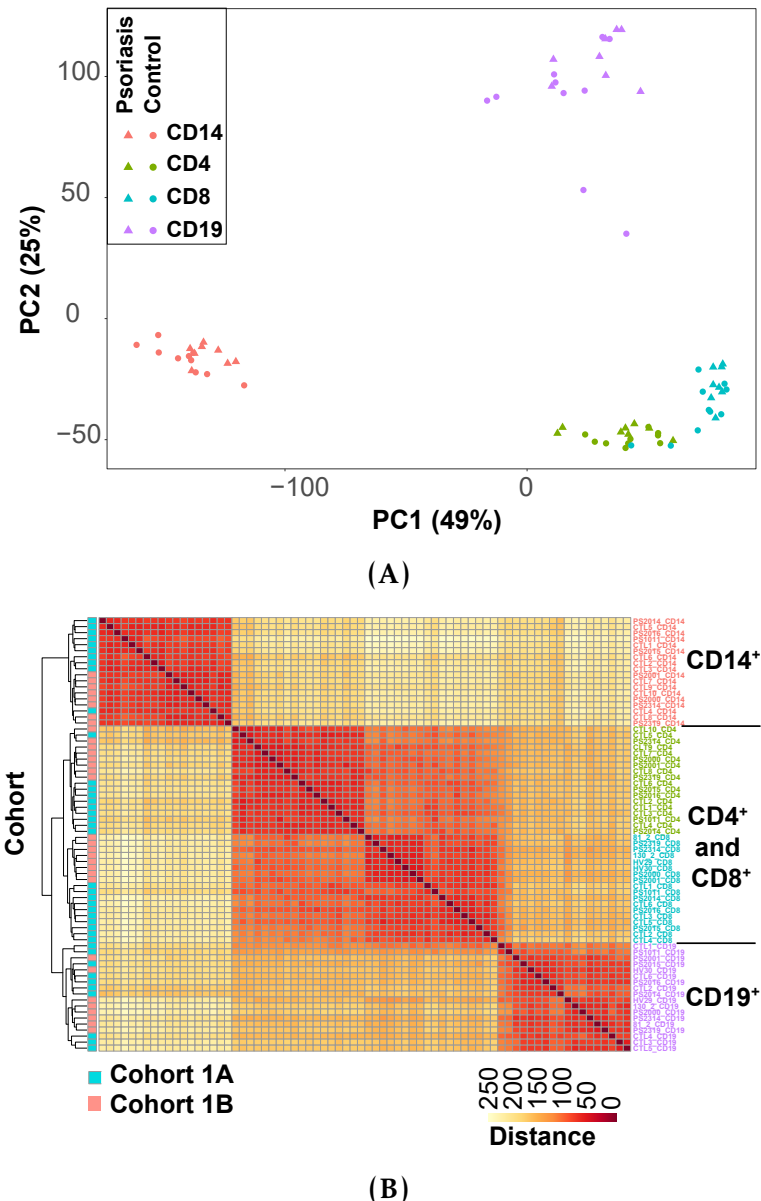


**Figure 3.8: PCA and sample distance heatmap with hierarchical clustering illustrating the sample variability based on the gene expression profiles for all 72 samples.** (A) The first and second PCs (x-axis and y-axis, respectively), where each point represents a sample, colour coding for cell type and the shape for cohort (batch). The proportion of variation explained by each principal component is indicated.(B) Distance matrix clustering based on normalised read counts mapping to 20,493 Ensembl featured remaining after appropriate filtering. Annotation of the clustering using cohort identity is included.

## Defining the genome-wide chromatin accessibility landscape and gene expression profile in psoriasis

change $\geq 1.5$  included *SOCS3* and *CXCR4* (Figure 3.9C). In CD4 $^{+}$  cells, the G protein-coupled receptor *GPR18* presented the most significant down-regulation with fold change 1.4. Overall, none of the detected genes showed dysregulation with extreme significance or fold change values in any of the 4 cell types.

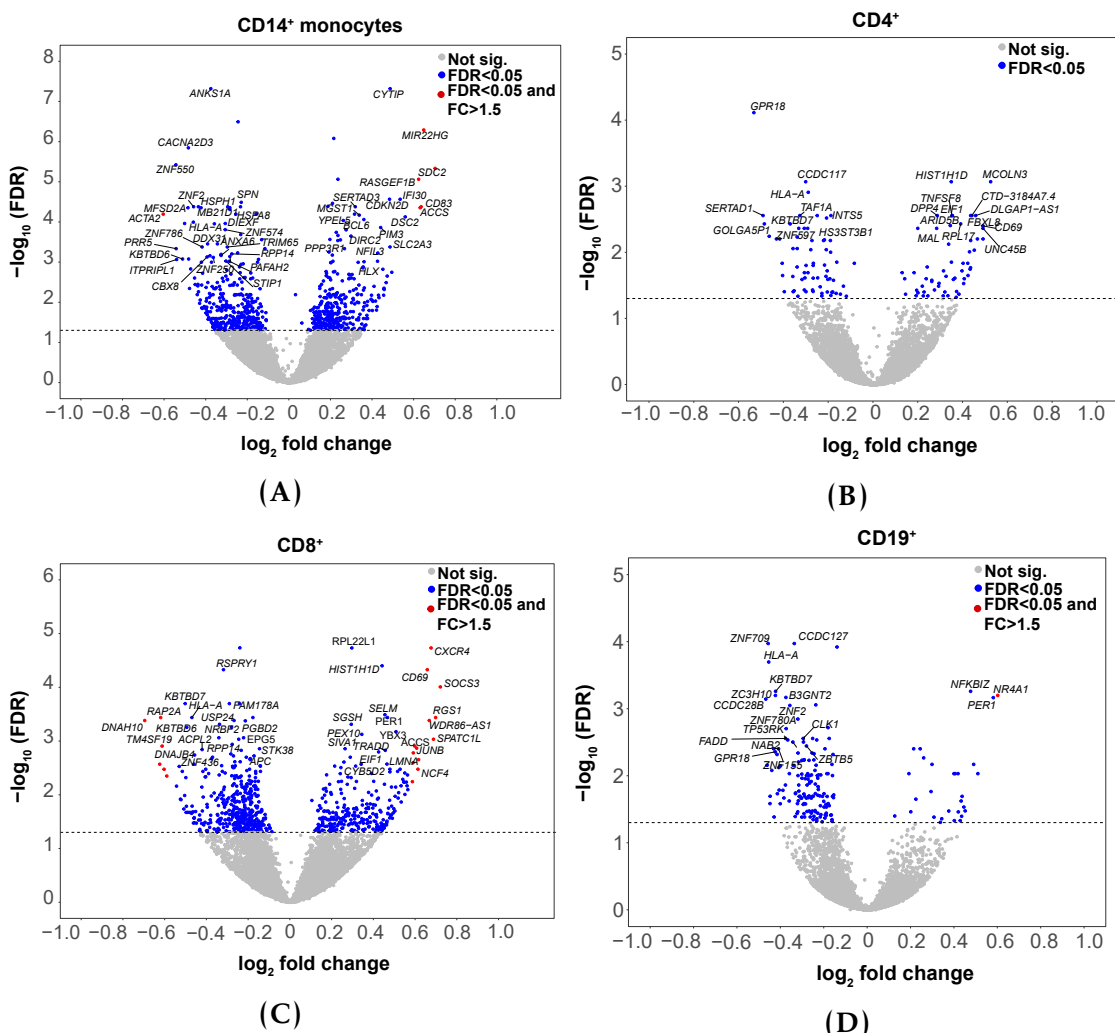


**Figure 3.9: Magnitude and significance of the gene expression changes between psoriasis patients and healthy controls in four immune cell types.** Volcano plots for the results of the DGE analysis in (A) CD14 $^{+}$  monocytes, (B) CD4 $^{+}$ , (C) CD8 $^{+}$  and (D) CD19 $^{+}$  cells. For each gene, the  $\log_2$  fold change represents the change in expression for that gene in the psoriasis group with reference to the healthy controls. Significant DEGs (FDR $<0.05$ ) in blue for fold change $<1.5$  and red for fold change $>1.5$ . The volcano plots include mRNAs and lncRNAs species.

Enrichment of significant DEGs (FDR $<0.05$ ) across the 4 cell types and genes associated with psoriasis from reported GWAS was analysed using the

## Defining the genome-wide chromatin accessibility landscape and gene expression profile in psoriasis

---

NHGRI-EBI catalog (<https://www.ebi.ac.uk/gwas>) (Table 3.7). CD8<sup>+</sup> was the cell type with the largest number of DEGs (7 hits) overlapping putative GWAS genes, followed by CD14<sup>+</sup> monocytes and CD4<sup>+</sup> (3 hits each). Some of the GWAS genes were found to be differentially expressed in more than one of the 4 cell types, including *NFKBIA*, *TNFAIP3* and *NFKBIZ*, amongst others. Only in CD4<sup>+</sup> and CD8<sup>+</sup> T cells, the overlap indicated statistically significant enrichment of GWAS genes amongst the differential genes when comparing patients vs controls (Fisher exact test, p-values 2.6x10<sup>-3</sup> and 9.36x10<sup>-4</sup>, respectively).

Cell type	Number of GWAS overlaps	Up-regulated genes	Down-regulated genes
CD14 <sup>+</sup>	3	<i>NFKBIA</i>	<i>IL23A, FASLG</i>
CD4 <sup>+</sup>	3	<i>TNFAIP3, NFKBIZ</i>	<i>FASLG</i>
CD8 <sup>+</sup>	7	<i>TNFAIP3, NFKBIA, ETS1, SOCS1, NFKBIZ</i>	<i>B3GNT2, FASLG</i>
CD19 <sup>+</sup>	2	<i>NFKBIZ</i>	<i>B3GNT2</i>

**Table 3.7:** Overlap between putative psoriasis GWAS genes and the reported significantly DEGs in CD14<sup>+</sup> monocytes, CD4<sup>+</sup>, CD8<sup>+</sup> and CD19<sup>+</sup> cells. DEGs list based on FDR<0.05.

## The role of lncRNAs in psoriasis circulating immune cells

In addition to protein coding genes, some of the DEGs identified were classified as lncRNAs. CD8<sup>+</sup> and CD14<sup>+</sup> monocytes were the two cell types showing the largest number of dysregulated lncRNAs between psoriasis patients and controls (Table 3.6).

The majority of the differentially expressed lncRNAs (FDR<0.05) were found to have a functional interacting partner based on NPInter database (Table A.4), which retrieves functional interactions between non-coding RNAs and biomolecules (proteins, RNAs and DNAs) which have been published (Hao et al. 2016). Some of the lncRNAs were also found to be differentially expressed

## **Defining the genome-wide chromatin accessibility landscape and gene expression profile in psoriasis**

---

in PBMCs when comparing PsA patients versus healthy controls in a study conducted by Dolcino and colleagues (Dolcino et al. 2018).

Examples of cell type-specific differentially expressed lncRNAs between psoriasis patients and healthy controls included *DYNLL1-AS1* (or *NAV*), *HOTAIRM1* and *NEAT1* in CD14<sup>+</sup> monocytes, *DLGAP1-AS1* in CD4<sup>+</sup>, *UBXN8* and *MIR146A* in CD8<sup>+</sup> and *LINC00324* in CD19<sup>+</sup>. Only one lncRNA, *RP11-218M22.1* appeared to be dysregulated between psoriasis and healthy controls in all the cell types.

Amongst the cell type-specific dysregulated lncRNAs, *DYNLL1-AS1* has been shown to affect the histone modifications of some critical IFN-stimulated genes (ISGs) including *IFITM3* and *MxA*, leading to down-regulation of their expression (Ouyang et al. 2014). *DYNLL1-AS1* was down-regulated in CD14<sup>+</sup> monocytes from psoriasis patients when compared to controls but no up-regulation of *IFITM3* and *MxA* was found. Conversely, *HOTAIRM1*, another CD14<sup>+</sup> monocytes specific lncRNA was up-regulated in psoriasis patients (Figure 3.10A). The experimentally validated target for *HOTAIRM1* reported by NPInter database was the RNA helicase and ATPase *UPF1* (Hao et al. 2016), which was found to be down-regulated in CD14<sup>+</sup> monocytes in psoriasis versus control samples in this data (Figure 3.10B). Lastly, *NEAT1*, was also up-regulated in psoriasis patients compared to controls in CD14<sup>+</sup> monocytes in line with a study in SLE CD14<sup>+</sup> monocytes (Zhang et al. 2016).

For CD8<sup>+</sup> cells, the miR *MIR146A* was the most interesting non-coding RNAs, showing down-regulation in psoriasis patients compared to controls and previously reported to have a role in negative regulation of the innate immunity, inflammatory response and antiviral pathways (Taganov et al. 2006).

## Defining the genome-wide chromatin accessibility landscape and gene expression profile in psoriasis

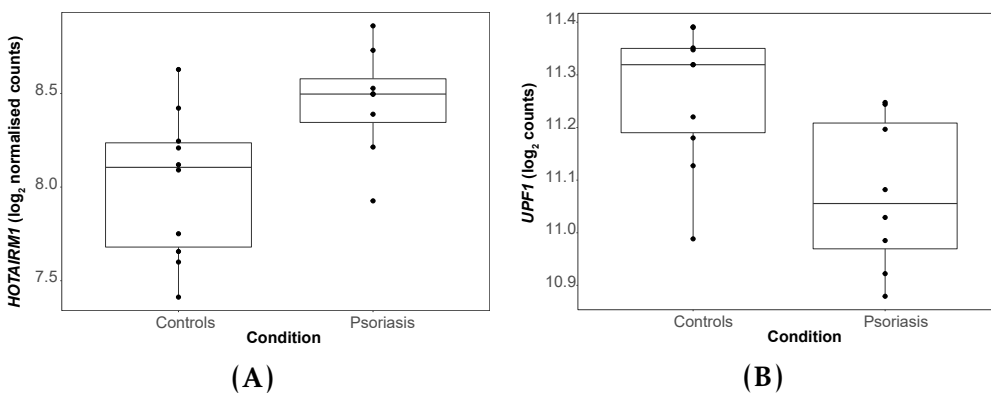


**Figure 3.10: RNA-seq expression levels of the lncRNA *HOTAIRM1* and its experimentally validated target *UPF1* in psoriasis and healthy controls CD14<sup>+</sup> monocytes.** Expression is illustrated as the log<sub>2</sub> of the normalised read counts mapping to (A) the lncRNA *HOTAIRM1* and (B) *UPF1*, which has been experimentally identified as one of the genes regulated by this lncRNA according to NPInter database.

### Pathway enrichment analysis for the DEGs

To investigate the biological role of the significantly modulated genes, pathway enrichment analysis was performed for each cell type using DEG with FDR<0.05 and no fold change cut-off. Biologically relevant pathways were significantly enriched (FDR<0.01) for CD14<sup>+</sup> monocytes and CD8<sup>+</sup> cells (Table 3.8 and A.5). In CD19<sup>+</sup> cells, only one pathway (generic transcription, p-value=8.2x10<sup>-12</sup>, fold change=6.26) was significantly enriched, while in CD4<sup>+</sup> cells no enrichment was seen for any pathways.

Two of the significant enriched pathways, MAPK signalling and IL-12 mediated signalling, were found to be enriched in both CD14<sup>+</sup> monocytes and CD8<sup>+</sup> cells (Table 3.8). MAPK signalling was of particular interest as DEGs contributing to the enrichment of this pathway in both cell types included a number of MAPK gene members differentially expressed between psoriasis patients and healthy controls (Figure 3.11). Two of those MAPK genes, *MAP3K4* and *MAPK14*, were down-regulated in psoriasis vs controls in CD14<sup>+</sup> monocytes and CD8<sup>+</sup> T cells (Figure 3.11A and B). *MAP3K4* is a member of the MAPKKK family, whose expression is down-regulated in LPS-stimulated PBMCs from Crohn's patients leading to a relative immune deficiency

## Defining the genome-wide chromatin accessibility landscape and gene expression profile in psoriasis

---

Cell type	Pathways
CD14 <sup>+</sup> monocytes	MAPK signalling $(p\text{-value}=1.3 \times 10^{-6}, \text{fold change}=2.83)$ IL-12 mediated signaling events $(p\text{-value}=3.2 \times 10^{-7}, \text{fold change}=4.82)$ Th-1 and Th-2 cell differentiation $(p\text{-value}=4.4 \times 10^{-5}, \text{fold change}=3.34)$ Th-17 cell differentiation $(p\text{-value}=4.7 \times 10^{-5}, \text{fold change}=3.21)$ TCR signalling $(p\text{-value}=5.3 \times 10^{-5}, \text{fold change}=3.18)$ Platelet-derived growth factor (PDGF- $\beta$ ) signalling $(p\text{-value}=3.2 \times 10^{-4}, \text{fold change}=2.59)$ Forkhead box O (FoxO) signalling $(p\text{-value}=1.6 \times 10^{-3}, \text{fold change}=2.38)$
CD8 <sup>+</sup>	Osteoclast differentiation $(p\text{-value}=3.4 \times 10^{-6}, \text{fold change}=3.45)$ MAPK signalling $(p\text{-value}=2.0 \times 10^{-4}, \text{fold change}=2.33)$ TNF signalling $(p\text{-value}=2.2 \times 10^{-4}, \text{fold change}=2.93)$ IL-12 mediated signalling events $(p\text{-value}=4.5 \times 10^{-5}, \text{fold change}=3.86)$ NF- $\kappa$ B signalling $(p\text{-value}=5.3 \times 10^{-4}, \text{fold change}=2.95)$ Chemokine signalling $(p\text{-value}=6.6 \times 10^{-4}, \text{fold change}=2.43)$

**Table 3.8: Pathways enriched for DEGs between psoriasis patients and healthy controls in CD14<sup>+</sup> monocytes and CD8<sup>+</sup> cells.** The enrichment analysis was conducted using significantly DEGs FDR<0.05 and no fold change threshold. Enriched pathways had FDR<0.01 and a minimum of ten gene members overlapping with DEGs for that particular cell type.

## **Defining the genome-wide chromatin accessibility landscape and gene expression profile in psoriasis**

---

in TLR-mediated cytokine production. Moreover, DGE of members of the dual-specificity phosphatases (DUSP) family, involved in fine-tuning the immune response (Qian et al. 2009), also contributed to the enrichment of the MAPK pathway in CD14<sup>+</sup> monocytes and CD8<sup>+</sup> cells. *DUSP10* was down-regulated in psoriasis only in CD14<sup>+</sup> monocytes (Figure 3.11C) and knock-out in mice has been associated with enhanced inflammation (Qian et al. 2009). Conversely, *DUSP4* was up-regulated in psoriasis CD8<sup>+</sup> cells vs healthy controls (Figure 3.11D) and has been demonstrated to have a pro-inflammatory role in a sepsis mice model (Cornell et al. 2010).

Regarding enrichment of the IL-12 signalling, CD14<sup>+</sup> monocytes from psoriasis showed down-regulation of *STAT4* and *STAT5A* in patients compared to controls. Neither *STAT4* and *STAT5A* were differentially expressed in CD8<sup>+</sup> cells. By contrast, *IFNG* expression in psoriasis patients was lower than in healthy controls in CD8<sup>+</sup> cells but showed no differences in CD14<sup>+</sup> monocytes. Also, *IL2RA* only showed up-regulation in CD8<sup>+</sup> T cells from psoriasis patients which may have an effect in the formation of the IL2-R $\alpha$  and the signalling by this cytokine involved in effector and regulatory T cell differentiation (Malek and Immunity 2010).

The platelet-derived growth factor (PDGF- $\beta$ ) signalling pathway was only enriched in CD14<sup>+</sup> monocytes (Table 3.8). Within this pathway the *SLA* gene was down-regulated in psoriasis patients. A *SLA* knock-out mice model has shown impaired IL-12 and TNF- $\alpha$  and failure of T cell stimulation by GM-CSG treated bone marrow-derived DCs (Liontos et al. 2011).

A number of very relevant inflammatory pathways in psoriasis were enriched only in CD8<sup>+</sup> cells. These included TNF, NF- $\kappa$ B and chemokine signalling (Table 3.8), with some of the DEGs contributing to the enrichment of more than one of the pathways. NF- $\kappa$ B inhibitor A (*NFKBIA*) and the TNF- $\alpha$  induced protein 3 (*TNFAIP3*) were unexpectedly up-regulated in CD8<sup>+</sup>

## Defining the genome-wide chromatin accessibility landscape and gene expression profile in psoriasis

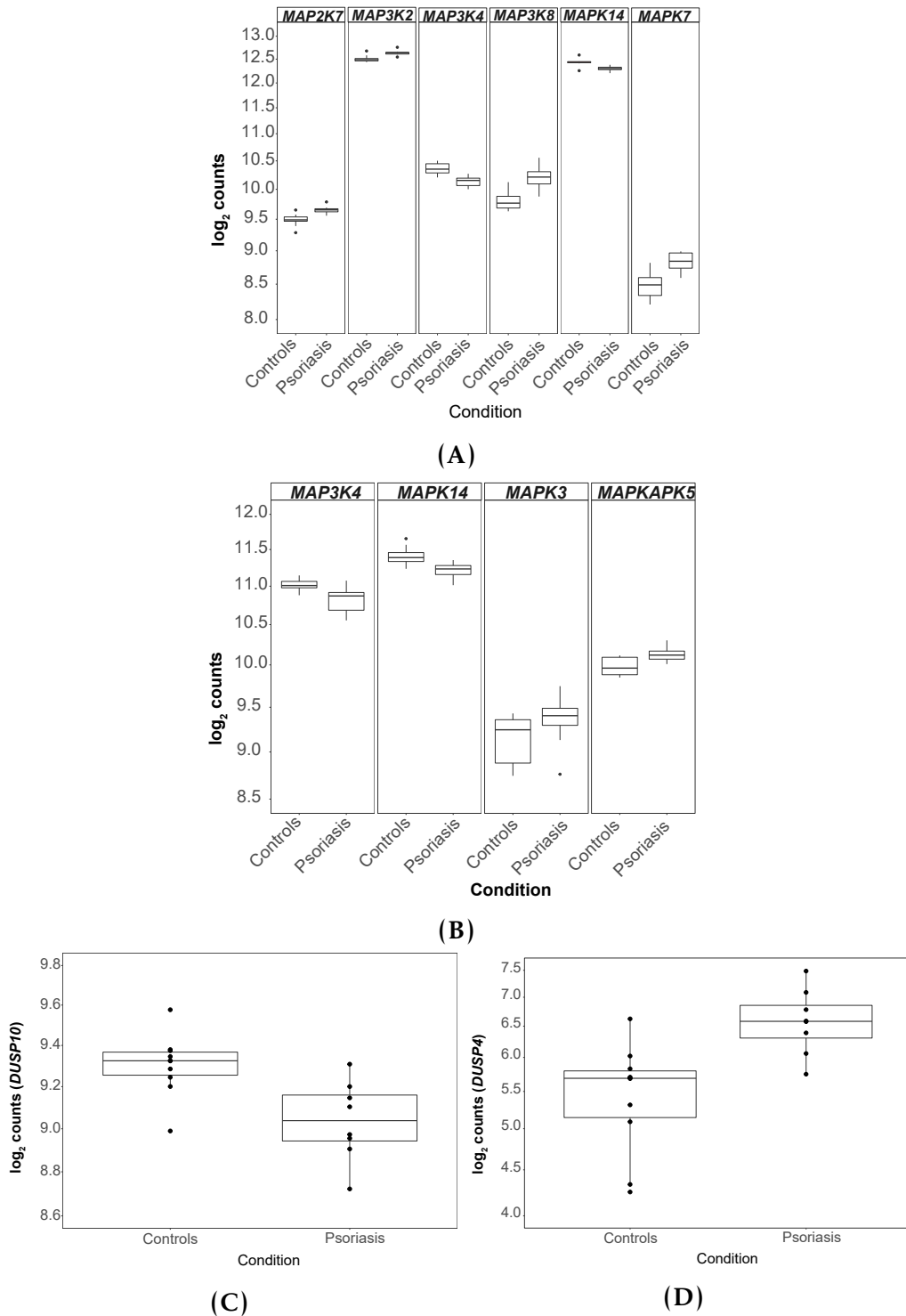


**Figure 3.11: Differential expression between psoriasis and healthy controls of MAPK and DUSP genes contributing to MAPK signalling enrichment in CD14<sup>+</sup> monocytes and CD8<sup>+</sup> T cells.** Expression for MAPK genes in psoriasis patients and controls is illustrated as the log<sub>2</sub> of the normalised read counts, including (A) *MAP2K7*, *MAP3K2*, *MAP3K4*, *MAP3K8*, *MAPK14* and *MAPK7* in CD14<sup>+</sup> monocytes and (B) *MAP3K4*, *MAPK14*, *MAPK3* and *MAPKAPK5* in CD8<sup>+</sup> T cells. Similarly, expression as log<sub>2</sub> of the normalised read counts is also illustrated for the DUSP gene members (C) *DUSP10* in CD14<sup>+</sup> monocytes and (D) *DUSP4* in CD8<sup>+</sup> T cells, in patients and control samples.

## Defining the genome-wide chromatin accessibility landscape and gene expression profile in psoriasis

---

cells from psoriasis compared to healthy controls. *NFKBIA* up-regulation contributed to the enrichment of all three pathways (Figure 3.12A in green box and B) and *TNFAIP3* was a member of the TNF and NF- $\kappa$ B pathways (Figure 3.12A in green box). Moreover, *NFKBIA* and *TNFAIP3* are two of the psoriasis GWAS associated genes and were also up-regulated in psoriasis CD14 $^{+}$  monocytes and CD4 $^{+}$  cells, respectively (Table 3.7). The enrichment of these three pathways in CD8 $^{+}$  cells was also driven by a mix of up-regulation (*JUNB*, *RELA*, *RELB* and *NFKB2*) and down-regulation (*ATF2* and *ATF4*) of pro-inflammatory genes, which effect on the overall immune response is difficult to predict.

Up-regulation and down-regulation of specific chemokines was seen in CD8 $^{+}$  cells from psoriasis patients when compared to healthy controls (Figure 3.12B), including up-regulation of *CCR10*, the receptor for the chemotactic skin-associated chemokine CCL27. Other up-regulated chemokine receptors included *CXCR4* gene, the receptor for the chemokine SDF-1, highly expressed in skin (Zgraggen et al. 2014). Of note, none of the genes coding for well-known psoriasis drug target genes, including TNF- $\alpha$ , IL-17 and IL-6, were up-regulated in any of the 4 cells types from psoriasis patients compared to healthy controls.

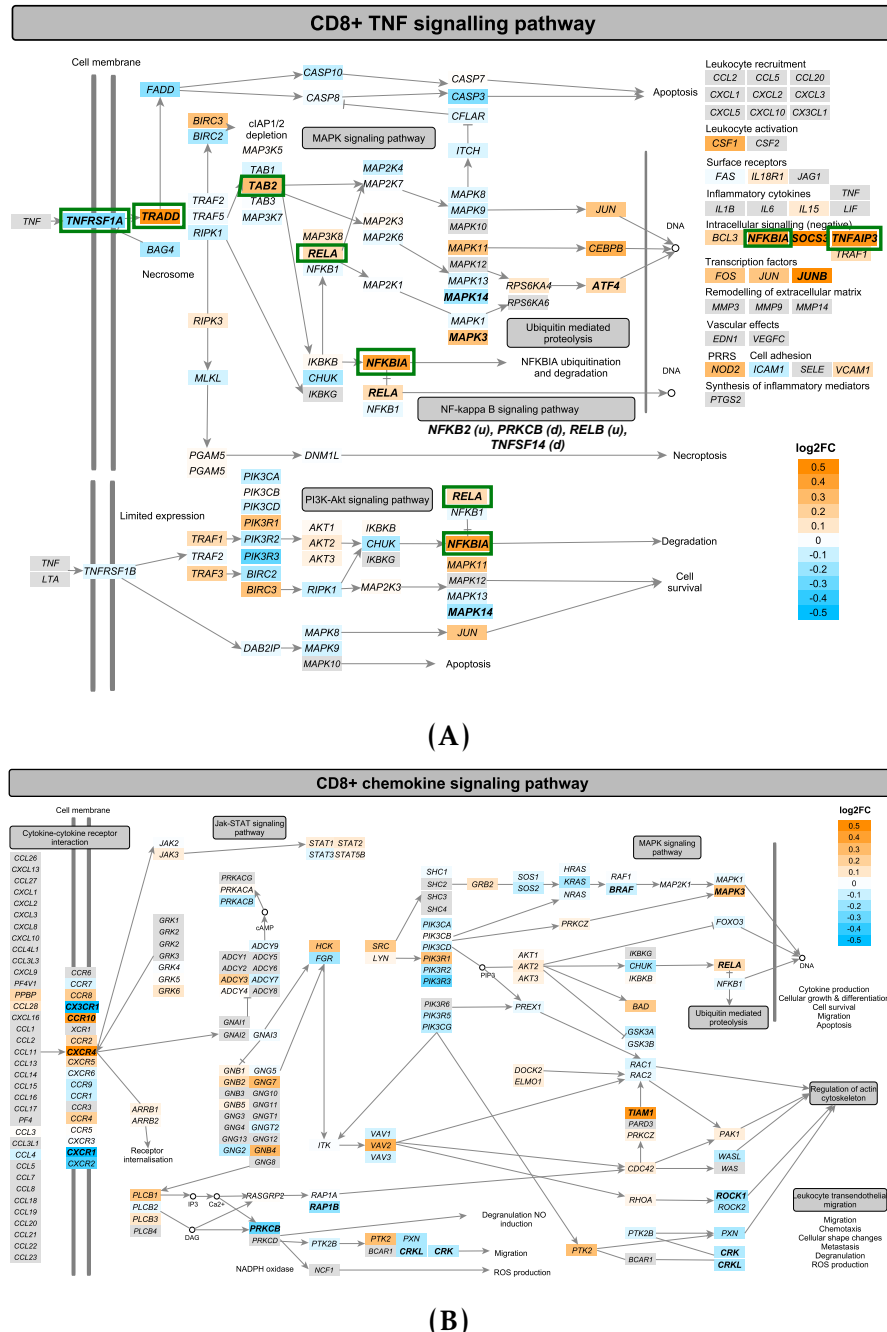
### 3.3.5 RNA-seq in epidermis from psoriasis patients

#### Data processing and quality control

For the three paired uninvolved-lesional samples (Table ??), all had a mapping rate greater than 80% (Figure B.8A). The number of reads after filtering mapped to Ensembl genes ranged between 29.5 and 33.2 million (Figure B.8B). The mapping rate and final number of reads mapping to genes was greater in the lesional samples compared to the controls (Figure B.8).

PCA using the normalised number of reads mapping to the genes after filtering revealed separation of the lesional samples from the uninvolved by

# Defining the genome-wide chromatin accessibility landscape and gene expression profile in psoriasis



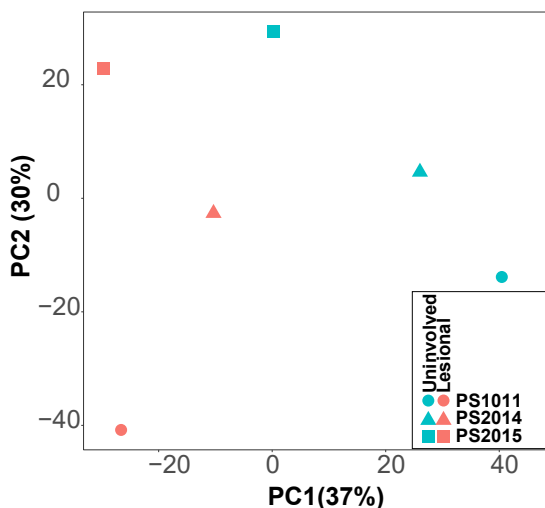


**Figure 3.13: PCA for the RNA-seq data in the uninvolved and lesional epidermis from psoriasis patients.** First and second component of the PCA analysis performed on the normalised number of reads mapping to the Ensembl list of mRNAs and lncRNAs detected in lesional and uninvolved epidermis isolated from psoriasis patient skin biopsies. Dots colour corresponds to condition (lesional or uninvolved) and shape refers to the patient ID.

the first PC, which explained 37% of the variance (Figure ??). The second PC explained 30% of the variance and correlated with the patient ID. Overall, PCA analysis revealed substantial variation between the lesional and uninvolved samples and biological variability across individuals, for which the paired design in the DGE analysis accounted.

### Summary of the differential gene expression results

DGE analysis revealed a total of 1,227 (FDR<0.05) and 702 (FDR<0.01) genes differentially expressed between uninvolved and lesional epidermis skin biopsies, including mRNAs and lncRNAs (Table ??). Amongst the 1,227 DEGs, a similar proportion of genes up- (559 genes) and down-regulated (629) in lesional skin when compared to uninvolved were identified (Figure 3.14) and 46 were annotated as lncRNAs (Table ??). The magnitude of changes in gene expression between lesional and uninvolved skin were notably larger when compared to the changes in expression from analysis in peripheral blood, with 874 out of 1,227 genes showing fold change>1.5.

## Defining the genome-wide chromatin accessibility landscape and gene expression profile in psoriasis

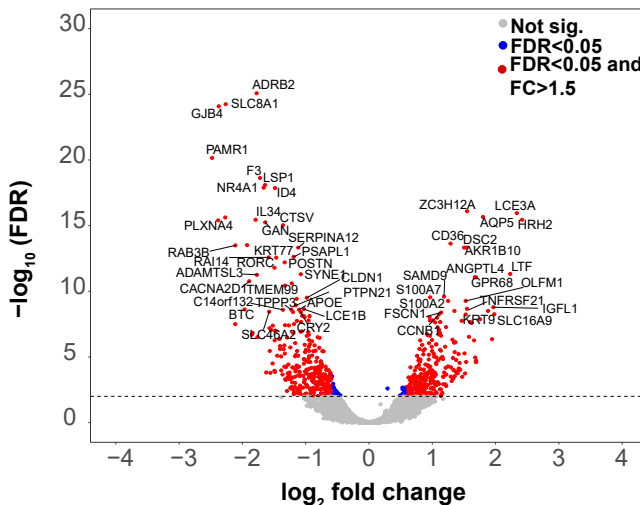


**Figure 3.14: Magnitude and significance of the gene expression changes between matched lesional and uninvolvled epidermal biopsies from three psoriasis patients.** The volcano plot represents for each gene the significance ( $-\log_{10}FDR$ ) of the  $\log_2$ fold change in expression for that gene in lesional skin group vs uninvolvled skin. Significant DEGs ( $FDR<0.05$ ) in blue for fold change $<1.5$  and red for fold change $>1.5$ . The volcano plot includes mRNAs and lncRNAs species.

Amongst the DEGs between the uninvolvled and lesional skin, five genes ( $FDR<0.05$ ) overlapped with putative GWAS genes (Table ??). *IFIH1*, *NOS2*, *LCE3D* and *STAT3* were up-regulated in lesional compared to uninvolvled skin, whereas *TNFAIP3* was down-regulated. Only *IFIH1* failed to show differential expression at an  $FDR<0.01$ .

FDR threshold	mRNA	lncRNA	Overlap with GWAS genes
0.05	1181	46	up( <i>IFIH1</i> , <i>NOS2</i> , <i>STAT3</i> , <i>LCE3D</i> ), down( <i>TNFAIP3</i> )
0.01	677	25	<i>NOS2</i> , <i>STAT3</i> , <i>TNFAIP3</i> , <i>LCE3D</i>

**Table 3.9: Summary results of the DGE analysis between uninvolvled and lesional psoriatic epidermal biopsies.** Number of differentially expressed mRNAs and lncRNAs are reported for two threshold of significance ( $FDR<0.05$  and  $FDR<0.01$ ). The DEGs overlapping putative psoriasis GWAS genes and the directionality in the change of expression are also specified.

## **Defining the genome-wide chromatin accessibility landscape and gene expression profile in psoriasis**

---

### **Overall comparison with other skin transcriptomic studies**

As detailed in Chapter 2, the approach to study DGE in skin is different from previously published studies using whole punch biopsies to compare lesional and uninvolved skin from psoriasis patients. During the course of this project a study was published by Tervaniemi and colleagues that also aimed to characterise the transcriptional profiles of the epidermis from psoriasis patients lesional and uninvolved skin (Tervaniemi et al. 2016). In order to explore the similarities between the two studies, a comparison for the DEGs identified between lesional and uninvolved matched samples was conducted.

Tervaniemi study showed a total of 2,589 DEGs (filtering criteria fold change $<0.75$  or fold change $>1.5$  and FDR $<0.05$ ), a larger number of DEGs compared to the number found in this thesis, and reported a larger number of up-regulated than down-regulated hits (Figure 3.15 bottom panel). A total of 359 out of the 1,227 DEGs (29.25%) identified by the in-house study were shared with the Tervaniemi results, of which 239 and 75 were up- and down-regulated, respectively (Figure 3.15 bottom panel). Some examples of this overlap included up-regulation of *STAT1*, genes from the *S100* family (e.g *S100A9* and *S100A12*) and genes nearby psoriasis GWAS loci such as *STAT3* and *IFIH1*. Notably, 45 genes were differentially expressed in both studies but showed opposite direction. For example *SERPINB2* was down-regulated in the in-house data and up-regulated in the Tervaniemi results.

In addition to the Tervaniemi study, our results were further contrasted to one of the most recent comprehensive RNA-seq studies comparing lesional and uninvolved full thickness skin biopsies from psoriasis patients (Tsoi et al. 2015). Out of the 3,725 DEGs reported by Tsoi and colleagues, 507 genes were shared between the two studies (41% of the in-house DEGs) and 24 corresponded to dysregulated lncRNAs. Out of the 507 commonly dysregulated genes in the

## Defining the genome-wide chromatin accessibility landscape and gene expression profile in psoriasis

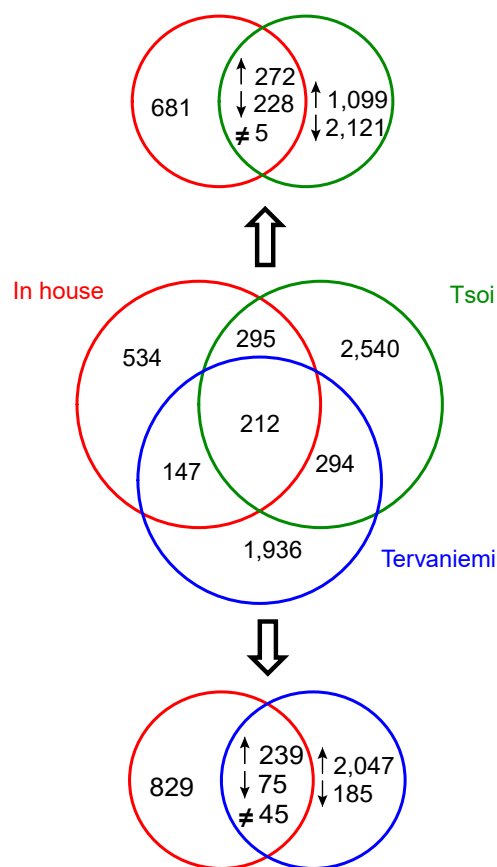


**Figure 3.15:** Overlap of the significantly differentially expressed genes between lesional and unininvolved epidermal sheets, split epidermis and full-thickness skin biopsies. The central venn diagram illustrated the DEGs overlapping between this study (in house), Tervaniemi *et al.*, 2016 split epidermis biopsies and Tsoi *et al.*, 2015 full thickness skin biopsies. Overlap is considered regardless the direction of the change. Two additional venn diagrams provide more detail about the total overlap and directionality in the change of gene expression between the in-house data and the Tsoi *et al.* (top) or Tervaniemi *et al.* (bottom).

## **Defining the genome-wide chromatin accessibility landscape and gene expression profile in psoriasis**

---

two datasets, 272 were up-regulated, 228 down-regulated and 7 showed opposite direction of change (Figure 3.15 top panel).

Overlap across the three studies only identified 212 DEGs shared by the three datasets. Despite having a the larger sample size, the Tsoi and colleagues study did not capture all the DEGs from the in-house or Tervaniemi (506 overlapping genes, Figure 3.15 middle panel) data.

### **Dysregulated lncRNAs in the psoriatic lesional skin**

In addition to protein coding genes, a total of 46 lncRNAs were also significantly (FDR<0.05) differentially expressed between uninvolved and lesional skin in the three psoriasis patients from this study. Out of the 46 differentially regulated lncRNAs, 37 had a functional experimental partner functionally validated according to NPInter database (Hao et al. 2016). An interesting example was *H19* which was significantly down-regulated in the lesional skin when compared to uninvolved. *H19* has been described to directly bind miR-130b-3p, which down-regulates Desmoglein 1 (*DSG1*), a gene promoting keratinocyte differentiation (Li et al. 2017). Nevertheless, *DSG1* did not appear as one of the DEGs between lesional and uninvolved skin.

Interestingly, four miRNAs (*MIR146A*, *MIR22HG*, *MIR31HG* and *MIR205HG*) were also captured with the standard library preparation for mRNAs and lncRNAs implemented in our project. The relevance of miR-146a has been already noted in the DGE analysis from circulating immune cells. In lesional skin *MIR146A* was up-regulated when compared to uninvolved skin, consistently with other studies (Lerman2014; Tsoi et al. 2015).

Another relevant finding was the up-regulation of *MIR31HG* in lesional skin, which has also been reported by (Tsoi et al. 2015). In a study in head and neck carcinoma, *MIR31HG* expression was identified to target *HIF-1A*, inducing up-regulation by an unknown mechanisms (Wang et al. 2018). In our data, *HIF-*

## Defining the genome-wide chromatin accessibility landscape and gene expression profile in psoriasis

---

*1A* showed up-regulation in lesional skin compared to uninvolved, and a trend for positive correlation ( $R=0.690$ ,  $p\text{-value}=0.12$ ) between normalised counts of this gene and the putative regulator *MIR31HG* was also observed (Figure B.9).

### Pathway enrichment analysis

In order to better understand the functional role of the DEGs ( $\text{FDR}<0.05$ ) between lesional and uninvolved epidermis from psoriasis patient skin biopsies, pathways enrichment analysis was performed. A number of pathways were significantly enriched ( $\text{FDR}<0.005$  and  $\text{fold change}>2$ ) for DEGs found in our analysis (Tables 3.10 and A.6).

---

#### Lesional versus uninvolved epidermis enriched pathways

---

IFN- $\alpha/\beta$ /signalling ( $p\text{-value}=6.1\times 10^{-6}$ , $\text{fold change}=3.65$ )
Peroxisome proliferator-activated receptors (PPAR) signalling ( $p\text{-value}=7.4\times 10^{-6}$ , $\text{fold change}=3.42$ )
NOD-like receptor signaling pathway ( $p\text{-value}=2.9\times 10^{-5}$ , $\text{fold change}=2.37$ )
IL-17 signalling ( $p\text{-value}=2.1\times 10^{-4}$ , $\text{fold change}=2.72$ )
IL2-mediated signalling ( $p\text{-value}=1.1\times 10^{-3}$ , $\text{fold change}=2.64$ )
Hypoxia-inducible factor 1 (HIF-1) signalling ( $p\text{-value}=8.8\times 10^{-4}$ , $\text{fold change}=2.31$ )
Glycolysis/gluconeogenesis ( $p\text{-value}=2.7\times 10^{-8}$ , $\text{fold change}=4.71$ )
Cell cycle ( $p\text{-value}=8.2\times 10^{-6}$ , $\text{fold change}=2.55$ )
Apoptosis ( $p\text{-value}=4.0\times 10^{-4}$ , $\text{fold change}=2.11$ )
Arginine and proline metabolism ( $p\text{-value}=1.3\times 10^{-9}$ , $\text{fold change}=5.28$ )

---

**Table 3.10:** Most relevant pathways enriched for DEGs between lesional and uninvolved epidermis isolated from psoriasis patients skin biopsies. Significant pathways for  $\text{FDR}<0.005$  and  $\text{fold change}>2$ . The analysis was performed using significantly DEGs ( $\text{FDR}<0.05$ ). Enriched pathways had a minimum of ten members overlapping with DEGs.

## Defining the genome-wide chromatin accessibility landscape and gene expression profile in psoriasis

A number of pathways were related to alterations in cell cycle and metabolic processes, including hypoxia-inducible factor 1 (HIF-1) signalling, arginine and proline metabolism, glycolysis/gluconeogenesis and metabolism of carbohydrates. HIF-1 signalling has been found to be up-regulated in psoriasis skin, likely through hypoxia caused by increased cell proliferation rates and epidermal thickening. In this data up-regulation of *HIF1A*, *VEGFA*, *ENO1* and the GWAS gene *NOS2*, amongst others, contributed to the enrichment of this pathway (Figure 3.17).

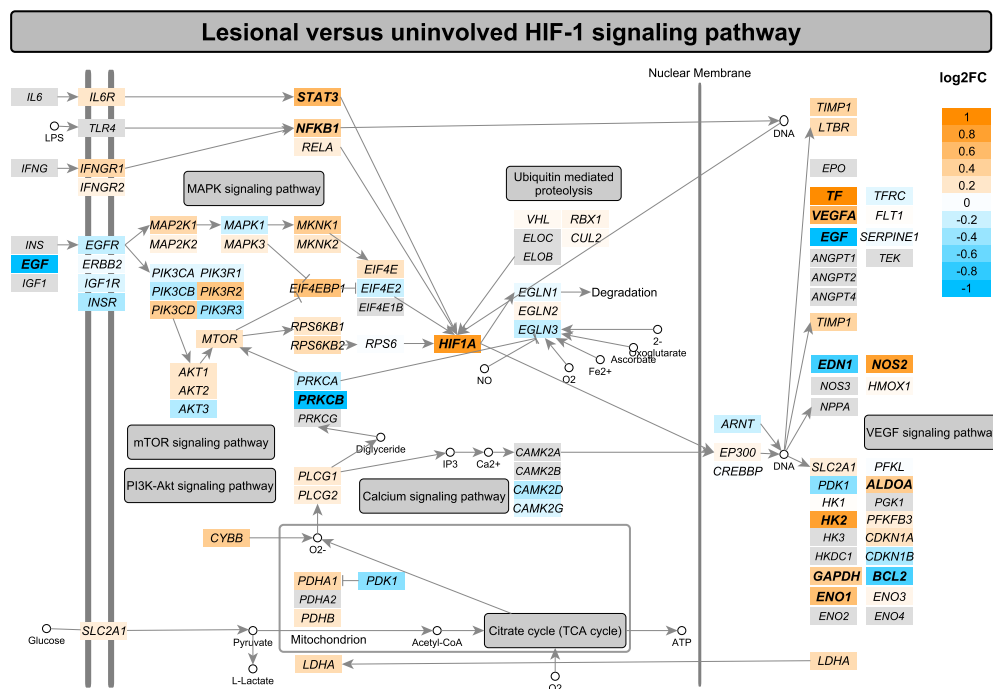


**Figure 3.16: Mapping of the DEGs between lesional and unininvolved epidermis from psoriasis patients onto the HIF-1 signalling pathway.** This pathway was sourced from KEGG, manually curated in a way that all member genes are maximised visually and then automatically color-coded by the log<sub>2</sub>fold change expression between the lesional and unininvolved epidermis. Significant DEGs (FDR<0.05) are highlighted in bold. This pathway was identified by pathway enrichment analysis using only DEGs (FDR<0.05).

Immune relevant pathways including IFN, IL-17 and NOD-like receptor signalling were also identified in this analysis. The NOD-like receptor pathway responsible for detecting various pathogens and generating innate immune responses through NF- $\kappa$ B and MAPK activation, was enriched with 23

## **Defining the genome-wide chromatin accessibility landscape and gene expression profile in psoriasis**

---

significantly DEGs , including *NOD2*, *CARD6* or *IFI16* (highly up-regulated) (Figure 3.17 in orange and bold) and *TNFAIP3* and *BCL-2* (down-regulated) (Figure 3.17 in blue and bold).

## Defining the genome-wide chromatin accessibility landscape and gene expression profile in psoriasis

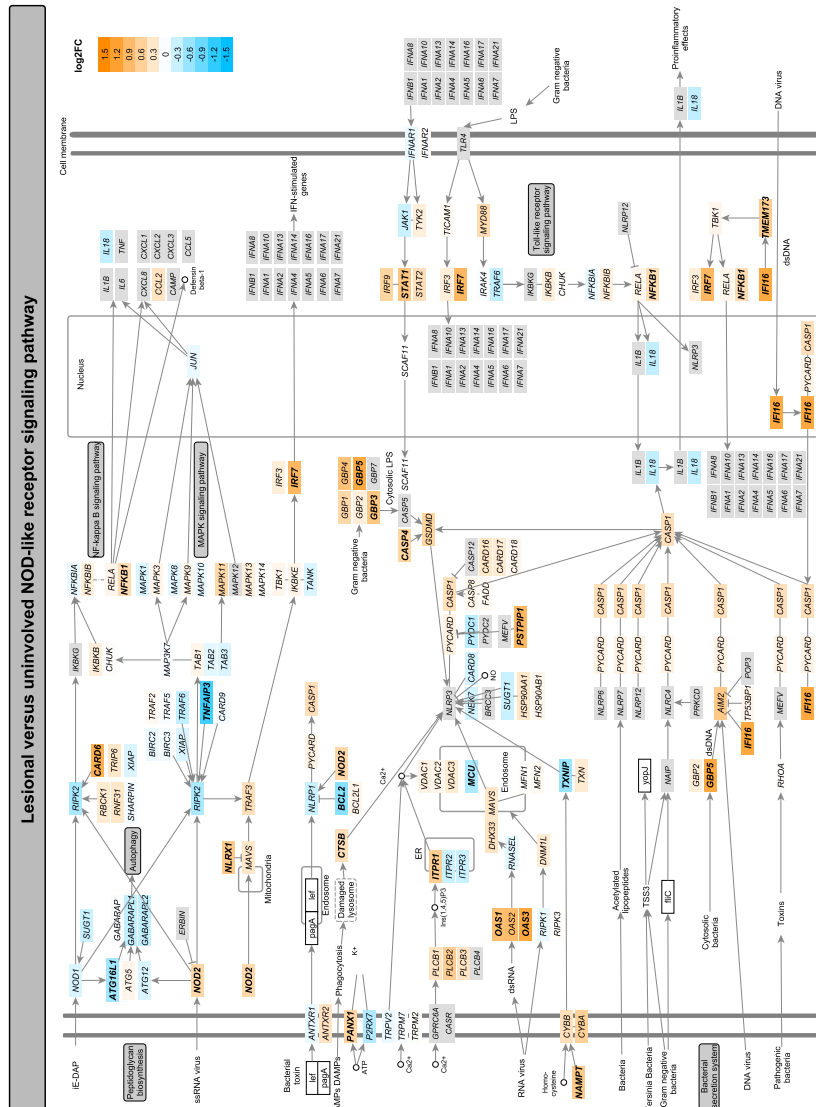


**Figure 3.17: Mapping of the DEGs between lesional and uninvolved epidermis from psoriasis patients onto the NOD-like signalling pathway.** This pathway was sourced from KEGG, manually curated in a way that all member genes are maximised visually and then automatically color-coded by the log<sub>2</sub>fold change expression between the lesional and uninvolved epidermis. Significant DEGs (FDR<0.05) are highlighted in bold. This pathway was identified by pathway enrichment analysis using only DEGs (FDR<0.05).

## **Defining the genome-wide chromatin accessibility landscape and gene expression profile in psoriasis**

---

In addition to the NOD-I signalling, IL-17 signalling was another enriched pathway well known to be relevant in the development of psoriasis. Enrichment of the IL-17 signalling pathway in our data is driven by up-regulation of the S100 protein family (*S100A7*, *S100A8* and *S100A9*) and chemokines such as *CCL20*, which binds the CCR6 receptor and is involved in DCs and T cell chemotaxis. *IL-17RE* which together with IL-17RA forms the receptor for IL-17C was down-regulated in lesional skin. Enrichment of DEGs between lesional and uninvolved skin for the peroxisome proliferator-activated receptor (PPAR) signalling highlighted the link between metabolic dysregulation (particularly lipids) and innate immunity. This pathway included up-regulation of the PPAR receptor  $\delta$  (*PPARD*), stearoyl-CoA desaturases such as *SCD* and *SCD5* involved in fatty acid synthesis and *CD36* which mediates fatty acid transport, also dysregulated in the Tsoi and/or Tervaniemi studies.

### **3.3.6 Comparison of systemic and tissue-specific gene expression signatures in psoriasis**

In order to investigate commonalities and differences in psoriasis gene expression at the affected tissue (skin) and the systemic level (circulating immune cells), overlap between the lists of DEGs was performed. Only modest overlap was found between DEGs in lesional skin compared to uninvolved and the DEGs identified in circulating immune cells. CD14 $^{+}$  monocytes and CD8 $^{+}$  cells showed the greatest overlap, although many of these genes did not show a consistent direction of change in differential expression (Table 3.11). Examples included *TNFAIP3*, which was up-regulated in psoriasis CD4 $^{+}$  and CD8 $^{+}$  cells compared to controls and down-regulated in lesional epidermis when compared to uninvolved.

Early growth response genes were up-regulated in CD14 $^{+}$  monocytes (*EGR1* and *EGR3*) and CD4 $^{+}$  T cells (*EGR1*, *EGR2* and *EGR3*). In lesional skin,

## Defining the genome-wide chromatin accessibility landscape and gene expression profile in psoriasis

---

*EGR2* and *EGR3* were also up-regulated with a much greater magnitude in the fold change ( $\log_2$ fold change -0.74 and -0.53, respectively) compared to the circulating immune cell types.

DEGs overlapping with skin	Total overlap	Same direction	Opposite direction
CD14 <sup>+</sup> monocytes	37	19	18
CD4 <sup>+</sup>	10	6	4
CD8 <sup>+</sup>	37	24	13
CD19 <sup>+</sup>	16	5	11

**Table 3.11: Overlap between the DEGs in the four circulating immune cell types (psoriasis patients versus controls) and the DEGs in psoriasis patients skin biopsies (lesional versus uninvolved).** DEGs based on FDR<0.05 for each of the comparisons

The limited overlap between circulating and skin DEGs was also reflected in the different enriched pathways identified for each analysis. The pathways enriched for CD14<sup>+</sup> and CD8<sup>+</sup> DEGs were mostly immune-related pathways, including TCR, IL-12, TNF and NF- $\kappa$ B signalling. In skin, the DEGs were not only enriched in immune-related pathways but also for pathways involved in metabolism, oxidative stress and cell cycle and genes contributing to the enrichment of immune-related pathways had a more pronounced pro-inflammatory signature, consistent with the skin being a site of more active inflammation compared to circulating immune cells in psoriasis.

### 3.3.7 Integration of chromatin accessibility and expression data for peripheral blood immune cells in psoriasis

The characterisation of the chromatin accessibility landscape and the transcriptome in circulating immune cells from psoriasis patients has revealed a greater effect of disease status on gene expression than chromatin accessibility. To investigate whether an integrated approach combining evidence of differential

## **Defining the genome-wide chromatin accessibility landscape and gene expression profile in psoriasis**

---

accessibility and expression, overlap between DEGs and the genes proximal to DARs ( $\leq 5\text{Kb}$ ) was investigated. Overlap was only found in CD8 $^{+}$  cells, where 6 out of the 53 DARs were annotated by proximity to an RNA-seq DEG in the same cell type (*ARL4A*, *ASCL2*, *ENTPD1*, *TIAM1*, *TRAT1* and *ZNF276*).

For example, T Cell lymphoma invasion and metastasis 1 (*TIAM1*), which activates IL-17 expression and T cell transendothelial migration during inflammation (Kurdi et al. 2016; Grard et al. 2009). This gene showed an increased expression (log<sub>2</sub>fold change 0.44) in psoriasis patients CD8 $^{+}$  cells (Figure 3.18A). Likewise, psoriasis CD8 $^{+}$  cells presented greater chromatin accessibility compared to healthy controls (log<sub>2</sub>fold change 0.41) in a region located at an intron of the *TIAM1* gene and annotated as an active enhancer according to the chromatin segmentation data in this cell type (Figure 3.18C). Common SNPs within this peak did not appear to be an eQTL regulating expression of any gene in CD8 $^{+}$  cells (Kasela et al. 2017) and chromatin conformation data did not reveal interaction of this particular region with the *TIAM1* promoter (Javiere2016), at least in unstimulated conditions, complicating the establishment of a mechanistic connection between chromatin accessibility and gene expression.

Another two relevant genes in the immune response for which ATAC and RNA-seq presented overlap were the ectonucleoside triphosphate diphosphohydrolase 1 (*ENTPD1*), which hydrolyses the pro-inflammatory mediator ATP attenuating the inflammation and acting as a modulator of the immune response, and the TCR-associated transmembrane adaptor 1 (*TRAT1*) gene, a positive regulator of TCR signalling (Antonioli et al. 2013; Valk et al. 2006). *TRAT1* showed up-regulated expression (Figure 3.18B) and increased chromatin accessibility (Figure 3.18D) in psoriasis patients CD8 $^{+}$  cells compared to healthy controls.

## Defining the genome-wide chromatin accessibility landscape and gene expression profile in psoriasis

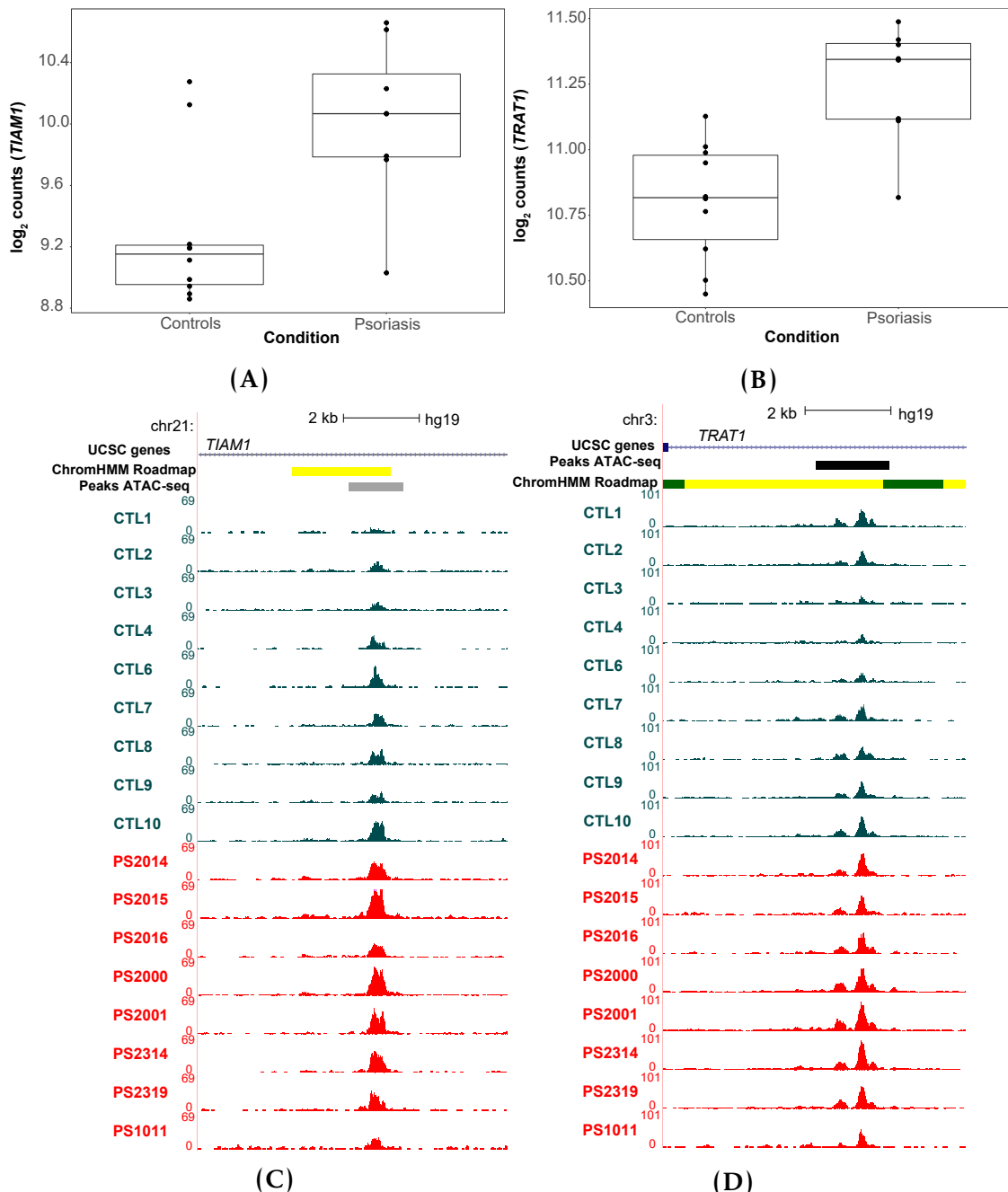


**Figure 3.18: Differential gene expression and chromatin accessibility landscape for *TIAM1* and *TRAT1* genes in  $CD8^+$  cells.** Boxplots represent RNA-seq  $\log_2$  normalised counts for (A) *TIAM1* and (B) *TRAT1* genes in psoriasis and healthy controls  $CD8^+$  cells. UCSC Genome Browser view illustrating the normalised ATAC read density (y-axis) at an intron of the *TIAM1* (C) and *TRAT1* (x-axis) in  $CD8^+$  cells. Both regions were identified as more accessible in psoriasis patients compared to healthy controls. Tracks are colour-coded by condition and assay: control(CTL)=dark turquoise and psoriasis (PS)=red. The Roadmap Epigenomic Project chromatin segmentation map for  $CD8^+$  cells is included.

### **3.3.8 Fine-mapping of psoriasis GWAS loci and functional interpretation**

#### **Fine-mapping using summary statistics data**

Due to the impossibility of accessing genotyping data, fine-mapping of psoriasis Immunochip GWAS loci was conducted using summary statistics of the GACP cohort (2,997 cases and 9,183 controls), one of the two included in the Immunochip psoriasis GWAS study from Tsoi *et al.*, 2012. Summary statistics of the second Immunochip cohort from Tsoi and colleagues (PAGE cohort) (Tsoi *et al.* 2012), were not publicly available through ImmunoBase at the time of this analysis. As explained in Chapter 2, fine-mapping from summary statistics with DIST used the statistics z-score of each of the genotyped SNPs from the GACP cohort to impute the z-scores for the missing SNPs based on the  $r^2$  relationship from the 1000 Genome Project Version 3 (Lee *et al.* 2013). Following z-score imputation for the non-genotypes SNPs, association analysis was performed and ABF, PP and credible set of SNPs were built for each of the signals (Tables 3.12 and A.7).

Fine-mapping was performed for 25 of the Immunochip GWAS loci reported by Tsoi *et al.*, 2012, excluding the MHC and those loci which were in high LD with missense mutations showing experimentally proved or highly confident predicted damaging effects. Out of the 25 regions, 9 loci did not reach  $\log_{10}\text{ABF}>3$  (cut-off used as in Bunt *et al.*, 2015) with 90% credible sets ranging from 19 to 853 SNPs (Table A.7). In 10 of the loci presenting  $\log_{10}\text{ABF}>3$ , the fine-mapping lead SNP was in low LD with the Tsoi *et al.*, 2012 GWAS lead SNP and/ or did not include it in the 90 or 50% credible set (Table 3.12 with \*). This is likely due to lack of power compared to Tsoi and colleagues Immunochip, as only summary statistics from the GACP cohort were available for this analysis.

**Defining the genome-wide chromatin accessibility landscape and gene expression profile in psoriasis**

**Table 3.12: Summary table of the psoriasis Immunochip GWAS loci presenting  $\log_{10}ABF > 3$  for the fine-mapping lead SNP.** For the 16 Immunochip psoriasis GWAS loci showing  $\log_{10}ABF > 3$ , the table reports the closer gene(s), FM lead SNP, RAF, imputation status, z-score, OR for the GAPC cohort lead SNP,  $\log_{10}ABF$  for the FM lead SNP, PP, number of SNPs included in the 90% credible set and the Tsai *et al.*, 2012 GWAS lead SNP. The imputation status indicates whether the SNP was genotypes by the Immunochip array (No) or not (Yes). If a SNP is imputed, the z-score statistic was determined by imputation based on LD with other SNPs, as previously explained. The sign of the z-score indicates whether the RAF allele increases (+) or decreases (-) risk of psoriasis. In 10 of those loci (\*) the fine-mapping lead SNP was in low LD ( $r^2 < 0.5$ ) with the psoriasis GWAS SNP and did not contain it that SNP in the credible set. FM=fine-mapping; RAF=reference panel allele frequency; OR=odds ratio; ABF=approximate Bayes factor; PP=posterior probability.

chr	Closer gene	FM lead SNP	RAF	Imputed	z	OR	$\log_{10}ABF$		PP	90% credible set	Tsai lead SNP
							GAPC	FM lead SNP			
1	<i>IL28RA</i>	rs61774731*	0.10	No	-7.68	1.21	11.5	0.99	1	rs7552167	
2	<i>FLJ16341/REL</i>	rs6714339*	0.14	No	-6.82	1.17	9.0	0.99	1	rs62149416	
2	<i>IFIH1</i>	rs2111485*	0.59	No	5.94	1.27	6.7	0.50	2	rs17716942	
5	<i>TNIP1</i>	rs17728338	0.06	No	7.45	1.59	10.6	0.40	6	rs2233278	
5	<i>IL12B/ADRA1B</i>	rs12188300	0.05	No	7.71	1.58	11.2	0.18	9	rs12188300	
6	<i>TNFAIP3</i>	rs1416173*	0.85	No	-6.36	1.23	7.7	0.15	10	rs582757	
14	<i>NFKBIA</i>	rs74243591	0.21	No	-5.23	1.16	5.0	0.30	12	rs8016947	
17	<i>NOS2</i>	rs117094752*	0.02	No	-6.53	1.22	7.3	0.94	1	rs28998802	
1	<i>SLC45A1/TNFRSF9</i>	rs425371	0.25	Yes	5.52	1.13	5.6	0.14	22	rs11121129	
1	<i>RUNX3</i>	rs61774731 *	0.10	No	-7.68	1.13	11.5	0.99	1	rs7536201	

**Defining the genome-wide chromatin accessibility landscape and gene expression profile in psoriasis**

---

2	<i>B3GNT2/TMEM17</i>	rs9309343*	0.33	Yes	4.92	1.12	4.3	0.66	34	rs10865331
(ch2p15)										
7	<i>ELMO1</i>	rs77840275*	0.10	No	-6.31	1.11	7.5	0.99	1	rs2700987
11	<i>ZC3H12C</i>	rs11213274	0.40	Yes	-4.78	1.14	4.0	0.05	69	rs4561177
16	<i>PRM3/SOCS1</i>	rs111251548*	0.02	No	-7.41	1.13	9.4	0.97	1	rs367569
17	<i>PTRF/STAT3</i>	rs963986	0.17	No	4.82	1.15	4.1	0.18	8	rs963986
19	<i>ILF3/CARM1</i>	rs34536443*	0.03	No	-7.43	1.17	9.7	0.93	1	rs892085

## **Defining the genome-wide chromatin accessibility landscape and gene expression profile in psoriasis**

---

The remaining 6 loci in high LD with the Tsoi *et al.*, 2012 GWAS lead SNP showed 90% credible set of SNPs ranging from 6 to 69 SNPs (Table 3.12). Of those 6 loci, *TNIP1*, *IL12B/ADRA1B* and *PTRF/STAT3* had 90% credible sets which included less than 10 SNPs. *TNIP1* and *IL12B/ADRA1B* had been previously fine-mapped by Das and colleagues using dense genotyping with a customised array followed by association analysis (Das *et al.* 2014). Interestingly, 2 (rs75851973 and rs2233278) and 3 SNPs (rs918519, rs918518 and rs733589) from the *TNIP1* and *IL12B/ADRA1B* 90% credible sets, respectively, were amongst the set of significant variants and perfect near proxies ( $r^2 > 0.9$ ) reported by Das *et al.* for those two same loci. Interestingly, only 2 of the 6 loci showed the fine-mapping lead SNP to be the same as the Tsoi GWAS lead SNP, supporting the sensitivity of the association analysis to sample size.

### **Integration with functional data**

A total of 126 unique SNPs formed the union of 90% credible sets from the 6 loci with fine-mapped lead SNPs presenting a  $\log_{10}ABF > 3$  and including the Tsoi *et al.*, 2012 GWAS lead SNP. None of the SNPs overlapped any of the DARs or differentially H3K27ac regions identified in CD14<sup>+</sup> monocytes, CD4<sup>+</sup>, CD8<sup>+</sup> and CD19<sup>+</sup> cells. Conversely, overlap with the consensus master list ATAC peaks from each of the cell types revealed a total of 16 SNPs from 5 loci located at accessible chromatin in at least one cell type (*NFKBIA*(1 SNP), *PTRF/STAT3*(1 SNP), *SLC45A1/TNFRSF9*(4 SNPs), *TNIP1*(4 SNPs) and *ZC3H12C*(6 SNPs)). However, no overlap was found for the 9 SNPs of the *IL12B/ADRA1B* 90% credible set. CD14<sup>+</sup> monocytes appeared as the cell type showing the largest proportion of accessible chromatin regions containing SNPs from the credible (2.3%), followed by CD19<sup>+</sup>, CD4<sup>+</sup> and CD8<sup>+</sup> cells (1.7, 1.6 and 1.05%, respectively) (Table 3.13). Altogether, integration of the SNPs from the credible set with ATAC accessible regions in four cell types allowed to

## Defining the genome-wide chromatin accessibility landscape and gene expression profile in psoriasis

---

further refine the number of genetic variants with a putative functional role in psoriasis for 5 of the 6 analysed loci. Moreover, in the *PTRF/STAT3* and *SLC45A1/TNFRSF9* loci all the SNPs from the credible set overlapping accessible chromatin appeared to be cell type specific (Table 3.12 and 3.13). Of the 8 SNPs in the *PTRF/STAT3* credible set, only 1 overlapped accessible chromatin in CD14<sup>+</sup> monocytes. Similarly, the *SLC45A1/TNFRSF9* locus presented only 4 out of the 22 SNPs from the 90% credible set within ATAC peaks, of which all were CD14<sup>+</sup> monocytes-specific.

ATAC cell type master list	90% credible set overlapping SNPs (number)	Cell type specific overlap
CD14 <sup>+</sup> monocytes	13	<i>PTRF/STAT3</i> (1), <i>SLC45A1/TNFRSF9</i> (4)
CD4 <sup>+</sup>	5	None
CD8 <sup>+</sup>	3	<i>TNIP1</i> (2)
CD19 <sup>+</sup>	5	None

**Table 3.13: SNPs from the 90% credible set of the successfully fine-mapped psoriasis loci overlapping ATAC accessible chromatin in four cell types.** The number of SNPs in the 90% credible set union (total 126 SNPs) from the 6 successfully fine-mapped loci overlapping ATAC accessible chromatin in each cell type master list are reported. Additionally, the number of SNPs only found to overlap open chromatin in one cell type are indicated together with the locus in which the SNP was fine-mapped.

### The functional landscape at *SLC45A1/TNFRSF9* locus

As previously mentioned, integration of the *SLC45A1/TNFRSF9* 90% credible set of SNPs with ATAC data further refined the number of candidate functional SNPs from 22 to 4. *SLC45A1/TNFRSF9* was one of the new intergenic GWAS associations reported by Tsoi *et al.*, 2012 and is shared with UC and celiac disease (<https://www.immunobase.org/>). Amongst the 4 SNPs overlapping CD14<sup>+</sup> monocyte ATAC-specific peaks was the fine-mapping lead SNP rs425371, located at an intergenic region, approximately 269.3Kb downstream *TNFRSF9* gene (Figure 3.19 top panel). The other 3 SNPs overlapping CD14<sup>+</sup> monocytes

## **Defining the genome-wide chromatin accessibility landscape and gene expression profile in psoriasis**

---

accessible chromatin included rs11121131, rs12745477 and rs417065 (Figure 3.19 top panel). Notably, the 2 ATAC peaks harbouring the 4 fine-mapped SNPs showed variable chromatin accessibility across individuals (Figure 3.19 bottom panel). Roadmap Epigenomic Project data showed enrichment for H3K4me1 in CD14<sup>+</sup> monocytes overlying the two ATAC peaks also overlapping with modest enrichment of in-house H3K27ac data in some of the samples. This was consistent with the designation of these two regions as enhancers by the CD14<sup>+</sup> monocytes chromatin segmentation map (Figure 3.19 bottom panel). No accessible chromatin was found at the location of the 4 fine-mapped SNPs in CD4<sup>+</sup>, CD8<sup>+</sup> and CD19<sup>+</sup> cells, in line with the classification of these two regions as heterochromatin or repressed chromatin by the chromatin segmentation maps in the same cell types. Furthermore, rs11121131, rs12745477 and rs417065 also overlapped with TFBSs identified by ENCODE ChIP-seq data in a number of cell types and rs11121131 was nearby a CpG island (Figure 3.19 bottom panel), altogether reinforcing a putative role of these two regions in regulating gene expression.

rs12745477 and rs425371 (p-values 0.01 and 0.04) had an effect in regulating PARK7 expression levels in CD14<sup>+</sup> monocytes treated with LPS for 24h and in whole blood (Westra2013; Fairfax et al. 2012).

### **3.3.9 Allele-specific differences in chromatin accessibility at the GWAS locus 2p15**

The chr2p15 psoriasis risk locus (lead SNP rs10865331, OR=1.12) represents one of the GWAS associations located in an intergenic region was identified by the Immunochip study from Tsoi *et al.*,2012. This locus is shared with other chronic inflammatory diseases including AS and CD (Jostins2012; Cortes et al. 2013). Although fine-mapping using summary statistics from the psoriasis GACP Immunochip identified a signal with the lead showing

## Defining the genome-wide chromatin accessibility landscape and gene expression profile in psoriasis

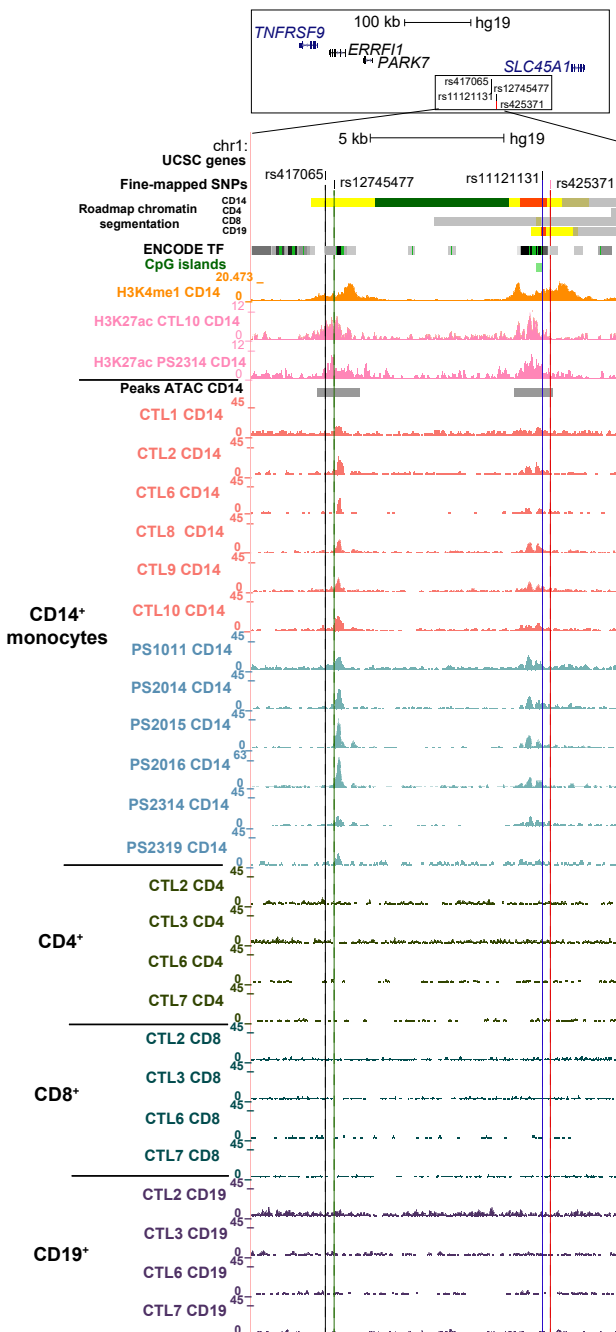


**Figure 3.19: Epigenetic landscape at the location of the SNPs in the 4 SNPs in the 90% credible set for the *SLC45A1/TNFRSF9* psoriasis GWAS locus.** The top panel illustrates the genomic location of the 4 SNPs in the *SLC45A1/TNFRSF9* fine-mapping 90% credible set overlapping ATAC accessible regions in CD14<sup>+</sup> monocytes and their distance from the *SLC45A1* and *TNFRSF9* genes. The bottom panel represents the UCSC Genome Browser view illustrating normalised ATAC read density and fold-enrichment of H3K27ac (both in-house dat(A) together with other publicly available epigenetic datasets (chromatin segmentation map, H3K4me1, ENCODE TF ChIP-seq and CpG islands) (y-axis) at the location of the 4 SNPs (rs425371, rs11121131, rs12745477 and rs417065) (x-axis) from the 90% credible set obtained in the fine-mapping analysis. ATAC and H3K27ac ChIPm data from some controls and psoriasis patients in the cohort are included for CD14<sup>+</sup> monocytes. Representative ATAC tracks from control samples are also shown for CD4<sup>+</sup>, CD8<sup>+</sup> and CD19<sup>+</sup> cells to illustrate the absence of accessible chromatin at the location of the 4 SNPs.

## **Defining the genome-wide chromatin accessibility landscape and gene expression profile in psoriasis**

---

$\log_{10}\text{ABF}=4.3$ , it was not in LD with the psoriasis GWAS lead SNPs. Fine-mapping analysis in the AS UK Immunochip performed by Dr Anna Sanniti implicated rs4672505 (risk allele rs4672505\_A) as the SNP with the greatest PP (0.4) of the 95% credible set, together with another two SNPs (rs6759298 and rs6759003). Rs4672505 was also identified as the lead SNP in a multi-disease meta-analysis from Ellinghaus and colleagues (Ellinghaus et al. 2016).

Rs4672505 overlaps a CD8<sup>+</sup> T cell specific ATAC region, not present in CD14<sup>+</sup> monocytes, CD4<sup>+</sup> and CD19<sup>+</sup> cells (Figure 3.20A), that was not differentially accessible between patients and controls but did show marked variability across individuals (Figure 3.20B), with some individuals (PS2314 and CTL1) demonstrating no ATAC signal at this location.

Integration with publicly available ENCODE and Roadmap Epigenomic Project DHS data confirmed accessible chromatin at this site in Th-1, Th-2 and Th-17 cells and CD8<sup>+</sup> T cells, respectively (Figure 3.20A). Variability across individuals was also observed for H3K27ac enrichment was also observed according to the ChIPm data generated in cohort 1B (Figure 3.20B). ENCODE ChIP-seq experimental data from GM12878 showed binding for RUNX3, a psoriasis and AS GWAS associated gene and is involved in CD8<sup>+</sup> cell differentiation (Wong et al. 2011). In addition, *in silico* TFBS prediction using PROMO (Messeguer et al. 2002) and ENCODE genomic DNase-I footprint in GM128778 predicted STAT1 binding at rs4672505. Altogether, integration of ATAC and publicly available epigenetic data indicated that rs4672505 was the most likely variant, amongst the three fine-mapped SNPs included in the 95% credible set from AS fine-mapping, to have a functional role which could explain the association of chr2p15 with psoriasis risk.

The genotype of each individual for rs4672505 was determined using Sanger sequencing. Amongst the eighteen samples (10 controls and 8 psoriasis patients), one (PS2314) was homozygous for the risk allele (A, MAF=0.43), 11

## Defining the genome-wide chromatin accessibility landscape and gene expression profile in psoriasis

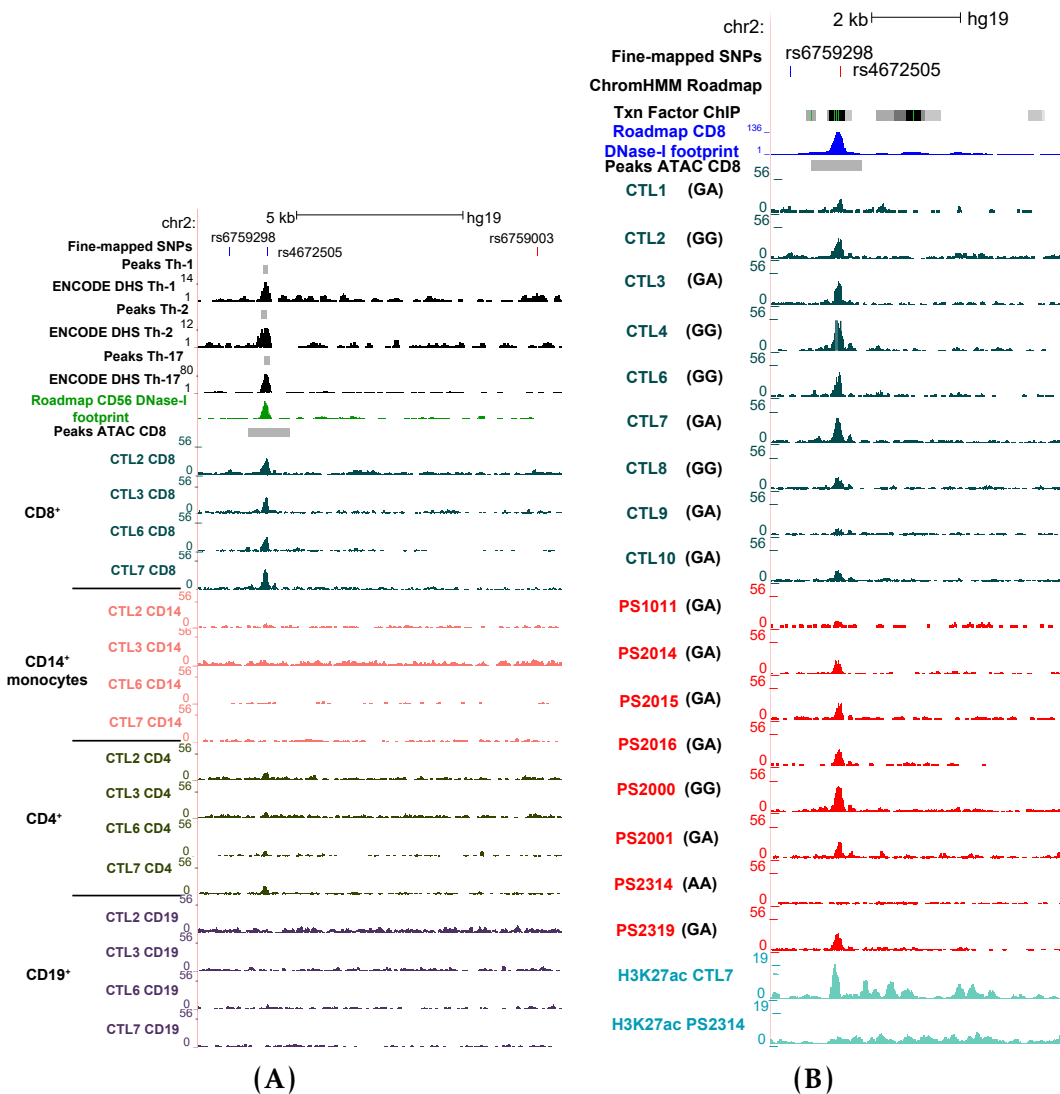


**Figure 3.20: Epigenetic landscape at the location of the 95% credible set of AS fine-mapped SNPs for the chr2p15.** (A) UCSC Genome Browser view illustrating normalised read density for in-house ATAC and a number of other publicly available epigenetic data (DHS, DNase-I footprint, chromatin segmentation map) (y-axis) snapping the 3 SNPs (rs6759298, rs4672505 and rs6759003) (x-axis) from the 95% credible set obtained in the fine-mapping analysis of the chr2p15 GWAS association in AS. Representative ATAC data from the same 4 controls in the cohort and the 4 cell types included in this study are shown. (B) UCSC Genome Browser view illustrating the normalised read density for CD8<sup>+</sup> ATAC (x-axis) generated in psoriasis patients and healthy controls, in-house H3K27ac ChIPm, ENCODE TF ChIP-seq and DNase-I footprint (y-axis) at the location of the SNP rs4672505 (y-axis). For each of the patients and controls of the cohort the Sanger sequencing genotype of rs4672505 is included.

## Defining the genome-wide chromatin accessibility landscape and gene expression profile in psoriasis

were heterozygous and 6 were homozygous for the protective allele (G) (Figure 3.20B). Interestingly, PS2314, the only homozygous individual for the risk allele, showed complete absence of the peak at rs4672505. To further investigate the role of rs4672505 genotype in the variability of chromatin accessibility across individuals, the normalised read counts at the ATAC peak chr2:62,559,749-62,561,442 were used as a dependent variable in linear model analysis based on rs4672505 genotype, using batch as a covariate.

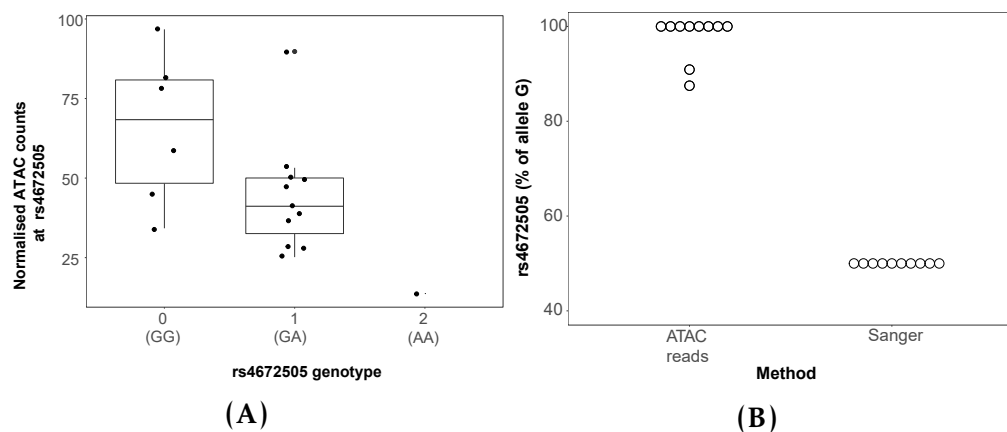


**Figure 3.21: rs4672505 genotype and chromatin accessibility at chr2:62,559,749-62,561,442 in CD8<sup>+</sup> cells.** (A) Boxplot illustrating the effect of the rs4672505 genotype on chromatin accessibility at the chr2:62,559,749-62,561,442 ATAC peak. Log<sub>2</sub> normalised ATAC counts adjusted for batch effect, also included as a covariate for the linear model, are plotted for each sample against the number of copies of the minor allele (G=0, AG=1, AA=2). (B) Representation of the percentage of ATAC reads overlapping rs4672505 and mapping to the major allele (G) in comparison to the Sanger genotype results for the eleven heterozygous individuals at this SNP.

Significant negative correlation ( $p\text{-value}=0.035$ ) was found, suggesting allele-dependent chromatin accessibility (Figure 3.21 a). Furthermore, allelic imbalance for the ATAC reads at rs4672505 position was investigated on those individuals identified as heterozygous by Sanger sequencing and for which 50% of the ATAC reads were expected to map to each of the alleles. This analysis demonstrated a larger percentage of ATAC reads (greater than the expected 50%) preferentially tagging the protective allele G (Figure 3.21 b). This finding was not driven by mapping bias, since A was the reference allele in the hg19 build used to map the ATAC data. Overall, these results showed evidence of greater chromatin

## Defining the genome-wide chromatin accessibility landscape and gene expression profile in psoriasis

accessibility in presence of the fine-mapped protective allele rs4672505(G) at the chr2p15 locus.

A major challenge with intergenic GWAs signals is the difficulty in determining the specific gene they may be modulating, for example through differential enhancer activity affecting gene expression. rs4672505 is located 140Kb downstream of *B3GNT2* and 150Kb upstream of *TMEM1*. Publicly available promoter capture data from Javierre *et al.* 2016 in CD8<sup>+</sup> revealed a genome-wide significant interaction (CHiCAGO score=7.67) between a region containing rs4672505 and the promoter of the *B3GNT2* gene (Figure 3.22A).

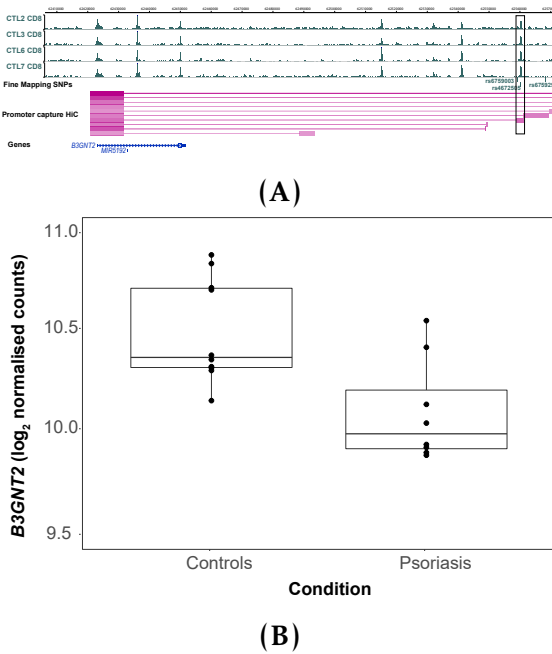


**Figure 3.22: Potential role of rs4672505 in regulating *B3GNT2* gene expression.** (A) WASHU Genome Browser track showing in CD8<sup>+</sup> cells normalised ATAC read density in four of the healthy controls, the location of the three SNPs of the 95% credible set and the promoter capture HiC data depicting the regions interacting with the bait at the *B3GNT2* promoter. (B) Boxplot illustrating the *B3GNT2* log<sub>2</sub> normalised RNA-seq counts adjusted for batch effect in the psoriasis and healthy control groups.

This interaction was not found in any of the additional 16 human primary hematopoietic cell included in the study. No upstream interaction with *TMEM1* promoter was identified. Investigation of the publicly available T cell eQTL dataset from Kasela *et al.* and Raj *et al.* did not show a significant eQTL for this SNPs or SNPs in high LD ( $r^2>0.8$ ) either in CD8<sup>+</sup> or CD4<sup>+</sup> (Raj *et al.*

## **Defining the genome-wide chromatin accessibility landscape and gene expression profile in psoriasis**

---

2014; Kasela et al. 2017). Similarly, no eQTL effect of rs4672505 was found in unstimulated or stimulated CD14<sup>+</sup> monocytes (Fairfax et al. 2014). However, a whole blood eQTL study from Jansen and colleagues revealed a significant *cis*-eQTL ( $\text{FDR}=1.34\times 10^{-5}$ ) with moderate effect size ( $\beta=-0.16$ ) for the minor allele (Jansen et al. 2017). In terms of gene expression based on disease state, significant ( $\text{FDR}<0.05$ ) down-regulation of *B3GNT2* was observed in psoriasis patients when compared to controls in CD8<sup>+</sup> cells ( $\log_2 \text{fold change}=-0.317$ ) (Figure 3.22B). These data provide evidence of allele-specific chromatin accessibility at chr2p15 in CD8<sup>+</sup> T cells involving a GWAS SNP, with chromatin conformation capture and gene expression data suggesting that this modulates, at a distance, expression of *B3GNT2*, providing insights into the possible mechanistic basis of the disease association seen in psoriasis and other inflammatory diseases, including AS.

## **3.4 Discussion**

### **3.4.1 Chromatin accessibility and H3K27ac landscape in psoriasis immune cells**

Comparison of chromatin accessibility and H3K27ac histone modifications has revealed a small number of differential regions between patients and controls in the four cells types under study. For both epigenetic features, CD14<sup>+</sup> monocytes and CD8<sup>+</sup> cells had the largest number of discrete changes. In ATAC, greater accessibility in CD8<sup>+</sup> cells from patients compared to controls was found at two regions proximal to *IL7R* and *TNFSF11*, respectively, that also overlap FANTOM eRNA in the same cell type. Both genes are well known for having a pro-inflammatory effect and be involved in chronic inflammatory diseases. For example, *TNFSF11* is downstream of the lead SNP for a CD risk locus, and its protein product RANKL was found to be overexpressed in epidermis from

## **Defining the genome-wide chromatin accessibility landscape and gene expression profile in psoriasis**

---

psoriasis patients, highlighting the role of this gene in the pathophysiology of psoriasis (Toberer et al. 2011).

Integration of the ATAC and H3K27ac ChIPm differential analysis only found one overlapping region at an intron of the *DTD1*, a D-Tyr-tRNA deacylase responsible for releasing D-aminoacids from the tRNAs, making them available to be loaded with L-aminoacids for the production of functional proteins (Bhatt2016). A role of aminoacylRNA synthetases, responsible for the loading of L-aminoacids into tRNAs, in modulation of inflammation and angiogenesis (Yao2013). Although, intronic variants in *DTD1* have been associated with anxiety, onset of sleep irregularities and age-related variation of DNA methylation through GWAS (<https://www.ebi.ac.uk/gwas/>), no evidence of *DTD1* involvement in chronic inflammation and psoriasis has yet been reported. Altogether, the lack of overlap between DARs and differentially H3K27ac modified regions might be expected given that chromatin accessibility is driven by the interaction between a number of histone modifications, TFs, and structural proteins, such as CTCF.

The results in this chapter suggest that disease status does not involve global differences in chromatin accessibility and H3K27ac between patients and controls in the studied circulating immune cells. Recent similar studies performing ATAC in B cells from SLE patients have revealed larger differences in the chromatin accessibility landscape between patients and controls , while H3K27ac mapping in mCD4<sup>+</sup> cells isolated from juvenile idiopathic arthritis synovial fluid found approximately one thousand differential enhancers when compared to healthy control circulating cells (Scharer et al. 2016; Peeters et al. 2015). Conversely only small differences were found when comparing mCD4<sup>+</sup> from peripheral blood of patients and controls, highlighting the specificity of the disease signature at the site of inflammation and importance of studying the most disease relevant cell types and tissues. Moreover, it may be necessary

## **Defining the genome-wide chromatin accessibility landscape and gene expression profile in psoriasis**

---

to study changes in chromatin accessibility in the context of genotype and under exogenous inflammatory stimuli that may manifest those differences (**Calderon2018**; Alasoo et al. 2018).

### **3.4.2 Dysregulation of gene expression in psoriasis circulating immune cells**

Comparison of gene expression between psoriasis and healthy controls in a cell type specific manner identified larger numbers of DEGs compared to DARs or differential H3K27ac modifications. As for ATAC and ChIPm, CD14<sup>+</sup> monocytes and CD8<sup>+</sup> cells showed the largest number of transcriptomic changes in disease. This may suggest greater relevance of these two cell types in the systemic footprint of psoriasis. The more dysregulated gene expression in CD8<sup>+</sup> compared to CD4<sup>+</sup> may suggest that, as in skin, CD8<sup>+</sup> are the main effector cells upon induced-activation by CD4<sup>+</sup> cells (Nickoloff and Wrone-Smith 1999). The importance of monocytes/macrophages in psoriasis has also been demonstrated by their presence in psoriatic skin where TNF- $\alpha$  production contributes towards maintenance of inflammation (**Nickoloff2000**; Wang et al. 2006).

For example, *MAP3K4* down-regulation in LPS stimulated PBMCs has been identified as an immune-suppressive feature in CD leading to reduced expression of the cytokine IL-1 $\alpha$ . In the IL-12 signalling pathway which leads to T cell proliferation and IFN- $\gamma$  production through activation of TFs from the STAT family, CD14<sup>+</sup> cells presented down-regulation of *STAT4* and *STAT5A* in psoriasis versus controls. *STAT2*, other member of the STAT family, was found to be down-regulated in psoriasis PBMCs and in AS monocyte-derived macrophages when compared to controls but was not differentially expressed in my data (Coda et al. 2012; Smith et al. 2008). In other chronic inflammatory diseases such as T2D, persistent STAT5 phosphorylation has been found in circulating monocytes isolated from patients upon GM-CSF (Litherland et al.

## **Defining the genome-wide chromatin accessibility landscape and gene expression profile in psoriasis**

---

2005). Further investigation to determine phosphorylated STAT4 and STAT5 protein abundance will be required to determine if the down-regulation at the transcript level observed in psoriasis CD14<sup>+</sup> monocytes is biologically relevant.

A very interesting observation in this data was the down-regulation of *IFNG* in psoriasis CD8<sup>+</sup> cells, a gene member of the IL-12 signalling pathway. This has previously been reported in unstimulated and stimulated macrophages derived from AS patients, in synovial fluid from SpA patients compared to RA and in a SpA rat model (Smith et al. 2008; Fert et al. 2014). In AS monocytes and in the SpA rat model, *IFNG* down-regulation was accompanied by an overall inverse transcriptional response of IFN-regulated genes, which was not seen in my data. Reduced expression of *IFNG* in knock-out mice has been shown to increase activation of the IL-23/IL-17 axis, which is pivotal in psoriasis pathogenesis, resulting in a pro-inflammatory effect (Cañete et al. 2000; Chu et al. 2007). Nevertheless, either IL-23 or IL-17 were up-regulated in psoriasis CD8<sup>+</sup> T cells compared to healthy controls.

In CD8<sup>+</sup> specifically, DEGs showed significant enrichment for three very relevant pathophysiological pathways in psoriasis: NF-κB, TNF and chemokine signaling. Important cross-talk between the NF-κB and TNF signaling pathway was observed, with a number of dysregulated genes contributing to both. Interestingly, the enrichment of these pathways involved up-regulation of pro-inflammatory genes (e.g *ATF2*, *ATF4*, *RELA*, *RELB*) but also increased expression of well-characterised immunoregulatory genes. These included *NFKBIA* and *TNFAIP3*, also up-regulated in CD14<sup>+</sup> monocytes and CD4<sup>+</sup> cells respectively, and both associated with psoriasis risk and a number of other chronic inflammatory diseases, including MS, RA, SLE and T1D (Vereecke et al. 2011). *NFKBIA* inhibits NF-κB by binding it and preventing translocation to the nucleus. Similarly, *TNFAIP3* undergoes upregulation upon inflammatory stimuli and NF-κB activation to inhibit the NF-κB TNF-mediated response and

## **Defining the genome-wide chromatin accessibility landscape and gene expression profile in psoriasis**

---

promote the return to homeostasis. *NFKBIA* and *TNFAIP3* were not found to be dysregulated in psoriasis PBMCs by Coda *et al.*, Lee *et al.* and Mesko *et al.* or in PBMCs from PsA patients versus controls (Dolcino *et al.* 2015). Interestingly, qPCR analysis in PBMCs from mild ( $\text{PASI} < 4.84$ ) and severe ( $\text{PASI} > 4.84$ ) psoriasis vulgaris revealed a significant negative correlation between *TNFAIP3* expression and disease severity (Jiang *et al.* 2012). This study also demonstrated *TNFAIP3* down-regulation in PBMCs from the mild group of patients, but not from the severe one, when compared to healthy controls. This would be consistent with my findings, with the caveat that all patients from my cohort would be classified as severe ( $\text{PASI} > 4.84$ ) according to Jian and colleagues (Jian2012). Altogether, the up-regulated expression of *TNFAIP3* and *NFKBIA* compared to healthy controls may be the result of a feedback loop reflecting a persistent inflammatory stimuli in psoriasis peripheral blood and a mechanism that limits the systemic inflammatory response to some extent (Idel *et al.* 2003).

Amongst the differential expression of chemokines, up-regulation of the chemokine receptor *CCR10* in  $\text{CD8}^+$  cells from psoriasis patients was of particular interest. In circulation, expression of *CCR10* is restricted to a subset of circulating mCD4 $^+$  and mCD8 $^+$  T cells expressing the cutaneous lymphocyte-associated antigen (CLA), and preferentially recruited to cutaneous sites of inflammation (Hudak *et al.* 2002). Indeed, an increase of  $\text{CCR10}^+$  infiltrated T lymphocytes in psoriatic skin, where keratinocytes express *CCR10* ligand *CCL27*, has been demonstrated (Homey *et al.* 2002). The up-regulation of *CCR10* in my data could potentially suggest an increase of mCD8 $^+$   $\text{CCR10}^+$  cells ready to migrate into the skin lesions. Overall, these data have revealed differential gene expression between psoriasis patients and controls for relevant immune genes showing pro- and anti-inflammatory effects in peripheral blood immune cells. Although down-regulation of pro-inflammatory genes and up-regulation of anti-

## **Defining the genome-wide chromatin accessibility landscape and gene expression profile in psoriasis**

---

inflammatory genes has been observed, understanding the overall effect of those interactions in the inflammatory response requires further investigation.

### **3.4.3 Correlation between changes in chromatin accessibility and gene expression**

In this chapter, greater changes in gene expression have been identified compared to chromatin accessibility. Strikingly, in CD8<sup>+</sup> cells, 687 transcripts were differentially expressed between psoriasis and healthy controls but only 55 regions showed differential chromatin accessibility when performing the same contrast and only six of the 687 were proximal to a DAR. This may relate to the complexity of gene regulation with a multi-component regulatory process manifesting in differential gene expression, to which chromatin accessibility is only one part. Correlation between chromatin accessibility measured by ATAC and gene expression has been reported to some extent in a number of studies, with limitations in establishing relationships between enhancer regions and the regulated target gene (Ackermann et al. 2016; Wang et al. 2018).

Two relevant DEG nearby a DAR were *TIAM1* and *TRAT1*, showing increased chromatin accessibility and gene expression in psoriasis CD8<sup>+</sup> cells compared to healthy controls. The T cell lymphoma invasion and metastasis 1 *TIAM1* is involved in IL-17 expression and cell migration into the inflamed tissue (Kurdi et al. 2016; Grard et al. 2009). However, no eQTL or chromatin conformation data in this cell type has been found to formally establish a link between the region harbouring this DAR and *TIAM1* expression. The TCR associated transmembrane adaptor 1 *TRAT1* gene is a positive regulator for TCR signalling and has been observed to be down-regulated in Tregs (**Birzele**).

### **3.4.4 Transcriptomic profiles in lesional and uninvolved psoriatic epidermis**

Investigation of differences in the transcriptomic profile between paired lesional and uninvolved skin was conducted for three psoriasis patients. Most previous transcriptional studies in psoriasis have used full thickness skin biopsies, comprising a mix of cell types including fibroblast, adipocytes, keratinocytes from the epidermis and dermis and infiltrated immune cells. A study from Ahn and colleagues demonstrated large differences in gene expression between whole biopsies and FACS-isolated keratinocytes, and the former may be masking keratinocyte-specific pathophysiological differences in many previous studies using psoriasis skin biopsies (Ahn2016). In this chapter, RNA-seq was conducted on epidermal sheets isolated from whole biopsies and a total of 1,227 DEGs were identified. Comparison with the Tervaniemi *et al.* study contrasting gene expression between lesional and uninvolved epidermis split biopsies, mainly formed by epidermis, revealed an overlap of only 359 out of the 1,227 DEGs detected in my data (12.1% of Tervaniemi *et al.* DEGs). Interestingly, the overlap with the Tsoi *et al.* study using whole biopsies was similar (505, 13.1% of Tsoi *et al.* DEGs) and only 5 genes had opposite direction of change, in contrast with the 75 showing discrepancies with Tervaniemi's study. The similar percentage overlap with the Tsoi study despite the different source material could simply be the result of greater power in that study.

Genes consistently up-regulated across the three studies included genes from the *S100A* family. The *S100* family are located in the chr1p21 locus, which harbours genes involved in keratinocytes differentiation, act as calcium sensors and may also have a chemotactic effect (Eckert *et al.* 2004). In particular, *S100A9* and *S100A12* undergo up-regulation in psoriasis (Broome *et al.* 2003), with the latter involved in the T cell proliferative response and IFN- $\gamma$  and IL-2 production (Moser *et al.* 2007). *LCE3B*, also at the chr1p21 locus, was

## **Defining the genome-wide chromatin accessibility landscape and gene expression profile in psoriasis**

---

also upregulated in lesional skin compared to uninvolved in all three studies. *LCE3B/C\_del*, a psoriasis GWAS association, is found in approximately 60 to 70% of European psoriasis patients (Cid et al. 2009). As explained in Chapter 1, *LCE* gene expression is induced upon disruption of the skin barrier, and expression of *LCE3B* and *LCE3D* has been only detected in lesional but not uninvolved psoriatic skin of heterozygous individuals (Cid et al. 2009; Bergboer et al. 2011).

Pathway enrichment analysis for the DEGs between lesional and uninvolved skin revealed a number of relevant biological processes for psoriasis pathophysiology. These highlighted alterations in cell cycle and metabolic processes, including amino acid metabolism, glycolysis, and hypoxia (HIF-I signalling), which had been identified in other studies performing DGE analysis between lesional and uninvolved skin or genome-wide pathway analysis (Coda et al. 2012; Gudjonsson et al. 2010; Aterido et al. 2016; Tervaniemi et al. 2016). Up-regulation of the hypoxia-inducible TFs HIF-1 $\alpha$  and HIF-2 $\alpha$  has been reported in lesional skin, correlating with an increase in *VEGF* transcript levels, a gene regulated by HIFs that mediates pathological angiogenesis also characteristic of psoriasis (Rosenberg 2007). No correlation was observed between *HIF*A and *VEGF* in the data presented here, likely due to the small sample size. Moreover, HIF-I signalling is also involved in regulating Th-17/Treg ratios and therefore in perpetuation and termination of the immune response (Dang et al. 2011).

Immune-related pathway enrichment were also found, including Th-17, IL-12 and NOD-like signalling. Interestingly, NOD-like signalling was found to be enriched in DEGs between lesional and uninvolved skin in a contemporary study by Tervaniemi and colleagues (Tervaniemi et al. 2016). Tervaniemi mainly attributed this novel pathway to the greater sensitivity of RNA-seq compared to microarrays to detect changes in gene expression for genes involved in this pathway. The fact that Tsoi *et al.* also used RNA-seq and did not show enrichment for NOD-like signalling is likely due to the type of biopsy, highlighting the value

## **Defining the genome-wide chromatin accessibility landscape and gene expression profile in psoriasis**

---

of studying epidermis instead of full thickness skin to uncover dysregulation of functional pathways in keratinocytes. NOD-like signalling involves signal transduction by NOD-like receptors, a type of pattern-recognition receptors, which can recruit and activate caspases into the inflammasomes or trigger inflammation through NF- $\kappa$ B and MAPK. Amongst the genes contributing to this pathway *CARD6*, *IFI16*, *NOD2* and *NLRX1* overlapped with Tervaniemis data and showed up-regulation in both. Notably, polymorphisms in *NOD2* have been linked to inflammatory diseases such as CD, atopic eczema and arthritis and potentially with psoriasis and PsA (Zhong et al. 2013; Zhu et al. 2012).

Lastly, PPAR signaling appeared as one of the most significantly enriched pathways and represents a link between metabolic and innate immunity dysregulation in psoriasis. PPARs are TFs activated by fatty acid signaling with an anti-inflammatory role in the development of metabolic diseases and chronic inflammation such as RA (Straus and immunology 2007; Ji et al. 2001). Similarly to my study, *PPARD* was up-regulated in psoriatic lesional skin, and molecular studies have demonstrated a role of this PPAR in keratinocyte hyperproliferation through induction of heparin-binding EGF-like growth factor (HB-EGF) (Romanowska et al. 2008).

### **3.4.5 LncRNAs in psoriasis**

The largest number of differentially expressed lncRNAs between psoriasis patients and controls were found in CD14 $^{+}$  monocytes and CD8 $^{+}$  T cells (28 and 31, respectively for FDR<0.05) with 46 lncRNAs differentially expressed between lesional and uninvolved skin (FDR<0.05). Several studies have contrasted lncRNAs in lesional compared to uninvolved or healthy skin (Ahn2016; Li et al. 2014; Gupta et al. 2016; Tsoi et al. 2015) but no study has been conducted to identify differentially lncRNAs in a cell type-specific manner in peripheral blood

## **Defining the genome-wide chromatin accessibility landscape and gene expression profile in psoriasis**

---

from psoriasis patients. The role of lncRNAs has been studied in RA, SLE, AS, and PsA (Muller 2014; Shi et al. 2014; Zhang et al. 2017; Dolcino et al. 2018).

Characterisation of lncRNA biological function is a developing field, which represents a limitation when interpreting these results (B et al. 2018). Some of the well-characterised dysregulated lncRNAs have a role in the immune response. For example, in psoriasis CD14<sup>+</sup> monocytes the up-regulation of *HOTAIRM1* was found to be associated with down-regulation of the predicted target gene *USP1*. *UPF1* is involved in nonsense-mediated decay and in partnership with the monocyte chemotactic protein-1-induced protein-1 (*MCPIP1*) gene drives degradation of inflammation-related mRNAs to ensure maintenance of homeostasis (Mino et al. 2015). Down-regulation of *UPF1* in psoriasis CD14<sup>+</sup> monocytes may suggest impairment of this homeostatic mechanism, contributing to disease pathophysiology in this cell type. Another example of a relevant lncRNA up-regulated in CD14<sup>+</sup> monocytes was *NEAT1*, which has also shown up-regulation in SLE CD14<sup>+</sup> monocytes. Knock-down demonstrated impairment of TLR4 signalling and down-regulation of inflammatory genes including IL-6 and CXCL10 (Zhang et al. 2016).

*MIR146A* was found to be differentially expressed between lesional and uninvolved skin and also when comparing psoriasis CD8<sup>+</sup> T cells to healthy controls. Molecular studies have suggested a role for miR-146a as a negative regulator of the TLR4 pathway through inhibition of TNF associated factor 6 (*TRAF6*) and IL-1 receptor-associated kinase 1 (*IRAK1*) expression (Taganov et al. 2006). The up-regulation of *MIR146A* expression in lesional epidermis compared to uninvolved has been observed in other studies, and was also shown to be increased in lesional skin versus healthy biopsies (Lerman 2014; Tsoi et al. 2015; Li et al. 2014). Down-regulation of miR-146a levels in CD8<sup>+</sup> cells would support failure of one of the check-points controlling sustained inflammation and the subsequent pathophysiological implications, while the up-regulation in lesional

## **Defining the genome-wide chromatin accessibility landscape and gene expression profile in psoriasis**

---

skin would not be expected given the exacerbated inflammatory response in skin characteristic of psoriasis.

Other dysregulated non-coding RNAs in lesional epidermis relevant to psoriasis pathophysiology were *HG19* and *MIR31HG*, found to be down- and up-regulated, respectively. Silencing miR-31hg in keratinocyte immortal cell line HaCaT induced cell cycle arrest and inhibited cell proliferation, consistent with two characteristic aspects dysregulated in psoriatic keratinocytes (Gao et al. 2018). Overall, the lncRNA differential analysis conducted in this chapter gives an overview of dysregulation in blood and skin of psoriasis patients. A more comprehensive analysis could be performed to identify putative targets for all the identified lncRNAs. Those interactions could then be used to identify relevant biological processes through network and pathway analysis using only those dysregulated lncRNAs matching dysregulated target genes, similarly to the strategy used by Dolcino *et al.*, 2018. However, such an analysis would likely require increased sample size to be appropriately powered.

### **3.4.6 Differences in transcriptional dysregulation in peripheral blood and skin**

Comparison of the dysregulated genes in circulating immune cells and in psoriatic skin revealed very limited overlap. CD14<sup>+</sup> monocytes and CD8<sup>+</sup> cells showed the greatest overlap of DEGs; however, almost half of the genes showed opposite direction in differential expression, consistent with a report by Coda comparing DEGs genes in psoriasis patients and controls PBMCs to genes dysregulated between lesional and uninvolved skin biopsies (Coda et al. 2012). Genes showing opposite changes in circulation and in skin included the GWAS gene *TNFAIP3*, *EGR2* and *EGR3*, amongst others. As previously mentioned, *TNFAIP3* down-regulation in lesional skin may reflect complete loss of an NF- $\kappa$ B pathway check-point to control and terminate the inflammatory response

## **Defining the genome-wide chromatin accessibility landscape and gene expression profile in psoriasis**

---

at the site of inflammation. Similarly, *EGR2* and *EGR3* are pivotal for control of inflammation and antigen-induced proliferation. In addition to its role in regulating inflammation, down-regulation of *EGR2* in skin may also increase keratinocyte proliferation as has been shown in certain types of cancer (Wu et al. 2010).

Differences are also observed in the distinct enriched pathways. For example, DEGs in skin not only showed enrichment for immune-related functions but also highlighted metabolic dysregulation that appears to be characteristic of this site of inflammation. Moreover, immune related pathway such as NOD-like signalling was only seen in skin. Likewise, up-regulation of genes from the *S100* family in lesional skin, such as *S100A7*, *S100A8*, *S100A9*, contributed to enrichment of IL-17 signalling and appeared to be a feature of dysregulated inflammation only in skin. Notably, these genes had also been reported as a specific hallmark of skin inflammation when compared to inflamed synovium from matched PsA patients, supporting the better outcomes for IL-17 antagonists in skin lesions compared to the inflammation of the synovium (Belasco et al. 2015).

### **3.4.7 Fine-mapping using summary statistics and integration with epigenetic data**

Fine-mapping of GWAS loci is one strategy to narrow down putative functionally relevant variants identified by GWAS studies. Using summary statistics from the psoriasis Immunochip GWAS GPC cohort, 26 of the genome-wide significant loci reported by Tsoi and colleagues were fine-mapped (Tsoi et al. 2012). Successful fine-mapping based on ABF cut-off was achieved for 16 loci, 10 of them which association signal identified by the fine-mapping was not in LD with the GWAS signal reported by Tsoi and colleagues. This is consequence of a reduced power in the association analysis compared to Tsoi and colleagues (Tsoi

## **Defining the genome-wide chromatin accessibility landscape and gene expression profile in psoriasis**

---

et al. 2012), supporting the sensitivity of the association analysis to sample size, previously shown by other studies (Bunt et al. 2015). In contrast, 6 of the loci were successfully fine-mapped, with the fine-mapping lead SNP in high LD with the GWAS lead SNP. Fine-mapping successfully reduced the number of putative causal SNPs, with some loci showing less than 10 SNPs in the 90% credible set, such as *TNIP1*, *IL12B/ADRA1B* and *PTRF/STAT3*. Interestingly, the credible set of *TNIP1* included 6 SNPs, a lower number of putative causal SNPs compared to the 9 SNPs (which only included those in LD  $r^2 \geq 0.9$ ) reported by a study performing dense genotyping and association analysis for 8 psoriasis loci (Das et al. 2014). Integration of DARs and differentially H3K27ac modified regions with the SNPs from the credible set of the loci successfully fine-mapped did not reveal any overlap. In contrast, 16 SNPs out of the 126 forming the union of credible set of SNPs from 6 successfully fine-mapped loci, co-localised with accessible chromatin, and some of the with cell type specific ATAC peaks. Interestingly, integration with ATAC data further reduced the credible set of SNPs in the *SLC45A1/TNFRSF9* locus from 22 to 4, all of them overlapping CD14<sup>+</sup>-specific ATAC peaks. Integration of eQTL publicly available data showed regulation of *PARK7* expression by rs12745477 and rs425371 genotype. *PARK7* is a sensor for oxidative stress causing early-onset of Parkinson's disease (Bonifati2003). A role for *PARK7* in inflammation has been described in Tregs development and in bone marrow-derived macrophages, where *PARK7* impairs LPS response with implications in sepsis pathogen clearance (Singh2015; Amatullah2017).

Similar approaches integrating fine-mapping SNPs and tissue-specific chromatin accessibility maps have led to successful prioritisation of putative causal variants in other diseases (Stefan et al. 2014). Moreover, tools such as Risk Variant Inference using Epigenomic Reference Annotation (RiVIERA) has been applied to perform fine-mapping for the Immunochip GWAS associated loci, including psoriasis, using summary statistics and incorporating in the model

## **Defining the genome-wide chromatin accessibility landscape and gene expression profile in psoriasis**

---

the 43 ENCODE and Roadmap Epigenomic Project annotation features most enriched for psoriasis GWAS loci (Li et al. 2016). For example, Li and colleagues only reported 2 SNPs to explain the association of the *SLC45A1/TNFRSF9* locus to psoriasis but none was in LD with the GWAS signal from Tsoi *et al.*, 2012.

### **Allelic differences in chromatin accessibility at the chr2p15 locus**

One of the particularly interesting psoriasis GWAS associations is the chr2p15 locus, where the lead SNP is located in an intergenic region 140Kb and 150Kb away from *B3GNT2* and *TMEM1* respectively and is also associated with CD and AS (**ostins2012**; Cortes et al. 2013). Fine-mapping at chr2p15 using psoriasis summary stats from the GAPC cohort failed to identify a signal in LD with the psoriasis GWAS from Tsoi and colleagues (Tsoi et al. 2012). The results published by Li and colleagues also failed to fine-map this locus. Conversely, fine-mapping analysis in AS implicated rs4672505, in high LD with the psoriasis Immunochip chr2p15 SNP, which was found to overlapped a CD8<sup>+</sup>-specific ATAC peak. This SNP is also the 4<sup>th</sup> variant prioritised by the fine-mapping algorithm published by Farh and colleagues (**Farh2014**). Chromatin accessibility was observed to vary between individuals, with complete loss of ATAC peak in some individuals. Integration of genotyping data with ATAC revealed allele-dependent chromatin accessibility, with loss of chromatin accessibility correlating with the risk allele. Promoter capture-C data linked rs4672505 to the *B3GNT2* promoter only in CD8<sup>+</sup> cells, suggesting the accessible chromatin at rs4672505 may be highlighting an enhancer element interacting with *B3GNT2* promoter as a priming event (**Javierre2016**). *B3GNT2* is a major polylactosamine synthase involved in the post-translational modifications of carbohydrate chains, which are essential for cellcell, receptorligand and carbohydratecarbohydrate interactions. Interestingly, *B3GNT2* knock-out mice demonstrated more sensitive and strongly proliferating T cell and B cell responses to stimulation compared to

## **Defining the genome-wide chromatin accessibility landscape and gene expression profile in psoriasis**

---

wild-type (Togayachi et al. 2010). In T cells, this effect was linked to a reduction of polylactosamine chains in co-stimulatory accessory molecules such as CD28, overall leading to enhanced initiation of the immune response *in vitro*.

Up-regulation of *B3GNT2* in this context could be contributing to attenuation and modulation of CD8<sup>+</sup> activation. Under this scenario, the presence of the risk allele (A) at this stimulus-specific enhancer could increase risk of disease by reducing chromatin accessibility, in both homozygous and heterozygous individuals. Similar examples have been found in other diseases, for example in T2D, where only one SNP from the credible set located at a *TCF7L2* intron overlapped FAIRE-seq accessible chromatin, with the risk allele showing greater abundance at open chromatin and increased enhancer activity (Gaulton et al. 2010; Stefan et al. 2014). Nevertheless, establishing of a more comprehensive and accurate model to further explain the functional role of rs4672505 in psoriasis susceptibility will require additional work.

### **3.4.8 Limitations in the approach**

Although the work in this chapter has shed light on the chromatin landscape and gene expression in psoriasis in a cell type and tissue specific manner, a number of limitations are noted. Due to difficulties in optimising ATAC protocols to yield good quality data, mapping chromatin accessibility in lesional and uninvolved keratinocytes was not achieved.

Other limitations in this study include its relatively small sample size, lack of genotyping data and skin biopsies only being available for 3 patients in the cohort. These limitations are intrinsic to time and project budget constraints and will be addressed as the study continues.

Finally, the analytical methods and strategies used in this chapter to perform data analysis, particularly incorporation of genotyping data into the differential analysis of chromatin accessibility and histones modifications.

## **Defining the genome-wide chromatin accessibility landscape and gene expression profile in psoriasis**

---

Further analysis could also be performed with the differentially expressed lncRNA integrating their experimentally validated targets to identify specific processes regulated by these RNA species in the context of disease.

### **3.4.9 Conclusions**

In this chapter, use of contemporary methods for epigenetic profiling (as established in the previous chapter) together with gene expression quantification has allowed characterisation of the regulatory landscape in relevant cell types isolated from psoriasis patients and healthy individuals. Minor differences in chromatin accessibility and H3K27ac modifications between psoriasis and healthy controls have been identified in circulating immune cells. Conversely, a number of relevant biological processes dysregulated in the context of psoriasis have been shown at the transcriptional level both, in circulating cells and in psoriatic epidermis. Moreover, this chapter illustrates how GWAS signals may be interpreted through integration of multiple data types. Overall, the protocols established and data generated in this chapter provide a valuable resource that may be built upon in future work.

# Appendices

<b>A Tables</b>	<b>155</b>
A.1 Chapter 3 Tables . . . . .	155
A.2 Chapter 4 Tables . . . . .	155
A.3 Chapter 5 Tables . . . . .	162
<b>B Additional figures</b>	<b>165</b>
B.1 Chapter 3 Figures . . . . .	165
B.2 Chapter 4 Figures . . . . .	168
B.3 Chapter 5 Figures . . . . .	171
<b>Bibliography</b>	<b>206</b>

# List of Tables

A.1 Enrichment of ATAC-seq reads across the TSS for the CD14 <sup>+</sup> monocytes and CD4 <sup>+</sup> samples fresh, frozen and fixed. . . . .	155
A.2 Evaluation of ChiPm library complexity for the psoriasis and control chort 1B ChIPm assay. . . . .	156
A.3 Size of the master lists generated by DiffBind for the H3K27ac differential analysis between psoriasis patients and healthy controls in CD14 <sup>+</sup> monocytes, CD4 <sup>+</sup> , CD8 <sup>+</sup> and CD19 <sup>+</sup> cells. . . . .	157
A.4 Functional interactions and overlap with another study for the differentially expressed lncRNAs in each cell type. . . . .	157
A.5 Additional enriched pathways for DEGs between psoriasis and healthy controls in CD14 <sup>+</sup> monocytes and CD8 <sup>+</sup> cells. . . . .	158
A.6 Additional enriched pathways for DEGs between lesional and uninvolved epidermis isolated from psoriasis patients skin biopsies.	159
A.7 Loci from the psoriasis GWAS Immunochip presenting log <sub>10</sub> ABF< 3 for the fine-mapping lead SNP in the association analysis. . . . .	161
A.8 Additional enriched pathways for the DEGs between SF and PB CD14 <sup>+</sup> monocytes from the CC-mixed and CC-IL7R subpopulations.	162

A.9 PsA GWAS Immunochip loci presenting $\log_10\text{ABF} < 3$ for the fine-mapping lead SNP in the association analysis. . . . .	163
--	-----

## List of Figures

B.1 Distribution of the background read counts from all the master list peaks absent in each sample. . . . .	165
B.2 Pre-sequencing profiles of relative abundance of DNA library fragment sizes for a psoriatic lesional keratinocytes ATAC 1 library generated using 40 min of transposition. . . . .	165
B.3 Assessment of TSS enrichment from ATAC 1 and Fast-ATAC in healthy and psoriasis KCs isolated from skin biopsy samples. . . . .	166
B.4 Fast-ATAC and Omni-ATAC NHEK pre-sequencing profiles of relative abundance of DNA library fragment sizes. . . . .	167
B.5 Percentage of MT reads and called peaks after IDR p-value filtering in the ATAClibraries generated in CD14 <sup>+</sup> monocytes, CD4 <sup>+</sup> , CD8 <sup>+</sup> and CD19 <sup>+</sup> isolated from psoriasis patients and healthy controls. . . . .	168
B.6 PCA analysis illustrating batch effect in ATAC and RNA-seq samples. . . . .	169
B.7 Mapping rate and total reads after filtering (million) mapping to Ensembl genes in all the RNA-seq samples from psoriasis patients and controls in four cell types. . . . .	169
B.8 Mapping quality control for the RNA-seq data in the uninvolved and lesional epidermis from psoriasis patients. . . . .	170
B.9 Correlation in gene expression between the miRs <i>MIR31HG</i> and the target gene <i>HIF-1A</i> in lesional and uninvolved skin. . . . .	170
B.10 Assessment of the percentage of mitochondrial and duplicated reads and the number of called peaks after filtering in the ATAC data from peripheral blood and synovial fluid of PsA patients samples. . . . .	171
B.11 Enrichment of eQTL SNPs for the consensus list of ATAC peaks used to perform differential chromatin accessibility analysis in each cell type. . . . .	171
B.12 Permutation analysis SF vs PB in CD14 <sup>+</sup> monocytes,CD4m <sup>+</sup> ,CD8m <sup>+</sup> and NK. . . . .	172
B.13 Enrichment of DARs in the 15 chromatin states of the cell type specific Roadmap Epigenomic Project segmentation maps. . . . .	173
B.14 Heatmap for the top 20 marker genes of the CC-mixed and CC-IL7R CD14 <sup>+</sup> monocytes subpopulations. . . . .	174
B.15 Identification of the CD14 <sup>+</sup> monocytes populations from bulk SFMCs and PBMCs using scRNA-seq transcriptomes. . . . .	175
B.16 Quantification of cytokine levels in plasma and synovial fluid from 10 PsA patients. . . . .	176

# Appendix A

## Tables

### A.1 Chapter 3 Tables

Cell type	Condition	TSS enrichment		
		CTL1	CTL2	CTL3
CD14	Fresh	17.4	19.6	14.11
	Frozen	26.3	25.2	27.1
	Fixed	2.5	16.5	22.4
CD4	Fresh	5.3	5.6	7.7
	Frozen	17.9	14.1	16.1
	Fixed	7.9	23.0	14.3

Table A.1: Enrichment of ATAC-seq reads across the TSS for the CD14<sup>+</sup> monocytes and CD4<sup>+</sup> samples fresh, frozen and fixed.

### A.2 Chapter 4 Tables

## Tables

---

Sample ID	NRF	PBC1/PBC2
PS2000 CD14	77.6	0.60/2.5
PS2001 CD14	84.9	0.70/3.0
PS2314 CD14	81.1	0.60/1.8
PS2319 CD14	79.9	0.60/2.2
CTL7 CD14	81.1	0.65/2.2
CTL8 CD14	83.9	0.66/2.3
CTL9 CD14	80.7	0.60/2.3
CTL10 CD14	83.1	0.65/2.1
PS2000 CD4	84.8	0.75/3.4
PS2001 CD4	82.0	0.72/2.9
PS2314 CD4	82.9	0.71/2.8
PS2319 CD4	82.4	0.73/3.2
CTL7 CD4	78.6	0.68/2.5
CTL8 CD4	81.8	0.71/2.9
CTL9 CD4	81.6	0.74/3.3
CTL10 CD4	77.6	0.61/1.9
PS2000 CD8	77.0	0.76/4.5
PS2001 CD8	74.7	0.74/4.0
PS2314 CD8	74.2	0.75/4.1
PS2319 CD8	72.2	0.75/4.0
CTL7 CD8	32.7	0.32/1.5
CTL8 CD8	70.1	0.70/3.3
CTL9 CD8	73.9	0.73/3.7
CTL10 CD8	68.2	0.65/2.9
PS2000 CD19	38.0	0.42/1.9
PS2001 CD19	71.4	0.71/3.7
PS2314 CD19	29.4	0.34/1.8
PS2319 CD19	76.1	0.78/4.8
CTL7 CD19	74.2	0.69/3.1
CTL8 CD19	68.4	0.67/3.2
CTL9 CD19	75.1	0.76/4.6
CTL10 CD19	61.7	0.59/2.6

**Table A.2: Evaluation of ChiPm library complexity for the psoriasis and control cohort 1B ChiPm assay.** NRF, PBC1 and PBC2 are the three measures used according to the ENCODE standards as referred in Chapter 2.  $0.5 \leq \text{NRF} < 0.8$  acceptable;  $0.8 \leq \text{NRF} \leq 0.9$  compliant;  $\text{NRF} > 0.9$  ideal;  $0.5 \leq \text{PBC1} < 0.8$  and  $1 \leq \text{PBC2} < 3$  moderate bottlenecking;  $0.8 \leq \text{PBC1} < 0.9$  and  $3 \leq \text{PBC2} < 10$  mild bottlenecking.

## Tables

---

Cell type	Master list size genome-wide	Master list size enhancers
CD14 <sup>+</sup>	99,862	60,962
CD4 <sup>+</sup>	110,353	56,282
CD8 <sup>+</sup>	137,194	51,607
CD19 <sup>+</sup>	199,014	88,722

**Table A.3: Size of the master lists generated by DiffBind for the H3K27ac differential analysis between psoriasis patients and healthy controls in CD14<sup>+</sup> monocytes, CD4<sup>+</sup>, CD8<sup>+</sup> and CD19<sup>+</sup> cells.** In the genome-wide analysis, the master list size refers to the number of H3K27ac enriched sites included in the consensus list built using DiffBind to perform the differential analysis. In the analysis restricted to enhancers, the size of the master list was reduced to only those sites from the genome-wide master list annotated as enhancers (weak and strong) according to the chromatin segmentation map for each particular cell type.

Cell type	LncRNAs with functional interactions	LncRNAs overlapping Dolcino <i>et al.</i> , 2018
CD14 <sup>+</sup>	24	4 ( <i>HOTAIRM1*</i> , <i>ILF3-AS1*</i> , <i>MMP24-AS1</i> , <i>RP11-325F22.2</i> )
CD4 <sup>+</sup>	10	1 ( <i>MMP24-AS1</i> )
CD8 <sup>+</sup>	21	1( <i>CTB-25B13.12</i> )
CD19 <sup>+</sup>	5	0

**Table A.4: Functional interactions and overlap with another study for the differentially expressed lncRNAs in each cell type.** For each cell type the number of differentially expressed lncRNAs (FDR<0.05) for which a functional interaction has been experimentally validated based on NPInter database is shown. NPInter documents functional interactions between noncoding RNAs (except tRNAs and rRNAs) and biomolecules (proteins, RNAs and DNAs) which have published experimental validation. This table also records the number of differentially expressed lncRNAs overlapping with the Dolcino *et al.*, 2018 study, where PBMCs from PsA patients and healthy controls are contrasted.(\*) indicates dysregulation in the opposite direction between this data and Dolcino *et al.*.

## Tables

---

---

### CD14<sup>+</sup> monocytes additional enriched pathways in psoriasis

---

Generic transcription ( <i>p-value</i> = $2.8 \times 10^{-8}$ , <i>fold change</i> =2.66)
RNA transport ( <i>p-value</i> = $3.3 \times 10^{-6}$ , <i>fold change</i> =2.98)
GnRH signalling ( <i>p-value</i> = $4.4 \times 10^{-5}$ , <i>fold change</i> =3.61)
Ribosome biogenesis in eukaryotes ( <i>p-value</i> = $7.7 \times 10^{-5}$ , <i>fold change</i> =3.42)
Neurotrophin signaling ( <i>p-value</i> = $1.2 \times 10^{-4}$ , <i>fold change</i> =2.96)
Spliceosome ( <i>p-value</i> = $6.6 \times 10^{-4}$ , <i>fold change</i> =2.51)
Autophagy ( <i>p-value</i> = $4.6 \times 10^{-3}$ , <i>fold change</i> =2.18)
Protein processing in endoplasmic reticulum ( <i>p-value</i> = $4.6 \times 10^{-4}$ , <i>fold change</i> =2.05)

---

### CD8<sup>+</sup> additional enriched pathways in psoriasis

---

Epstein-Barr virus infection ( <i>p-value</i> = $2.8 \times 10^{-4}$ , <i>fold change</i> =2.33)
RNA Polymerase I and III, and mitochondrial transcription ( <i>p-value</i> = $3.5 \times 10^{-4}$ , <i>fold change</i> =2.79)
Apoptosis ( <i>p-value</i> =0.001, <i>fold change</i> =2.41)

**Table A.5: Additional enriched pathways DEGs between psoriasis and healthy controls in CD14<sup>+</sup> monocytes and CD8<sup>+</sup> cells.** Significant pathways for FDR<0.01. All the enriched pathways contained a minimum of ten DEGs FDR<0.05 from the analysis.

**Table A.6: Additional enriched pathways for DEGs between lesional and uninvolved epidermis isolated from psoriasis patients skin biopsies.** Significant pathways for FDR<0.005. All the enriched pathways contained a minimum of ten DEGs FDR>0.05 from the analysis.

### Lesional versus uninvolved epidermis additional enriched pathways

Genes encoding extracellular matrix and extracellular matrix-associated proteins ( $p\text{-value}=1.4\times10^{-10}$ ,  $fold\ change=3.3$ ), Serine/threonine-protein kinase (PLK1) signalling ( $p\text{-value}=4.0\times10^{-8}$ ,  $fold\ change=4.6$ ), Genes encoding secreted soluble factors ( $p\text{-value}=7.4\times10^{-6}$ ,  $fold\ change=3.42$ ), FOXM1 transcription factor network ( $p\text{-value}=1.5\times10^{-7}$ ,  $fold\ change=4.76$ ), Phase 1 functionalization of compounds ( $p\text{-value}=6.8\times10^{-7}$ ,  $fold\ change=4.29$ ), Biological oxidations ( $p\text{-value}=2.7\times10^{-6}$ ,  $fold\ change=3.02$ ), G2/M Checkpoints ( $p\text{-value}=6.0\times10^{-6}$ ,  $fold\ change=3.86$ ), Aurora B signaling ( $p\text{-value}=1.1\times10^{-5}$ ,  $fold\ change=3.92$ ), Chemical carcinogenesis ( $p\text{-value}=6.0\times10^{-6}$ ,  $fold\ change=3.86$ ), Serotonergic synapse ( $p\text{-value}=6.0\times10^{-6}$ ,  $fold\ change=3.86$ ), Drug metabolism-cytochrome P450 ( $p\text{-value}=4.4\times10^{-5}$ ,  $fold\ change=3.45$ ), Mitotic M-M/G1 phases ( $p\text{-value}=6.0\times10^{-5}$ ,  $fold\ change=2.16$ ), MicroRNAs in cancer ( $p\text{-value}=8.6\times10^{-5}$ ,  $fold\ change=2.18$ ), Glycosaminoglycan metabolism ( $p\text{-value}=5.0\times10^{-5}$ ,  $fold\ change=2.36$ ), E2F transcription factor network ( $p\text{-value}=5.7\times10^{-4}$ ,  $fold\ change=2.49$ ), p73 transcription factor network ( $p\text{-value}=6.7\times10^{-4}$ ,  $fold\ change=2.45$ ), Fc-epsilon receptor I signaling in mast cells ( $p\text{-value}=1.5\times10^{-3}$ ,  $fold\ change=2.54$ ), Tight junction ( $p\text{-value}=1.6\times10^{-3}$ ,  $fold\ change=2.13$ ), Origin recognition complex subunit 1 (Orc1) removal from chromatin ( $p\text{-value}=1.8\times10^{-3}$ ,  $fold\ change=2.38$ )

## **Tables**

---

## Tables

---

**Table A.7: Loci from the psoriasis GWAS Immunochip presenting  $\log_{10}ABF < 3$  for the fine-mapping lead SNP in the association analysis.**  
 For each of the locus the closer gene, FM lead SNP,  $\log_{10}ABF$ , Tsoi *et al.*, 2012 GWAS lead SNP, the OR in the GAPC cohort and the number of SNPs in the 90% credible set are reported. FM=fine-mapping; ABF=approximated Bayesian factor; OR=odd ratio.

chr	Closer gene	FM lead SNP	$\log_{10}ABF$	FM lead SNP	GWAS lead SNP	GAPC OR	90% credible set
10	<i>ZMIZ1</i>	rs1316431	2.4		rs1250546	1.09	401
11	<i>RPS6KA4/PRDX5</i>	rs58779949	0.3		rs645078	1.06	334
20	<i>RNF114</i>	rs13041638	3.1		rs1056198	1.11	116
6	<i>EXOC2/IRF4</i>	rs113866081	2.4		rs9504361	1.14	400
6	<i>TAGAP</i>	rs62431928	2.2		rs2451258	1.11	853
9	<i>DDX58</i>	rs7045087	0.4		rs11795343	1.05	167
9	<i>KLF4</i>	rs6477612	2.1		rs10979182	1.12	80
11	<i>ETS1</i>	rs10893884	3.5		rs3802826	1.15	19
18	<i>POL1/STARD6</i>	rs11661229	1.6		rs545979	1.11	121

## Tables

---

### A.3 Chapter 5 Tables

CC-mixed CD14 <sup>+</sup> monocytes additional enriched pathways	
SLE	
Translation	
3'-UTR-mediated translational regulation	
Th-1 and Th-2 cell differentiation	
Peptide chain elongation	
Rheumatoid arthritis	
Metabolism of proteins	
Cell adhesion molecules (CAMs)	
Th-17 cell differentiation	
Nonsense mediated decay enhanced by the exon junction complex	
SRP-dependent co-translational protein targeting to membrane	
Hemostasis	
Metabolism of mRNA	
Platelet activation, signalling and aggregation	
HTLV-I infection	
Innate immune system	
Adaptive immune system	
CC-IL7R CD14 <sup>+</sup> monocytes additional enriched pathways	
SLE	
Tuberculosis	
Epstein-Barr virus infection	
Immune System	

**Table A.8: Additional enriched pathways for the DEGs between SF and PB CD14<sup>+</sup> monocytes from the CC-mixed and CC-IL7R subpopulations.** All the enriched pathways contained a minimum of ten DEGs from the analysis and were significant at an FDR<0.01.

## Tables

**Table A.9: PsA GWAS Immunochip loci presenting  $-\log_{10} \text{ABF} < 3$  for the fine-mapping lead SNP in the association analysis.** For each of the signals chromosome (chr), genes nearby,  $\log_{10} \text{ABF} < 3$  for the fine-mapping (FM) lead SNP, the PsA GWAS lead SNP including p-value in the study and the number of SNPs in the 99% credible set reported by Bowes *et al.* for that signal. NA refers to the locus reported as fine-mapped by Bowes *et al.*. OR=odd ratio

chr	Closer gene	FM lead SNP	$\log_{10} \text{ABF}$	GWAS lead SNP	SNP (p-value)	OR	lead SNP	Bowes FM	Bowes 99% credible set
2	<i>B3GNT2/TMEM17</i>	2:62501912(INS)	1.8	rs6713082 (4.59x10 <sup>-5</sup> )		1.2	rs6713082	22	
17	<i>CARD14</i>	rs11150848	0.8	rs11652075 (0.014)		1.1	NA	NA	
9	<i>DDX58</i>	rs138398872	0.5	rs1133071 (3.36x10 <sup>-5</sup> )		1.2	NA	NA	
7	<i>ELMO1</i>	rs10279209	1.1	rs73112675 (0.0041)		1.1	NA	NA	
6	<i>ERAP1/ERAP2</i>	rs58711860	2.7	rs62376445 (0.00017)		1.4	NA	NA	
1	<i>SLC45A1/TNFRSF9</i>	rs11367773	1.7	rs11121129 (0.00093)		1.1	NA	NA	
11	<i>ETS1/FLI1</i>	rs7935286	0.6	rs4936059 (0.0014)		1.1	NA	NA	
1	<i>LCE3B/LCE3A</i>	rs11205042	2.8	rs6693105 (0.0028)		1.1	NA	NA	
22	<i>LOC150223</i>	rs371643642	1.2	rs2298428 (4.38x10 <sup>-5</sup> )		1.2	NA	NA	
11	<i>ZC3H12C</i>	rs1648153	0.2	rs4561177 (0.0037)		1.1	NA	NA	
9	<i>LOC392382</i>	rs36015268	0.8	rs12236285 (0.038)		1.2	NA	NA	
17	<i>NOS2A</i>	rs4795067	1.9	rs4795067 (1.94x10 <sup>-7</sup> )		1.2	rs4795067	2	

## Tables

---

2	<i>PAPOLG/REL</i>	rs60685986	2.0	rs1306395 ( $2.99 \times 10^{-5}$ )	1.2	rs1306395	32
18	<i>POLI</i>	18:51926806	0.3	rs602422 (0.0047)	1.1	NA	NA
14	<i>NFKBIA</i>	rs35309046	0.9	rs8016947 ( $9.65 \times 10^{-5}$ )	1.2	NA	NA
11	<i>RPS6KA4</i>	rs146881600	1.3	rs645078 (0.00086)	1.1	NA	NA
6	<i>RSPH3/TAGAP</i>	rs11754601	1.3	rs1973919 (0.018)	1.1	NA	NA
6	<i>TNFAIP3</i>	rs1890370	2.0	rs610604 (0.00032)	1.1	NA	NA
5	<i>TNIP1/ANXA6</i>	rs75851973	2.8	rs76956521 ( $4.98 \times 10^{-9}$ )	1.5	rs76956521	24
10	<i>ZMIZ1</i>	rs2395526	0.9	rs1972346 (0.0082)	1.1	NA	NA
20	<i>ZNF313</i>	rs73129222	1.6	rs6063454 ( $2.90 \times 10^{-5}$ )	1.2	NA	NA
16	<i>ZNF668</i>	rs9939243	0.9	rs7197717 (0.0035)	1.1	NA	NA

# Appendix B

## Additional figures

### B.1 Chapter 3 Figures

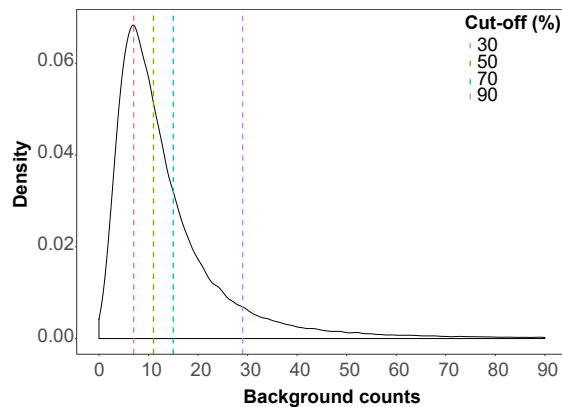


**Figure B.1: Distribution of the background read counts from all the master list peaks absent peaks in each sample.** Each cut-off corresponds to the number of background counts showed by a particular percentage of the total number of absent peaks.

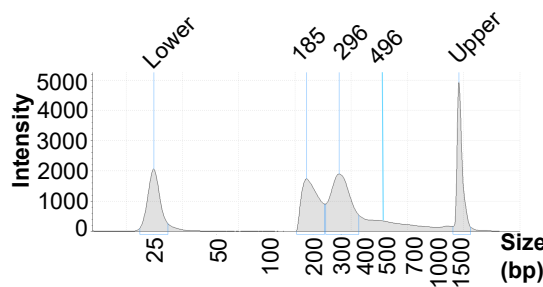


**Figure B.2: Pre-sequencing profiles of relative abundance of DNA library fragment sizes for a psoriatic lesional keratinocytes ATAC 1 library generated using 40 min of transposition.** Pre-sequencing quantification of DNA fragment sizes from the ATAC library generated using 50,000 keratinocytes isolated from a psoriatic lesional skin biopsy and the ATAC 1 protocol (detailed in Table ??) and transposition for 40 min.

## **Additional figures**

---

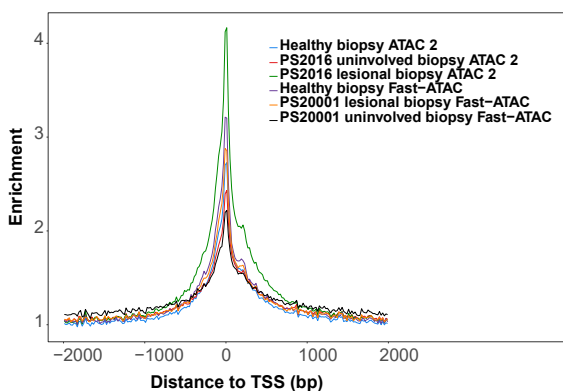


**Figure B.3: Assessment of TSS enrichment from ATAC 1 and Fast-ATAC in healthy and psoriasis KCs isolated from skin biopsy samples.** Fold-enrichment of ATAC fragments across the Ensembl annotated TSS from the different ATAC libraries.

## Additional figures

---

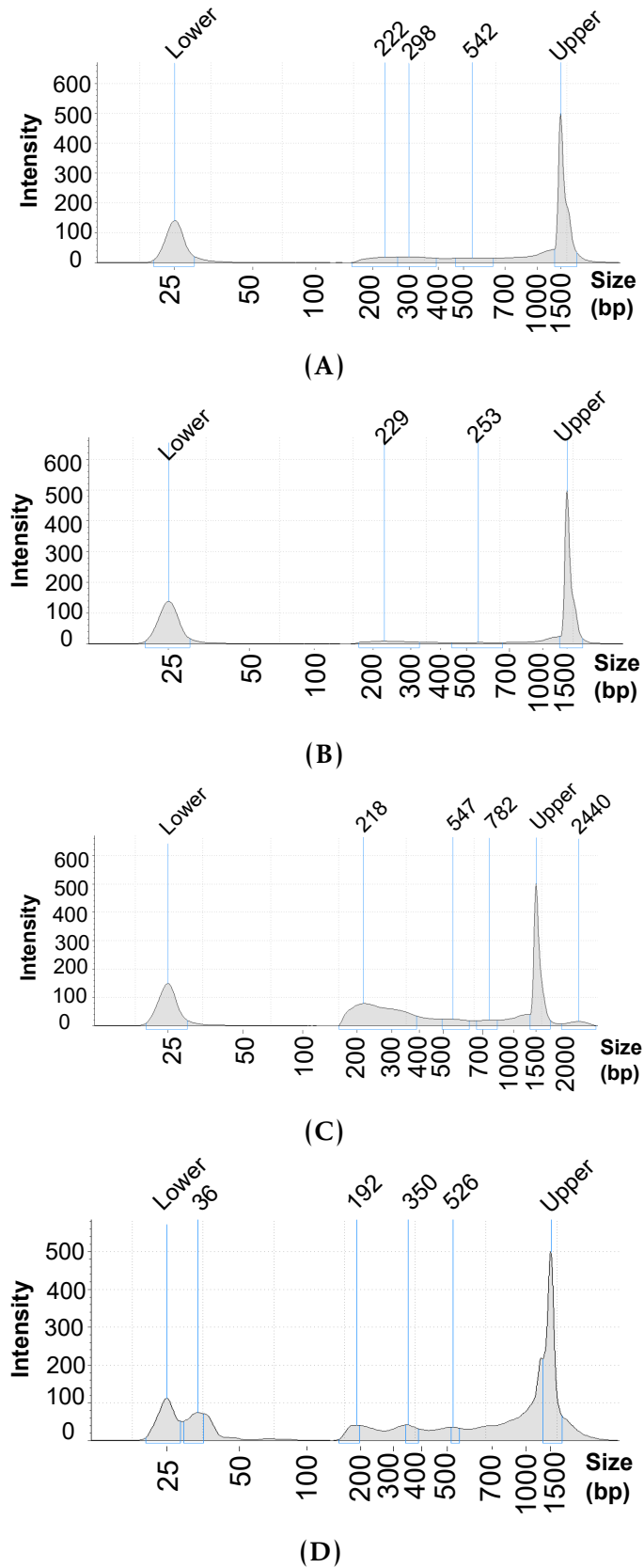


**Figure B.4: Fast-ATAC and Omni-ATAC NHEK pre-sequencing profiles of relative abundance of DNA library fragment sizes.** Pre-sequencing quantification of DNA fragment sizes from the libraries generated using the (A) C2, (B) C3, and (C) C4 versions of the Fast-ATAC protocol based on modifications in the detergent and Tn5 concentration and (D) Omni-ATAC. C2, C3 and C4 detergent and Tn5 concentrations are detailed in Table ??.

## Additional figures

---

### B.2 Chapter 4 Figures

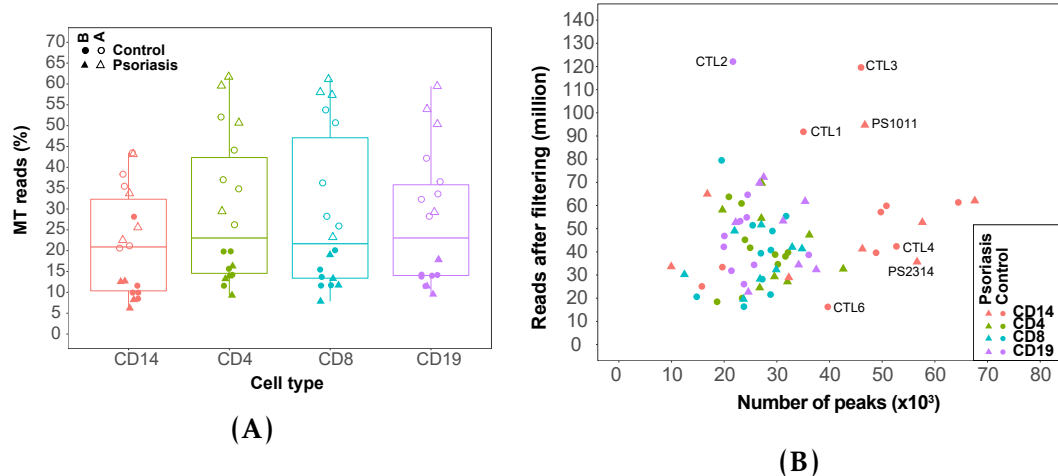


**Figure B.5: (A) Percentage of MT reads in the ATAC-seq samples generated in CD14<sup>+</sup> monocytes, CD4<sup>+</sup>, CD8<sup>+</sup> and CD19<sup>+</sup> isolated from psoriasis patients and healthy controls.** Samples from cohort 1A (open circles and triangles) were generated with the standard ATAC-seq protocol from Buenrostro *et al.*, 2013 whereas samples from cohort 1B (filled circles and triangles) were processed using FAST-ATAC (Corces *et al.* 2016). (B) For each of the ATAC libraries, representation of the number of significant peaks based on IDR optimal p-value filtering versus the total million of reads after filtering.

## Additional figures

---

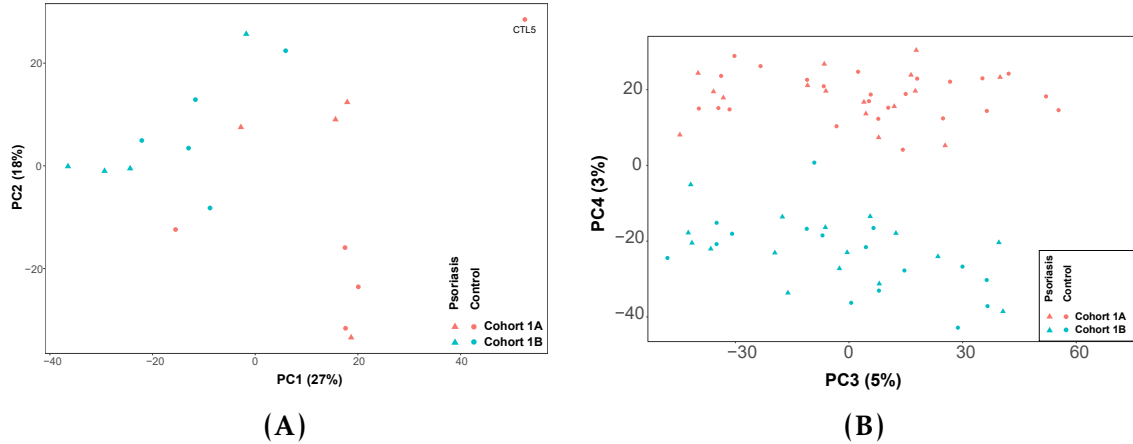


**Figure B.6: PCA analysis illustrating batch effect in ATAC and RNA-seq samples.** (A) First and second component of the PCA analysis performed using the normalised ATAC counts in a master list of consensus regions across all the combined tCD8<sup>+</sup> samples from psoriasis patients and healthy controls. b) Third and fourth component of the PCA analysis performed on the normalised number of reads mapping to the Ensembl list of mRNAs and lncRNAs detected in tCD8<sup>+</sup> cells from psoriasis patients and healthy controls. For each dot colour corresponds to cohort ID (batch) and shape to condition (psoriasis or control).

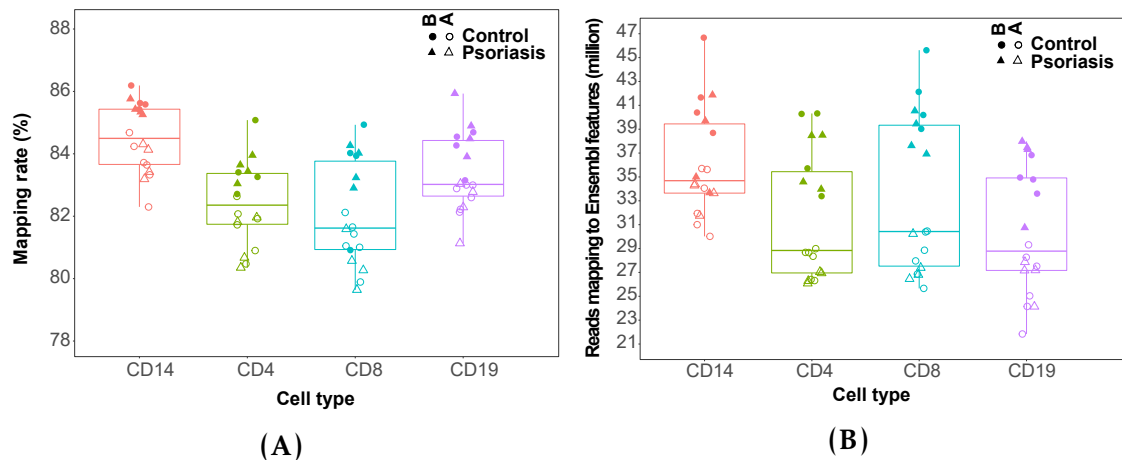


**Figure B.7: Mapping rate and total reads after filtering (million) mapping to Ensembl genes in all the RNA-seq samples from psoriasis patients and controls in four cell types.** (A) The mapping rate refers to the percentage of total sequenced reads from each sample that uniquely mapped to a particular site of the genome. (B) The total number of reads after filtering for non-uniquely mapped and duplicated reads that mapped to Ensembl features, including coding protein genes and lncRNAs.

## Additional figures

---

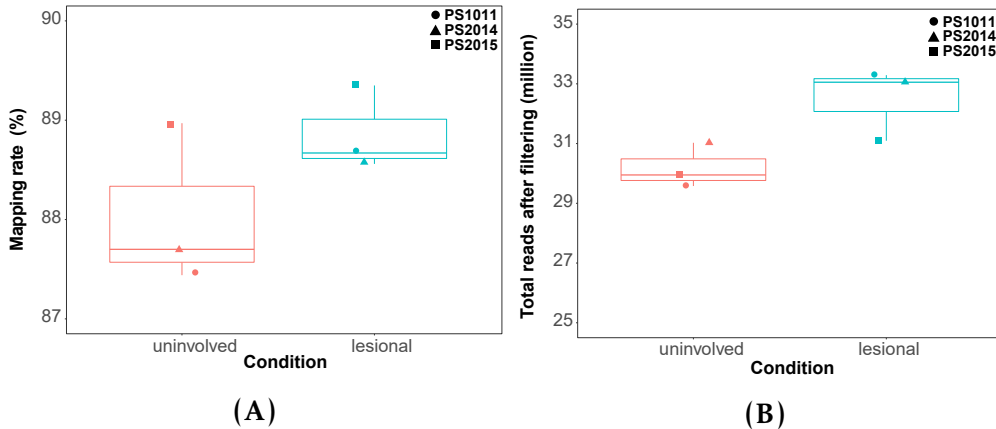


**Figure B.8: Mapping quality control for the RNA-seq data in the uninvolved and lesional epidermis from psoriasis patients.** (A) Mapping rate calculated as the proportion of sequencing reads mapping uniquely to a particular region of the genome. (B) The total number of reads mapping to an Ensembl feature (including protein coding genes and lncRNAs) after removing the non-uniquely mapped and duplicated reads.

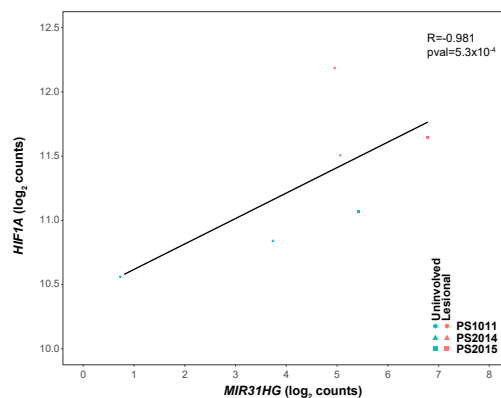


**Figure B.9: Correlation in gene expression between the miRs *MIR31HG* and the target gene *HIF-1A* in lesional and uninvolved skin.** Plot showing the correlation in  $\log_2$  normalised read counts for *MIR31HG* and *HIF-1A*. Pearson correlation values ( $R$ ) and significance ( $p$ -value) are included. Each of the dots represents one samples, where colour represents condition (lesional or uninvolved) and shape corresponds to the patient ID.

## Additional figures

---

### B.3 Chapter 5 Figures

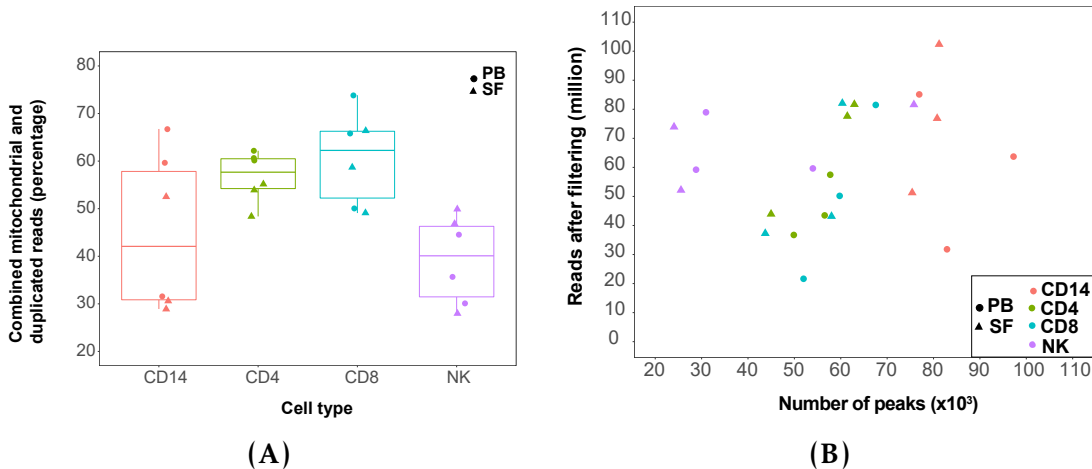


**Figure B.10: Assessment of the percentage of mitochondrial and duplicated reads and the number of called peaks after filtering in the ATAC data from peripheral blood and synovial fluid of PsA patients samples.** For each of the cell types and samples (A) boxplot representing percentage of duplicated and mitochondrial reads combined and (B) representation of the number of significant peaks after filtering based on IDR optimal p-values versus the total million reads after filtering for each of the samples. For each point, colour codes for cell type and shape for tissue (SF=synovial fluid; PB=peripheral blood).

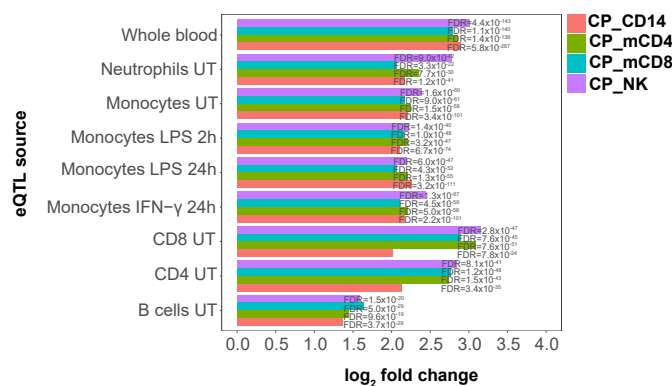


**Figure B.11: Enrichment of eQTL SNPs for the consensus list of ATAC peaks used to perform differential chromatin accessibility analysis in each cell type.** Barplot illustrating for the consensus list of ATAC peaks in of the 4 assayed cell types the log<sub>2</sub> fold change and significance (FDR) of the top enriched GTEx eQTL dataset (whole blood) and the publicly available eQTL datasets in immune cell types. Although enrichment of eQTL SNPs in the majority of GTEx datasets for the consensus list of peaks in the 4 cell types was found, whole blood presented the largest and most significant enrichment amongst all of them

## Additional figures

---

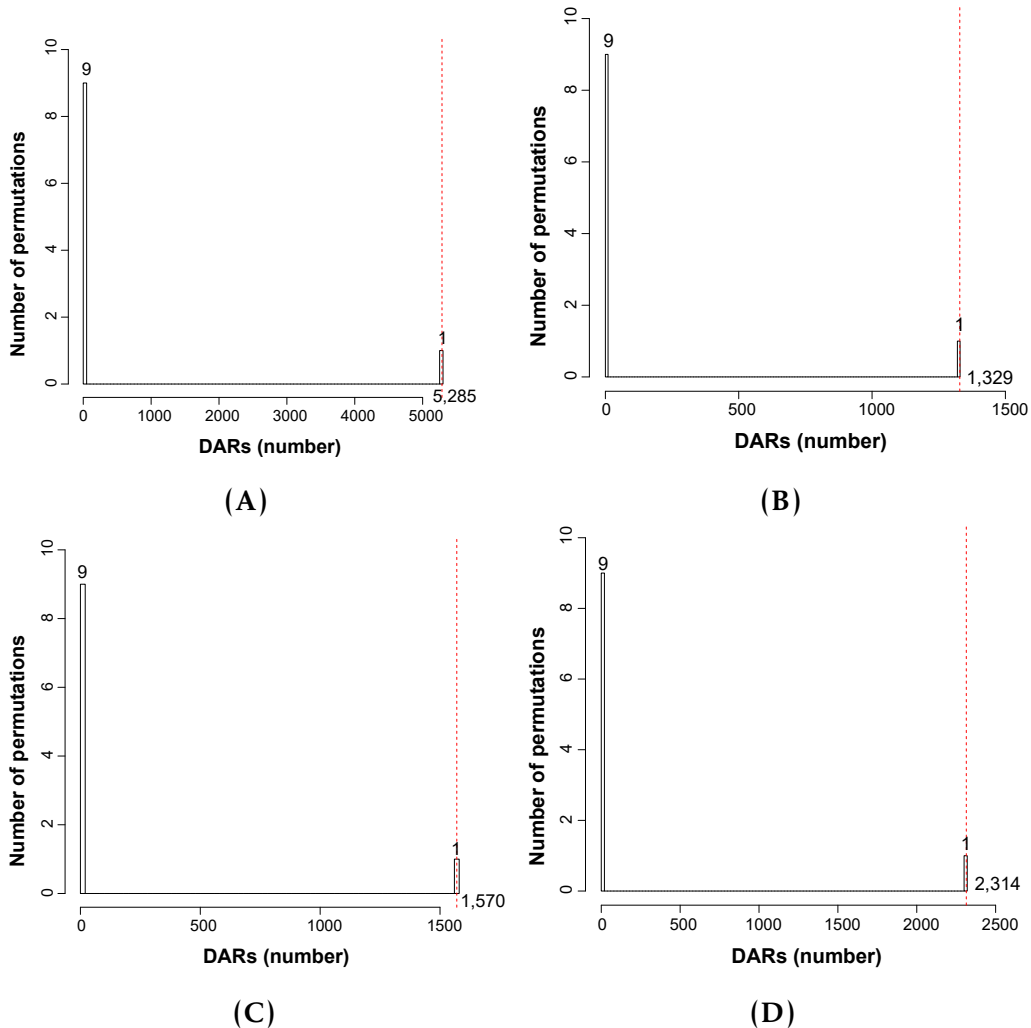


**Figure B.12: Permutation analysis SF vs PB in CD14<sup>+</sup> monocytes, CD4m<sup>+</sup>, CD8m<sup>+</sup> and NK.** Sample labels were permuted within each cell type to achieve the ten unique possible combinations and differential analysis was performed. The number of significant DARs (FDR<0.01 and no abs(FC)>1.5) across all permutations is plotted for (A) CD14<sup>+</sup> monocytes, (B) mCD4<sup>+</sup>, (C) mCD8<sup>+</sup> and (D) NK, demonstrating that the true observation (dashed red line) is significantly more than expected by chance ( $p\text{-value}<0.1$ , the lowest  $p\text{-value}$  for the maximum number of permutations that can be conducted with this sample size) in all four cell types.

## Additional figures

---

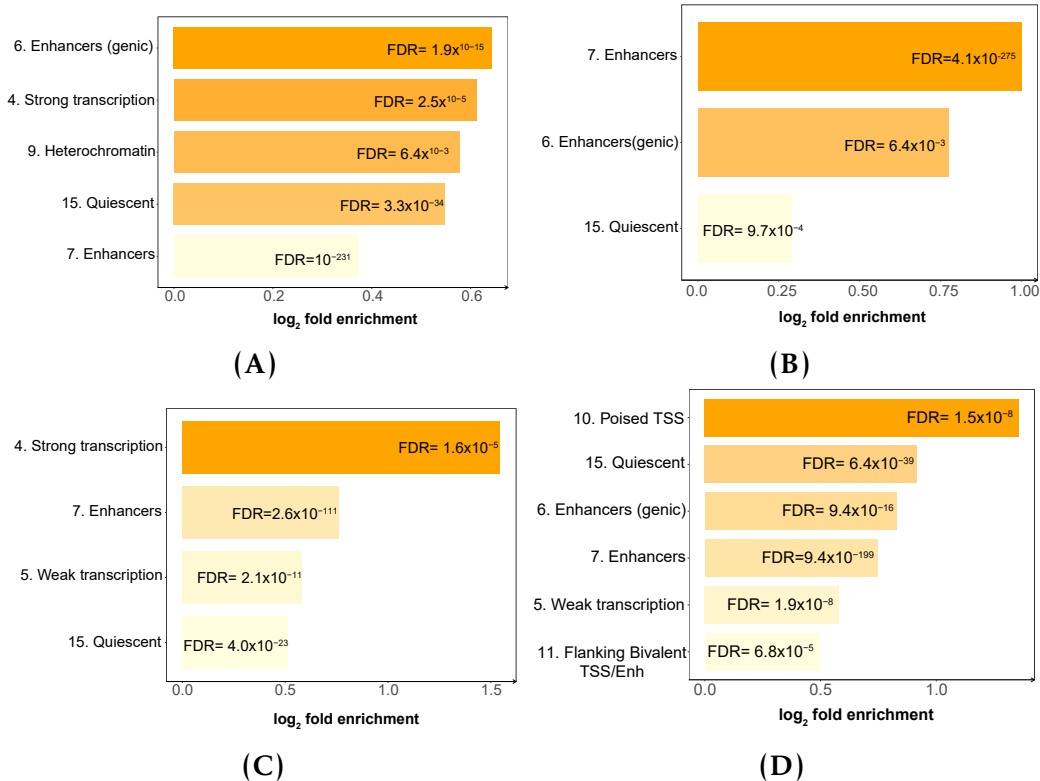


**Figure B.13: Enrichment of DARs in the 15 chromatin states of the cell type specific Roadmap Epigenomic Project segmentation maps.** Barplots illustrating the chromatin states significantly enriched ( $FDR < 0.01$ ) in DARs from the differential chromatin accessibility analysis between synovial fluid and peripheral blood in (A) CD14<sup>+</sup> monocytes, (B) mCD4<sup>+</sup>, (C) mCD8<sup>+</sup> and (D) NK cells. For each of the enriched chromatin states the statistical significance (FDR) and the magnitude ( $\log_2$  fold change) of the enrichment is included.

## Additional figures

---

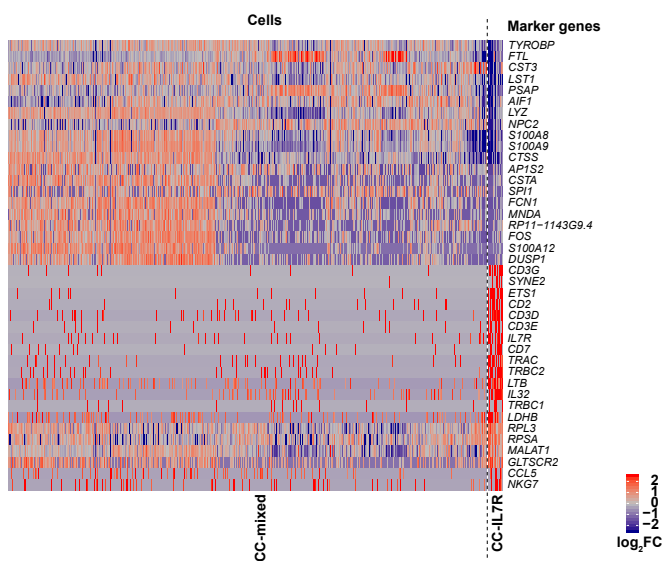


**Figure B.14: Heatmap for the top 20 marker genes of the CC-mixed and CC-IL7R CD14<sup>+</sup> monocytes subpopulations.** Rows are the top 20 marker genes for each of the two subpopulations (total of 40 genes). The columns represent each of the cells members of the CC-mixed (left) or CC-IL7R (right) clusters. The colour scale represents the log<sub>2</sub>FC in the expression of the marker gene in a particular cell of the cluster compared to the average expression of all the cells from the other cluster.

## Additional figures

---

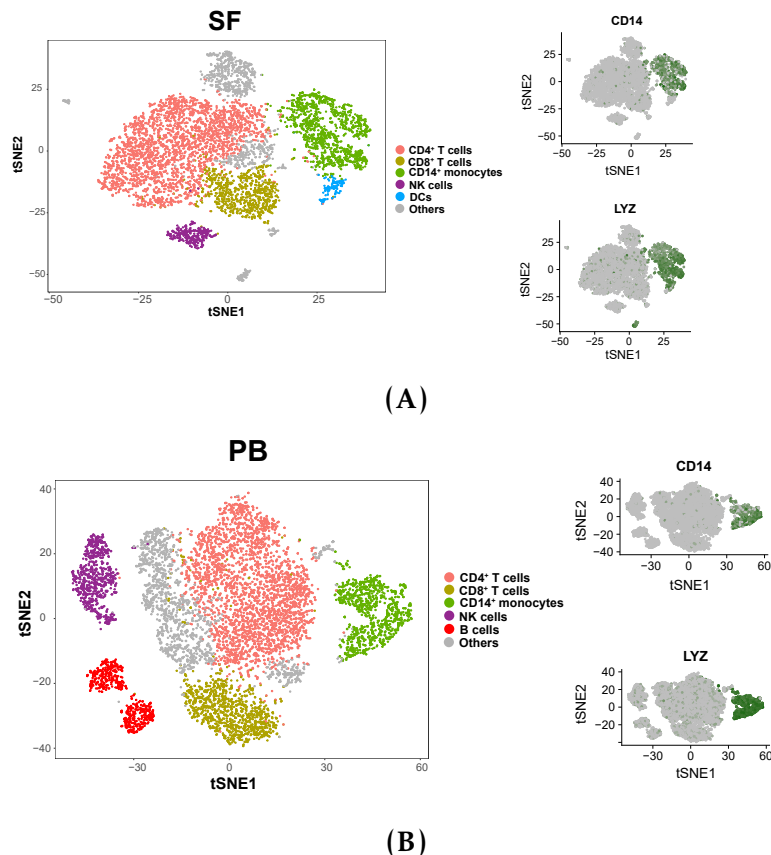


**Figure B.15: Identification of the CD14<sup>+</sup> monocytes populations from bulk SFMCs and PBMCs using scRNA-seq transcriptomes.** Visualisation using t-SNE dimensional reduction of the cell subpopulations identified in (A) SFMCs and (B) PBMCs and the overlay of CD14<sup>+</sup> monocytes characteristic markers (left hand side panel of (A) and (B)) for a representative PsA sample. Clustering performed using recommended resolution (res=0.6) allowed to identify CD4<sup>+</sup> (pink), CD8<sup>+</sup> (khaki), CD14<sup>+</sup> monocytes (green), NK (purple), DCs (blue), B cells (red) and others (grey). On the left hand side panel, expression for two characteristics CD14<sup>+</sup> monocytes markers (CD14 and LYZ) used to subset this population (dark green dots) is overlaid on the t-SNE visual representation of all the cells in each of the tissues.

## Additional figures

---

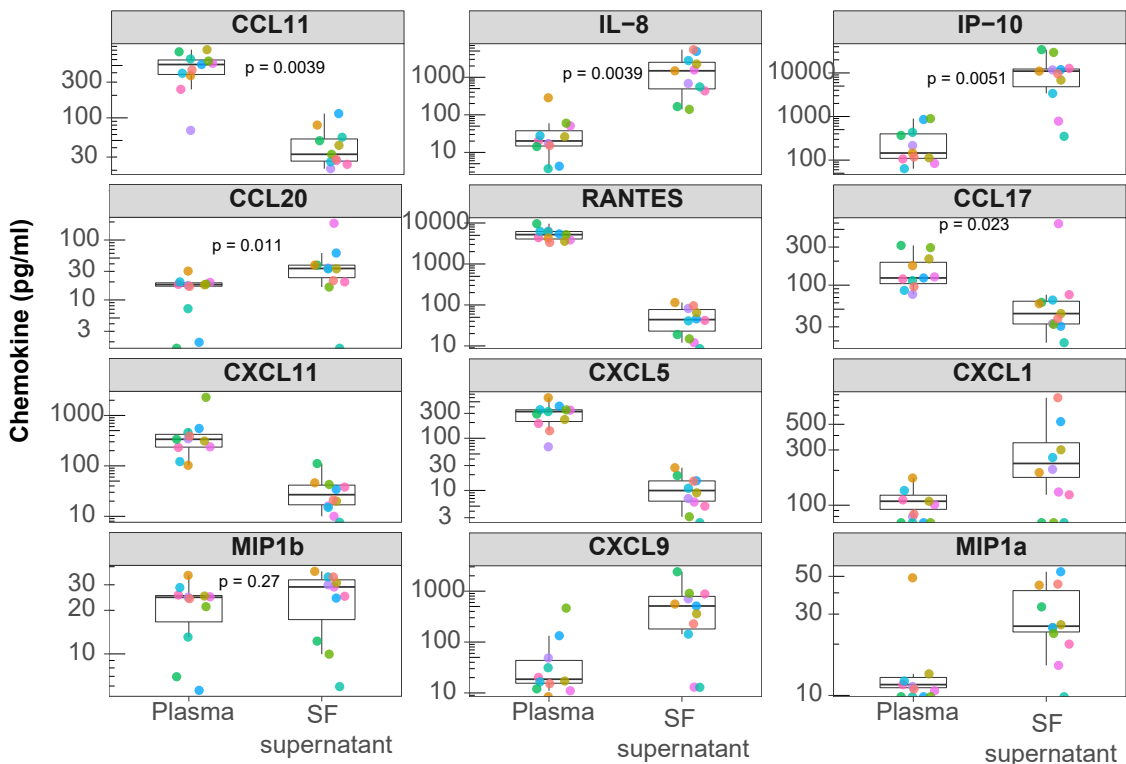


**Figure B.16: Quantification of cytokine levels in plasma and synovial fluid from 10 PsA patients.** Boxplots illustrating the concentration in pg/mL (x-axis  $\log_{10}$  scale) for a number of cytokines measured in supernatant from synovial fluid and plasma from peripheral blood of 10 PsA patients. The experiment was conducted by collaborators in Basle using enzyme-linked immunosorbent assay (ELISA). Each circle represents one sample and patient identity is colour coded. For some of the cytokines, the significance of the difference in concentration between the two tissues has been determined using Wilcoxon signed-rank test and the corresponding p-value is included.

# Bibliography

- Abecasis, G. R., Auton, A., Brooks, L. D., DePristo, M. A., Durbin, R. M., et al. (2012). "An integrated encyclopedia of DNA elements in the human genome". *Nature* 489: pp. 57–74.
- Abraham, Gad and Inouye, Michael (2014). "Fast principal component analysis of large-scale genome-wide data". *PloS one* 9.
- Abramson, SR. and Khattri, S (2016). "A Review of Current Evidence for TNF Inhibitor Switching in Psoriatic Arthritis". *Journal of Psoriasis and Psoriatic arthritis*.
- Ackermann, A. M., Wang, Z., Schug, J., and Naji, A. (2016). "Integration of ATAC-seq and RNA-seq identifies human alpha cell and beta cell signature genes". *Molecular*.
- Adams, D., Altucci, L., Antonarakis, S. E., and Nature, Ballesteros-J. (2012). "BLUEPRINT to decode the epigenetic signature written in blood". *Nature*.
- Adey, Andrew, Morrison, Hilary G., Asan, Xun, Xu, Kitzman, Jacob O., et al. (2010). "Rapid, low-input, low-bias construction of shotgun fragment libraries by high-density in vitro transposition". *Genome Biology* 11.
- Alasoo, K., Rodrigues, J., Mukhopadhyay, S., and Nature, Knights-A. J. (2018). "Shared genetic effects on chromatin and gene expression indicate a role for enhancer priming in immune response". *Nature*.
- Alrefai, H, Muhammad, K, Rudolf, R, and Nature, DAT (2016). "NFATc1 supports imiquimod-induced skin inflammation by suppressing IL-10 synthesis in B cells". *Nature*.
- Ameres, S. L., Horwich, M. D., Hung, J. H., and, Xu-J. (2010). "Target RNAdirected trimming and tailing of small silencing RNAs" ..
- Anders, S., Pyl, P. T., and Bioinformatics, Huber-W. (2015). "HTSeq Python framework to work with high-throughput sequencing data". *Bioinformatics*.
- Andersson, Robin, Gebhard, Claudia, Miguel-Escalada, Irene, Hoof, Ilka, Bornholdt, Jette, et al. (2014). "An atlas of active enhancers across human cell types and tissues". *Nature* 507: p. 455.
- Antonioli, L., Pacher, P., Vizi, E. S., and medicine, Hask-G. in molecular (2013). "CD39 and CD73 in immunity and inflammation". *Trends in molecular medicine*.
- Appel, H., Maier, R., and Arthritis, Wu-P. (2011). "Analysis of IL-17+ cells in facet joints of patients with spondyloarthritis suggests that the innate immune pathway might be of greater relevance than the Th17-mediated adaptive immune response." *Arthritis*.
- Arend, W. P., Palmer, G., and reviews, Gabay-C. (2008). "IL1, IL18, and IL33 families of cytokines". *Immunological reviews*.

## BIBLIOGRAPHY

---

- Armstrong, AW, Harskamp, CT, and, Dhillon JS journal of (2014). "Psoriasis and smoking: a systematic review and metaanalysis". *British journal of*.
- Assassi, S., Reveille, J. D., and of, Arnett-F. C. (2010). "Whole-blood gene expression profiling in ankylosing spondylitis shows upregulation of toll-like receptor 4 and 5". *The Journal of*.
- Aterido, Adrià, Julià, Antonio, Ferrández, Carlos, Puig, Lluís, Fonseca, Eduardo, et al. (2016). "Genome-Wide Pathway Analysis Identifies Genetic Pathways Associated with Psoriasis." *J. Invest. Dermatol.* 136: pp. 593–602.
- Attar, M., Sharma, E., Li, S., Bryer, C., and reports, Cubitt-L. (2018). "A practical solution for preserving single cells for RNA sequencing". *Scientific reports*.
- Austin, Lisa M., Ozawa, Maki, Kikuchi, Toyoko, Walters, Ian B., and Krueger, James G. (1999). "The majority of epidermal T cells in psoriasis vulgaris lesions can produce type 1 cytokines, interferon-, interleukin-2, and tumor necrosis factor-, defining TC1 (Cytotoxic T Lymphocyte) and TH1 effector populations: 1 a type 1 differentiation bias is also measured in circulating blood T cells in psoriatic patients". *Journal of Investigative Dermatology* 113: pp. 752–759.
- B, Uszczynska-Ratajczak, Lagarde, J, and resource, Frankish A (2018). "Towards a complete map of the human long non-coding RNA transcriptome". *resource*.
- Baechler, E. C., Batliwalla, F. M., and the, Karypis-G. of (2003). "Interferon-inducible gene expression signature in peripheral blood cells of patients with severe lupus". *Proceedings of the*.
- Baeten, D., Breban, M., Lories, R., and, Schett-G. (2013). "Are spondylarthritides related but distinct conditions or a single disease with a heterogeneous phenotype?" *Arthritis &*.
- Baker, K. F. and diseases, Isaacs-J. D. of the rheumatic (2017). "Novel therapies for immune-mediated inflammatory diseases: What can we learn from their use in rheumatoid arthritis, spondyloarthritis, systemic lupus erythematosus". *Annals of the rheumatic diseases*.
- Bannister, AJ and research, Kouzarides T (2011). "Regulation of chromatin by histone modifications". *Cell research* 21: pp. 381–395.
- Bannister, AJ, Zegerman, P, Partridge, JF, and Nature, Miska EA (2001). "Selective recognition of methylated lysine 9 on histone H3 by the HP1 chromo domain". *Nature*.
- Bao, Xiaomin, Rubin, Adam J, Qu, Kun, Zhang, Jiajing, Giresi, Paul G, et al. (2015). "A novel ATAC-seq approach reveals lineage-specific reinforcement of the open chromatin landscape via cooperation between BAF and p63". *16*: p. 284.
- Barski, A., Cuddapah, S., Cui, K., Roh, T. Y., and Cell, Schones-D. E. (2007). "High-resolution profiling of histone methylations in the human genome". *Cell*.

## BIBLIOGRAPHY

---

- Batliwalla, F. M., Li, W., Ritchlin, C. T., and Molecular, Xiao-X. (2005). "Microarray analyses of peripheral blood cells identifies unique gene expression signature in psoriatic arthritis". *Molecular*.
- Belasco, J, Louie, JS, Gulati, N, and &, Wei N (2015). "Comparative genomic profiling of synovium versus skin lesions in psoriatic arthritis". *Arthritis &*.
- Bell, A. C. and Nature, Felsenfeld-G. (2000). "Methylation of a CTCF-dependent boundary controls imprinted expression of the Igf2 gene". *Nature*.
- Benjamin, Michael and McGonagle, Dennis (2009). *The enthesis organ concept and its relevance to the spondyloarthropathies*. The enthesis organ concept and its relevance to the spondyloarthropathies. Springer: pp. 57–70.
- Bergboer, J. G. M., Tjabringa, G. S., and of, Kamsteeg-M. journal (2011). "Psoriasis risk genes of the late cornified envelope-3 group are distinctly expressed compared with genes of other LCE groups". *The American journal of*.
- Bernstein, B. E. and Nature, Stamatoyannopoulos-J. A. (2010). "The NIH roadmap epigenomics mapping consortium". *Nature*.
- Black, A. P. B. and ArdernJones, M. R. (2007). "Human keratinocyte induction of rapid effector function in antigenspecific memory CD4+ and CD8+ T cells". *European journal of*.
- Blais, M. E., Dong, T., and Immunology, RowlandJones-S. (2011). "HLAC as a mediator of natural killer and Tcell activation: spectator or key player?" *Immunology*.
- Blauvelt, A., Papp, K. A., Griffiths, C. E. M., and American, Randazzo-B. of the (2017). "anti-interleukin-23 monoclonal antibody, compared with adalimumab for the continuous treatment of patients with moderate to severe psoriasis: results from the phase". *Journal of the American*.
- Bouaziz, JD, Yanaba, K, and, Venturi GM of the (2007). "Therapeutic B cell depletion impairs adaptive and autoreactive CD4+ T cell activation in mice". *Proceedings of the*.
- Bowes, J., Ho, P., Flynn, E., and the, Ali-F. of (2012). "Comprehensive assessment of rheumatoid arthritis susceptibility loci in a large psoriatic arthritis cohort". *Annals of the*.
- Bowes, John, Budu-Aggrey, Ashley, Huffmeier, Ulrike, Uebe, Steffen, Steel, Kathryn, et al. (2015). "Dense genotyping of immune-related susceptibility loci reveals new insights into the genetics of psoriatic arthritis". *Nature communications* 6: p. 6046.
- Boyle, A. P., Song, L., Lee, B. K., London, D., and Genome, Keefe-D. (2010). "High-resolution genome-wide in vivo footprinting of diverse transcription factors in human cells". *Genome*.
- Boyle, A. P., Hong, E. L., Hariharan, M., Cheng, Y., Schaub, M. A., et al. (2012). "Annotation of functional variation in personal genomes using RegulomeDB". *Genome Res* 22: pp. 1790–7.

## BIBLIOGRAPHY

---

- Boyman, O., Hefti, H. P., Conrad, C., Nickoloff, B. J., Suter, M., et al. (2004). "Spontaneous development of psoriasis in a new animal model shows an essential role for resident T cells and tumor necrosis factor-alpha". *J Exp Med* 199: pp. 731–6.
- Braun, J. E., Huntzinger, E., Fauser, M., and cell, Izaurrealde-E. (2011). "GW182 proteins directly recruit cytoplasmic deadenylase complexes to miRNA targets". *Molecular cell*.
- Brest, P., Lapaquette, P., Souidi, M., and Nature, Lebrigand-K. (2011). "A synonymous variant in IRGM alters a binding site for miR-196 and causes deregulation of IRGM-dependent xenophagy in Crohn's disease". *Nature*.
- Broome, AM, Ryan, D, and Histochemistry, Eckert RL of (2003). "S100 protein subcellular localization during epidermal differentiation and psoriasis". *Journal of Histochemistry*.
- Buck, M. J., Raaijmakers, L. M., Ramakrishnan, S., and Oncogene, Wang-D. (2014). "Alterations in chromatin accessibility and DNA methylation in clear cell renal cell carcinoma". *Oncogene*.
- Buenrostro, Jason D., Paul, G. Giresi, Lisa, C. Zaba, Howard, Y. Chang, and William, J. Greenleaf (2013). "Transposition of native chromatin for fast and sensitive epigenomic profiling of open chromatin, DNA-binding proteins and nucleosome position". *Nature Methods* 10: pp. 1213–1218.
- Buenrostro, Jason D., Wu, Beijing, Chang, Howard Y., and Greenleaf, William J. (2015). "ATAC seq: A Method for Assaying Chromatin Accessibility Genome Wide". *Current Protocols in Molecular Biology* 109: pp. 1–9.
- Bunt, M. van de, Cortes, A., Brown, M. A., and Morris, A. P. (2015). "Evaluating the Performance of Fine-Mapping Strategies at Common Variant GWAS Loci". *PLoS Genet* 11: pp. 1–14.
- Burgos-Pol, R. and Dermo, Martnez-Sesmero-J. M. (2016). "The cost of psoriasis and psoriatic arthritis in 5 European countries: a systematic review". *Actas Dermo*.
- Burton P., WTCCC2 (2007). "Genome-wide association study of 14,000 cases of seven common diseases and 3,000 shared controls". *Nature*.
- Butler, Andrew, Hoffman, Paul, Smibert, Peter, Papalexi, Efthymia, and Satija, Rahul (2018). "Integrating single-cell transcriptomic data across different conditions, technologies, and species". *Nature biotechnology* 36: p. 411.
- Cañete, JD, Martínez, SE, Farrés, J, and, Sanmartí R of the (2000). "Differential Th1/Th2 cytokine patterns in chronic arthritis: interferon is highly expressed in synovium of rheumatoid arthritis compared with seronegative". *Annals of the*.
- Capon, Francesca (2017). "The Genetic Basis of Psoriasis". *International Journal of Molecular Sciences* 18: p. 2526.

## BIBLIOGRAPHY

---

- Capon, Francesca, Bijlmakers, Marie-Jos J., Wolf, Natalie, Quaranta, Maria, Huffmeier, Ulrike, et al. (2008). "Identification of ZNF313/RNF114 as a novel psoriasis susceptibility gene". *Human molecular genetics* 17: pp. 1938–1945.
- Cargill, Michele, Schrodi, Steven J., Chang, Monica, Garcia, Veronica E., Brandon, Rhonda, et al. (2007). "A large-scale genetic association study confirms IL12B and leads to the identification of IL23R as psoriasis-risk genes". *The American Journal of Human Genetics* 80: pp. 273–290.
- Carrieri, Claudia, Cimatti, Laura, Biagioli, Marta, Beugnet, Anne, Zucchelli, Silvia, et al. (2012). "Long non-coding antisense RNA controls Uchl1 translation through an embedded SINEB2 repeat". *Nature* 491: pp. 454–457.
- Carter, K. W., Pluzhnikov, A., Timms, A. E., Miceli-Richard, C., Bourgain, C., et al. (2007). "Combined analysis of three whole genome linkage scans for ankylosing spondylitis". *Rheumatology* 46: pp. 763–771.
- Chandran, Vinod, Schentag, Catherine T., Brockbank, John E., Pellett, Fawnda J., Shanmugarajah, S., et al. (2009). "Familial aggregation of psoriatic arthritis". *Annals of the rheumatic diseases* 68: pp. 664–667.
- Chang, C. C., Chow, C. C., and, Lcam (2015). "Second-generation PLINK: rising to the challenge of larger and richer datasets" ..
- Chang, JC, Smith, LR, and, Froning KJ of the (1994). "CD8+ T cells in psoriatic lesions preferentially use T-cell receptor V beta 3 and/or V beta 13.1 genes". *Proceedings of the*.
- Chou, W. C., Zheng, H. F., Cheng, C. H., Yan, H., and reports, Wang-L. (2016). "A combined reference panel from the 1000 Genomes and UK10K projects improved rare variant imputation in European and Chinese samples". *Scientific reports*.
- Chu, CQ, Swart, D, Alcorn, D, and &, Tocker J (2007). "Interferon regulates susceptibility to collageninduced arthritis through suppression of interleukin17". *Arthritis &*.
- Cid, De R, E, Riveira-Munoz, and Nature, PLJM (2009). "Deletion of the late cornified envelope LCE3B and LCE3C genes as a susceptibility factor for psoriasis". *Nature*.
- Clegg, Daniel O., Reda, Domenic J., Mejias, Edwin, Cannon, Grant W., Weisman, Michael H., et al. (1996). "Comparison of sulfasalazine and placebo in the treatment of psoriatic arthritis. A Department of Veterans Affairs Cooperative Study". *Arthritis & Rheumatology* 39: pp. 2013–2020.
- Coates, L. C., FitzGerald, O., Helliwell, P. S., and and, Paul-C. in arthritis (2016a). "Psoriasis, psoriatic arthritis, and rheumatoid arthritis: Is all inflammation the same?" *Seminars in arthritis and*.
- Coates, Laura C., Kavanaugh, Arthur, Mease, Philip J., Soriano, Enrique R., Felquer, Maria, et al. (2016b). "Group for research and assessment of psoriasis and psoriatic arthritis 2015 treatment recommendations for psoriatic arthritis". *Arthritis & rheumatology* 68: pp. 1060–1071.

## BIBLIOGRAPHY

---

- Coda, A. B., Icen, M., Smith, J. R., and Genomics, Sinha-A. A. (2012). "Global transcriptional analysis of psoriatic skin and blood confirms known disease-associated pathways and highlights novel genomic hot spots for". *Genomics*.
- Cohen, A. D., Sherf, M., Vidavsky, L., Vardy, D. A., and Dermatology, Shapiro-J. (2008). "Association between psoriasis and the metabolic syndrome". *Dermatology*.
- Constant, S, Schweitzer, N, and, West J of (1995). "B lymphocytes can be competent antigen-presenting cells for priming CD4+ T cells to protein antigens in vivo." *The Journal of*.
- Corces, MR, Trevino, AE, Hamilton, EG, and Nature, Greenside PG (2017). "An improved ATAC-seq protocol reduces background and enables interrogation of frozen tissues". *Nature*.
- Corces, Ryan M., Buenrostro, Jason D., Wu, Beijing, Greenside, Peyton G., Chan, Steven M., et al. (2016). "Lineage-specific and single-cell chromatin accessibility charts human hematopoiesis and leukemia evolution". *Nature Genetics* 48: pp. 1193–1203.
- Cornell, T. T., Rodenhouse, P., Cai, Q., and and, Sun-L. (2010). "Mitogen-activated protein kinase phosphatase 2 regulates the inflammatory response in sepsis". *Infection and*.
- Cortes, Adrian and Brown, Matthew A. (2011). "Promise and pitfalls of the Immunochip". *Arthritis research & therapy* 13: p. 101.
- Cortes, Adrian, Hadler, Johanna, Pointon, Jenny P., Robinson, Philip C., Karaderi, Tugce, et al. (2013). "Identification of multiple risk variants for ankylosing spondylitis through high-density genotyping of immune-related loci". *Nature genetics* 45: p. 730.
- Cosma, M. P., Tanaka, T., and Cell, Nasmyth-K. (1999). "Ordered recruitment of transcription and chromatin remodeling factors to a cell cycleand developmentally regulated promoter". *Cell*.
- Creyghton, M. P. and the, Cheng-A. W. of (2010). "Histone H3K27ac separates active from poised enhancers and predicts developmental state". *Proceedings of the*.
- Cui, Y., Li, G., Li, S., and Biology, Wu-R. in (2010). "Designs for linkage analysis and association studies of complex diseases". *Statistical Methods in Molecular Biology*.
- Cusanovich, Darren A, Daza, Riza, Adey, Andrew, Pliner, Hannah A, Christiansen, Lena, et al. (2015). "Multiplex single-cell profiling of chromatin accessibility by combinatorial cellular indexing". 348: pp. 910–914.
- Dalbeth, N and Callan, MF. (2002). "A subset of natural killer cells is greatly expanded within inflamed joints". *& Rheumatism: Official Journal of the*.

## BIBLIOGRAPHY

---

- Dand, N., Mucha, S., Tsoi, L. C., and molecular, Mahil-S. K. (2017). "Exome-wide association study reveals novel psoriasis susceptibility locus at TNFSF15 and rare protective alleles in genes contributing to type I IFN signalling". *Human molecular*.
- Dang, EV, Barbi, J, Yang, HY, Jinanena, D, and Cell, Yu H (2011). "Control of TH17/Treg Balance by Hypoxia-Inducible Factor 1". *Cell*.
- Das, Sayantan, Stuart, Philip E., Ding, Jun, Tejasvi, Trilokraj, Li, Yanming, et al. (2014). "Fine mapping of eight psoriasis susceptibility loci". *European Journal of Human Genetics*.
- Davies, James O., Oudelaar, A. M., Higgs, Douglas R., and Hughes, Jim R. (2017). "How best to identify chromosomal interactions: a comparison of approaches". *Nature methods* 14: pp. 125–134.
- Delaneau, O., Marchini, J., and methods, Zagury-J. F. (2012). "A linear complexity phasing method for thousands of genomes". *Nature methods*.
- Derrien, Thomas, Johnson, Rory, Bussotti, Giovanni, Tanzer, Andrea, Djebali, Sarah, et al. (2012). "The GENCODE v7 catalog of human long noncoding RNAs: Analysis of their gene structure, evolution, and expression". *Genome Research* 22: pp. 1775–1789.
- Diluvio, L., Vollmer, S., Besgen, P., and of, Ellwart-J. W. (2006). "Identical TCR -chain rearrangements in streptococcal angina and skin lesions of patients with psoriasis vulgaris". *The Journal of*.
- Dimas, Antigone S., Deutsch, Samuel, Stranger, Barbara E., Montgomery, Stephen B., Borel, Christelle, et al. (2009). "Common regulatory variation impacts gene expression in a cell typedependent manner". *Science* 325: pp. 1246–1250.
- Dobin, Alexander, Davis, Carrie A., Schlesinger, Felix, Drenkow, Jorg, Zaleski, Chris, et al. (2013). "STAR: ultrafast universal RNA-seq aligner". *Bioinformatics* 29: pp. 15–21.
- Dolcino, M, Pelosi, A, Fiore, PF, and, Patuzzo G in (2018). "Long non coding RNAs play a role in the pathogenesis of Psoriatic Arthritis by regulating microRNAs and genes involved in inflammation and metabolic syndrome." *Frontiers in*.
- Dolcino, Marzia, Ottavia, Andrea, Barbieri, Alessandro, Patuzzo, Giuseppe, Tinazzi, Elisa, et al. (2015). "Gene Expression Profiling in Peripheral Blood Cells and Synovial Membranes of Patients with Psoriatic Arthritis." *PLoS ONE* 10: e0128262.
- Doyle, MS and Arthritis, Collins ES (2012). "New insight into the functions of the interleukin-17 receptor adaptor protein Act1 in psoriatic arthritis". *Arthritis*.
- Dozmorov, M. G., Dominguez, N., and insights, Bean-K. biology (2015). "B-cell and monocyte contribution to systemic lupus erythematosus identified by cell-type-specific differential expression analysis in RNA-seq data". *and biology insights*.

## BIBLIOGRAPHY

---

- Duffy, D. L., Spelman, L. S., and of, Martin-N. G. of the (1993). "Psoriasis in Australian twins". *Journal of the American Academy of*.
- Eckert, RL, Broome, AM, Ruse, M, and Investigative, Robinson N of (2004). "S100 proteins in the epidermis". *Journal of Investigative*.
- Eder, L, Law, T, and &, Chandran V care (2011). "Association between environmental factors and onset of psoriatic arthritis in patients with psoriasis". *Arthritis care &*.
- Edwards, S. L., Beesley, J., French, J. D., and Dunning, A. M. (2013). "Beyond GWASs: illuminating the dark road from association to function". *Am J Hum Genet* 93: pp. 779–97.
- Eedy, D., Burrows, D., Bridges, J., and Jones, F. (1990). "Clearance of severe psoriasis after allogenic bone marrow transplantation". *BMJ* 300.
- Ellinghaus, David, Jostins, Luke, Spain, Sarah L., Cortes, Adrian, Bethune, Jrn, et al. (2016). "Analysis of five chronic inflammatory diseases identifies 27 new associations and highlights disease-specific patterns at shared loci". *Nature Genetics* 48: pp. 510–518.
- Ellinghaus, E., Ellinghaus, D., Stuart, P. E., and Nair, R. P. (2010). "Genome-wide association study identifies a psoriasis susceptibility locus at TRAF3IP2". *Nature genetics* 42: pp. 991–996.
- ENCODE (2007). "Identification and analysis of functional elements in 1the human genome by the ENCODE pilot project". *Nature* 447: p. 799.
- Eppinga, H. and rheumatology, Konstantinov-S. R. (2014). "The microbiome and psoriatic arthritis". *Current rheumatology*.
- Ernst, J., Kheradpour, P., Mikkelsen, T. S., and Shores, N. (2011). "Mapping and analysis of chromatin state dynamics in nine human cell types". *Nature* 473: pp. 43–49.
- Ernst, Jason and Kellis, Manolis (2010). "Discovery and characterization of chromatin states for systematic annotation of the human genome". *Nat Biotechnol* 28: pp. 817–825.
- Evans, D. M., Spencer, C. C. A., Pointon, J. J., Su, Z., and Nature, Harvey-D. (2011). "Interaction between ERAP1 and HLA-B27 in ankylosing spondylitis implicates peptide handling in the mechanism for HLA-B27 in disease susceptibility". *Nature*.
- Eyerich, S, Eyerich, K, and, Pennino D of (2009). "Th22 cells represent a distinct human T cell subset involved in epidermal immunity and remodeling". *The Journal of*.
- Fabregat, Antonio, Jupe, Steven, Matthews, Lisa, Sidiropoulos, Konstantinos, Gillespie, Marc, et al. (2018). "The reactome pathway knowledgebase". *Nucleic acids research* 46.
- Faghhihi, Mohammad A., Modarresi, Farzaneh, Khalil, Ahmad M., Wood, Douglas E., Sahagan, Barbara G., et al. (2008). "Expression of a noncoding RNA is elevated in Alzheimer's disease and drives rapid feed-forward regulation of beta-secretase". *Nature medicine* 14: pp. 723–730.

## BIBLIOGRAPHY

---

- Fagny, M., Paulson, J. N., and the, Kuijjer-M. L. of (2017). "Exploring regulation in tissues with eQTL networks". *Proceedings of the*.
- Fairfax, Benjamin P., Makino, Seiko, Radhakrishnan, Jayachandran, Plant, Katharine, Leslie, Stephen, et al. (2012). "Genetics of gene expression in primary immune cells identifies cell type-specific master regulators and roles of HLA alleles". *Nature genetics* 44: pp. 502–510.
- Fairfax, Benjamin P., Humburg, Peter, Makino, Seiko, Naranbhai, Vivek, Wong, Daniel, et al. (2014). "Innate immune activity conditions the effect of regulatory variants upon monocyte gene expression". *Science* 343: p. 1246949.
- Fang, Hai, Knezevic, Bogdan, Burnham, Katie L., and Knight, Julian C. (2016). "XGR software for enhanced interpretation of genomic summary data, illustrated by application to immunological traits". *Genome Medicine* 8: p. 129.
- Farber, E. M., Nall, M. L., and dermatology, Watson-W. of (1974). "Natural history of psoriasis in 61 twin pairs". *Archives of dermatology*.
- Farh, Kyle, Carrasco-Alfonso, J., Dita, Mayer, Luckey, C., Nikolaos, A., et al. (2015). "Genetic and epigenetic fine mapping of causal autoimmune disease variants". *Nature* 518: 337343.
- Feil, Robert and Fraga, Mario F. (2012). "Epigenetics and the environment: emerging patterns and implications". *Nature Reviews Genetics* 13: p. 97.
- Feldmeyer, L, Keller, M, Niklaus, G, Hohl, D, and Biology, Werner S (2007). "The inflammasome mediates UVB-induced activation and secretion of interleukin-1 by keratinocytes". *Current Biology*.
- Ferlazzo, G, Pack, M, and, Thomas D of the (2004). "Distinct roles of IL-12 and IL-15 in human natural killer cell activation by dendritic cells from secondary lymphoid organs". *Proceedings of the*.
- Fert, I., Cagnard, N., Glatigny, S., and, Letourneau-F. (2014). "Reverse interferon signature is characteristic of antigenpresenting cells in human and rat spondyloarthritis". *Arthritis &*.
- Finlay, Andrew (2005). "Current severe psoriasis and the rule of tens". *British Journal of Dermatology* 152: pp. 861–867.
- Finzel, S., Sahinbegovic, E., and, Kocjan-R. (2014). "Inflammatory bone spur formation in psoriatic arthritis is different from bone spur formation in hand osteoarthritis". *Arthritis &*.
- Forrest, Alistair R. R., Kawaji, Hideya, Rehli, Michael, Baillie, Kenneth J., Hoon, Michiel J. L. de, et al. (2014). "A promoter-level mammalian expression atlas". *Nature* 507.
- Fredriksson, T. and Pettersson, U. (1978). "Severe psoriasisoral therapy with a new retinoid". *Dermatology*.
- Friedman, R. C., Farh, K. K. H., and research, Burge-C. B. (2008). "Most mammalian mRNAs are conserved targets of microRNAs". *Genome research*.

## BIBLIOGRAPHY

---

- Gandhapudi, S. K., Murapa, P., and Md (2013). "HSF1 is activated as a consequence of lymphocyte activation and regulates a major proteostasis network in T cells critical for cell division during stress". *(Baltimore)*.
- Gao, J., Chen, F., Hua, M., Guo, J., and Biological, Nong-Y. (2018). "Knockdown of lncRNA MIR31HG inhibits cell proliferation in human HaCaT keratinocytes". *Biological*.
- Gaulton, K. J., Nammo, T., Pasquali, L., and Nature, Simon-J. M. (2010). "A map of open chromatin in human pancreatic islets". *Nature*.
- Gelfand, J. M., Gladman, D. D., Mease, P. J., and Academy, Smith-N. (2005). "Epidemiology of psoriatic arthritis in the population of the United States". *the American Academy*.
- Gelfand, J. M., Neumann, A. L., Shin, D. B., and Jama, Wang-X. (2006). "Risk of myocardial infarction in patients with psoriasis". *Jama*.
- Giresi, P. G., Kim, J., McDaniell, R. M., and Genome, Iyer-V. R. (2006). "FAIRE (Formaldehyde-Assisted Isolation of Regulatory Elements) isolates active regulatory elements from human chromatin". *Genome*.
- Gladman, D. D., Anhorn, K. A., Schachter, R. K., and Mervart, H. (1986). "HLA antigens in psoriatic arthritis". *The Journal of Rheumatology* 13: pp. 586–592.
- Gladman, D. D., Antoni, C., Mease, P., and rheumatic, Clegg-D. O. of the (2005). "Psoriatic arthritis: epidemiology, clinical features, course, and outcome". *Annals of the rheumatic*.
- Glessner, J. T., Wang, K., Cai, G., Korvatska, O., and Nature, Kim-C. E. (2009). "Autism genome-wide copy number variation reveals ubiquitin and neuronal genes". *Nature*.
- Gobbi, De M., Viprakasit, V., Hughes, J. R., and, Fisher-C. (2006). "A regulatory SNP causes a human genetic disease by creating a new transcriptional promoter" ..
- Goldman, L and Schafer, AI (2011). "Goldman's Cecil Medicine E-Book".
- Gong, Chenguang and Maquat, Lynne E. (2011). "lncRNAs transactivate STAU1-mediated mRNA decay by duplexing with 3' UTRs via Alu elements". *Nature* 470: pp. 284–288.
- Goodnow, Christopher C., Sprent, Jonathon, Groth, Barbara, and Vinuesa, Carola G. (2005). "Cellular and genetic mechanisms of self tolerance and autoimmunity". *Nature* 435: p. 590.
- Gossec, L., Smolen, J. S., Ramiro, S., Wit, M. de, Cutolo, M., et al. (2016). "European League Against Rheumatism (EULAR) recommendations for the management of psoriatic arthritis with pharmacological therapies: 2015 update". *Annals of the rheumatic diseases* 75: pp. 499–510.
- Gradman, R. J., Ptacin, J. L., and Molecular, Bhasin-A. (2008). "A bifunctional DNA binding region in Tn5 transposase". *Molecular*.
- Grard, A., Kammen, R. A. van der, and Blood, Janssen-H. (2009). "The Rac activator Tiam1 controls efficient T-cell trafficking and route of transendothelial migration". *Blood*.

## BIBLIOGRAPHY

---

- Gregory, Adam P., Dendrou, Calliope A., Attfield, Kathrine E., Haghikia, Aiden, Xifara, Dionysia K., et al. (2012). "TNF receptor 1 genetic risk mirrors outcome of anti-TNF therapy in multiple sclerosis". *Nature* 488: p. 508.
- Griffiths, C. E. M. and Barker, JN. (2007). "Pathogenesis and clinical features of psoriasis". *The Lancet*.
- Griffiths, C. E. M., Reich, K., Lebwohl, M., and Lancet, Kerkhof-P. van de (2015). "Comparison of ixekizumab with etanercept or placebo in moderate-to-severe psoriasis (UNCOVER-2 and UNCOVER-3): results from two phase 3 randomised". *The Lancet*.
- Guan, Tianxia, Dominguez, Claudia X., Amezquita, Robert A., Laidlaw, Brian J., Cheng, Jijun, et al. (2018). "ZEB1, ZEB2, and the miR-200 family form a counterregulatory network to regulate CD8+ T cell fates". *Journal of Experimental Medicine* 215: pp. 1153–1168.
- Gudjonsson, J. E. and Karason, A. (2003). "Psoriasis patients who are homozygous for the HLACw\* 0602 allele have a 2.5fold increased risk of developing psoriasis compared with Cw6 heterozygotes". *British journal of*.
- Gudjonsson, J. E., Ding, J., Johnston, A., Tejasvi, T., Guzman, A. M., et al. (2010). "Assessment of the psoriatic transcriptome in a large sample: additional regulated genes and comparisons with in vitro models". *J Invest Dermatol* 130: pp. 1829–40.
- Gupta, R., Lai, K., and Chopra, N. (2016). "Network analysis of psoriasis reveals biological pathways and roles for coding and long non-coding RNAs". *BMC*.
- Gusev, Alexander, Lee, Hong S., Trynka, Gosia, Finucane, Hilary, Vilhjalmsson, Bjarni J., et al. (2014). "Partitioning heritability of regulatory and cell-type-specific variants across 11 common diseases". *The American Journal of Human Genetics* 95: pp. 535–552.
- GutowskaOwsiak, D. and Schaupp, A. L. (2012). "IL17 downregulates filaggrin and affects keratinocyte expression of genes associated with cellular adhesion". *Experimental dermatology* 21: pp. 104–110.
- Haddad, Amir and Chandran, Vinod (2013). "Arthritis Mutilans". *Current Rheumatology Reports* 15.
- Hammer, R. E., Maika, S. D., Richardson, J. A., and Cell, Tang-J. P. (1990). "Spontaneous inflammatory disease in transgenic rats expressing HLA-B27 and human 2m: an animal model of HLA-B27-associated human disorders". *Cell*.
- Hansen, K. H., Bracken, A. P., Pasini, D., and cell, Dietrich-N. (2008). "A model for transmission of the H3K27me3 epigenetic mark". *Nature cell*.
- Hanson, A. L., Cuddihy, T., Haynes, K., and, Loo-D. (2018). "Genetic Variants in ERAP1 and ERAP2 Associated With ImmuneMediated Diseases Influence Protein Expression and the Isoform Profile". *Arthritis &*.
- Hao, Yajing, Wu, Wei, Li, Hui, Yuan, Jiao, Luo, Jianjun, et al. (2016). "NPInter v3.0: an upgraded database of noncoding RNA-associated interactions". 2016.

## BIBLIOGRAPHY

---

- Harris, DP, Haynes, L, Sayles, PC, and Nature, Duso DK (2000). "Reciprocal regulation of polarized cytokine production by effector B and T cells". *Nature*.
- Harris, T. J., Grosso, J. F., Yen, H. R., and of, Xin-H. (2007). "Cutting edge: An in vivo requirement for STAT3 signaling in TH17 development and TH17-dependent autoimmunity". *The Journal of*.
- Hecht, I, Toporik, A, Podojil, JR, and, Vaknin I of (2018). "ILDR2 is a novel B7-like protein that negatively regulates T cell responses". *The Journal of*.
- Heintzman, N. D., Stuart, R. K., Hon, G., Fu, Y., and genetics, Ching-C. W. (2007). "Distinct and predictive chromatin signatures of transcriptional promoters and enhancers in the human genome". *genetics*.
- Henseler, T. and Christophers, E. (1985). "Psoriasis of early and late onset: characterization of two types of psoriasis vulgaris". *J Am Acad Dermatol* 13: pp. 450–6.
- Herman, J. G. and Baylin, S. B. (2003). "Gene silencing in cancer in association with promoter hypermethylation". *New England Journal of Medicine*.
- Hesselberth, J. R., Chen, X., Zhang, Z., and Nature, Sabo-P. J. (2009). "Global mapping of protein-DNA interactions in vivo by digital genomic footprinting". *Nature*.
- Hijnen, DJ, Knol, EF, Gent, YY, and Investigative, Giovannone B of (2013). "CD8+ T cells in the lesional skin of atopic dermatitis and psoriasis patients are an important source of IFN-, IL-13, IL-17, and IL-22". *Journal of Investigative*.
- Hirschhorn, Joel N. (2005). "Genetic Approaches to Studying Common Diseases and Complex Traits". *Pediatr Res* 57: pp. 74–77.
- Hitchon, Carol A., Danning, Carol L., Illei, Gabor G., El-Gabalawy, Hani S., and Boumpas, Dimitrios T. (2002). "Gelatinase expression and activity in the synovium and skin of patients with erosive psoriatic arthritis". *The Journal of rheumatology* 29: pp. 107–117.
- Hoffman, M. M., Ernst, J., Wilder, S. P., Kundaje, A., Harris, R. S., et al. (2013). "Integrative annotation of chromatin elements from ENCODE data". *Nucleic Acids Res* 41: pp. 827–41.
- Homey, B., Alenius, H., Mller, A., Soto, H., and medicine, Bowman-E. P. (2002). "CCL27CCR10 interactions regulate T cellmediated skin inflammation". *Nature medicine*.
- Hon, G., Wang, W., and biology, Ren-B. computational (2009). "Discovery and annotation of functional chromatin signatures in the human genome". *PLoS computational biology*.
- Howie, B. N., Donnelly, P., and genetics, Marchini-J. (2009). "A flexible and accurate genotype imputation method for the next generation of genome-wide association studies". *PLoS genetics*.
- Hsieh, I. N., Liou, J. P., Lee, H. Y., Lai, M. J., death, et al. (2014). "Preclinical anti-arthritic study and pharmacokinetic properties of a potent histone deacetylase inhibitor MPT0G009". *Cell death &*.

## BIBLIOGRAPHY

---

- Hu, Stephen, Yu, Hsin-Su, Yen, Feng-Lin, Lin, Chi-Ling, Chen, Gwo-Shing, et al. (2016). "Neutrophil extracellular trap formation is increased in psoriasis and induces human -defensin-2 production in epidermal keratinocytes". *Scientific Reports* 6: p. 31119.
- Huber, M., Brstle, A., and the, Reinhard-K. of (2008). "IRF4 is essential for IL-21-mediated induction, amplification, and stabilization of the Th17 phenotype". *Proceedings of the*.
- Hudak, S., Hagen, M., Liu, Y., and of, Catron-D. (2002). "Immune surveillance and effector functions of CCR10+ skin homing T cells". *The Journal of*.
- Hundhausen, C., Bertoni, A., Mak, R. K., and Investigative, Botti-E. of (2012). "Allele-Specific Cytokine Responses at the HLA-C Locus: Implications for Psoriasis". *Journal of Investigative*.
- Husted, J. A., care, and, Thavaneswaran-A. (2011). "Cardiovascular and other comorbidities in patients with psoriatic arthritis: a comparison with patients with psoriasis". *Arthritis care &*.
- Ibrahim, G., Waxman, R., and Helliwell, P. S. (2009). "The prevalence of psoriatic arthritis in people with psoriasis". *Arthritis Rheum* 61: pp. 1373–8.
- Idel, S., Dansky, H. M., and the, Breslow-J. L. of (2003). "A20, a regulator of NFB, maps to an atherosclerosis locus and differs between parental sensitive C57BL/6J and resistant FVB/N strains". *Proceedings of the*.
- Jabbari, Ali, Surez-Farias, Mayte, Dewell, Scott, and Krueger, James G. (2012). "Transcriptional profiling of psoriasis using RNA-seq reveals previously unidentified differentially expressed genes". *The Journal of investigative dermatology* 132: pp. 246–249.
- Jacobson, Christine C., Kumar, Sandeep, and Kimball, Alexa B. (2011). "Latitude and psoriasis prevalence". *Journal of the American Academy of Dermatology* 65: pp. 870–873.
- Jansen, R., Hottenga, J. J., and molecular, Nivard-M. G. (2017). "Conditional eQTL analysis reveals allelic heterogeneity of gene expression". *Human molecular*.
- Jenuwein, T. and Science, Allis-C. D. (2001). "Translating the histone code". *Science*.
- Ji, Jong, Cheon, Hyeonjoo, Jun, Jae, Choi, Seong, Kim, Ye, et al. (2001). "Effects of peroxisome proliferator-activated receptor- (PPAR- ) on the expression of inflammatory cytokines and apoptosis induction in rheumatoid synovial fibroblasts and monocytes". *Journal of autoimmunity* 17: pp. 215–221.
- Jiang, X, Tian, H, Fan, Y, Chen, J, et al. (2012). "Expression of tumor necrosis factor alpha-induced protein 3 mRNA in peripheral blood mononuclear cells negatively correlates with disease severity in psoriasis ". *Clinical and Vaccine*.
- Johansen, C., Kragballe, K., and of, Rasmussen-M. (2004). "Activator protein 1 DNA binding activity is decreased in lesional psoriatic skin compared with nonlesional psoriatic skin". *British Journal of*.

## BIBLIOGRAPHY

---

- John, S., Sabo, P. J., Canfield, T. K., and in, Lee-K. protocols (2013). "Genomescale mapping of DNase I hypersensitivity". *Current protocols in*.
- Johnson, D. S., Mortazavi, A., Myers, R. M., and Science, Wold-B. (2007). "Genome-wide mapping of in vivo protein-DNA interactions". *Science*.
- Jordan, C. T., Cao, L., Roberson, E. D. O., and of, Pierson-K. C. (2012a). "PSORS2 is due to mutations in CARD14". *The American Journal of*.
- Jordan, C. T., Cao, L., Roberson, E. D. O., and of, Duan-S. (2012b). "Rare and common variants in CARD14, encoding an epidermal regulator of NF-kappaB, in psoriasis". *The American Journal of*.
- Jung, M., Sabat, R., and of, Krtzschmar-J. journal (2004). "Expression profiling of IL10regulated genes in human monocytes and peripheral blood mononuclear cells from psoriatic patients during IL10 therapy". *European journal of*.
- Junta, CM and, SandrinGarcia - P (2009). "Differential gene expression of peripheral blood mononuclear cells from rheumatoid arthritis patients may discriminate immunogenetic, pathogenic and treatment "..
- Kagami, Shinji, Rizzo, Heather L, Lee, Jennifer J, Koguchi, Yoshinobu, and Blauvelt, Andrew (2010). "Circulating Th17, Th22, and Th1 cells are increased in psoriasis". 130: pp. 1373–1383.
- Kaminsky, Z. A., Tang, T., Wang, S. C., Ptak, C., and Nature, G. H. T. (2009). "DNA methylation profiles in monozygotic and dizygotic twins". *Nature*.
- Kanehisa, M. and Goto, S. (2000). "KEGG: kyoto encyclopedia of genes and genomes". *Nucleic acids research* 28: pp. 27–30.
- Kasela, Silva, Kisand, Kai, Tserel, Liina, Kaleviste, Epp, Remm, Anu, et al. (2017). "Pathogenic implications for autoimmune mechanisms derived by comparative eQTL analysis of CD4+ versus CD8+ T cells". *Plos Genet* 13: e1006643.
- Katschke, K. J., Rottman, J. B., Ruth, J. H., and, Qin-S. (2001). "Differential expression of chemokine receptors on peripheral blood, synovial fluid, and synovial tissue monocytes/macrophages in rheumatoid arthritis". *Arthritis &*.
- Keermann, M., Kks, S., and Bmc, Reimann-E. (2015). "Transcriptional landscape of psoriasis identifies the involvement of IL36 and IL36RN". *BMC*.
- Kent, James W., Sugnet, Charles W., Furey, Terrence S., Roskin, Krishna M., Pringle, Tom H., et al. (2002). "The Human Genome Browser at UCSC". *Genome Research* 12: pp. 996–1006.
- Kent, L. (2009). "Freezing and thawing human embryonic stem cells". *Journal of visualized experiments: JoVE*.
- Kent, W. J., Zweig, A. S., Barber, G., and, Hinrichs-A. S. (2010). "BigWig and BigBed: enabling browsing of large distributed datasets" ..
- Kichaev, G. and Pasaniuc, B. (2015). "Leveraging functional-annotation data in trans-ethnic fine-mapping studies". *The American Journal of Human Genetics*.

## BIBLIOGRAPHY

---

- Kim, G. K., of, clinical, and aesthetic, Del J. Q. (2010). "Drug-provoked psoriasis: is it drug induced or drug aggravated?: understanding pathophysiology and clinical relevance". *The Journal of clinical and aesthetic*.
- Kino, Tomoshige, Hurt, Darrell E., Ichijo, Takamasa, Nader, Nancy, and Chrousos, George P. (2010). "Noncoding RNA gas5 is a growth arrest- and starvation-associated repressor of the glucocorticoid receptor". *Science signaling* 3.
- Knight, J. C. (2014). "Approaches for establishing the function of regulatory genetic variants involved in disease". *Genome medicine*.
- Ku, C. S., Loy, E. Y., Salim, A., and genetics, Pawitan-Y. of human (2010). "The discovery of human genetic variations and their use as disease markers: past, present and future". *Journal of human genetics*.
- Kundaje, A., Meuleman, W., Ernst, J., Bilenky, M., and Nature, Yen-A. (2015). "Integrative analysis of 111 reference human epigenomes". *Nature*.
- Kurdi, A. T., Bassil, R., Olah, M., Wu, C., and Nature, Xiao-S. (2016). "Tiam1/Rac1 complex controls Il17a transcription and autoimmunity". *Nature*.
- Lai, A. Y., Mav, D., Shah, R., Grimm, S. A., and Genome, Phadke-D. (2013). "DNA methylation profiling in human B cells reveals immune regulatory elements and epigenetic plasticity at Alu elements during B cell activation". *Genome*.
- Lande, R., Gregorio, J., Facchinetto, V., Chatterjee, B., Wang, Y., et al. (2007). "Plasmacytoid dendritic cells sense self-DNA coupled with antimicrobial peptide". *Nature* 449.
- Landt, Stephen G., Marinov, Georgi K., Kundaje, Anshul, Kheradpour, Pouya, Pauli, Florencia, et al. (2012). "ChIP-seq guidelines and practices of the ENCODE and modENCODE consortia". *Genome research* 22: pp. 1813–1831.
- Langewouters, A. M. G., Erp, P. E. J., Jong, Emgj, and Kerkhof, P. C. M. (2008). "Lymphocyte subsets in peripheral blood of patients with moderate-to-severe versus mild plaque psoriasis". *Archives of dermatological research* 300: pp. 107–113.
- Langmead, B. and Salzberg, S. L. (2012). "Fast gapped-read alignment with Bowtie 2". *Nature methods*.
- Leanne, M, Johnson-Huang, L. M., McNutt, N. S., and Krueger, J. G. (2009). "Cytokine-producing dendritic cells in the pathogenesis of inflammatory skin diseases". *Journal of clinical*.
- Lee, Donghyung, Bigdelli, Bernard T., Riley, Brien P., Fanous, Ayman H., and Bacanu, Silviu-Alin (2013). "DIST: direct imputation of summary statistics for unmeasured SNPs". *Bioinformatics* 29: pp. 2925–2927.
- Lee, Edmund, Trepicchio, William L., Oestreicher, Judith L., Pittman, Debra, Wang, Frank, et al. (2004). "Increased expression of interleukin 23 p19 and p40 in lesional skin of patients with psoriasis vulgaris". *Journal of Experimental Medicine* 199: pp. 125–130.

## BIBLIOGRAPHY

---

- Lee, S. K., Jeon, E. K., Kim, Y. J., and of, Seo-S. H. (2009). "A global gene expression analysis of the peripheral blood mononuclear cells reveals the gene expression signature in psoriasis". *Annals of*
- Lee, Yoontae, Jeon, Kipyung, Lee, Jun, Kim, Sunyoung, and Kim, Narry V. (2002). "MicroRNA maturation: stepwise processing and subcellular localization". *The EMBO journal* 21: pp. 4663–4670.
- Lei, W., Luo, Y., Lei, W., Luo, Y., Yan, K., et al. (2009). "Abnormal DNA methylation in CD4+ T cells from patients with systemic lupus erythematosus, systemic sclerosis, and dermatomyositis". *Scandinavian journal*.
- Lewis, B. P., Burge, C. B., and cell, Bartel-D. P. (2005). "Conserved seed pairing, often flanked by adenosines, indicates that thousands of human genes are microRNA targets". *cell*.
- Li, B., Tsoi, L., Swindell, W., Gudjonsson, J., Tejasvi, T., et al. (2014). "Transcriptome analysis of psoriasis in a large case-control sample: RNA-seq provides insights into disease mechanisms". *J Invest Dermatol* 134: pp. 1828–1838.
- Li, Chun-xiao, Li, Hua-guo, Huang, Lin-ting, Kong, Yu-wei, Chen, Fu-ying, et al. (2017). "H19 lncRNA regulates keratinocyte differentiation by targeting miR-130b-3p". *Cell death & disease* 8.
- Li, H, Yao, Q, Mariscal, AG, Wu, X, and Nature, Hülse J (2018). "Epigenetic control of IL-23 expression in keratinocytes is important for chronic skin inflammation". *Nature*.
- Li, Heng, Handsaker, Bob, Wysoker, Alec, Fennell, Tim, Ruan, Jue, et al. (2009). "The sequence alignment/map format and SAMtools". *Bioinformatics* 25: pp. 2078–2079.
- Li, Y., and Kellis, M. (2016). "Joint Bayesian inference of risk variants and tissue-specific epigenomic enrichments across multiple complex human diseases". *Nucleic acids research*.
- Lin, Andrew M., Rubin, Cory J., Khandpur, Ritika, Wang, Jennifer Y., Riblett, MaryBeth, et al. (2011). "Mast Cells and Neutrophils Release IL-17 through Extracellular Trap Formation in Psoriasis". *The Journal of Immunology* 187: pp. 490–500.
- Linton, PJ, Bautista, B, and, Biederman E of (2003). "Costimulation via OX40L expressed by B cells is sufficient to determine the extent of primary CD4 cell expansion and Th2 cytokine secretion in vivo". *Journal of*
- Liontos, Larissa M., Dissanayake, Dilan, Ohashi, Pamela S., Weiss, Arthur, Dragone, Leonard L., et al. (2011). "The Src-like adaptor protein regulates GM-CSFR signaling and monocytic dendritic cell maturation". *The Journal of Immunology*: p. 903292.
- Litherland, SA, Xie, TX, and, Grebe KM of (2005). "Signal transduction activator of transcription 5 (STAT5) dysfunction in autoimmune monocytes and macrophages". *Journal of*

## BIBLIOGRAPHY

---

- Liu, Ting, Zhang, Lingyun, Joo, Donghyun, and Sun, Shao-Cong (2017). “NF-B signaling in inflammation”. *Signal Transduction and Targeted Therapy* 2: p. 17023.
- Liu, Y., Aryee, M. J., Padyukov, L., and Nature, Fallin-M. D. (2013). “Epigenome-wide association data implicate DNA methylation as an intermediary of genetic risk in rheumatoid arthritis”. *Nature*.
- Lizzul, P. F., Aphale, A., Malaviya, R., and Investigative, Sun-Y. of (2005). “Differential expression of phosphorylated NF-B/RelA in normal and psoriatic epidermis and downregulation of NF-B in response to treatment with”. *Journal of Investigative*.
- Lonsdale, J., Thomas, J., Salvatore, M., Phillips, R., and genetics, Lo-E. (2013). “The genotype-tissue expression (GTEx) project”. *genetics*.
- Love, M. I., Huber, W., and biology, Anders-S. (2014). “Moderated estimation of fold change and dispersion for RNA-seq data with DESeq2”. *Genome biology*.
- Lowes, MA, Kikuchi, T, and Investigative, Fuentes-Duculan - J of (2008). “Psoriasis vulgaris lesions contain discrete populations of Th1 and Th17 T cells”. *Journal of Investigative*.
- Lu, J, Ding, Y, Yi, X, and and, Zheng J of (2016). “CD19+ B cell subsets in the peripheral blood and skin lesions of psoriasis patients and their correlations with disease severity”. *Brazilian Journal of Medical and*.
- Luger, K., Mder, A. W., Richmond, R. K., Sargent, D. F., and Nature, Richmond-T. J. (1997). “Crystal structure of the nucleosome core particle at 2.8 resolution”. *Nature*.
- M, Bar-Eli, Gallily, R, and Investigative, Cohen HA of (1979). “Monocyte function in psoriasis.” *Journal of Investigative*.
- M., Martin (2011). “Cutadapt removes adapter sequences from high-throughput sequencing reads”. *EMBnet. journal*.
- Mahil, Satveer K., Capon, Francesca, and Barker, Jonathan N. (2016). “Update on psoriasis immunopathogenesis and targeted immunotherapy”. *Seminars in Immunopathology* 38: pp. 11–27.
- Malek, T. R. and Immunity, Castro-I. (2010). “Interleukin-2 receptor signaling: at the interface between tolerance and immunity”. *Immunity*.
- Marouli, E., Graff, M., Medina-Gomez, C., Lo, K. S., and Nature, Wood-A. R. (2017). “Rare and low-frequency coding variants alter human adult height”. *Nature*.
- Marrakchi, S., Guigue, P., and of, Renshaw-B. R. (2011). “Interleukin-36receptor antagonist deficiency and generalized pustular psoriasis”. *England Journal of*.
- Marshall, C. R., Howrigan, D. P., and Nature, Merico-D. (2017). “Contribution of copy number variants to schizophrenia from a genome-wide study of 41,321 subjects”. *Nature*.

## BIBLIOGRAPHY

---

- Martin-Fontechá, Alfonso, Thomsen, Lindy L, Brett, Sara, Gerard, Craig, Lipp, Martin, et al. (2004). "Induced recruitment of NK cells to lymph nodes provides IFN- for T H 1 priming". *5*: p. 1260.
- Maurano, M. T., Humbert, R., Rynes, E., and Thurman-R. E. (2012). "Systematic localization of common disease-associated variation in regulatory DNA" ..
- McGeachy, Mandy J., Chen, Yi, Tato, Cristina M., Laurence, Arian, Barbara, Joyce-Shaikh, et al. (2009). "The interleukin 23 receptor is essential for the terminal differentiation of interleukin 17-producing effector T helper cells in vivo." *Nat. Immunol.* 10: pp. 314–24.
- McGonagle, Dennis, Ash, Zoe, Dickie, Laura, McDermott, Michael, and Aydin, Sibel (2011). "The early phase of psoriatic arthritis". *Annals of the Rheumatic Diseases* 70.
- Mease, Philip J. (2011). "Measures of psoriatic arthritis: Tender and Swollen Joint Assessment, Psoriasis Area and Severity Index (PASI), Nail Psoriasis Severity Index (NAPSI), Modified Nail Psoriasis Severity Index (mNAPSI), Mander/Newcastle Enthesitis Index (MEI), Leeds Enthesitis Index (LEI), Spondyloarthritis Research Consortium of Canada (SPARCC), Maastricht Ankylosing Spondylitis Enthesis Score (MASES), Leeds Dactylitis Index (LDI), Patient Global for Psoriatic Arthritis, Dermatology Life Quality Index (DLQI), Psoriatic Arthritis Quality of Life (PsAQOL), Functional Assessment of Chronic Illness TherapyFatigue (FACITF), Psoriatic Arthritis Response Criteria (PsARC), Psoriatic Arthritis Joint Activity Index (PsAJAI), Disease Activity in Psoriatic Arthritis (DAPSA), and Composite Psoriatic Disease Activity Index (CPDAI)". *Arthritis Care & Research* 63.
- Meglio, Di P, Cesare, Di A, Laggner, U, and one, Chu CC (2011). "The IL23R R381Q gene variant protects against immune-mediated diseases by impairing IL-23-induced Th17 effector response in humans". *PloS one*.
- Meglio, Paola, Villanova, Federica, and Nestle, Frank O. (2014). "Psoriasis". *Cold Spring Harbor Perspectives in Medicine* 4.
- Menon, B., Gullick, N. J., and, Walter-G. J. (2014). "Interleukin17+ CD8+ T cells are enriched in the joints of patients with psoriatic arthritis and correlate with disease activity and joint damage progression". *Arthritis &*.
- Mensah, K. A., Schwarz, E. M., and reports, Ritchlin-C. T. rheumatology (2008). "Altered bone remodeling in psoriatic arthritis". *Current rheumatology reports*.
- Menter, Alan, Korman, Neil J., Elmets, Craig A., Feldman, Steven R., Gelfand, Joel M., et al. (2009). "Guidelines of care for the management of psoriasis and psoriatic arthritis Section 3. Guidelines of care for the management and treatment of psoriasis with topical therapies". *Journal of the American Academy of Dermatology* 60: pp. 643–659.
- Mesko, B., Poliskal, S., and Szegedi, A. (2010). "Peripheral blood gene expression patterns discriminate among chronic inflammatory diseases and healthy controls and identify novel targets". *BMC medical*.

## BIBLIOGRAPHY

---

- Messeguer, X., Escudero, R., Farr, D., and, Nez-O. (2002). "PROMO: detection of known transcription regulatory elements using species-tailored searches" ..
- Miao, Y. L., Xiao, Y. L., Du, Y., and of, Duan-L. P. (2013). "Gene expression profiles in peripheral blood mononuclear cells of ulcerative colitis patients". *World Journal of*.
- Mino, T., Murakawa, Y., Fukao, A., and Cell, Vandenbon-A. (2015). "Regnase-1 and roquin regulate a common element in inflammatory mRNAs by spatiotemporally distinct mechanisms". *Cell*.
- Moll, J. M. H., in, arthritis, and rheumatism, Wright-V. (1973). "Psoriatic arthritis". *Seminars in arthritis and rheumatism*.
- Mortazavi, Ali, Williams, Brian A., McCue, Kenneth, Schaeffer, Lorian, and Wold, Barbara (2008). "Mapping and quantifying mammalian transcriptomes by RNA-Seq". *Nature methods* 5: pp. 621–628.
- Moser, B, Desai, DD, Downie, MP, and, Chen Y of (2007). "Receptor for advanced glycation end products expression on T cells contributes to antigen-specific cellular expansion in vivo". *The Journal of*.
- Müller, Nike, Dring, Frank, Klapper, Maja, Neumann, Katrin, Schulte, Dominik M., et al. (2014). "Interleukin-6 and tumour necrosis factor- differentially regulate lincRNA transcripts in cells of the innate immune system in vivo in human subjects with rheumatoid arthritis". *Cytokine* 68: pp. 65–68.
- Nagano, T., Lubling, Y., Stevens, T. J., and Nature, Schoenfelder-S. (2013). "Single-cell Hi-C reveals cell-to-cell variability in chromosome structure". *Nature*.
- Nair, R. P., Ruether, A., Stuart, P. E., Jenisch, S., Tejasvi, T., et al. (2008). "Polymorphisms of the IL12B and IL23R genes are associated with psoriasis". *J Invest Dermatol* 128: pp. 1653–61.
- Nair, R. P., Duffin, K. C., Helms, C., Ding, J., Stuart, P. E., et al. (2009). "Genome-wide scan reveals association of psoriasis with IL-23 and NF-kappaB pathways". *Nat Genet* 41: pp. 199–204.
- Naranbhai, Vivek, Fairfax, Benjamin P, Makino, Seiko, Humburg, Peter, Wong, Daniel, et al. (2015). "Genomic modulators of gene expression in human neutrophils". *Nat Commun* 6: p. 7545.
- Nestle, Frank O., Conrad, Curdin, Tun-Kyi, Adrian, Homey, Bernhard, Gombert, Michael, et al. (2005). "Plasmacytoid dendritic cells initiate psoriasis through interferon- production". *The Journal of Experimental Medicine* 202: pp. 135–143.
- Nestle, Frank O., Kaplan, Daniel H., and Barker, Jonathan (2009). "Psoriasis". *New England Journal of Medicine* 361: pp. 496–509.
- Nica, Parts, Glass, Nisbet, Barrett, et al. (2011). "The Architecture of Gene Regulatory Variation across Multiple Human Tissues: The MuTHER Study". *The Architecture of Gene Regulatory Variation across Multiple Human Tissues: The MuTHER Study* 7: pp. 1–9.
- Nickoloff, B. and Nestle, F. (2004). "Recent insights into the immunopathogenesis of psoriasis provide new therapeutic opportunities". *J Clin Invest* 113.

## BIBLIOGRAPHY

---

- Nickoloff, B. J. and Wrone-Smith, T. (1999). "Injection of pre-psoriatic skin with CD4+ T cells induces psoriasis". *Am J Pathol* 155: pp. 145–58.
- Nora, Elphge P. P., Goloborodko, Anton, Valton, Anne-Laure L., Gibcus, Johan H., Uebersohn, Alec, et al. (2017). "Targeted Degradation of CTCF Decouples Local Insulation of Chromosome Domains from Genomic Compartmentalization". *Cell* 169: pp. 930–1073741824.
- Okada, Y., Han, B., Tsoi, L. C., and of, Stuart-P. E. (2014). "Fine mapping major histocompatibility complex associations in psoriasis and its clinical subtypes". *The American Journal of*.
- Oliveira, Mfsp, Rocha, B. O., and de, Duarte-G. V. brasileiros (2015). "Psoriasis: classical and emerging comorbidities". *Anais brasileiros de*.
- Organization, World Health (2016). *Global report on psoriasis*. Report.
- Ortega, C, S, FernándezA, and, Carrillo JM of leukocyte (2009). "IL17producing CD8+ T lymphocytes from psoriasis skin plaques are cytotoxic effector cells that secrete Th17related cytokines". *Journal of leukocyte*.
- Ottaviani, C, Nasorri, F, and Bedini, C (2006). "CD56brightCD16 NK cells accumulate in psoriatic skin in response to CXCL10 and CCL5 and exacerbate skin inflammation". *European journal of*.
- Oudelaar, A. M., Davies, J. O. J., and acids, Downes-D. J. (2017). "Robust detection of chromosomal interactions from small numbers of cells using low-input Capture-C". *Nucleic acids*.
- Ouyang, Jing, Zhu, Xiaomei, Chen, Yuhai, Wei, Haitao, Chen, Qinghuang, et al. (2014). "NRAV, a long noncoding RNA, modulates antiviral responses through suppression of interferon-stimulated gene transcription". *Cell host & microbe* 16: pp. 616–626.
- Palau, Nuria, Juli, Antonio, Ferrndiz, Carlos, Puig, Llus, Fonseca, Eduardo, et al. (2013). "Genome-wide transcriptional analysis of T cell activation reveals differential gene expression associated with psoriasis". *BMC genomics* 14: p. 825.
- Pan, G., Tian, S., Nie, J., Yang, C., Ruotti, V., et al. (2007). "Whole-genome analysis of histone H3 lysine 4 and lysine 27 methylation in human embryonic stem cells". *Cell stem cell*.
- Pandey, R. R., Mondal, T., Mohammad, F., and cell, Enroth-S. (2008). "Kcnq1ot1 antisense noncoding RNA mediates lineage-specific transcriptional silencing through chromatin-level regulation". *Molecular cell*.
- Pang, Ken C., Dinger, Marcel E., Mercer, Tim R., Malquori, Lorenzo, Grimmond, Sean M., et al. (2009). "Genome-wide identification of long noncoding RNAs in CD8+ T cells". *Journal of immunology (Baltimore, Md. : 1950)* 182: pp. 7738–7748.
- Pedersen, OB, Svendsen, AJ, and oEjstrup, L (2008). "On the heritability of psoriatic arthritis. Disease concordance among monozygotic and dizygotic twins". *Annals of the*.

## BIBLIOGRAPHY

---

- Peeters, J. G. C., Vervoort, S. J., Tan, S. C., and reports, Mijnheer-G. (2015). “Inhibition of super-enhancer activity in autoinflammatory site-derived T cells reduces disease-associated gene expression”. *Cell reports*.
- Pène, J., Chevalier, S., and, Preisser L of (2008). “Chronically inflamed human tissues are infiltrated by highly differentiated Th17 lymphocytes”. *The Journal of*.
- Pepeñella, S., Murphy, K. J., and Chromosoma, Hayes-J. J. (2014). “Intra-and inter-nucleosome interactions of the core histone tail domains in higher-order chromatin structure”. *Chromosoma*.
- Perera, G. K., Di Meglio, P., and Nestle, F. O. (2012). “Psoriasis”. *Annu Rev Pathol* 7: pp. 385–422.
- Petersen, C. P., Bordeleau, M. E., Pelletier, J., and cell, Sharp-P. A. (2006). “Short RNAs repress translation after initiation in mammalian cells”. *Molecular cell*.
- Petronis, Arturas (2010). “Epigenetics as a unifying principle in the aetiology of complex traits and diseases”. *Nature* 465: p. 721.
- Pickrell, J. K., Marioni, J. C., Pai, A. A., and Nature, Degner-J. F. (2010). “Understanding mechanisms underlying human gene expression variation with RNA sequencing”. *Nature*.
- Pivarcsi, A., Sthle, M., and dermatology, Sonkoly-E. (2014). “Genetic polymorphisms altering microRNA activity in psoriasis a key to solve the puzzle of missing heritability?” *Experimental dermatology*.
- Pogribny, I. P., Tryndyak, V. P., and of, Bagnyukova-T. V. (2009). “Hepatic epigenetic phenotype predetermines individual susceptibility to hepatic steatosis in mice fed a lipogenic methyl-deficient diet”. *Journal of*.
- Polach, K. J., Lowary, P. T., and biology, Widom-J. of molecular (2000). “Effects of core histone tail domains on the equilibrium constants for dynamic dna site accessibility in nucleosomes1”. *Journal of molecular biology*.
- Polachek, A., Li, S., care, and, Chandran-V. (2017). “Clinical Enthesitis in a Prospective Longitudinal Psoriatic Arthritis Cohort: Incidence, Prevalence, Characteristics, and Outcome”. *Arthritis care &*.
- Ponts, N., Harris, E. Y., Prudhomme, J., and Genome, Wick-I. (2010). “Nucleosome landscape and control of transcription in the human malaria parasite”. *Genome*.
- Poole, C. D., Lebmeier, M., Ara, R., and Rheumatology, Rafia-R. (2010). “Estimation of health care costs as a function of disease severity in people with psoriatic arthritis in the UK”. *Rheumatology*.
- Porcher, R., SaidNahal, R., and, D'Agostino-M. A. (2005). “Two major spondylarthropathy phenotypes are distinguished by pattern analysis in multiplex families”. *Arthritis Care &*.
- Proksch, E., Brandner, J. M., and Jensen, J. M. (2008). “The skin: an indispensable barrier”. *Exp Dermatol* 17: pp. 1063–72.

## BIBLIOGRAPHY

---

- Qian, F., Deng, J., Cheng, N., and Embo, Welch-E. J. (2009). "A nonredundant role for MKP5 in limiting ROS production and preventing LPSinduced vascular injury". *The EMBO*.
- Qu, K., Zaba, L. C., Satpathy, A. T., Giresi, P. G., Li, R., et al. (2017). "Chromatin Accessibility Landscape of Cutaneous T Cell Lymphoma and Dynamic Response to HDAC Inhibitors". *Cancer Cell*.
- Qu, Kun, Zaba, Lisa C., Giresi, Paul G., Li, Rui, Longmire, Michelle, et al. (2015). "Individuality and variation of personal regulomes in primary human T cells". *Cell systems* 1: pp. 51–61.
- Quinlan, A. R. and Hall, I. M. (2010). "BEDTools: a flexible suite of utilities for comparing genomic features". *Bioinformatics*.
- Raj, Towfique, Rothamel, Katie, Mostafavi, Sara, Ye, Chun, Lee, Mark N., et al. (2014). "Polarization of the effects of autoimmune and neurodegenerative risk alleles in leukocytes". *Science* 344: pp. 519–523.
- Ray-Jones, H. F., McGovern, A., Warren, P., Duffus, Martin K., Eyre, S., et al. (2017). "[Abstract] Capture Hi-C identifies chromatin interactions between psoriasis-associated genetic loci and disease candidate genes." *UNPUBLISHED*.
- Reich, K. (2012). "The concept of psoriasis as a systemic inflammation: implications for disease management". *Journal of the European Academy of Dermatology* 26: pp. 3–11.
- Reich, K., Krger, K., and Dermatology, MSSNER-R. OF (2009). "Epidemiology and clinical pattern of psoriatic arthritis in Germany: a prospective interdisciplinary epidemiological study of 1511 patients with plaque-type psoriasis". *Journal of Dermatology*.
- Reich, Kristian, Papp, Kim A., Matheson, Robert T., Tu, John H., Bissonnette, Robert, et al. (2015). "Evidence that a neutrophilkeratinocyte crosstalk is an early target of IL17A inhibition in psoriasis". *Experimental Dermatology* 24: pp. 529–535.
- Rendeiro, Andr F., Schmidl, Christian, Strefford, Jonathan C., Walewska, Renata, Davis, Zadie, et al. (2016). "Chromatin accessibility maps of chronic lymphocytic leukaemia identify subtype-specific epigenome signatures and transcription regulatory networks". *Nature communications* 7: p. 11938.
- Rizova, E. and Coroller, M. (2001). "Topical calcitriolstudies on local tolerance and systemic safety". *British Journal of Dermatology* 144: pp. 3–10.
- Romanowska, M, Yacoub, Al N, and Investigative, Seidel H of (2008). "PPAR enhances keratinocyte proliferation in psoriasis and induces heparin-binding EGF-like growth factor". *Journal of Investigative*.
- Rossetto, Cyprian C. and Pari, Gregory (2012). "KSHV PAN RNA associates with demethylases UTX and JMJD3 to activate lytic replication through a physical interaction with the virus genome". *PLoS pathogens* 8.
- Rotem, A., Ram, O., Shores, N., and Nature, Sperling-R. A. (2015). "Single-cell ChIP-seq reveals cell subpopulations defined by chromatin state". *Nature*.

## BIBLIOGRAPHY

---

- Ruchusatsawat, K, Wongpiyabovorn, J, and pathology, Protjaroen P (2011). “Parakeratosis in skin is associated with loss of inhibitor of differentiation 4 via promoter methylation”. *Human pathology*.
- Rudwaleit, M., Heijde, Van D., and the, Landew-R. of (2009). “The development of Assessment of Spondyloarthritis International Society (ASAS) classification criteria for axial spondyloarthritis (part II): validation and final selection”. *Annals of the*.
- Russell, T. J., Schultes, L. M., and of, Kuban-D. J. (1972). “Histocompatibility (HL-A) antigens associated with psoriasis”. *New England Journal of*.
- S., Andrews (2010). “FastQC: a quality control tool for high throughput sequence data. Available online at: <http://www.bioinformatics.babraham.ac.uk/projects/fastqc>”.
- Sampogna, Francesca, Tabolli, Stefano, and Abeni, Damiano (2012). “Living with psoriasis: prevalence of shame, anger, worry, and problems in daily activities and social life”. *Acta dermato-venereologica* 92: pp. 299–303.
- Scharer, Christopher D., Blalock, Emily L., Barwick, Benjamin G., Haines, Robert R., Wei, Chungwen, et al. (2016). “ATAC-seq on biobanked specimens defines a unique chromatin accessibility structure in naïve SLE B cells”. *Scientific reports* 6: p. 27030.
- Schett, G., Coates, L. C., and Arthritis, Ash-Z. R. (2011). “Structural damage in rheumatoid arthritis, psoriatic arthritis, and ankylosing spondylitis: traditional views, novel insights gained from TNF blockade, and”. *Arthritis*.
- Schmid, P., Itin, P., and interferon, Cox-D. of (1994). “The type I interferon system is locally activated in psoriatic lesions”. *Journal of interferon*.
- Schmidl, Christian, Rendeiro, Andr F., Sheffield, Nathan C., and Bock, Christoph (2015). “ChIPmentation: fast, robust, low-input ChIP-seq for histones and transcription factors”. *Nature methods* 12: p. 963.
- Schmitt, J. and of, Rosumeck-S. (2014). “Efficacy and safety of systemic treatments for moderate-to-severe psoriasis: metaanalysis of randomized controlled trials”. *British Journal of*.
- Schmitt, J. and Wozel, G. (2005). “The psoriasis area and severity index is the adequate criterion to define severity in chronic plaque-type psoriasis”. *Dermatology*.
- Schork, N. J., Murray, S. S., Frazer, K. A., and Topol, E. J. (2009). “Common vs. rare allele hypotheses for complex diseases”. *Curr Opin Genet Dev* 19: pp. 212–9.
- Sellars, M. L., Huh, J. R., Day, K., Issuree, P. D., and Nature, Galan-C. (2015). “Regulation of DNA methylation dictates Cd4 expression during the development of helper and cytotoxic T cell lineages”. *Nature*.
- Shapiro, J., Cohen, A. D., David, M., and American, Hodak-E. of the (2007). “The association between psoriasis, diabetes mellitus, and atherosclerosis in Israel: a case-control study”. *Journal of the American*.
- Shi, Lihua, Zhang, Zhe, Yu, Angela M., Wang, Wei, Wei, Zhi, et al. (2014). “The SLE transcriptome exhibits evidence of chronic endotoxin exposure and has widespread dysregulation of non-coding and coding RNAs”. *PloS one* 9.

## BIBLIOGRAPHY

---

- Shu, Jin, Li, Ling, Zhou, Lan-Bo, Qian, Jun, Fan, Zhi-Dan, et al. (2017). "IRF5 is elevated in childhood-onset SLE and regulated by histone acetyltransferase and histone deacetylase inhibitors". *Oncotarget* 8: p. 47184.
- Small, K. S., Hedman, K, Grundberg, E., and Nature, Nica-A. C. (2011). "Identification of an imprinted master trans regulator at the KLF14 locus related to multiple metabolic phenotypes". *Nature*.
- Smallwood, SA, Lee, HJ, Angermueller, C, and Nature, Krueger F (2014). "Single-cell genome-wide bisulfite sequencing for assessing epigenetic heterogeneity". *Nature* 507: pp. 371–375.
- Smemo, S., Tena, J. J., Kim, K. H., Gamazon, E. R., and Sakabe, N. J. (2014). "Obesity-associated variants within FTO form long-range functional connections with IRX3". *Nature* 507: pp. 371–375.
- Smith, Emily M., Lajoie, Bryan R., Jain, Gaurav, and Dekker, Job (2016). "Invariant TAD Boundaries Constrain Cell-Type-Specific Looping Interactions between Promoters and Distal Elements around the CFTR Locus". *American journal of human genetics* 98: pp. 185–201.
- Smith, Judith A., Barnes, Michael D., Hong, Dihua, DeLay, Monica L., Inman, Robert D., et al. (2008). "Gene expression analysis of macrophages derived from ankylosing spondylitis patients reveals interferon dysregulation". *Arthritis & Rheumatism: Official Journal of the American College of Rheumatology* 58: pp. 1640–1649.
- Soccio, Raymond E., Chen, Eric R., Rajapurkar, Satyajit R., Safabakhsh, Pegah, Marinis, Jill M., et al. (2015). "Genetic variation determines PPAR function and anti-diabetic drug response in vivo". *Cell* 162: pp. 33–44.
- Solomon, M. J., Larsen, P. L., and Cell, Varshavsky-A. (1988). "Mapping proteinDNA interactions in vivo with formaldehyde: Evidence that histone H4 is retained on a highly transcribed gene". *Cell*.
- Spain, S. L. and Barrett, J. C. (2015). "Strategies for fine-mapping complex traits". *Human molecular genetics*.
- Springate, D. A., Parisi, R., and of, Kontopantelis-E. (2017). "Incidence, prevalence and mortality of patients with psoriasis: a UK populationbased cohort study". *British Journal of*.
- Stefan, M., Wei, C., Lombardi, A., Li, C. W., Concepcion, E. S., et al. (2014). "Genetic-epigenetic dysregulation of thymic TSH receptor gene expression triggers thyroid autoimmunity". *Proc Natl Acad Sci U S A* 111: pp. 12562–7.
- Strange, A., Capon, F., Spencer, C. C., Knight, J., Weale, M. E., et al. (2010). "A genome-wide association study identifies new psoriasis susceptibility loci and an interaction between HLA-C and ERAP1". *Nat Genet* 42: pp. 985–90.
- Stratis, Athanasios, Pasparakis, Manolis, Rupec, Rudolf A., Markur, Doreen, Hartmann, Karin, et al. (2006). "Pathogenic role for skin macrophages in a mouse model of keratinocyte-induced psoriasis-like skin inflammation". *Journal of Clinical Investigation* 116: pp. 2094–2104.

## BIBLIOGRAPHY

---

- Straus, DS and immunology, Glass CK in (2007). "Anti-inflammatory actions of PPAR ligands: new insights on cellular and molecular mechanisms". *Trends in immunology*.
- Stuart, Philip E., Nair, Rajan P., Ellinghaus, Eva, Ding, Jun, Tejasvi, Trilokraj, et al. (2010). "Genome-wide association analysis identifies three psoriasis susceptibility loci". *Nature genetics* 42: pp. 1000–1004.
- Stuart, Philip E., Nair, Rajan P., Tsoi, Lam C., Tejasvi, Trilokraj, Das, Sayantan, et al. (2015). "Genome-wide association analysis of psoriatic arthritis and cutaneous psoriasis reveals differences in their genetic architecture". *The American Journal of Human Genetics* 97.
- Sullivan, KE, Reddy, ABM, and biology, Dietzmann K cellular (2007). "Epigenetic regulation of tumor necrosis factor alpha". *and cellular biology*.
- Sun, Lian-Dang, Cheng, Hui, Xue-Qin, Yang, Jian-Zhong, Zhang, Ai, E., et al. (2010). "Association analyses identify six new psoriasis susceptibility loci in the Chinese population". *Nature Genetics* 42.
- Swindell, W. R. and Remmer, H. A. (2015). "Proteogenomic analysis of psoriasis reveals discordant and concordant changes in mRNA and protein abundance". *Genome*.
- Swindell, W. R., Sarkar, M. K., Liang, Y., Xing, X., and reports, Baliwag-J. (2017). "RNA-seq identifies a diminished differentiation gene signature in primary monolayer keratinocytes grown from lesional and uninvolved psoriatic skin". *Scientific reports*.
- Taganov, K. D., Boldin, M. P., and the, Chang-K. J. of (2006). "NF-B-dependent induction of microRNA miR-146, an inhibitor targeted to signaling proteins of innate immune responses". *Proceedings of the*.
- Tang, F., Barbacioru, C., Wang, Y., Nordman, E., and Nature, Lee-C. (2009). "mRNA-Seq whole-transcriptome analysis of a single cell". *Nature methods* 6: p. 377.
- Tang, Fuchou, Barbacioru, Catalin, Nordman, Ellen, Li, Bin, Xu, Nanlan, et al. (2010). "RNA-Seq analysis to capture the transcriptome landscape of a single cell". *Nature protocols* 5: pp. 516–535.
- Tang, H., Jin, X., Li, Y., Jiang, H., Tang, X., et al. (2014). "A large-scale screen for coding variants predisposing to psoriasis". *Nature*.
- Taylor, W, Gladman, D, and &, Helliwell P (2006). "Classification criteria for psoriatic arthritis: development of new criteria from a large international study". *Arthritis &*.
- Telfer, NR, Chalmers, RJ, Whale, K, and Colman, G (1992). "The role of streptococcal infection in the initiation of guttate psoriasis." *Arch Dermatol* 128: pp. 39–42.
- Tervaniemi, Mari H., Katayama, Shintaro, Skoog, Tiina, Siitonen, Annika H., Vuola, Jyrki, et al. (2016). "NOD-like receptor signaling and inflammasome-related pathways are highlighted in psoriatic epidermis". *Scientific reports* 6: p. 22745.

## BIBLIOGRAPHY

---

- Thrastardottir, T and international, Love TJ (2018). "Infections and the risk of psoriatic arthritis among psoriasis patients: a systematic review". *Rheumatology international*.
- Tiilikainen, A., Lassus, A., Karvonen, J., Vartiainen, P., and Julin, M. (1980). "Psoriasis and HLA Cw6". *British Journal of Dermatology* 102: pp. 179–184.
- Toberer, Ferdinand, Sykora, Jaromir, Gttel, Daniel, Ruland, Vincent, Hartschuh, Wolfgang, et al. (2011). "Tissue microarray analysis of RANKL in cutaneous lupus erythematosus and psoriasis". *Experimental dermatology* 20: pp. 600–602.
- Tobin, AM, Lynch, L, Kirby, B, and immunity, O'Farrelly - C of innate (2011). "Natural killer cells in psoriasis". *Journal of innate immunity*.
- Togayachi, Akira, Kozono, Yuko, Kuno, Atsushi, Ohkura, Takashi, Sato, Takashi, et al. (2010). "3GnT2 (B3GNT2), a major polylactosamine synthase: analysis of B3GNT2-deficient mice". 479: pp. 185–204.
- Tomfohrde, J., Silverman, A., and, Barnes-R. (1994). "Gene for familial psoriasis susceptibility mapped to the distal end of human chromosome 17q" ..
- Tonel, Giulia, Conrad, Curdin, Laggner, Ute, Di Meglio, Paola, Grys, Katarzyna, et al. (2010). "Cutting edge: A critical functional role for IL-23 in psoriasis." *J. Immunol.* 185: pp. 5688–91.
- Trynka, G. and Raychaudhuri, S. (2013a). "Using chromatin marks to interpret and localize genetic associations to complex human traits and diseases". *Current opinion in genetics & development* 23: pp. 635–641.
- Trynka, G., Hunt, K. A., Bockett, N. A., Romanos, J., and Nature, Mistry-V. (2011). "Dense genotyping identifies and localizes multiple common and rare variant association signals in celiac disease". *Nature*.
- Trynka, Gosia and Raychaudhuri, Soumya (2013b). "Using chromatin marks to interpret and localize genetic associations to complex human traits and diseases". *Curr Opin Genetics Dev* 23: pp. 635–641.
- Tsoi, L. C., Spain, S. L., Knight, J., Ellinghaus, E., Stuart, P. E., et al. (2012). "Identification of 15 new psoriasis susceptibility loci highlights the role of innate immunity". *Nat Genet* 44: pp. 1341–8.
- Tsoi, L. C., Stuart, P. E., Tian, C., and Nature, Gudjonsson-J. E. (2017). "Large scale meta-analysis characterizes genetic architecture for common psoriasis associated variants". *Nature*.
- Tsoi, Lam C., Iyer, Matthew K., Stuart, Philip E., Swindell, William R., Gudjonsson, Johann E., et al. (2015). "Analysis of long non-coding RNAs highlights tissue-specific expression patterns and epigenetic profiles in normal and psoriatic skin". *Genome Biology* 16: p. 24.
- Valdimarsson, H. and Thorleifsdottir, R. H. (2009). "Psoriasis as an autoimmune disease caused by molecular mimicry". *Trends in*.
- Valk, E., Leung, R., Kang, H., Kaneko, K., and Immunity, Rudd-C. E. (2006). "T cell receptor-interacting molecule acts as a chaperone to modulate surface expression of the CTLA-4 coreceptor". *Immunity*.

## BIBLIOGRAPHY

---

- Vandooren, B, Kruithof, E, Yu, DTY, and, Rihl M of (2004). "Involvement of matrix metalloproteinases and their inhibitors in peripheral synovitis and downregulation by tumor necrosis factor blockade in spondylarthropathy". *: Official Journal of*.
- Vence, L., Schmitt, A., and Medical, Meadows-C. E. (2015). "Recognizing guttate psoriasis and initiating appropriate treatment". *West Virginia Medical*.
- Vereecke, L, Beyaert, R, and Loo, G van (2011). "Genetic relationships between A20/TNFAIP3, chronic inflammation and autoimmune disease".
- Vierstra, Jeff, Wang, Hao, John, Sam, Sandstrom, Richard, and Stamatoyannopoulos, John A. (2014). "Coupling transcription factor occupancy to nucleosome architecture with DNase-FLASH". *Nature Methods*.
- Villanova, Federica, Meglio, Paola, and Nestle, Frank O. (2013). "Biomarkers in psoriasis and psoriatic arthritis". *Annals of the rheumatic diseases* 72.
- Visscher, PM, Wray, NR, Zhang, Q, and, Sklar P of (2017). "10 years of GWAS discovery: biology, function, and translation". *The American Journal of*.
- Wang, H., Kess, D., Lindqvist, A. K. B., and of, Peters-T. (2008). "A 9-centimorgan interval of chromosome 10 controls the T cell-dependent psoriasisform skin disease and arthritis in a murine psoriasis model". *The Journal of*.
- Wang, Honglin, Peters, Thorsten, Kess, Daniel, Sindrilaru, Anca, Oreshkova, Tsvetelina, et al. (2006). "Activated macrophages are essential in a murine model for T cellmediated chronic psoriasisform skin inflammation". *Journal of Clinical Investigation* 116: pp. 2105–2114.
- Wang, Jie, Zibetti, Cristina, Shang, Peng, Sripathi, Srinivasa R, Zhang, Pingwu, et al. (2018). "ATAC-Seq analysis reveals a widespread decrease of chromatin accessibility in age-related macular degeneration". 9: p. 1364.
- Wang, Jun, Al-Lamki, Rafia S., Zhu, Xinwang, Liu, Hanzhe, Pober, Jordan S., et al. (2014). "TL1-A can engage death receptor-3 and activate NF-kappa B in endothelial cells". *BMC nephrology* 15: p. 178.
- Ward, L. D. and Kellis, M. (2012). "Interpreting noncoding genetic variation in complex traits and human disease". *Nature biotechnology*.
- Weaver, CT, Hatton, RD, and Rev, Mangan PR (2007). "IL-17 family cytokines and the expanding diversity of effector T cell lineages". *Annu. Rev.*
- Weiss, G., Shemer, A., and Academy, Trau-H. of the (2002). "The Koebner phenomenon: review of the literature". *Journal of the European Academy*.
- Welter, D., MacArthur, J., Morales, J., and acids, Burdett-T. (2013). "The NHGRI GWAS Catalog, a curated resource of SNP-trait associations". *Nucleic acids*.
- Wikramanayake, T. C., Stojadinovic, O., and Tomic-Canic, M. (2014). "Epidermal Differentiation in Barrier Maintenance and Wound Healing". *Adv Wound Care (New Rochelle)*. Vol. 3: pp. 272–280.
- Williams, Fionnuala, Meenagh, Ashley, Sleator, Carole, Cook, Daniel, Fernandez-Vina, Marcelo, et al. (2005). "Activating Killer Cell Immunoglobulin-Like Receptor Gene KIR2DS1 Is Associated With Psoriatic Arthritis". *Human Immunology* 66: pp. 836–841.

## BIBLIOGRAPHY

---

- Winchester, R., Minevich, G., and, Steshenko-V. (2012). "HLA associations reveal genetic heterogeneity in psoriatic arthritis and in the psoriasis phenotype". *Arthritis &*
- Wolk, K, Witte, E, Wallace, E, and, Döcke WD journal of (2006). "IL22 regulates the expression of genes responsible for antimicrobial defense, cellular differentiation, and mobility in keratinocytes: a potential role in psoriasis". *European journal of*
- Wong, W. F., Kohu, K., Chiba, T., Sato, T., and Immunology, Satake-M. (2011). "Interplay of transcription factors in Tcell differentiation and function: the role of Runx". *Immunology*.
- Woolacott, N., Hawkins, N., Kainth, A., and Khadjesari, Z. (2006). "Etanercept and Efalizumab for the Treatment of Moderate to Severe Psoriasis". *Etanercept and Efalizumab for the Treatment of Moderate to Severe Psoriasis*.
- Wray, Naomi R. (2005). "Allele frequencies and the r<sup>2</sup> measure of linkage disequilibrium: impact on design and interpretation of association studies". *Twin Research and Human Genetics* 8: pp. 87–94.
- Wrone-Smith, T. and Nickoloff, B. J. (1996). "Dermal injection of immunocytes induces psoriasis". *The Journal of clinical*.
- Wu, Q, Jin, H, Yang, Z, Luo, G, Lu, Y, et al. (2010). "MiR-150 promotes gastric cancer proliferation by negatively regulating the pro-apoptotic gene EGR2". *Biochemical and*
- Xia, Yu-Ping, Li, Baosheng, Hylton, Donna, Detmar, Michael, Yancopoulos, George D, et al. (2003). "Transgenic delivery of VEGF to mouse skin leads to an inflammatory condition resembling human psoriasis". 102: pp. 161–168.
- Yamazaki, H., Hiramatsu, N., and of, Hayakawa-K. (2009). "Activation of the Akt-NF-B pathway by subtilase cytotoxin through the ATF6 branch of the unfolded protein response". *The Journal of*
- Yan, Di, Issa, Naiem, Afifi, Ladan, Jeon, Caleb, Chang, Hsin-Wen, et al. (2017). "The Role of the Skin and Gut Microbiome in Psoriatic Disease". *Current Dermatology Reports* 6: pp. 94–103.
- Yan, Hai, Yuan, Weishi, Velculescu, Victor E., Vogelstein, Bert, and Kinzler, Kenneth W. (2002). "Allelic variation in human gene expression". *Science* 297: pp. 1143–1143.
- Yanaba, K, Kamata, M, and, Ishiura N of leukocyte (2013). "Regulatory B cells suppress imiquimodinduced, psoriasislike skin inflammation". *Journal of leukocyte*.
- Yang, J., Benyamin, B., McEvoy, B. P., Gordon, S., Henders, A. K., et al. (2010). "Common SNPs explain a large proportion of the heritability for human height". *Nat Genet* 42: pp. 565–9.
- Yen, J. H., Moore, B. E., Nakajima, T., and of, Scholl-D. (2001). "Major histocompatibility complex class Irecognizing receptors are disease risk genes in rheumatoid arthritis". *Journal of*

## BIBLIOGRAPHY

---

- Yin, Xianyong, Low, Hui Q., Wang, Ling, Li, Yonghong, Ellinghaus, Eva, et al. (2015). "Genome-wide meta-analysis identifies multiple novel associations and ethnic heterogeneity of psoriasis susceptibility". *Nature communications* 6: pp. 1–11.
- Yogo, T, Nagamiya, H, Seto, M, and, Sasaki S of medicinal (2016). "Structure-Based Design and Synthesis of 3-Amino-1,5-dihydro-4H-pyrazolopyridin-4-one Derivatives as Tyrosine Kinase 2 Inhibitors". *Journal of medicinal*.
- Yosef, N and Regev, A (2016). "Writ large: Genomic dissection of the effect of cellular environment on immune response". 354: pp. 64–68.
- Zgraggen, S., Huggerberger, R., Kerl, K., and One, Detmar-M. (2014). "An important role of the SDF-1/CXCR4 axis in chronic skin inflammation". *PLoS One*.
- Zhang, Chen, Wang, Chen, Jia, Zhenyu, Tong, Wenwen, Liu, Delin, et al. (2017). "Differentially expressed mRNAs, lncRNAs, and miRNAs with associated co-expression and ceRNA networks in ankylosing spondylitis". 8: p. 113543.
- Zhang, F., Wu, L., Qian, J., Qu, B., Xia, S., et al. (2016). "Identification of the long noncoding RNA NEAT1 as a novel inflammatory regulator acting through MAPK pathway in human lupus". *Journal of*.
- Zhang, P., Su, Y., Chen, H., Zhao, M., and dermatological, Lu-Q. of (2010). "Abnormal DNA methylation in skin lesions and PBMCs of patients with psoriasis vulgaris". *Journal of dermatological*.
- Zhang, X., Cowper-Sal, R., Bailey, S. D., and Genome, Moore-J. H. (2012). "Integrative functional genomics identifies an enhancer looping to the SOX9 gene disrupted by the 17q24.3 prostate cancer risk locus". *Genome*.
- Zhang, X. J., Huang, W., Yang, S., Sun, L. D., and Zhang, F. Y. (2009). "Psoriasis genome-wide association study identifies susceptibility variants within LCE gene cluster at 1q21". *Psoriasis genome-wide association study identifies susceptibility variants within LCE gene cluster at 1q21*.
- Zhang, Y., Liu, T., and Genome, Meyer-C. A. (2008). "Model-based analysis of ChIP-Seq (MACS)". *Genome*.
- Zhao, S., Fung-Leung, W. P., Bittner, A., Ngo, K., and one, Liu-X. (2014). "Comparison of RNA-Seq and microarray in transcriptome profiling of activated T cells". *PloS one*.
- Zhong, Y, Kinio, A, and immunology, Saleh M in (2013). "Functions of NOD-like receptors in human diseases". *Frontiers in immunology*.
- Zhu, K. J., Zhu, C. Y., Shi, G., and Research, Fan-Y. M. (2012). "Association of IL23R polymorphisms with psoriasis and psoriatic arthritis: a meta-analysis". *Inflammation Research*.
- Zuk, O., Hechter, E., and the, Sunyaev-S. R. of (2012). "The mystery of missing heritability: Genetic interactions create phantom heritability". *Proceedings of the*.

## BIBLIOGRAPHY

---

Zuo, Xianbo, Sun, Liangdan, Yin, Xianyong, Gao, Jinping, Sheng, Yujun, et al. (2015). "Whole-exome SNP array identifies 15 new susceptibility loci for psoriasis". *Nature communications* 6: p. 6793.